

Electronic Thesis and Dissertation Repository

12-14-2011 12:00 AM

Effects of Internals Configurations on Heat Transfer and Hydrodynamics in Bubble Columns - With and Without Solid Particles

Anil Kumar Jhawar, *The University of Western Ontario*

Supervisor: Dr. Anand Prakash, *The University of Western Ontario*

A thesis submitted in partial fulfillment of the requirements for the Doctor of Philosophy degree in Chemical and Biochemical Engineering

© Anil Kumar Jhawar 2011

Follow this and additional works at: <https://ir.lib.uwo.ca/etd>



Part of the [Transport Phenomena Commons](#)

Recommended Citation

Jhawar, Anil Kumar, "Effects of Internals Configurations on Heat Transfer and Hydrodynamics in Bubble Columns - With and Without Solid Particles" (2011). *Electronic Thesis and Dissertation Repository*. 339. <https://ir.lib.uwo.ca/etd/339>

This Dissertation/Thesis is brought to you for free and open access by Scholarship@Western. It has been accepted for inclusion in Electronic Thesis and Dissertation Repository by an authorized administrator of Scholarship@Western. For more information, please contact wlsadmin@uwo.ca.

EFFECTS OF INTERNALS CONFIGURATIONS ON HEAT TRANSFER AND
HYDRODYNAMICS IN BUBBLE COLUMNS –WITH AND WITHOUT SOLID
PARTICLES

(Spine title: Effects of Internals on Heat Transfer in Bubble Columns)

(Thesis format: Integrated Article)

by

Anil Kumar Jhawar

Graduate Program in Chemical and Biochemical Engineering

A thesis submitted in partial fulfilment
of the requirements for the degree of
Doctor of Philosophy

The School of Graduate and Postdoctoral Studies
The University of Western Ontario
London, Ontario, Canada

© Anil Kumar Jhawar 2011

CERTIFICATE OF EXAMINATION

Supervisor

Examiners

Dr. Anand Prakash

Dr. Argyrios Margaritis

Supervisory Committee

Dr. George Nakhla

Dr. Ajay Ray

Dr. Ernest Yanful

Dr. Argyrios Margaritis

Dr. Krishna Nigam

The thesis by

Anil Kumar Jhawar

entitled:

**Effects of Internals Configurations on Heat Transfer and Hydrodynamics in
Bubble Columns –With and Without Solid Particles**

is accepted in partial fulfillment of the
requirements for the degree of
Doctor of Philosophy

Date

Chair of the Thesis Examination Board

ABSTRACT

Internals of different types are required in a number of industrial applications of bubble columns to achieve the desired mixing or to remove the heat of reaction to maintain desired temperature and isothermal conditions of operation. Some of these applications include Fischer-Tropsch synthesis, methanol synthesis, and production of dimethyl ether (DME). The presence of internals however can alter the column hydrodynamics and mixing patterns which could influence reactor performance. A fast response probe capable of capturing bubble dynamics, as well as detecting flow direction is used to study the effect of internals on local heat transfer and column hydrodynamics in a bubble column with and without solid particles. It captured the temporal variations in heat transfer coefficients due to changes in local hydrodynamic conditions. Measurements obtained in presence of different configurations and combinations of internals are compared with those without internals to elucidate the effects of internals design and configurations. Comparisons are based on average values and fluctuating component of local temporal variations of the heat transfer coefficient obtained with the fast response probe. The average gas holdup, center line liquid, and bubble rise velocities obtained with and without internals are also compared. The observed differences are discussed based on the insights provided by these comparisons. The heat transfer coefficient and gas holdup increases in presence of internals. Relationships between local heat transfer measurements and hydrodynamic conditions with internals are shown and discussed. The observed increase in heat transfer coefficients with scale can be related to increase in liquid circulation velocity with column diameter, which in turn is related to an increase in large bubbles rise velocity.

Keywords: Local heat transfer, Bubble columns, Hydrodynamics, Internals design, Liquid circulation velocity, Bubble fractions

CO-AUTHORSHIP

Title: Heat transfer in slurry bubble column reactor – a critical overview

Authors: A. K. Jhavar, A. Prakash

All literature survey was done by A. K. Jhavar under the guidance of advisor A. Prakash. All drafts of the manuscripts were written by A. K. Jhavar. Modification of the drafts was undertaken under the close supervision of thesis advisor A. Prakash.

Title: Influence of bubble column diameter on local heat transfer and related hydrodynamics

Authors: A. K. Jhavar, A. Prakash

All portions of experimental work and data analysis were undertaken by A. K. Jhavar under the guidance of advisor A. Prakash. All drafts of the manuscripts were written by A. K. Jhavar. Modification of the drafts was undertaken under the close supervision of thesis advisor A. Prakash.

ACKNOWLEDGEMENTS

First of all, I would like to express my deep sense of gratitude to my supervisor Dr. Anand Prakash. His wide knowledge and his logical way of thinking have been of great value for me. His understanding, encouraging and personal guidance have provided a good basis for the present thesis.

I warmly thank to Department of Chemical and Biochemical Engineering for their tremendous support from time to time. I also want to extend my thanks to Joanna Bloom, April Finkenhoefer and Souheil Afara for their help and kindness to me. The valuable help of University Machine Services staff and Electronic Stores staff in establishing the experimental setup is gratefully acknowledged.

I also thank my friends and colleagues Kandlakuti Venkat Reddy, Abhishek Shukla, Kai Pisters, Krupal Pal and Srikanth Bhattad at the University of Western Ontario for their continued and untiring support during tough times.

In the last but not least, I owe my loving thanks to my parents, my wife Arpana, son Archit and family. Without their encouragement and understanding it would have been impossible for me to finish this work.

TABLE OF CONTENTS

CERTIFICATE OF EXAMINATION	ii
ABSTRACT.....	iii
CO-AUTHORSHIP	iv
ACKNOWLEDGEMENTS	v
TABLE OF CONTENTS	vi
LIST OF TABLES.....	ix
LIST OF FIGURES	x
LIST OF APPENDICES	xvi
CHAPTER 1. INTRODUCTION.....	1
1.1 Introduction.....	2
1.2 Scope and Objectives	4
1.3 Research Contributions.....	5
1.4 Thesis Format.....	5
1.5 References.....	6
CHAPTER 2. HEAT TRANSFER IN SLURRY BUBBLE COLUMN REACTOR – A CRITICAL OVERVIEW.....	8
2.1. Introduction.....	9
2.2.1 Cataloging of Slurry Bubble Column Reactors	10
2.2. Flow Regimes and Effects on Heat Transfer.....	12
2.3. Effect of Operating Variables on Heat Transfer	18
2.3.1. Effects of Superficial Gas Velocity	18
2.3.2. Effects of Superficial Liquid Velocity	19
2.3.3. Effects of Liquid Properties	19
2.3.4. Effects of Particles Properties and Concentration	21
2.3.5. Effects of Operating Pressure	23

2.3.6.	Effects of Column Diameter	24
2.3.7.	Effects of Internals	25
2.3.8.	Effects of Axial and Radial Location.....	26
2.4.	Correlations of Heat Transfer Coefficients	27
2.5.	Conclusions.....	30
2.6.	Notations	31
2.7.	References.....	33
CHAPTER 3. EFFECTS OF INTERNALS OF DIFFERENT CONFIGURATIONS ON LOCAL HEAT TRANSFER AND HYDRODYNAMICS IN BUBBLE COLUMN.....		42
3.1	Introduction.....	43
3.2	Experimental	44
3.3	Results and discussion	48
3.3.1	Local Heat Transfer Coefficients.....	48
3.3.2	Gas Holdup and Bubbles Fractions.....	55
3.3.3	Local Liquid Velocity and Related Hydrodynamics	60
3.3.4	Estimation of Centerline Liquid Velocity for Type A Internal.....	66
3.4	Conclusions.....	73
3.5	Notations	73
3.6	References.....	75
CHAPTER 4. INVESTIGATIONS OF HEAT TRANSFER PROFILE AND HYDRODYNAMICS IN A SLURRY BUBBLE COLUMN INSERTED WITH INTERNALS		80
4.1	Introduction.....	81
4.2	Experimental	82
4.3	Results and discussion	86
4.3.1	Local Heat Transfer Coefficients.....	86
4.3.2	Gas Holdup and Bubbles Fractions.....	98
4.3.3	Local Liquid Velocity and Related Hydrodynamics	104
4.4	Conclusions.....	109
4.5	Notations	110

4.6	References.....	111
CHAPTER 5. INFLUENCE OF BUBBLE COLUMN DIAMETER ON LOCAL HEAT TRANSFER AND RELATED HYDRODYNAMICS.....		115
5.1	Introduction.....	116
5.2	Experimental Setup	117
5.3	Results and Discussion.....	120
5.4	Conclusions.....	134
5.5	Notations	134
5.6	References.....	136
CHAPTER 6. ANALYSIS OF BUBBLE DYNAMICS AND COLUMN HYDRODYNAMICS BASED ON INSTANTANEOUS HEAT TRANSFER COEFFICIENTS IN SLURRY BUBBLE COLUMNS – WITH AND WITHOUT INTERNALS		140
6.1	Introduction.....	141
6.2	Experimental	142
6.3	Results and Discussion.....	144
6.3.1	Response of Probe at Column Center	144
6.3.2	Probe Response in Central and Wall Regions	144
6.3.3	Estimation of peak-height distribution.....	147
6.3.4	Peak-height distribution.....	151
6.3.5	Average Peak Area Analysis	156
6.4	Conclusions.....	158
6.5	Notations	159
6.6	References.....	160
CHAPTER 7. CONCLUSIONS AND RECOMMENDATIONS.....		164
7.1	Conclusions.....	165
7.2	Recommendations.....	167
CURRICULUM VITAE.....		196

LIST OF TABLES

Table 3.1. Details of internals used in air-water system	48
Table 4.1. Details of internals used in air-water-glass beads system.....	86
Table G.1. Physicochemical properties of the glass beads	192

LIST OF FIGURES

Figure 2.1. Schematic of slurry bubble column reactor.....	11
Figure 2.2a. Flow regimes in 3-D bubble column and gas-liquid-solid fluidization system (Adapted from Chen et al. (1994)).....	13
Figure 2.2b. Gas holdup obtained with a fine and coarse sparger (from Jhawar and Prakash (2007)).....	14
Figure 2.3. Changes in gas holdup profile due to addition of fine particles in liquid (from Krishna et al. 1997).....	15
Figure 2.4. Variation of heat transfer coefficients with superficial gas velocity for fine and coarse sparger ($z = 0.91$ m) (Adapted from Jhawar and Prakash (2007))	16
Figure 2.5. Radial profile of heat transfer coefficients obtained with fine and coarse sparger ($z = 0.91$ m) (Adapted from Jhawar and Prakash (2007)).....	17
Figure 2.6. Variations of heat transfer coefficients with liquid or slurry velocities in gas- liquid and gas-liquid-solid systems (adapted from Magiliotou et al. (1988); Kumar et al. (1993); Muroyama et al. (2003)).....	20
Figure 2.7. Effect of slurry concentration on Thermophysical properties.....	23
Figure 3.1. Schematic diagram of experimental setup.....	46
Figure 3.2a. Top view of the tube bundle used (Type A).....	47
Figure 3.2b. Top view of bubble diffuser used (Type B).....	47
Figure 3.3. Comparison of heat transfer coefficient measurements in bubble column with and without internals, $r/R=0$ (air-water system).....	49
Figure 3.4a. Instantaneous heat transfer coefficients of air-water system (with and without internals) at $r/R=0$	50
Figure 3.4b. Instantaneous heat transfer coefficients of air-water system (with and without internals) at $r/R=0.624$	51
Figure 3.5. Comparison of heat transfer coefficient measurements in bubble column with and without internals, $r/R=0.624$ (air-water system).....	52
Figure 3.6. Variations of heat transfer coefficient at two radial locations with internal A and B2.....	53

Figure 3.7a. Comparison of the radial profile of heat transfer coefficient obtained with and without internals in air-water system	54
Figure 3.7b. Comparison of the radial profile of heat transfer coefficient obtained with Type A and without internals in air-water system	55
Figure 3.8. Comparison of gas holdup measurements obtained with and without internals (air-water system).....	56
Figure 3.9a. Comparison of small bubbles holdup in bubble columns equipped with and without internals in air-water system.....	57
Figure 3.9b. Comparison of large bubbles holdup in bubble columns equipped with and without internals in air-water system.....	58
Figure 3.10. Comparison of standard deviation of heat transfer coefficient in bubble columns with and without internals in: (a) central ($r/R=0$) (b) wall region ($r/R=0.624$)	59
Figure 3.11. Local heat transfer coefficients for different probe orientations in presence of internals Type A in air-water system ($r/R = 0$).....	61
Figure 3.12. Comparison of liquid velocities estimated at the center in bulk section of the column by equation (3.3) in air water system.....	62
Figure 3.13. Comparison of liquid velocities estimated at the wall ($r/R =0.624$) in bulk section of the column by equation (3) in air water system	63
Figure 3.14. Comparison of differential radial liquid velocities with different internals in bulk section of the column.....	64
Figure 3.15. Comparison of time series heat transfer coefficients obtained with internals A and AB2 in the annular region	65
Figure 3.16. Comparison of estimated liquid circulation velocity in core region in bubble columns equipped with Type A internals	72
Figure 4.1. Schematic diagram of experimental setup	84
Figure 4.2a. Top view of the tube bundle used (Type A).....	85
Figure 4.2b. Top view of bubble diffuser used (Type B)	85
Figure 4.3. Comparison of heat transfer coefficient measurements in bubble column with and without internals, $r/R=0$ (air-water-glass beads system).....	87

Figure 4.4. Effect of slurry concentration on heat transfer coefficients in bubble columns (a) Without Internals (b) Internals A	88
Figure 4.5. Variation of heat transfer coefficient with slurry concentration in bubble columns in central region with and without internals	89
Figure 4.6a. Instantaneous heat transfer coefficients of air-water-glass beads system (with and without internals) at $r/R=0$	90
Figure 4.6b. Instantaneous heat transfer coefficients of air-water-glass beads system (with and without internals) at $r/R=0.624$	91
Figure 4.7. Comparison of instantaneous heat transfer coefficients for air-water and air-water-glass beads system with internal type A (a) $r/R = 0$ (b) $r/R=0.624$...	92
Figure 4.8. Comparison of heat transfer coefficient measurements in slurry bubble column with and without internals, $r/R=0.624$ (air-water-glass beads system)	93
Figure 4.9. Variation of heat transfer coefficient with slurry concentration in bubble columns in central region with and without internals	95
Figure 4.10. Variations of heat transfer coefficient at two radial locations with internal A and B (air-water-glass beads system)	96
Figure 4.11. Comparison of the radial profile of heat transfer coefficient obtained with and without internals in air-water-glass beads system	97
Figure 4.12. Comparison of the radial profile of heat transfer coefficient obtained with type A and without internals (air-water-glass beads system)	98
Figure 4.13. Comparison of gas holdup measurements obtained with and without internals (air-water-glass beads systems) (a) 10 vol. % (b) 20 vol. %	99
Figure 4.14. Comparison of bubble holdup in slurry bubble columns with and without internals in air-water-glass beads system (a) small (b) large	101
Figure 4.15. Effect of slurry concentration on bubble holdup in slurry bubble columns with and without internals in air-water-glass beads system (a) small (b) large	102
Figure 4.16. Comparison of standard deviation of heat transfer coefficient in slurry bubble columns with and without internals in (a) central (b) wall region.	105

Figure 4.17. Local heat transfer coefficients for different probe orientations in presence of internals Type A in air-water-glass beads system (slurry conc. 10 vol. %) ($r/R = 0$)	106
Figure 4.18. Comparison of slurry velocities estimated at the center in bulk section of the column by equation (4.3) in air- water –glass beads system	107
Figure 4.19. Comparison of slurry velocities estimated at the wall ($r/R=0.624$) in bulk section of the column by equation (4.3) in air- water –glass beads system	108
Figure 4.20. Comparison of differential radial liquid velocities with different internals in bulk section of the column.....	109
Figure 5.1. Schematic diagram of experimental setup	119
Figure 5.2. Comparison of measured heat transfer coefficients with literature studies effects of column diameter: (a) air-water system. (b) air-water-glass beads system	121
Figure 5.3. Heat transfer coefficient data obtained in different column diameter from Saxena et al. (1989).....	122
Figure 5.4. Comparison of average gas holdup obtained with literature studies	123
Figure 5.5. Comparison of bubble rise velocity with literature studies: a) air-water system (b) air-water-5 vol.% glass beads systems (c) air-water-10 vol.% glass beads system	125
Figure 5.6. Local heat transfer coefficients for different probe orientations in bulk section ($z = 0.91$ m; $r/R = 0.0$) for air-water system.....	126
Figure 5.7. Comparison of liquid velocities estimated by equation (5.3) with predictions by literature correlations (air-water system).....	127
Figure 5.8. Radial distribution of liquid velocity in heterogeneous flow regime from Krishna et al. (1999)	128
Figure 5.9. Effect of column diameter on centerline liquid velocity	129
Figure 5.10. Comparison of predicted and experimental value of heat transfer coefficient for vertical orientation of heat flux sensor.....	130
Figure 5.11. Prediction of Radial profile of heat transfer coefficient using equation (5.6): (a) this study (b) literature studies in different column diameter.....	132

Figure 6.1.	Instantaneous heat transfer coefficient obtained at center in bulk section in air – water system (a) Without Internals (b) Type A.	145
Figure 6.2.	Instantaneous heat transfer coefficient obtained at center and in wall region in bulk section in air – water system (a) Without Internals (b) Type A. ...	146
Figure 6.3.	Instantaneous heat transfer coefficient obtained in bulk section of the bubble columns with Type A and without internals in air – water system(a) center ($r/R=0$) (b) wall ($r/R=0.624$) region.....	148
Figure 6.4.	Peak-height distribution in bubble columns with Type A and without internals at different gas velocities in air – water system ($r/R=0$).	150
Figure 6.5.	Comparison of average peak height in bubble column with and without internals and with literature studies in air-water and air-water-glass beads system	152
Figure 6.7.	Comparison of average peak height with slurry concentration in bubble columns in central region with Type A and without internals.....	154
Figure 6.8.	Comparison of average peak area in bubble column with and without internals and with literature studies in air-water and air-water-glass beads system	155
Figure 6.9.	Variation of average peak area with slurry concentration in bubble columns in central region (a) Without internals (b) Type A	157
Figure C.1 .	Schematic diagram of experimental setup	173
Figure C.2 .	Schematic diagram of the dual sparger design (Gandhi, 1997).....	174
Figure C.3.	Schematic diagram of the heat transfer probe.....	175
Figure C.4.	Microfoil Heat Flux Sensor Dimensions	176
Figure C.5.	Schematic diagram of tube bundle internal (type A).....	177
Figure C.6.	Schematic diagram of six-blade baffle (type B)	178
Figure D.1.	95% Confidence interval of heat transfer data in hollow bubble columns and with internals (air-water-system) at center	180
Figure D.2.	95% Confidence interval of heat transfer data in hollow bubble columns and with internals (air-water-glass beads system) at center	181
Figure D.3.	95% Confidence interval of heat transfer data in hollow bubble columns and with internals (air-water-system) in wall region.....	182

Figure D.4. 95% Confidence interval of gas holdup data in hollow bubble columns and with tube bundle type internal (air-water-system).....	183
Figure D.5. 95% Confidence interval of gas holdup data in hollow bubble columns and with tube bundle type internal (air-water-glass beads system).....	184
Figure E.1. Calibration curve for distributor section pressure transducer (OMEGA type PX541-15GI).....	186
Figure E.2. Calibration curve for disengagement section pressure transducer (OMEGA type PX541-7.5GI).....	187
Figure F.1. Calibration curve for bulk thermocouple located at the center.....	189
Figure F.2. Calibration curve for bulk thermocouple located close to the wall	190

LIST OF APPENDICES

Appendix A.	Local Liquid velocity	169
Appendix B.	Calculation procedure for gas hold-up from pressure difference in bubble and slurry bubble column.....	172
Appendix C	Experimental setup and internals drawings	173
Appendix D.	Reproducibility of heat transfer and gas holdup data	179
Appendix E.	Pressure transducers calibration.....	185
Appendix F	Calibration of Bulk Thermocouples.....	188
Appendix G.	Solid Characteristics	191

CHAPTER 1. INTRODUCTION

1.1 Introduction

Bubble column reactors are widely used in a number of industrial processes such as oxidation (adiponitrile synthesis), hydrogenation (saturation of fatty acids), fermentation (production of ethanol and mammalian cells), biological waste water treatment, flue gas desulphurization, coal liquefaction, dimethyl ether production, chlorination (production of aliphatic and aromatic chlorinated compounds, polymerization (production of polyolefins), biomedical engineering (blood oxygenator) (Shah et al.,1982; Fan, 1989; Duduković and Devanathan, 1992; Deckwer and Schumpe, 1993; Li, 1998; Prakash et al.,1999; Prakash et al., 2001; Duduković et al.,2002). An important and growing area of application of multiphase reactor systems is production of clean and renewable fuels such as production of sulfur-free diesel by the Fischer-Tropsch process, dimethyl ether (DME) and bioethanol processes. For a large number of these processes, there is a need for proper design of heat removal in these reactor systems to allow optimal temperature control for desired product quality and yield (Duduković et al.,2002).

Bubble columns (BC) belong to a larger class of multiphase reactor of relatively simple construction. In bubble columns gas is usually the discontinuous phase and is sparged at the bottom of the column through a sparger and the resulting buoyancy-driven flow creates strong liquid recirculation. These reactors where fine particles used as catalyst or reactive solids are suspended in liquid phase are called slurry bubble column (SBC) reactors. Compared to other multiphase reactors (i.e. stirred tank reactors, trickle bed reactors, three-phase fluidized bed or ebullated bed reactors), BC and SBC reactors offer several advantages (Deckwer and Schumpe, 1993; Kluytmans et al., 2001; Li and Prakash, 2002; Li et al., 2003; Barghi et al., 2004):

- Simplicity of construction and ease of operation
- Low construction, operating and maintenance costs
- No problems with sealing due to absence of moving parts

- Excellent temperature control
- High heat and good mass transfer rates
- On-line catalyst addition and withdrawal to maintain constant catalyst activity
- Solids can be handled without serious erosion or plugging problems
- High liquid (slurry) phase content for the reaction to take place
- Washing effect of the liquid on catalyst
- Little floor space is required and good mixing of the phases by gas aeration only

Though BCs and SBCs are simple in construction, the design, scale-up and modeling of BCs and SBCs is a difficult task because of lack of information on the effect of different parameters such as operating conditions, reactor geometry, distributor type, physico-chemical properties of the phases, and slurry concentrations on hydrodynamics, heat and mass transfer in these reactors. The crucial design considerations include: phase holdup structure, operating flow regimes, mixing and circulation pattern, axial and radial dispersion of liquid (slurry) and gas phase, heat and mass transfer coefficient, and interfacial area. These parameters are affected by various variables such as:

- Superficial gas and liquid (slurry) velocity.
- Operating conditions (temperature and pressure).
- Physical characteristics of gas phase (density) and liquid (slurry) phase properties (surface tension, viscosity, density and thermal conductivity, particles concentration and size distribution)
- Column diameter
- Internals and their design (e.g. heat transfer surface).

Effects of some parameters such as superficial gas velocity, distributor type, liquid viscosity, operating pressure etc. have been investigated in some detail (Wilkinson et al., 1992; Zahradník et al., 1997; Su et al., 2006). However, the effects of other variables such as column diameter, internals design have received less attention in

literature. A common type of internal used in these reactors for heat removal is a tube bundle. A few literature studies have investigated potential design configurations of this internal type with some interesting results on column hydrodynamics (Youssef and Al-Dahhan, 2009; Larachi et al., 2006; Chen et al., 1999). There are indications that column hydrodynamics and hence performance can be affected by the internals design. In some applications, there may be a need to use a combination of internals to achieve desired hydrodynamic effects or to mitigate less desirable effects of the main internal.

1.2 Scope and Objectives

Based on above, there is a need to systematically investigate effects of internals design and configurations on flow patterns and mixing and heat transfer profile in bubble and slurry bubble columns. Two main type internals selected are a tube bundle and a six-blade baffle based on initial investigations. The study also combines tube bundle type internals with the baffle type to study improvements. The influence of column diameter is investigated for scale up effects and comparisons are made with internals. The study investigates the effects of two important variables namely superficial gas velocity and slurry concentration on heat transfer and hydrodynamic parameters including radial heat transfer profiles, gas holdup structure, bubble population fractions and potential back mixing effects.

This thesis has seven chapters including the first introductory chapter. Chapter 2 presents a critical overview of heat transfer in slurry bubble columns and observed differences have been analyzed based on available data and appropriate recommendations are made. In Chapters 3 and 4 the heat transfer coefficients obtained in bubble columns with and without solids in presence of different configuration of internals are compared with those without internals to elucidate the effects of different internals design. Comparisons are based on average values and temporal variation of local near instantaneous heat transfer coefficient obtained with the fast response probe. The average gas holdup, center line liquid velocity, and

bubble holdup obtained with and without internals are also compared. The observed differences are discussed based on the insights provided by these comparisons. With some internals, the heat transfer coefficient and gas holdup may increase or decrease. The reasons for these increase or decrease are pointed out in this study. Relationships between local heat transfer measurements and hydrodynamic conditions in presence of internals are shown and discussed. In Chapter 5 the heat transfer coefficient data obtained in this study has been compared with the literature data to determine scale-up effects. The hydrodynamic parameters such as gas holdup profile, liquid circulation velocity profile, and bubble rise velocity are compared with the available literature data to get the insights of effect of these parameters on the heat transfer coefficient with the increase in column size. A simplified scale-up procedure is presented based on available data and suitably modified literature correlations for heat transfer coefficient. In chapter 6, the temporal variations of heat transfer measurements obtained with and without are compared. The temporal variations of heat transfer coefficients are also analyzed to study the bubble-wake properties and local column hydrodynamics Finally Chapter 7 presents the important conclusions of this study. The scope of future work and recommendations are also included in Chapter 7.

1.3 Research Contributions

The main contributions of this research are: 1) The internals developed can be used alone or in combination to reduce average bubble size, thereby increasing the interfacial area and improving the mass transfer. 2) The backmixing in bubble and slurry bubble column is reduced by using combination of internals developed, thereby improving the product selectivity and reaction rate.

1.4 Thesis Format

This thesis is written in the format of ‘Integrated Article thesis’ as specified by the Faculty of Graduate Studies of the University of Western Ontario. Individual chapters are presented as technical papers with an abstract. Each chapter has its own

conclusions and references with symbols and abbreviations listed at the end of each chapter. Appendix is presented together at the end all chapters.

1.5 References

Barghi, S., Prakash, A., Margaritis, A. and Bergounou, M.A., 2004. Flow regime identification in a slurry bubble column from gas holdup and pressure fluctuation analysis. *The Canadian Journal of Chemical Engineering*. 82, 865-870.

Bhattacharya, S., 1999. Internal filtration system for three-phase slurry bubble column. Thesis, MEng. University of Western Ontario, London, Ontario, Canada.

Chen, J., Li, F., Degaleesan, S., Gupta, P., Al-Dahhan, M.H., Dudukovic, M.P., Toseland, B.A., 1999. Fluid dynamic parameters in bubble columns with internals. *Chem. Eng. Sci.* 54, 2187-2197.

Deckwer, W.D., Schumpe, A., 1993. Improved tools for bubble column reactor design and scale-up. *Chemical Engineering Science*. 48, 889-911.

Duduković, M.P., Devanathan, N., 1992. Bubble column reactors: some recent developments. *Nato ASI Series E Applied Sciences*. 225, 353-377.

Duduković, M.P., Larachi, F., Mills, P.L., 2002. Multiphase catalytic reactors: a perspective on current knowledge and future trends. *Catalysis Reviews*. 44, 123-246.

Fan, L. S., 1989. *Gas-liquid-solid fluidization engineering*. Butterworths, Stoneham, MA.

Kluytmans, J.H.J., van Wachem B.G.M., Kuster, B.F.M. and Schouten J.C., 2001. Gas holdup in a slurry bubble column: influence of electrolyte and carbon particles. *Industrial Engineering Chemical Research*. 40, 5326-5333.

Kurten, H., Zehner, P., 1979. Slurry reactors. *German Chemical Engineering*. 2, 220-227

Larachi, F., Desvigne D., Donnat, L., Schweich, D., 2006. Simulating the effects of liquid circulation in bubble columns with internals. *Chemical Engineering Science*. 61, 4195-4206.

Li, H., 1998. Heat transfer and hydrodynamics in a three-phase slurry bubble column. Thesis, PhD University of Western Ontario, London, Ontario.

Li, H., Prakash A., 2002. Analysis of flow patterns in bubble and slurry bubble columns based on local heat transfer measurements. *Chemical Engineering Journal*. 86, 269-276.

Li, H., Prakash A., Margaritis, A., Bergougnou, M.A., 2003. Effects of micron-sized particles on hydrodynamics and local heat transfer in a slurry bubble column. *Powder Technology*. 133, 171-184

Li, H., Prakash, A., 1997. Heat transfer and hydrodynamics in a three-phase slurry bubble column. *Industrial Engineering Chemical Research*. 36, 4688-4694.

Prakash, A., Margaritis, A., Li, H., Bergougnou, M.A., 2001. Hydrodynamics and local heat transfer measurements in a bubble column with suspension of yeast. *Biochemical Engineering Journal*. 9, 155-163.

Prakash, A., Margaritis, A., Saunders, R.C., Vijayan, S., 1999. Ammonia removal at high concentrations by the cyanobacterium *plectonema boryanum* in a photobioreactor system. *Canadian Journal of Chemical Engineering*. 77, 99-106

Shah, Y.T., Godbole, S.P., Deckwer, W.D., 1982. Design parameters estimation for bubble column reactors. *AIChE Journal*. 28, 353-379.

Su, X., Hol, P.D., Talcott, S.M., Staudt, A.K., Heindel, T.J., 2006. The effect of bubble column diameter on gas holdup in fiber suspensions. *Chemical Engineering Science*. 61, 3098-3104.

Wilkinson, P.M., Spek, A.P., van Dierendonck, L.L., 1992. Design parameters estimation for scale-up of high-pressure bubble columns. *AIChE Journal*. 38, 544-554.

Youssef. A.A., Al-Dahhan, M.H., 2009. Impact of Internals on the Gas Holdup and Bubble Properties of a Bubble Column. *Industrial and Engineering Chemistry Research*. 48, 8007-8013.

Zahradník, J., Fislová, M., Růžička, M., Drahoš, J., Kaštánek, F., 1997. Duality of the gas-liquid flow regimes in bubble column reactors. *Chemical Engineering Science*. 52, 3811-3826.

CHAPTER 2. HEAT TRANSFER IN SLURRY BUBBLE COLUMN REACTOR – A CRITICAL OVERVIEW¹

Abstract

Studies of heat transfer in slurry bubble column reactors (SBCR) have been reviewed and observed differences analyzed based on available data. Heat transfer in these reactors is a strong function of some parameters and weak function of others. The parameters significantly influencing heat transfer in these reactors are the superficial gas velocity, thermophysical properties of liquid and solid particles, and size and concentration of particles. Moreover the rate of change with a parameter is dependent on operating flow regime, particles properties, and presence of internals. Of all the parameters, the effect of particles is more complex and inadequately understood because particles influence flow regime transition, thermophysical and rheological properties of the suspension which in turn affect hydrodynamic behavior and associated heat transfer characteristics. Effects of column diameter and internals have been investigated by a limited number of studies. A comparison of available data shows that the effect of column diameter on heat transfer diminishes above 0.3 m. This however, requires confirmation from larger diameter studies together with associated hydrodynamic studies and appropriate modeling. Literature correlations for heat transfer coefficient have been reviewed and their limitations and applicability discussed. Axial and radial variations of heat transfer coefficients reported in literature studies require appropriate design considerations.

Key Words: Slurry bubble column reactor, Multiphase reactors, Heat transfer, Hydrodynamics, Flow regime, Operating variables; Column diameter

¹ A Version of this chapter is accepted for publication in Industrial and Engineering Chemistry Research (2012).

2.1. Introduction

Applications of multiphase reactors are quite diverse spanning a broad range from large scale operations such as heavy oil upgrading to manufacture of fine chemicals and pharmaceuticals. Literature studies have reviewed different types of multiphase reactors and their application areas (Hulet et al., 2009; Wang et al., 2007, Kantarci et al., 2005a; Dudukovic et al., 2002; Dudukovic et al., 1999; Nigam and Schumpe., 1999; Shah et al., 1982). An important and growing area of application of multiphase reactor systems is production of clean and renewable fuels such as production of sulfur free diesel by Fischer-Tropsch process, dimethyl ether (DME) and bioethanol processes. For a large number of these processes, there is need for proper design of heat removal arrangement in these reactor systems to allow optimal temperature control for desired product quality and yield. The reactor type commonly used for these applications is three-phase gas-liquid-solid reactor wherein fine catalyst particles ($<100\mu\text{m}$) are suspended by flow of gas or gas and liquid. These reactors, commonly known as slurry bubble column reactor (SBCR) are the main focus of this review while references are made to other reactor systems as appropriate. The main distinguishing feature of SBCR is more homogeneous distribution of fine solid particles in the reactor. For low concentration of solid particles, the behavior of these reactors approaches that of solids-free bubble columns (Dudukovic et al., 2002). Detailed review on flow modeling and design of bubble column reactors is presented in literature studies (Joshi., 2001; Degaleesan et al., 1996; Chen et al., 1994; Jakobsen et al., 1997; Jakobsen et al., 2005). The heat transfer process in these reactor systems is dictated by the highly mixed hydrodynamic structure induced by the rising gas bubbles through suspension. This link has been established by several literature studies (Jhavar and Prakash., 2007; Jhavar and Prakash., 2011; Lin and Hung-Tzu., 2003; Lin and Hung-Tzu., 2001) and it is further expanded and highlighted in this review.

2.2.1 Cataloging of Slurry Bubble Column Reactors

Slurry bubble column reactors are a subset of a larger group of three-phase sparged reactors. Classification of three-phase sparged reactors (TPSR) has been attempted by several researchers over the years (Fan., 1989; Fan et al., 1987; Tsutsumi et al., 1987; Deckwer et al., 1984). Two main types of three-phase sparged reactors based on hydrodynamic considerations are referred to as SBCR and three-phase fluidized bed (TPFB). For a given gas-liquid-solid system, particle size and resulting axial solids profile distinguish the reactor type. The particle size is usually less than 100 μm in SBCR and larger than 500 μm in TPFB, however, these values can change with particle type and liquid phase properties. When the particle size is between these two limits, a significant axial profile of solids concentration can develop and the operation can be classified as three-phase bubble column (Tsutsumi et al., 1987) Apart from particle size, their density and loading and liquid physical properties can also influence hydrodynamic behavior of these reactors and affect classification (Pandit and Joshi., 1984; Khare and Joshi., 1990). A more general classification of these reactors based on particles settling velocity (U_t) has been presented by Fan and co-workers (Fan., 1989; Fan et al., 1987). The three phase fluidized bed operate in expanded bed regime covering particle terminal settling velocity in a liquid medium from 3 to 50 cm/s. Detailed review on hydrodynamics and heat transfer in three phase fluidized bed are available in literature studies (Fan., 1989; Kim and Kang., 1997; Kumar et al., 1993; Wild et al., 1984). Slurry bubble column can operate in both expanded and transport regime covering U_t from 0.03 to 7 cm/s. There is overlap in operating range for both fluidized bed and slurry bubble column operations in the expanded bed regime for U_t from 3 to 7 cm/s (Fan., 1989; Fan et al., 1987). This classification based on particles settling velocity is less restrictive since momentum and energy balance equations governing the performance of these reactors depend on this velocity.

For SBCR, usually a key consideration would be ease of particles suspension in the liquid by gas alone. The gas sparged at the bottom of the column creates buoyancy-driven flow resulting in strong liquid recirculation. The solids follow the liquid

motion, and the relative velocity between liquid and solid particles is nearly zero as the particles get smaller (Dudukovic et al., 2002). Figure 2.1 shows schematic diagram of a slurry bubble column. In these reactors, pseudo-homogeneous phase can operate in either batch or continuous mode since superficial gas velocity is the dominant variable driving the dynamics of the entire system. The fine particles can be uniformly distributed throughout the reactor even at low superficial gas velocities. The hydrodynamic characteristics of the slurry bubble column reactor are closer to solid free bubble column reactor due to fine particles used. Therefore some predictive correlations developed for bubble column reactors can be applied to three-phase slurry reactor especially at low solids loadings. A common application of these reactors is exothermic catalytic reactions where catalysts particles in the range of 35 to 60 μm are used to minimize internal diffusion resistance as well allow easy separation from liquid product (Gamwo et al., 2005; Krishna and Sie., 2000).

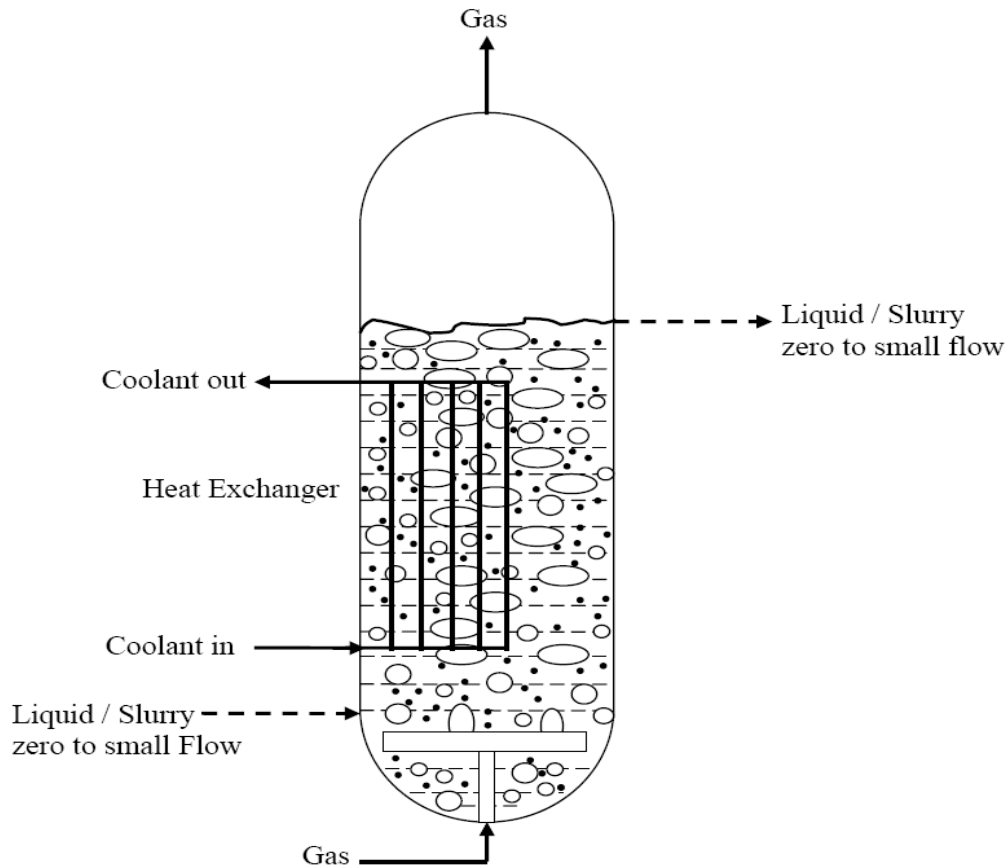


Figure 2.1. Schematic of slurry bubble column reactor

In three-phase fluidized beds, the bed is divided into two regions - the lower one is a dense region concentrated with solid particles and the upper one is solid-free region. Solids are uniformly distributed in the lower dense region. Solid particles are mainly suspended by the upward flow of liquid phase in the lower dense region. The gas phase in these reactor types can either help suspension or settle the suspension of particles causing the bed to expand or contract (El-Temtamy et al., 1979; Epstein., 1976; Epstein and Nicks., 1976; Darton and Harrison., 1975; Kim et al., 1975; Darshinamurty et al., 1971; Ostergaard and Thiesen., 1966). Epstein and coworkers (El-Temtamy et al., 1979; Epstein., 1976; Epstein and Nicks., 1976) explained this phenomenon based on bubble wake model, while Joshi and co-workers (Joshi et al., 2001; Joshi, 1983) explained this behavior depending upon whether the gas phase supplies energy to the bed or extracts energy from the bed.

2.2. Flow Regimes and Effects on Heat Transfer

Demarcation of flow regimes in multiphase reactors and the applicable criteria have been the subject of a number of investigations (Wallis, 1969; Michelsen and Ostergaard, 1970; Kawagoe et al., 1976; Matsuura and Fan, 1984; Drahos and Cermak, 1989; Vial et al., 2000; Olmos et al., 2003a; Olmos et al., 2003b; Memon, 2004; Barghi et al., 2004; Thorat and Joshi, 2004). Three primary flow regimes commonly reported are: dispersed bubble regime (homogeneous or bubble flow regime), heterogeneous regime (coalesced bubble or churn turbulent regime), and slugging. In addition a transition regime is observed to occur in between dispersed bubble regime and coalesced bubble regime (Chen et al., 1994). The slugging regime mainly occurs in small diameter experimental columns (< 0.05 m), usually with high flow rates. In this regime the gas bubble expands easily up to the column diameter creating 'slugs' which nearly occupy the entire cross-section of the column. This flow regime is seldom encountered in industrial scale reactors. Figure 2.2a from Chen et al. (1994) depicts approximate flow structure observed with increasing gas flow. The dispersed bubble flow regime (I) is characterized by nearly uniform bubble size and radially uniform gas holdup. This is followed by transition regime (II) when

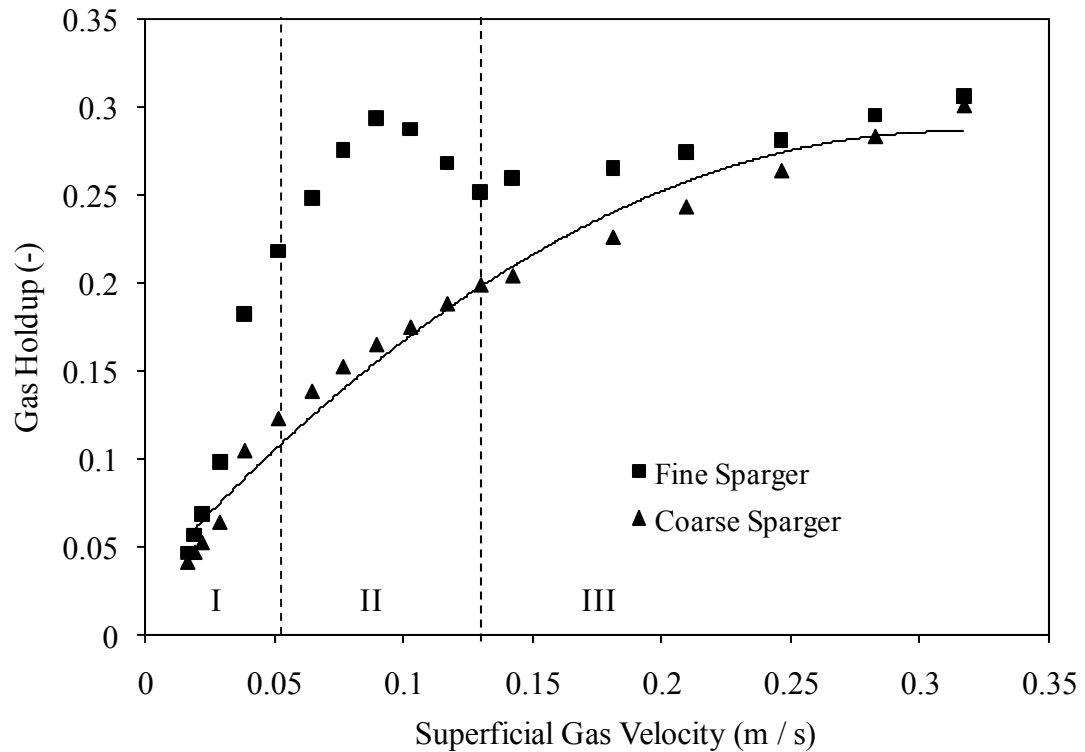


Figure 2.2b. Gas holdup obtained with a fine and coarse sparger (from Jhawar and Prakash (2007))

Krishna et al. (1997) reported gas holdup measurements obtained with a fine sparger with increasing solids concentration in the liquid phase. As shown in Figure 2.3, the addition of fine particles into liquid lowered the gas holdup and the transition velocity. For high solids concentrations, the bubbly flow regime essentially disappeared and the gas holdup profile became similar to that of a coarse sparger (Figure 2.3). This indicates increased bubble coalescence in presence of fine particles in the suspension.

Variation of heat transfer with flow regime in bubble column has been reported by Jhawar and Prakash (2007) while Pandit and Joshi (1986) presented a review from studies in fluidized beds. Jhawar and Prakash (2007) compared average heat transfer coefficients obtained with a fine and coarse sparger at column center (Figure 2.4). It can be seen that in the bubble flow regime, difference between the two spargers is large and stays nearly constant. In the transition regime, heat transfer with the fine

sparger increases quickly due to emergence of larger bubbles and approaches that with coarse sparger. In the fully developed heterogeneous regime, heat transfer coefficients obtained with the two spargers are similar. A comparison of Figures 2.2b and 2.4 shows that with the fine sparger in the transition flow regime, the gas holdup increases rapidly until it reaches a maximum and then decreases, but heat transfer continues to increase. This indicates that there is no direct relationship between gas holdup structure and heat transfer coefficient in the bubble flow and transition regime. Heat transfer process is mainly governed by strength of liquid circulation patterns created by rising gas bubbles and their wake region. A decrease in gas holdup with increase in velocity indicates increase in average bubble size and corresponding bubble rise velocity.

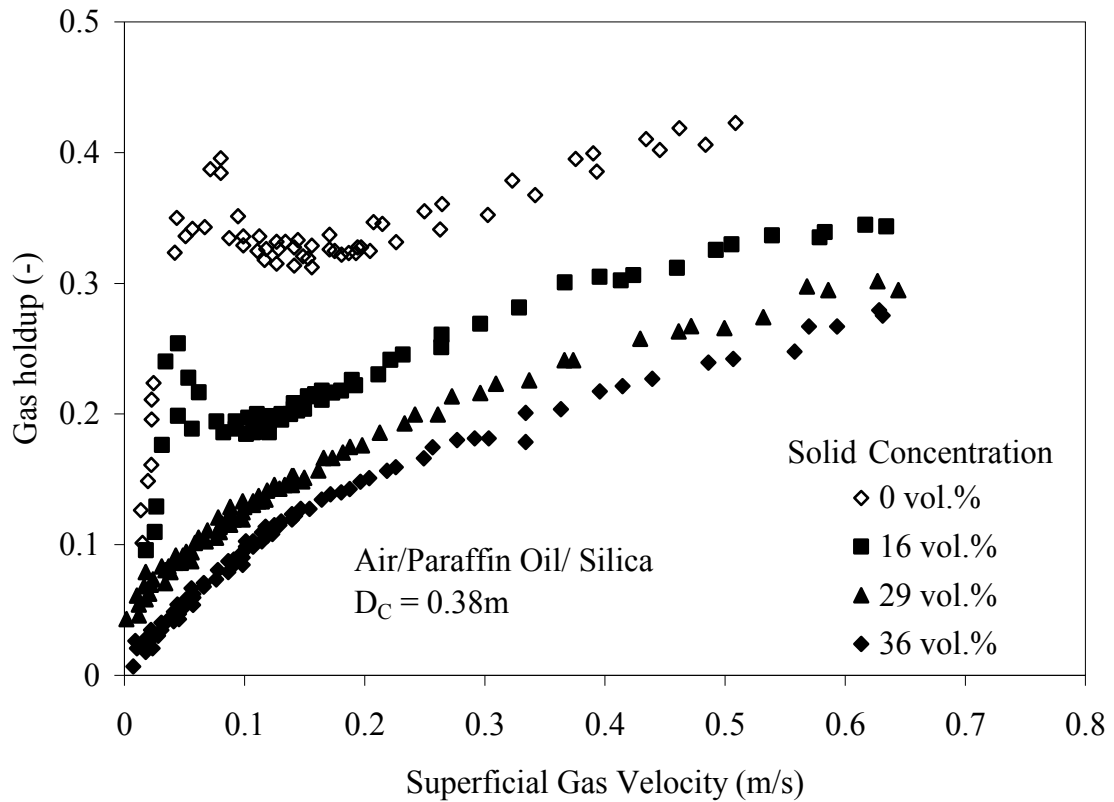


Figure 2.3. Changes in gas holdup profile due to addition of fine particles in liquid (from Krishna et al. 1997)

In the heterogeneous flow regime, the average gas holdup and heat transfer is not affected by primary bubble size, but is related to gross circulation pattern created by

fast rising large bubbles (Jhawar and Prakash, 2007; Vial et al., 2000; Lin et al., 2001). In this regime, the column hydrodynamics and heat transfer tend to become essentially independent of the effects of primary gas dispersion orifice diameter and the bubble bed is primarily determined by bulk liquid circulation (Jhawar and Prakash, 2007; Joshi et al., 1984). There is currently no data available to show the effects of particles addition on the heat transfer coefficient, with the two types of spargers. However based on the above, it is expected that difference between the coarse and fine spargers would decrease with increasing solids concentration in the suspension.

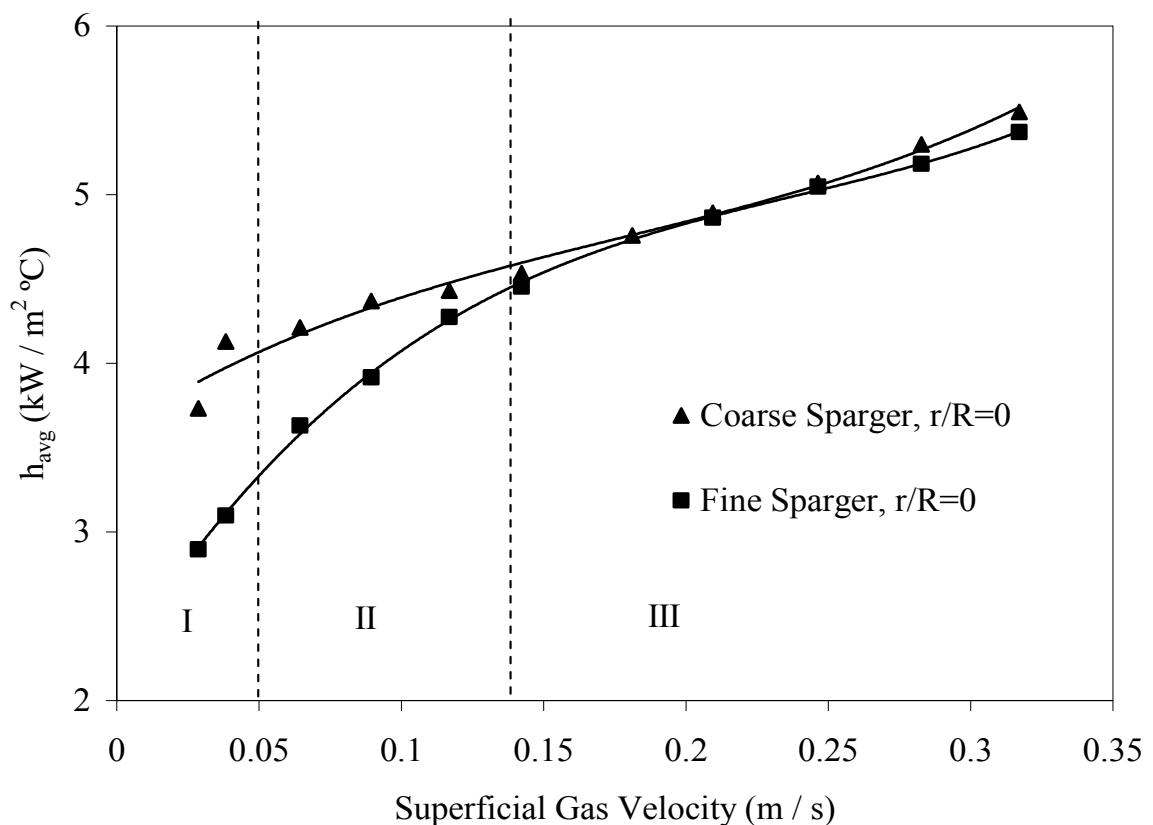


Figure 2.4. Variation of heat transfer coefficients with superficial gas velocity for fine and coarse sparger ($z = 0.91$ m) (Adapted from Jhawar and Prakash (2007))

Jhawar and Prakash (2007) also presented radial profile of the heat transfer coefficient for different gas velocities in bulk zone (Figure 2.5) which further illustrated the link between flow regime and heat transfer. The radial profile is nearly flat at a gas velocity ($= 0.038$ m/s) in the bubble flow regime obtained with fine

sparger. However, with increasing gas velocity, the profile was no more flat - indicating absence of bubble flow regime. Figure 2.5 shows that the radial profile became steeper as the flow moved to transition and heterogeneous flow at higher gas velocities. It can also be seen that with increasing gas velocity, heat transfer coefficients increased much faster in the central region compared to the wall region. This is related to faster moving large bubbles moving through the central region compared to the wall region. The radial profile is also dependent on the axial distance from the sparger. In the literature, it has been reported that the radial profile of the heat transfer coefficients is relatively flat in zones other than bulk zone (Li and Prakash, 2002) Radial profile may also be influenced by presence of internals and their configurations. Additional work which includes hydrodynamic and local turbulence measurements would provide further insights and confirm the observations on the radial variation of heat transfer coefficient.

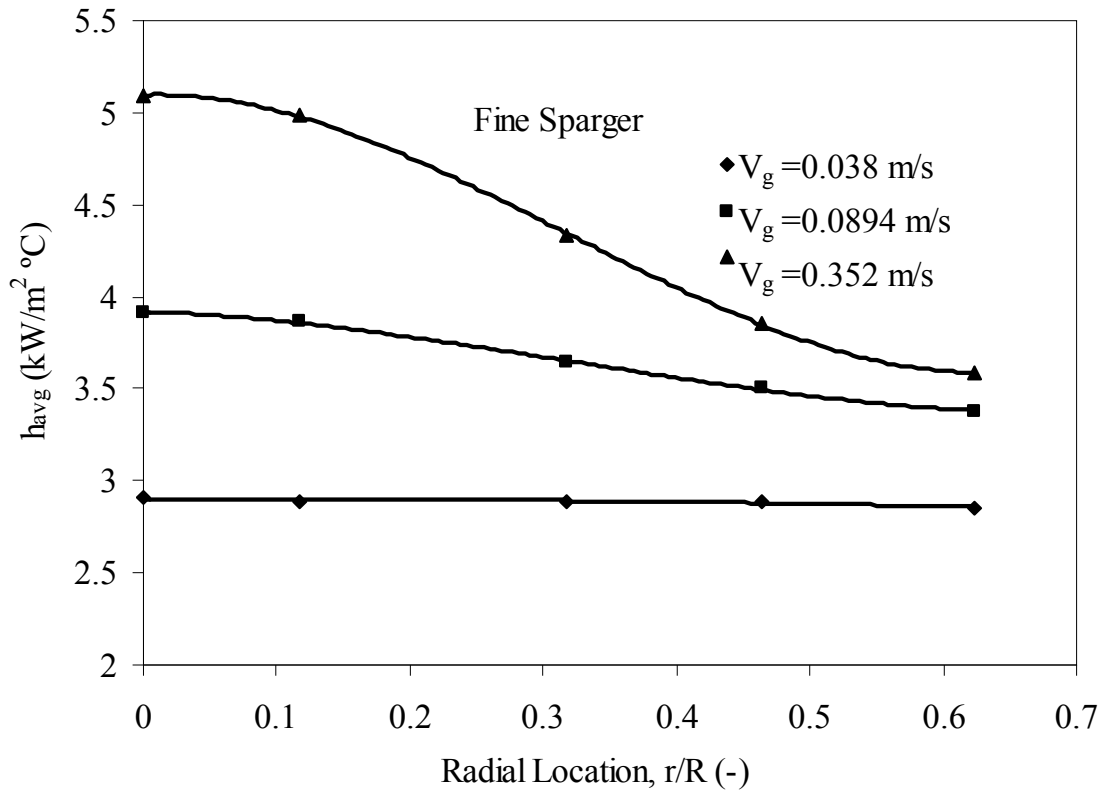


Figure 2.5. Radial profile of heat transfer coefficients obtained with fine and coarse sparger ($z = 0.91$ m) (Adapted from Jhavar and Prakash (2007))

2.3. Effect of Operating Variables on Heat Transfer

The high heat transfer rate in three phase sparged reactors helps to maintain required temperature to maximize the yield of the desired product. The heat transfer can take place between the bed and the wall or between the bed and the immersed surface. Bed-to-wall heat transfer has been studied by few researchers (Viswanathan et al., 1985; Kato et al., 1980; Kato et al., 1981; Chiu and Ziegler, 1983; Chiu and Ziegler, 1985). Heat transfer between the bed and the immersed surfaces is more widely used in industry and has been subject of several studies in literature (Jhawar and Prakash, 2007; Li and Prakash, 2002; Saxena et al., 1989; Saxena et al., 1990a; Saxena et al., 1990b; Saxena et al., 1991a; Saxena et al., 1991b; Saxena et al., 1992b; Saxena and Patel, 1990; Li and Prakash, 1997; Li and Prakash, 1999; Li and Prakash, 2001; Prakash et al., 2001; Quiroz et al., 2003; Li and Prakash) to name a few. An important link between column hydrodynamics and the heat transfer process has also been well established by literature studies (Jhawar and Prakash, 2007; Jhawar and Prakash, 2011; Lin and Hung-Tzu., 2003; Lin and Hung-Tzu, 2001).

Therefore the design and operating variables which affect hydrodynamics will also influence the heat transfer rate. These parameters can be divided into two main categories: 1) operational parameters; 2) geometric parameters. The first category includes variables such as superficial gas and liquid velocity, operating pressure and temperature, liquid thermophysical properties, particles properties and concentration. The second category includes column dimensions, internals design and location, axial and radial position of heat transfer surface. Important effects of these variables on heat transfer are discussed in the following sections.

2.3.1. Effects of Superficial Gas Velocity

The heat transfer coefficient increases with superficial gas velocity irrespective of the liquid velocity, gas density and pressure, liquid physical properties, column diameter, distributor type, internals, temperature, particle size, concentration and its physical properties and the axial and radial location of heat transfer probe/internals. This

increase in heat transfer coefficient with superficial gas velocity can be attributed to the buoyancy driven turbulence generated by the bubble due to the introduction of the gas in the column. The rate of increase in heat transfer coefficient with gas velocity is high till fully developed churn turbulent flow is reached ($V_g \approx 0.15$ m/s) beyond which there is slow increase with gas velocity (Jhavar and Prakash, 2007; Saxena et al., 1989; Saxena et al., 1990a; Saxena et al., 1990b; Saxena et al., 1992b; Li and Prakash, 1997; Wu et al., 2007; Li, 1998). This behavior can be attributed to evolving hydrodynamics and turbulence characteristics. The degree of turbulence distribution becomes poorer owing to non-uniform distribution of bubbles in the column at high gas velocities. This leads to less isotropic turbulence which dampens the effect of turbulence intensity on the heat transfer (Kim and Kang, 1997).

2.3.2. Effects of Superficial Liquid Velocity

The liquid and slurry velocities have only small effects on heat transfer coefficient in bubble and slurry bubble columns compared to three-phase fluidized bed. This is because bubble-wake-induced circulation velocity in bubble and slurry bubble columns reactors has a dominant effect (Yu and Kim, 1991; Michele and Hempel, 2002) while the liquid flow has little influence on the overall energy balance (Pandit and Joshi, 1986). However, as particle size increases and the bed operation moves towards three-phase sparged reactor or fluidized bed, liquid velocity effects become more significant. In three-phase fluidized beds, particles movements and collision effects with heat transfer surface are also important (Muroyama et al., 1984). This effect increases with liquid velocity up to a critical value and then decreases as the particles agitation effect becomes smaller with increasing voidage. These observations from different literature studies are presented in Figure 2.6.

2.3.3. Effects of Liquid Properties

From well documented single phase studies, liquid phase thermal conductivity and heat capacity are expected to affect the heat transfer rate. Addition of solid particles would increase or decrease the average properties of suspension depending on solids

properties (Deckwer et al., 1980). The important role of liquid viscosity affecting heat transfer rate in multiphase systems is also well documented in literature (Kim and Kang, 1997). Heat transfer coefficient decreases with increasing liquid viscosity in multiphase reactors (Kang et al., 1985; Kim et al., 1986; Kumar and Fan, 1994; Cho et al., 2002) regardless of the particle size and fluid velocities. The decrease in heat transfer rate has been attributed

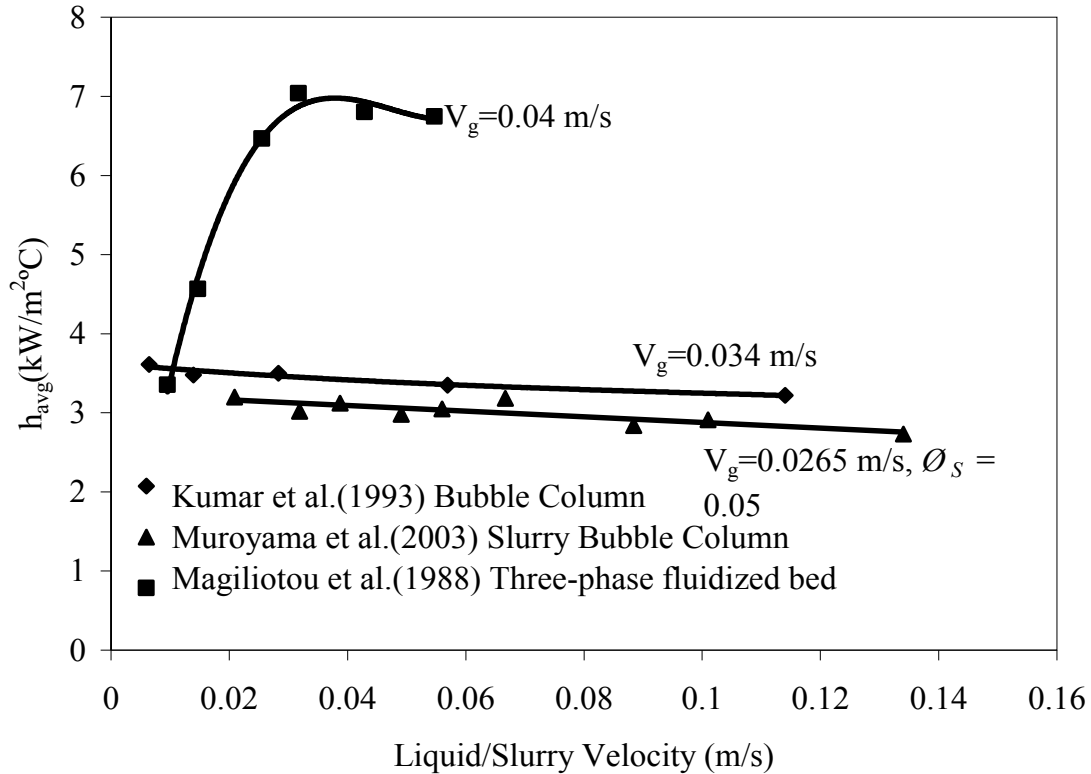


Figure 2.6. Variations of heat transfer coefficients with liquid or slurry velocities in gas-liquid and gas-liquid-solid systems (adapted from Magiliotou et al. (1988); Kumar et al. (1993); Muroyama et al. (2003))

to increase in thermal boundary sub-layer thickness of laminar flow around the heating surface with increasing viscosity due to decrease in turbulence and increase in viscous friction loss between the phases - thus increasing resistance for conduction heat transfer (Kang et al., 1985) Moreover, the particle movement is retarded with increasing viscosity, thereby reducing their attack on the thermal boundary layer around the heating source (Kim and Kang, 1997). Yang et al.(2000) reported increase in heat transfer coefficient in a slurry bubble column with increase in temperature.

This was mainly attributed to decrease in liquid viscosity of liquid with increase in temperature compared to other effects. Availability of data to consider the effect of other physico-chemical properties of the liquid such as: surface tension, thermal conductivity, heat capacity, ionic strength and density on heat transfer coefficient are either limited or unavailable (Kim and Kang, 1997)

2.3.4. Effects of Particles Properties and Concentration

While a number of literature studies have reported improved heat transfer with addition of fine particles in liquid (Saxena et al., 1990a; Deckwer et al., 1980; Yang et al., 2000) a few others have reported a decrease (Li and Prakash., 1997; Li, 1998). Addition of fine solid particles into a liquid changes average thermophysical properties of the suspension and increases its apparent viscosity (Deckwer et al., 1980). An increase in thermal conductivity and heat capacity of suspension would have a positive effect on heat transfer rate while increase in suspension viscosity would have a negative effect due to increase in hydrodynamic boundary layer thickness. The heat transfer mechanism in bubble columns has been elucidated based on Higbie’s surface renewal (Higbie, 1935) concept by Deckwer (Deckwer, 1980). Unsteady heat transfer occurs with fluid elements visiting the surface transitorily. The average heat flux during the contact time (θ_c) of fluid eddy at the heat exchanger area can be calculated.

$$q = 2 \sqrt{\frac{\alpha}{\pi \theta_c}} \rho C_p (T_w - T_B) \dots\dots\dots (2.1)$$

Comparing the above equation with heat transfer coefficient definition yields

$$h \sim \left(\frac{k \rho C_p}{\theta_c} \right)^{0.5} \dots\dots\dots (2.2)$$

An estimation of the contact time (θ_c) was obtained by applying Kolmogoroff’s theory of isotropic turbulence (Deckwer, 1980). If the Reynolds number of the turbulent fluid motion is high then Kolmogoroff’s theory (Hinze, 1958) postulates that the “the energy dissipation by the micro scale eddies is locally isotropic, no

matter whether the large scale eddies move isotropic or not". Subsequently Deckwer et al. (1980) proposed the following equation for heat transfer coefficient in slurry bubble column.

$$h_w = 0.1(k_{sl}^{0.5} \rho_{sl}^{0.75} C_{p,sl}^{0.5} \mu_{sl}^{-0.25} g^{0.25} V_g^{0.25}) \dots\dots\dots (2.3)$$

where

$$\rho_{sl} = \phi_s \rho_s + (1 - \phi_s) \rho_l \dots\dots\dots (2.4)$$

$$C_{p,sl} = w_s C_{p,s} + (1 - w_s) C_{p,l} \dots\dots\dots (2.5)$$

Thermal conductivities of suspensions were estimated by equation proposed by Tareef (Tareef, 1940):

$$k_{sl} = k_l \frac{2k_l + k_s - 2\phi_s(k_l - k_s)}{2k_l + k_s - \phi_s(k_l - k_s)} \dots\dots\dots (2.6)$$

For estimation of apparent slurry viscosity equation proposed by Vand (1948) is used:

$$\mu_{sl} = \mu_l \exp \left[\frac{2.5\phi_s}{1 - 0.609\phi_s} \right] \dots\dots\dots (2.7)$$

Equation 2.3 could be rearranged into three groups: 1) thermophysical properties (TP) to include thermal conductivity, heat capacity and density; 2) apparent slurry viscosity; and 3) gas velocity. Since suspension viscosity will increase with particles concentration, any increase in heat transfer coefficient for a given gas velocity, can be attributed to dominant effect of thermophysical properties. Ratios of thermophysical properties of slurry to the liquid phase are plotted in Figure 2.7 as a function of slurry concentration for different literature studies. It is observed that the ratio is above one for studies reporting higher heat transfer coefficients with slurries. The effects of apparent slurry viscosity may begin to dominate over thermophysical properties with increasing slurry concentration. However, this is not clear from available literature studies. There is need to systematically study effects of slurry rheology on heat transfer coefficient in SBCR.

The effects of particle size on heat transfer coefficient in SBCR have been investigated by a limited number of studies. (Saxena et al., 1990a; Saxena and Patel, 1990; Li et al., 2003). Saxena and coworkers (Saxena et al., 1990a; Saxena and Patel, 1990) have generally reported a weak dependence on particle size. Their data also shows influence of column diameter and presence of internals. Li et al. (2003) observed that the effect of particle size is not significant in the wall region but heat transfer coefficient decreases with increase in particle size in center of the column. The larger effect of particle size at column center could be attributed to its effects on wake formation process which is dominant in the central region of the column.

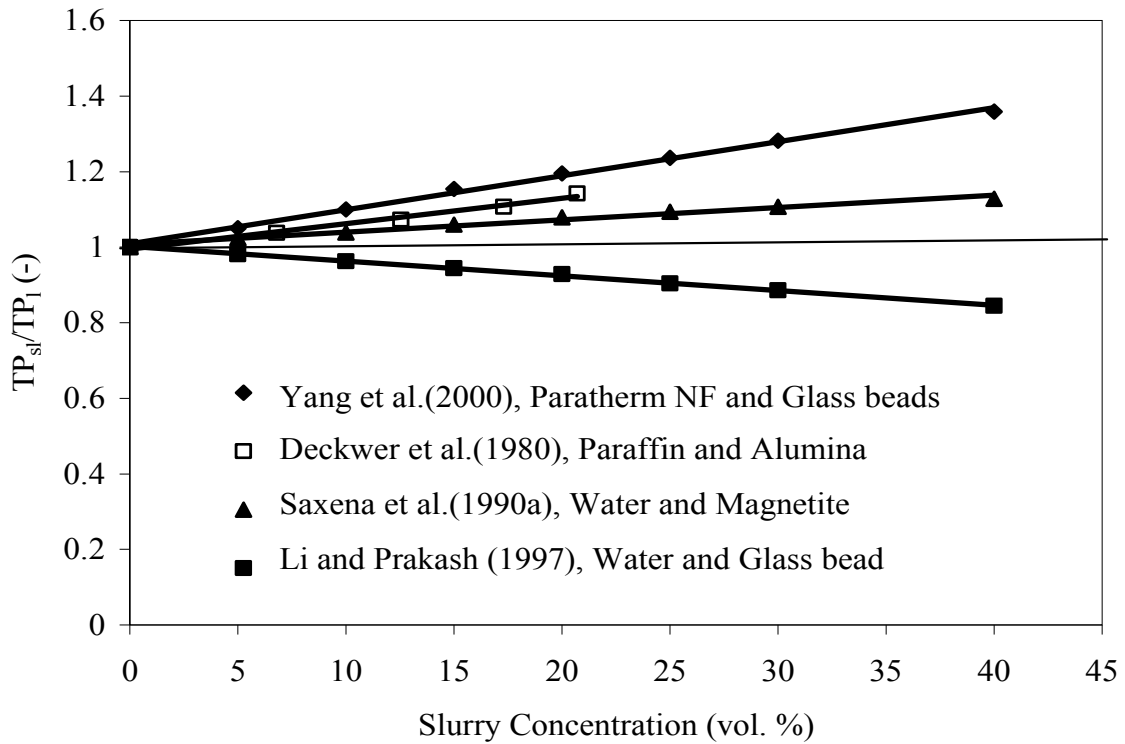


Figure 2.7. Effect of slurry concentration on Thermophysical properties

2.3.5. Effects of Operating Pressure

Heat transfer coefficients in BC and SBC have been observed to decrease with increase in operating pressure (Wu et al., 2007; Yang et al., 2000). This behavior can be attributed largely to reduced bubble size and to a smaller extent to increase in

liquid viscosity. Literature studies have shown that higher operating pressure in bubble columns result in smaller average bubble size and higher gas holdup (Lin et al., 1998; Wilkinson et al., 1992). The effect of pressure on physico-chemical properties of liquid except viscosity is small (Reid et al., 1977). Luo et al. (1999) pointed out that increase in gas density due to increase in pressure results in decrease of the initial bubble size from the sparger as well increases the bubble breakup rate. The reduced wake size of the resulting smaller bubbles would reduce bubble wake enhanced heat transfer rate in the dispersion. In three-phase fluidized beds of 2.1 and 3 mm glass beads however, heat transfer coefficients were observed to increase with pressure up to a critical pressure and decreased thereafter (Luo et al., 1997) This points to different hydrodynamic conditions in the two reactor systems. In three-phase fluidized bed, increase in gas holdup due to decrease in bubble size would reduce liquid holdup (ϵ_l) which would result in higher interstitial velocity (V_l/ϵ_l) leading to higher heat transfer rate. Literature studies have pointed to the role of interstitial or linear liquid velocity on heat and mass transfer in three-phase fluidized beds (Chiu and Ziegler, 1983; Prakash et al., 1987).

2.3.6. Effects of Column Diameter

Heat transfer data from different literature studies obtained with different column diameters are presented in Figure 2.8. Trend lines are shown for column diameter $\geq 0.15\text{m}$ where wall effects are expected to be negligible. It can be observed that column diameter effects seem to diminish above diameter of 0.3 m. There is some scatter in data at higher column diameter therefore measurements in a 0.6 m or greater diameter column can confirm the trend. Jhawar and Prakash (2011) demonstrated that the increase in heat transfer coefficient was related to increasing liquid recirculation velocity with column diameter. Their observations are, however, based on column diameter upto 0.3 m. and need to be verified for larger diameter column.

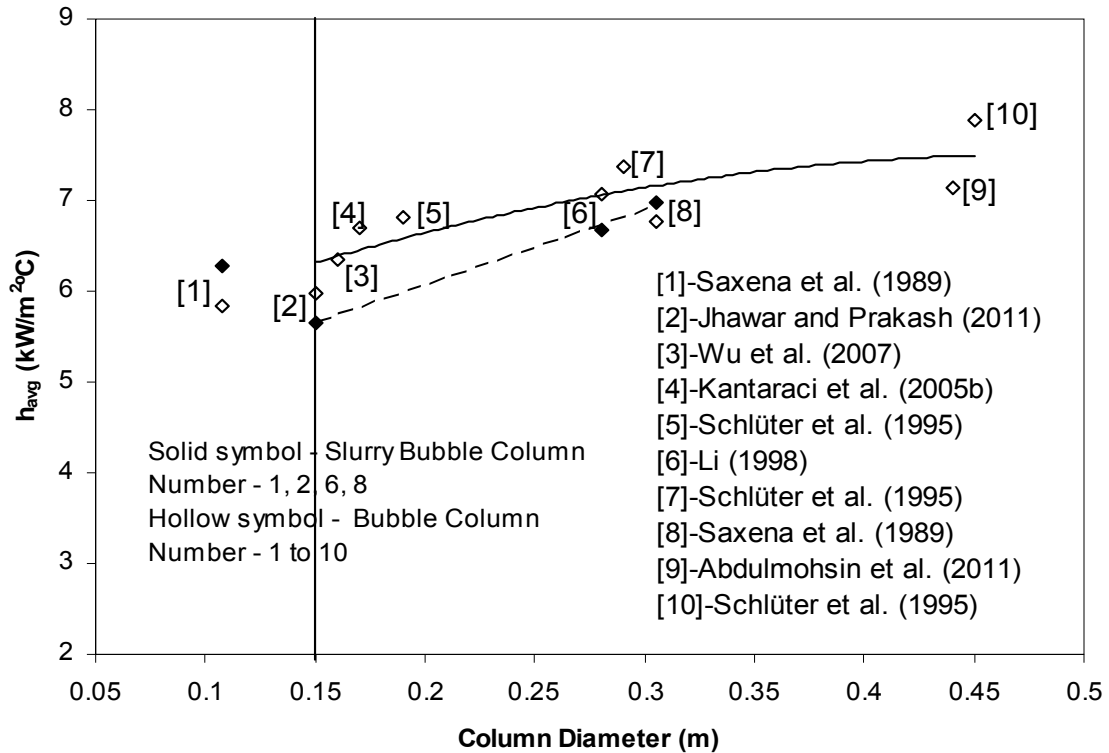


Figure 2.8. Effect of column diameter on heat transfer coefficients ($V_g = 0.2$ m/s)

2.3.7. Effects of Internals

The effect of internals on heat transfer coefficient in BC and SBC reactors has been studied by only a few researchers (Saxena et al., 1990b; Saxena et al., 1992b; Schlüter et al., 1995). Saxena et al. (1990b) reported that the effect of internals on heat transfer coefficient in large diameter (0.3 m) is not significant but the effect is significant in smaller diameter column (0.108 m). In the small diameter column with seven tube bundle, the heat transfer coefficients obtained by Saxena et al. (1990b) are similar to those obtained in large diameter column. They pointed out that the presence of internals can help in promoting the better mixing in small diameter columns by limiting the maximum stable size of the bubbles. It is however, likely that the small diameter column used by Saxena et al. (1990b) exhibited more slug like flow behavior without the internals. Presence of internals, however would have changed the hydrodynamic conditions leading to increase in turbulence and heat transfer enhancement. Schlüter et al.(1995) observed that the tube pitch has no significant

effect on heat transfer coefficient in low viscosity and it has only a small effect in case of highly viscous liquid. There is a need for additional work to investigate the role of internals design of different configurations on heat transfer and hydrodynamics in different size columns.

2.3.8. Effects of Axial and Radial Location

Heat transfer coefficient has been found to depend on axial and radial location in the column (Jhawar and Prakash, 2007; Li and Prakash, 2002; Saxena et al., 1992b; Li and Prakash, 1997; Li and Prakash, 1999; Li and Prakash, 2001; Prakash et al., 2001; Li et al., 2003; Wu et al., 2007). In the radial direction highest heat transfer coefficient is obtained at the center and lowest near the column wall (Li and Prakash, 1997; Li and Prakash, 2001; Wu et al., 2007). It is also pointed out that wall region heat transfer coefficient is not affected by particle size and column diameter (Jhawar and Prakash, 2011; Li and Prakash, 2001). Li and Prakash (2002), pointed out that the radial profile of the heat transfer coefficient is relatively flat in distributor, intermediate and disengagement zone compared to the bulk zone. Radial profile of heat transfer coefficient was found to be affected by slurry concentration up to 20 vol. % and the effect became insignificant for higher slurry concentrations (Li and Prakash, 2001). Saxena et al.(1992b) reported that the heat transfer coefficient increases as the axial distance from the distributor increases. They attributed this to the variation of liquid mixing along the column height. Li and Prakash (2002) also observed that the heat transfer coefficient increases with increase in distance from the sparger, but in the fully developed bulk zone the effect of axial position becomes insignificant. These observations need to be taken into consideration for proper design and arrangement of heat transfer surface.

2.4. Correlations of Heat Transfer Coefficients

A number of empirical and semi-empirical correlations have been proposed in literature for bubble columns over the years. The first correlation was reported by Kölbl et al. (1958) based on their experimental results:

$$Nu_{(d_i)} = 34.7 Re_{G,d_i}^{0.22} \text{ for } Re_{G,d_i} > 150 \dots\dots\dots(2.8)$$

$$Nu_{(d_i)} = 22.4 Re_{G,d_i}^{0.36} \text{ for } Re_{G,d_i} < 150 \dots\dots\dots(2.9)$$

It is of the form usual for convective heat transfer but does not account for the thermophysical properties of the liquid phase. First semi-theoretical correlation to estimate heat transfer coefficient in bubble columns was proposed by Kast (1962), by analyzing the fluid element motion around the rising gas bubble in column wall region. The general form of the equation is

$$St = f \left(Re^a Fr^b Pr^c \right)^m \dots\dots\dots(2.10)$$

The proposed values of constant and exponents are, $f = 0.1$, $a = 1$, $b = 1$, $c = 2$ and $m = -0.22$. The values of f, a, b, c and m were subsequently modified by several researchers (Kölbl et al., 1964; Burkel, 1972; Shaykhutdinov et al., 1971; Hart, 1976; Steiff and Weinspach, 1978) to fit their experimental data. The general equation accounts for the system properties and superficial gas velocity. The correlations can use any characteristic length (i.e. column diameter, heater diameter, particle diameter etc.), since it cancels out between Reynolds number and Froude number. Deckwer (1980) improved theoretical interpretation of heat transfer model proposed by Kast (1962) and applied Higbie's surface renewal theory (Higbie, 1935) of interphase mass transfer and Kolmogoroff's theory of isotropic turbulence and obtained the values of constant in general equation as $f = 1$, $a = 1$, $b = 1$, $c = 2$, $m = -0.25$. This equation was extended to slurry bubble columns by Deckwer et al.(1980) The modified equation for slurry bubble column can be expressed as shown in equation (2.3).

Li and Prakash (2001) observed that the correlation by Deckwer et al. (1980) well predicted the wall region heat transfer coefficient of their study. Saxena et al.

(1992b) pointed out that the correlation proposed by Deckwer et al.(1980) required modification to take the effect of temperature in account. They modified the correlation based on their experimental data obtained in a slurry bubble column of 0.305 m in diameter. It was reported that the effect of temperature on the term $(k_{sl} \rho_{sl} C_{p,sl})^{0.5}$ is minimal. They concluded that the major change in average heat transfer coefficient with temperature occurs due to the changes in $(\rho_{sl} g / \mu_{sl})^{0.25}$. The correlation proposed by Saxena et al. (1992b) is:

$$h_w = 0.0035 (k_{sl} \rho_{sl} C_{p,sl})^{0.5} \left(\frac{\rho_{sl} g}{\mu_{sl}} \right)^{0.47} V_g^{0.25} \dots\dots\dots (2.11)$$

Joshi et al. (1980) proposed a correlation to estimate heat transfer coefficient in bubble columns based on the analogy with mechanically agitated contactors.

$$\frac{h_w D_c}{k_l} = 0.4 \left(\frac{D_c V_l \rho_l}{\mu_l} \right)^{2/3} \left(\frac{C_{p,l} \mu_l}{k_l} \right)^{1/3} \left(\frac{\mu_l}{\mu_{l,w}} \right)^{0.14} \dots\dots\dots (2.12)$$

$$V_l = 1.31 \left[g D_c (V_g - \epsilon_g V_{B\infty}) \right]^{1/3} \dots\dots\dots (2.13)$$

This correlation accounts for system properties, superficial gas velocity and column diameter effect. It needs information on terminal rise velocity of a bubble to estimate liquid velocity, which is difficult to get. Zehner (1986a; 1986b) proposed a model to estimate heat transfer coefficient using approach similar to Joshi et al. (1980). They assumed that the circulation velocity of large eddies is an important parameter affecting the heat transfer in bubble columns. The model is derived from the heat transfer in single-phase flow over a flat surface by introducing the liquid circulation velocity as the characteristic velocity and the average distance of the bubbles as the characteristic length.

$$h_w = 0.18 (1 - \epsilon_g)^3 \sqrt[3]{ \left(k_l^2 \rho_l C_{p,l} \frac{V_l^2}{l_w} \right) } \dots\dots\dots (2.14)$$

$$V_l = \sqrt[3]{\frac{1}{2.5} \frac{(\rho_l - \rho_g) g D_C V_g}{\rho_l}} \dots\dots\dots (2.15)$$

$$l = d_B \sqrt[3]{\frac{\pi}{6 \epsilon_g}} \dots\dots\dots (2.16)$$

This correlation accounts for system properties, superficial gas velocity and column diameter effect. It needs the mean bubble diameter which is not easily available in bubble columns due to complex hydrodynamic nature.

Correlations obtained in bubble columns can be easily extended to slurry bubble columns by using effective slurry properties as proposed by Deckwer et al. (1980). In bubble columns the particle size is small and the particle movement relative to fluid is negligible and they don't contribute much to the surface renewal. Magiliotou et al. (1988) extended the equation of Deckwer et al. (1980) to three-phase fluidized beds. In three-phase fluidized bed, particle size is large and their movement relative to fluid is significant and play an important role in surface renewal in addition to fluid eddies.

While most literature correlations provide wall region heat transfer coefficient, Jhawar and Prakash (2011) presented a procedure to estimate heat transfer coefficient at any radial location in the column. Based on available data in columns ranging from 15 cm to 30.5 cm, they modified the correlation proposed by Joshi et al. (1980) to estimate heat transfer coefficient in the central region in bubble column.

$$\frac{h_c D_C}{k_l} = 0.084 \left(\frac{D_C V_l \rho_l}{\mu_l} \right)^{0.8} \left(\frac{C_{p,l} \mu_l}{k_l} \right)^{1/3} \left(\frac{\mu_l}{\mu_{l,w}} \right)^{0.14} \dots\dots\dots (2.17)$$

To estimate liquid velocity, the authors recommend correlation proposed by Riquarts (1981).

$$V_{l,c} = 0.21 \sqrt{g D_C} \left(\frac{V_g^3}{v_l g} \right)^{\frac{1}{8}} \dots\dots\dots (2.18)$$

To determine values at any radial location, following equation from Jhawar and Prakash (2007) is recommended.

$$\frac{h_c - h(r)}{h_c} = \left(\frac{n-1}{n}\right) \left(\frac{r}{R}\right)^n \dots\dots\dots (2.19)$$

Where, recommended value of n in this equation is 1.4. This correlation is valid in central region (r/R = 0.0 to 0.75). For the wall region correlation of Deckwer et al.(1980) is recommended. There is need to test this procedure in columns of diameter larger than 0.3m.

2.5. Conclusions

Slurry bubble column reactors belong to a subset of multiphase reactors. In these reactors, liquid-solid suspension can be treated as a pseudo homogeneous phase due to small size particles used. The average properties of the suspension can be estimated using fraction of the two phases. Strong link between column hydrodynamics and heat transfer has been reviewed and clarified. Based on available data, it is recommended that these reactors should be operated in heterogeneous regime to achieve high heat transfer rates. The review has also attempted to clarify some conflicting results in literature studies related to particle type, size and concentration. For example observed increase in heat transfer rate with addition of particles into liquid phase can be attributed to enhanced thermophysical properties of the suspension. Effects of operating variables have been discussed and their relative importance is pointed out. The review also points out that based on available data, the effect of column diameter becomes small above diameter of 0.3m. There is however, need for confirmation tests in larger diameter reactors with appropriate theoretical modeling and analysis. For proper heat transfer estimation in the column, axial and radial variations and effects of internals also need be taken into consideration. This can be assisted by CFD modeling with proper validation.

2.6. Notations

a	Exponent of dimensionless number in equation (2.10)
b	Exponent of dimensionless number in equation (2.10)
c	Exponent of dimensionless number in equation (2.10)
C_p	Heat capacity, (J/kg K)
d_B	mean bubble diameter, m
D_C	Column diameter, (m)
d_p	Diameter of particle, (m)
d_t	Tube diameter, (m)
f	Constant in equation (2.10)
Fr	Froude number, $\left(\frac{V_g^2}{gD_C} \right)$
g	Acceleration due to gravity, (m/s ²)
h	Heat transfer coefficient, (kW/m ² °C)
k	Thermal conductivity, (W/m K)
l	Mean distance between bubbles, (m)
m	Exponent of group of dimensionless number in equation (2.10)
n	Constant in equation (2.19)
Nu	Nusselt number, $\left(\frac{hD_c}{k_l} \right)$
Pr	Prandtl number, $\left(\frac{C_{p,l} \mu_l}{k_l} \right)$
q	Heat flux, W/m ²
r	Radial location, (m)

R	Radius of the column, (m)
Re	Reynolds number, $\left(\frac{\rho_l V_g D_c}{\mu_l} \right)$
St	Stanton number, $\left(\frac{h}{\rho_l C_{p,l} V_g} \right)$
T	Temperature, (°C)
TP	Thermophysical properties
U_t	Particle terminal rise velocity, (m/s)
V	Superficial velocity, (m/s)
$V_{B\infty}$	Terminal rise velocity of a bubble, (m/s)
w_s	weight fraction of the solid in the column
z	Axial location from the bottom of the column, (m)

Greek Symbols

α	Thermal diffusivity, $k/(\rho C_p)$, m^2/s
ρ	Density (kg/m^3)
Π	Constant (=3.14)
θ_c	Contact time, s
ν	Kinematic viscosity, (m^2/s)
ε	phase holdup (-)
ϕ_s	Volume fraction of solids in slurry phase
μ	Viscosity, (Pa.s)

Subscripts

avg	Average
g	Gas
l	Liquid
s	Solid
sl	Slurry
W	Wall
B	Bulk
c	Center

2.7. References

Abdulmohsin, R.S., Abid, B.A., Al-Dahhan, M.H., 2011. Heat transfer study in a pilot-plant scale bubble column. *Chemical Engineering Research and Design*. 89, 78-84.

Barghi, S., Prakash, A., Margaritis, A., Bergougnou, M.A., 2004. Flow regime identification in a slurry bubble column from gas holdup and pressure fluctuation analysis. *Canadian Journal of Chemical Engineering*. 82, 865-870.

Burkel, W., 1972. Der wärmeübergang an heiz- und kühlflächen in begasten flüssigkeiten. (Heat transfer at heating and cooling surfaces in gassed liquids). *Chemie Ingenieur Technik*. 44, 265 - 268.

Chen, R.C., Reese, J., Fan, L.S., 1994. Flow structure in a three-dimensional bubble column and three-phase fluidized bed. *AIChE Journal*. 40, 1093-1104.

Chiu, T.M., Ziegler, E.N., 1983. Heat transfer in three phase fluidized beds. *AIChE Journal*. 29, 677-685.

Chiu, T.M.; Ziegler, E.N., 1985. Liquid holdup and heat transfer coefficients in liquid solid three phase fluidized beds. *AIChE Journal*. 31, 1504-1509

- Cho, Y.J., Woo K.J., Kang, Y., Kim, S.D., 2002. Dynamic characteristics of heat transfer coefficient in pressurized bubble columns with viscous liquid medium. *Chemical Engineering and Processing*. 41, 699-706.
- Dakshinamurty, P., Subramhanyam, V., Rao, J.N., 1971. Bed porosities in gas-liquid fluidization. *Industrial and Engineering Chemistry Process Design and Development*. 10, 322-328.
- Darton, R.C., Harrison, D., 1975. Gas and liquid hold-up in three phase fluidization. *Chemical Engineering Science*. 30, 581-586.
- Deckwer, W.D., 1980. On the mechanism of heat transfer in bubble column reactors. *Chemical Engineering Science*. 33, 1341-1346.
- Deckwer, W.D., Louisi, Y., Zaldi, A., Ralek, M., 1980. Hydrodynamic properties of the Fischer-Tropsch slurry process. *Industrial and Engineering Chemistry Process Design and Development*. 19, 699-708.
- Deckwer, W.D., Schumpe, A., 1984. Transport phenomena in three phase reactors with fluidized solids. *German Chemical Engineering*. 7, 168-177.
- Degaleesan, S., Roy, S., Kumar, S.B., Duduković, M.P., 1996. Liquid mixing based on convection and turbulent dispersion in bubble columns. *Chemical Engineering Science*. 51, 1967-1976.
- Drahoš, J., Čermák, J., 1989. Diagnostic of gas-liquid flow patterns in chemical engineering systems. *Chemical Engineering and Processing*. 26, 147-164.
- Duduković, M.P., Larachi, F., Mills, P.L., 1999. Multiphase reactors – revisited. *Chemical Engineering Science*. 54, 1975-1995.
- Duduković, M.P., Larachi, F., Mills, P.L., 2002. Multiphase catalytic reactors: a perspective on current knowledge and future trends. *Catalysis Reviews*. 44, 123-246.
- El-Temtamy, S. A., Epstein, N., 1979. Contraction or expansion of three-phase fluidized beds containing fine/light solids. *The Canadian Journal of Chemical Engineering*. 57, 520–522.
- Epstein, N., 1976. Criterion for initial contraction or expansion of three-phase fluidized beds. *The Canadian Journal of Chemical Engineering*. 54, 259-263.
- Epstein, N., Nicks, D., 1976. Contraction or expansion of three-phase fluidized beds, in *Fluidization Technology*, D. L. Keairns (ed.), Hemisphere Publishing, Washington D.C. 1, 389-397.

- Fan, L. S., 1989. Gas-liquid-solid fluidization engineering. Butterworths, Stoneham, MA.
- Fan, L.S., Jean, R.H., Kitano, K., 1987. On the operating regimes of cocurrent upward gas-liquid-solid systems with liquid as the continuous phase. *Chemical Engineering Science*. 42, 1853-1855.
- Gamwo, I.K., Gidaspow, D., Jung, J., 2005. Optimum catalyst size for slurry bubble column reactors. *Ind. Eng. Chem. Res.* 44, 6393-6402.
- Hart, W.F., 1976. Heat transfer in bubble-agitated systems. A general correlation. *Industrial and Engineering Chemistry, Process Design and Development*. 15, 109 - 114.
- Higbie, R., 1935. The rate of absorption of a pure gas into a still liquid during short periods of exposure. *Transactions of the A.I.Ch.E.* 31, 365–389.
- Hikita, H., Asai, S., Kikukawa, H., Zaike, T., Ohue, M., 1981. Heat transfer coefficient in bubble columns. *Ind. Eng. Chem. Process Des. Dev.* 20, 540-545.
- Hinze, J. O., 1958. *Turbulence*. New York: McGraw-Hill.
- Hulet, C., Clement, P., Tochon, P., Schweich, D., Dromard, N, Anfray, J., 2009. Literature Review on Heat Transfer in Two- and Three-Phase Bubble Columns. *International Journal of Chemical Reactor Engineering*. 7, R1, 1-94.
- Jakobsen, H.A., Lindborg, H., Dorao, C.A., 2005. Modeling of bubble column reactors: progress and limitations. *Industrial and Engineering Chemistry Research*. 44, 5107-5151.
- Jakobsen, H.A., Sannæs, B.H., Grevskott, S., Svendsen, H. F., 1997. Modeling of vertical bubble-driven flows. *Industrial and Engineering Chemistry Research*. 36, 4052-4074.
- Jhavar, A.K., Prakash, A., 2007. Analysis of local heat transfer coefficient in bubble column using fast response probes. *Chemical Engineering Science*. 62, 7274-7281.
- Jhavar, A.K., Prakash, A., 2011. Influence of bubble column diameter on local heat transfer and related hydrodynamics. *Chemical Engineering Research and Design*. 89, 1996-2002
- Joshi, J.B., 1983. Solid-liquid fluidized beds: some design aspects. *Chemical Engineering Research and Design*. 61, 143-161.
- Joshi, J.B., 2001. Computational flow modeling and design of bubble column reactors. *Chemical Engineering Science*. 56, 5893-5933.

- Joshi, J.B., Deshpande, N.S., Dinkar, M., Phanikumar, D.V., 2001. Hydrodynamic stability of multiphase reactors. *Advances in Chem. Eng.* 26, 1-130.
- Joshi, J.B., Lali, A.M., 1984. Velocity–holdup relationship in multiphase contactors-a unified approach, in: Doraiswamy, L.K. and Mashelkar, R.A. (Eds.) *Frontiers in Chemical Reaction Engineering*, vol. I. Wiley Eastern, New Delhi. 314-329.
- Joshi, J.B., Sharma, M.M., Shah, Y.T., Singh, C.P.P., Ally, M., Klinzing, G.E., 1980. Heat transfer in multiphase contactors. *Chemical Engineering Communications.* 6, 257-271.
- Kang, Y., Suh, I.S., Kim, S.D., 1985. Heat transfer characteristics of three phase fluidized beds. *Chemical Engineering Communications.* 34, 1-13.
- Kantarci, N., Borak, F., Ulgen, K.O., 2005a. Bubble column reactors. *Process Biochemistry.* 40, 2263-2283.
- Kantarci, N., Ulgen, K.O., Borak, F., 2005b. A study on hydrodynamics and heat transfer in a bubble column reactor with yeast and bacterial cell suspensions. *Canadian Journal of Chemical Engineering.* 83, 764-773.
- Kast, W., 1962. Analyse des wärmeübergangs in blasensäulen. *International Journal of Heat and Mass Transfer.* 5, 329-336.
- Kato, Y., Uchida, K., Kago, T., S. Morooka., 1980. Wall-bed heat transfer characteristics of three-phase packed and fluidized bed. *Kagaku Kogaku Ronbunshu.* 6, 579-584.
- Kato, Y., Uchida, K., Kago, T., S. Morooka., 1981. Liquid holdup and heat transfer coefficient between bed and wall in liquid-solid and gas-liquid-solid fluidized beds. *Powder Technology.* 28, 173-179.
- Kawagoe, K.; Inoue, T.; Nakao, K.; Otake, T. Flow pattern and gas holdup conditions in gas sparged contactors. *Journal of Chemical Engineering of Japan.* 1976, 8, 254-256.
- Khare, A.S., Joshi, J.B., 1990. Effect of fine particles on gas hold-up in three phase sparged reactors. *Chemical Engineering Journal.* 44, 11-25.
- Kim, S.D., Baker, C.G.J, Bergougnou, M.A., 1975. Phase holdup characteristics of three phase fluidized beds. *The Canadian Journal of Chemical Engineering.* 53, 134–139.
- Kim, S.D., Kang, Y., 1997. Heat and mass transfer in three-phase fluidized-bed reactors – an overview. *Chemical Engineering Science.* 52, 3639-3660.

- Kim, S.D., Kang, Y., Kwon, H.K., 1986. Heat transfer characteristics in two- and three-phase slurry-fluidized beds. *AIChE Journal*. 32, 1397-1400.
- Kölbel, H., Langemann, H., 1964. Wärmeübergang in blasensäulen. *Erdöl-Z.* 80, 405-415.
- Kölbel, H., Siemens, W., Maas, R., Müller, K., 1958. Wärmeübergang in blasensäulen. *Chem.-Ing.-Tech.* 30, 400-404.
- Krishna, R., de Swart, W.A., Ellenberger, J., Martina, G.B., Maretto, C., 1997. Gas holdup in slurry bubble columns: effect of column diameter and slurry concentrations. *AIChE Journal*. 43, 311-316.
- Krishna, R., Sie, S.T., 2000. Design and scale-up of the Fischer-Tropsch bubble column slurry reactor. *Fuel Processing Technology*. 64, 73-105.
- Kumar, S., Fan, L.S., 1994. Heat-transfer characteristics in viscous gas-liquid and gas-liquid-solid system. *AIChE Journal*. 40, 745-754.
- Kumar, S., Kusakabe, K., Fan, L.S., 1993. Heat transfer in three-phase fluidization and bubble-columns with high gas holdups. *AIChE Journal*. 39, 1399-1405.
- Li, H., 1998. Heat transfer and hydrodynamics in a three-phase slurry bubble column. Thesis, PhD, University of Western Ontario, London, Ontario.
- Li, H., Prakash, A., 1997. Heat transfer and hydrodynamics in a three-phase slurry bubble column. *Industrial and Engineering Chemistry Research*. 36, 4688-4694.
- Li, H., Prakash, A., 1999. Analysis of bubble dynamics and local hydrodynamics based on instantaneous heat transfer measurements in a slurry bubble column. *Chemical Engineering Science*. 54, 5265-5271.
- Li, H., Prakash, A., 2001. Survey of heat transfer mechanisms in a slurry bubble column. *Canadian Journal of Chemical Engineering*. 79, 717-725.
- Li, H., Prakash, A., 2002. Analysis of flow patterns in bubble and slurry bubble columns based on local heat transfer measurements. *Chemical Engineering Journal*. 86, 269-276.
- Li, H., Prakash, A., Margaritis, A., Bergougnou, M.A., 2003. Effects of micron-sized particles on hydrodynamics and local heat transfer in a slurry bubble column. *Powder Technology*. 133, 171-184.
- Lin, T.J., Hung-Tzu, C., 2003. Effects of macroscopic hydrodynamics on heat transfer in a three-phase fluidized bed. *Catalysis Today*. 79-80, 159-167.

- Lin, T.J., Juang, R.C., Chen, Y.C., Chen, C.C., 2001. Predictions of flow transitions in a bubble column by chaotic time series analysis of pressure fluctuation signals. *Chemical Engineering Science*. 56, 1057-1065
- Lin, T.J., Tsuchiya, K., Fan, L.S., 1998. Bubble flow characteristics in bubble columns at elevated pressure and temperature. *AIChE J.* 44, 545-560.
- Lin, T.J., Wang, S.P., 2001. Effects of macroscopic hydrodynamics on heat transfer in bubble columns. *Chemical Engineering Science*. 56, 1143 - 1149.
- Luo, X., Jiang, P., Fan, L.S., 1997. High-pressure three-phase fluidization: hydrodynamics and heat transfer. *AIChE Journal*. 43, 2432-2445.
- Luo, X., Lee, D.J., Lau, R., Yang, G.Q., Fan, L.S., 1999. Maximum stable bubble size and gas holdup in high-pressure slurry bubble columns. *AIChE Journal*. 45, 665-680.
- Magiliotou, M., Chen, Y.M., Fan, L.S., 1988. Bed-immersed object heat transfer in a three-phase fluidized bed. *AIChE Journal*. 34, 1043-1047.
- Matsuura, A., Fan, L.S., 1984. Distribution of bubble properties in a gas-liquid-solid fluidized bed. *AIChE Journal*. 30, 894-903.
- Memon, A.I., 2004. Flow regime transitions in bubble and slurry bubble columns. Thesis, MEng. University of Western Ontario, London, Ontario, Canada.
- Michele, V., Hempel, D.C., 2002. Liquid flow and phase holdup – measurement and CFD modeling for two-and three-phase bubble columns. *Chemical Engineering Science*. 57, 1899-1908.
- Michelsen, M.L., Østergaard, K., 1970. Hold-up and fluid mixing in gas liquid fluidized beds. *Chemical Engineering Journal*. 1, 37-46.
- Muroyama, K., Fukuma, M., Yasunishi, A., 1984. Wall-to-bed heat transfer coefficient in gas-liquid-solid fluidized beds. *Canadian Journal of Chemical Engineering*. 62, 199-208.
- Muroyama, K., Kato, T., Masuda, T., Kinoshita, S., 2003. Vertical cylinder-to-slurry heat transfer in gas-slurry transport bed. *Canadian Journal of Chemical Engineering*. 81, 426-432.
- Nigam, K.D.P., Schumpe, A., 1996. Three-phase sparged reactors. Gordon and Breach, London.
- Olmos, E., Gentric, C., Poncin, S., Midoux, N., 2003a. Description of flow regime transitions in bubble columns via laser Doppler anemometry signals processing. *Chemical Engineering Science*. 58, 1731-1742.

Olmos, E., Gentric, C., Poncin, S., Midoux, N., 2003b. Identification of flow regimes in a flat gas-liquid bubble column via wavelet transforms. *Canadian Journal of Chemical Engineering*. 81, 382-388.

Østergaard, K., Thiesen, P.I., 1966. The effect of particle size and bed height on the expansion of mixed phase (gas-liquid) fluidized beds. *Chemical Engineering Science*. 21, 413- 417.

Pandit, A.B., Joshi, J.B., 1984. Three phase sparged reactors: some design aspects. *Reviews in Chem. Eng.* 2, 1-84.

Pandit, A.B., Joshi, J.B., 1986. Mass and heat transfer characteristics of three phase sparged reactors. *Chem. Eng. Res. Des.* 64, 125-157.

Prakash, A., Briens, C.L., Bergougnou, M.A., 1987. Mass transfer between solid particles and liquid in a three phase fluidized bed. *Canadian Journal of Chemical Engineering*. 65, 228-236.

Prakash, A., Margaritis, A., Li, H.; Bergougnou, M.A., 2001. Hydrodynamics and local heat transfer measurements in a bubble column with suspension of yeast. *Biochemical Engineering Journal*. 9, 155-163.

Quiroz, I., Herrera, I., Mendizabal, D.G., 2003. Experimental study on convective coefficients in a slurry bubble column. *International Communications in Heat and Mass Transfer*. 30, 775-786.

Reid, R.C., Prausnitz, J.M., Sherwood, T.K., 1977. *The properties of gases and liquids*. McGraw-Hill. New York.

Riquarts, H.P., 1981. Strömungsprofile, impulsaustausch und durchmischung der flüssigen phase in bläsensäulen. *Chem Ing Techn.* 53, 60–61.

Saxena, S.C., Patel, B.B., 1990. Heat transfer and hydrodynamic investigations in a baffled bubble column: air-water-glass bead system. *Chemical Engineering Communications*. 98, 65-88.

Saxena, S.C., Rao, N.S., Saxena, A.C., 1990a. Heat transfer from a cylindrical probe immersed in a three-phase slurry bubble column. *Chemical Engineering Journal*. 44, 141-156.

Saxena, S.C., Rao, N.S., Saxena, A.C., 1990b. Heat-transfer and gas-holdup studies in a bubble column: air-water-glass bead system. *Chemical engineering Communication*. 96, 31-55.

- Saxena, S.C., Rao, N.S., Saxena, A.C., 1992b. Heat transfer and gas holdup studies in a bubble column: air-water-sand system. *Canadian Journal of Chemical Engineering*. 70, 33-41.
- Saxena, S.C., Rao, N.S., Yousuf, M., 1991a. Hydrodynamic and heat transfer investigations conducted in a bubble column with fine powders and a viscous liquid. *Powder Technology*. 67, 265-275.
- Saxena, S.C., Rao, N.S., Yousuf, M., 1991b. Heat transfer and hydrodynamic investigations conducted in a bubble column with powders of small particles and a viscous liquid. *Chemical Engineering Journal*. 47, 91-103.
- Saxena, S.C., Vandivel, R., Saxena, A.C., 1989. Gas holdup and heat transfer from immersed surfaces in two- and three- phase systems in bubble columns. *Chemical Engineering communications*. 85, 63-83.
- Schlüter, S., Steiff, A., Weinspach, P.M., 1995. Heat transfer in two- and three-phase bubble column reactors with internals. *Chemical Engineering and Processing*. 34, 157-172.
- Shah, Y.T., Kelkar, B.G., Godbole, S. P., 1982. Design parameters estimations for bubble column reactors. *AIChE Journal*. 28, 353-379.
- Shaykhutdinov, A.G., Bakirov, N.U., Usmanov, A.G., 1971. Determination and mathematical correlation of heat transfer coefficient under conditions of bubble flow, cellular, and turbulent foam. *International Chemical Engineering Journal*. 11, 641 - 645.
- Steiff, A., Weinspach, P.M., 1978. Heat transfer in stirred and non-stirred gas-liquid reactors. *German Chemical Engineering*. 1, 150 - 161.
- Tareef, B. M., 1940. Thermal Conductivity of Colloidal Systems. *Colloidal J. USSR*. 6, 545.
- Thorat, B.N., Joshi, J.B., 2004. Regime transition in bubble columns: experimental and predictions. *Experimental Thermal and Fluid Science*. 28, 423-430
- Tsutsumi, A., Kim, Y.H., Togawa, S., Yoshida, K., 1987. Classification of three-phase reactors. *Sādhanā*. 10, 247-259.
- Vand, V., 1948. Viscosity of solutions and suspensions.I. Theory. *Journal of Physical Chemistry*. 52, 277-299.
- Vial, C., Camarasa, E., Poncin, S., Wild, G., Midoux, N., Bouillard, J., 2000. Study of hydrodynamics behaviour in bubble columns and external loop airlift reactors through analysis of pressure fluctuations. *Chemical Engineering Science*. 55, 2957-2973.

Viswanathan, S., Kakar, A.S., Murti, P.S., 1965. Effect of dispersing bubbles into liquid fluidized beds on heat transfer and hold-up at constant bed expansion. *Chemical Engineering Science*. 20, 903-910.

Wallis, G.B., 1969. *One dimensional two-phase flow*. McGraw Hill, New York.

Wang, T., Wang, J., Jin, Y., 2007. Slurry reactors for gas-to-liquid processes: A Review. *Ind. Eng. Chem. Res.* 46, 5824-5847.

Wild, G., Saberian, M., Schwartz, J.L., Charpentier, J.C., 1984. Gas-liquid-solid fluidized-bed reactors. State of the art and industrial possibilities. *International chemical Engineering*. 24, 639-677.

Wilkinson, P.M., Spek, A.P., van Dierendonck, L.L., 1992. Design parameters estimation for scale-up of high-pressure bubble columns. *AIChE J.* 38, 544-554.

Wu, C., Al-Dahhan, M.H., Prakash, A., 2007. Heat transfer coefficients in a high-pressure bubble column. *Chemical Engineering Science*. 62, 140-147.

Yang, G.Q., Luo, X., Lau, R., Fan, L.S., 2000. Heat-transfer characteristics in slurry bubble columns at elevated pressures and temperatures. *Industrial and Engineering Chemistry Research*. 39, 2568-2577.

Yu, Y.H., Kim, S.D., 1991. Bubble properties and local liquid velocity in the radial direction of cocurrent gas-liquid flow. *Chemical Engineering Science*. 46, 313-320.

Zehner, P., 1986a. Momentum, mass and heat transfer in bubble columns. Part 1. Flow model of the bubble column and liquid velocities. *International Chemical Engineering*. 26, 22-28.

Zehner, P., 1986b. Momentum, mass and heat transfer in bubble columns. Part 2. Axial blending and heat transfer. *International Chemical Engineering*. 26, 29-34.

CHAPTER 3. EFFECTS OF INTERNALS OF DIFFERENT CONFIGURATIONS ON LOCAL HEAT TRANSFER AND HYDRODYNAMICS IN BUBBLE COLUMN

Abstract

Local heat transfer and column hydrodynamics are investigated in a 0.15m ID bubble column in presence of internals of different configurations. Local heat transfers variations are measured with a fast response probe capable of capturing bubble dynamics as well detect local flow direction. Tap water is the liquid phase and gas phase used is oil free compressed air at flow rates varied from 0.03 to 0.35 m/s. Measurements obtained in presence of internals are compared with those without internals to elucidate the effects of internals design. Comparisons are based on average values and fluctuating component of local instantaneous heat transfer coefficient obtained with the fast response probe. The average gas holdup, center line liquid and bubble holdups obtained with and without internals are also compared. The observed differences are discussed based on the insights provided by these comparisons. The heat transfer coefficient and gas holdup can increase or decrease depending on internal type. The reasons for these increase or decrease are pointed out in this study. Relationships between local heat transfer measurements and hydrodynamic conditions in presence of internals are shown and discussed.

Key words: Bubble columns, Local heat transfer, Internals design, Hydrodynamics, Gas holdup, Bubbles fractions, Liquid circulation velocity

3.1 Introduction

Bubble columns (BC) are becoming the reactor of choice for a number of industrial applications owing to a number of attractive features the most notable of which include excellent heat transfer properties, isothermal conditions of operation, low maintenance cost due to simple construction and absence of any moving parts (Deckwer and Schumpe, 1993; Kluytmans et al., 2001; Li and Prakash, 2002; Li et al., 2003). In addition they offer good mass transfer rates, high selectivity and conversion per pass, online catalyst addition and withdrawal and washing effect of the liquid on catalyst. The rule of thumb is that the heat transfer in these reactors is between 10 and 100 times greater than it is in single-phase liquid flow for the same flow rates with respect to the column cross-section (Kast, 1962; Deckwer, 1980; Deckwer, 1992). The above benefits make these as the reactor of choice in variety of industrial applications such as Fischer-Tropsch synthesis, methanol synthesis, heavy oil upgrading, fermentation, biological waste water treatment, flue gas desulphurization, coal liquefaction, dimethyl ether production, chlorination and hydrogenation (Shah et al., 1982; Fan, 1989; Duduković and Devanathan, 1992; Deckwer and Schumpe, 1993; Li, 1998; Prakash et al., 1999; Prakash et al., 2001; Duduković et al., 2002).

In order to obtain desired performance, for a given application bubble column may need to be equipped with different internals type. These include baffles, heat transfer tubes and gas/liquid distributors of different configurations. The internals presence and arrangement in bubble columns would affect hydrodynamics and mixing pattern, there by affecting the reactor performance and heat transfer characteristics. A limited number of literature studies have investigated effects of internals on bubble column hydrodynamics (Youssef and Al-Dahhan, 2009; Larachi et al., 2006; Chen et al., 1999; Schlüter et al., 1995; Saxena et al., 1992). These studies clearly point to alterations in flow pattern, mixing intensities and general hydrodynamics due to insertion of internals in a hollow bubble column. Most of these studies have focused on different arrangements of heat exchanger tubes aimed at applications in exothermic such as Fischer-Tropsch synthesis, methanol synthesis and production of

dimethyl ether (DME). By appropriate selection and arrangement of internals, it is also possible to improve mass transfer and reduce back mixing effects in these reactors. In this study attempts are made to get further insights into the local hydrodynamics based on heat transfer coefficient measurements and study of bubble populations in presence of internals of different types. The heat transfer coefficient data obtained in this study has been compared with the data obtained in bubble columns without internals to point out the effects. The hydrodynamic parameters such as gas holdup profile, liquid circulation velocity profile, and bubble holdup are compared in bubble columns with and without internals to get the insights of affect of these parameters on the heat transfer coefficient in air-water system.

3.2 Experimental

Experiments were conducted in a Plexiglas column of 0.15 m internal diameter and height of 2.5 m with (Figure 3.1). The column was supported by rigid metallic structure to keep it vertical and minimize mechanical vibrations which might affect pressure and heat transfer signals. The gas was introduced in the column using a coarse sparger. The detailed design of the coarse sparger is explained elsewhere (Gandhi, 1997). The sparger had two levels, upper level had seven (1.9 mm diameter) and lower level had five (1.9 mm diameter) downward facing holes on each of four arms. Two types of internals and their combination were used in this study. Top view of tube bundle type internal studied (Type A) is shown in Figure 3.2a. A flow deflector type six-blade concentric baffle studied is shown in Figure 3.2b. It was located at two separate axial positions 21 cm and 36 cm from the bottom of the column. Specific details about internals used are provided in Table 3.1. Oil-free compressed air was used as gas phase; tap water was used as the liquid phase. The gas flow rate was measured using three calibrated sonic nozzles of different diameter (0.7mm, 1.5 mm and 2.5 mm). The superficial gas velocity was varied from 0.03 to 0.35 m/s. The unaerated water height in the column was maintained around 1.45 m. A measuring tape was provided on the column to note the liquid level and dispersion height. Two pressure transducers (OMEGA Type PX541-7.5GI and Type PX541-

15GI) were used to measure the pressure fluctuations in distributor ($z = 0.027$ m) and disengagement section ($z = 1.318$ m), as shown in Figure 3.1. The pressure transducers were connected to a DC power supply and generated a voltage proportional to measured pressure. The response time of the pressure transducers was 2 ms and data were recorded for 105 seconds at a rate of 60 Hz. Instantaneous heat flux was measured using a micro-foil heat flux sensor (Rdf, Model number 20453-1 G161). The sensor was flush mounted on the surface of a brass cylinder of 11 mm outer diameter. A small cartridge heater (Chromalox, model number CIR-1012) was installed inside the brass cylinder. The AC power was supplied to the cartridge heater through a variac to regulate supplied power in the range of 20 to 40V. The detailed design of the heat flux probe is explained elsewhere (Li and Prakash., 1997; Li, 1998). Probe location could be changed both axially and radially and it could also be rotated to study effects of sensor orientation on measured values. The temperature of the liquid phase was measured using two copper-constantan thermocouples (ANSI type T). These thermocouples were located at two radial locations: one at center and other close to the wall. Axial position of the thermocouple could be changed. The response time of micro-foil heat flux sensor was 20 ms and data were recorded for 180 s at a rate of 60 Hz. The probe generated microvolt signals, which were amplified to millivolts by a suitable amplification circuit using 15V DC supply. A minimum of three test runs were performed at each condition and average values are reported. For the heat flux sensor, the following equation can be derived for liquid film heat transfer coefficient (Li and Prakash, 2001):

$$\frac{1}{h_i} = \frac{T_{su} - T_b}{q / A} - \frac{\Delta x}{k} \dots\dots\dots(3.1)$$

The second term on the right hand side of Equation 3.1 is negligible compared to the first term (< 1%) due to high thermal conductivity (k) and small thickness (Δx) of the thermal barrier film. Therefore instantaneous heat transfer coefficient could be determined by measurement of heat flux and the difference between surface and bulk temperatures at a given time. The time-averaged heat transfer coefficient at a given location was obtained by averaging the instantaneous heat transfer data collected.

$$h_{avg} = \frac{1}{N} \sum_{i=1}^N \frac{q / A}{T_{Su} - T_b} \dots\dots\dots(3.2)$$

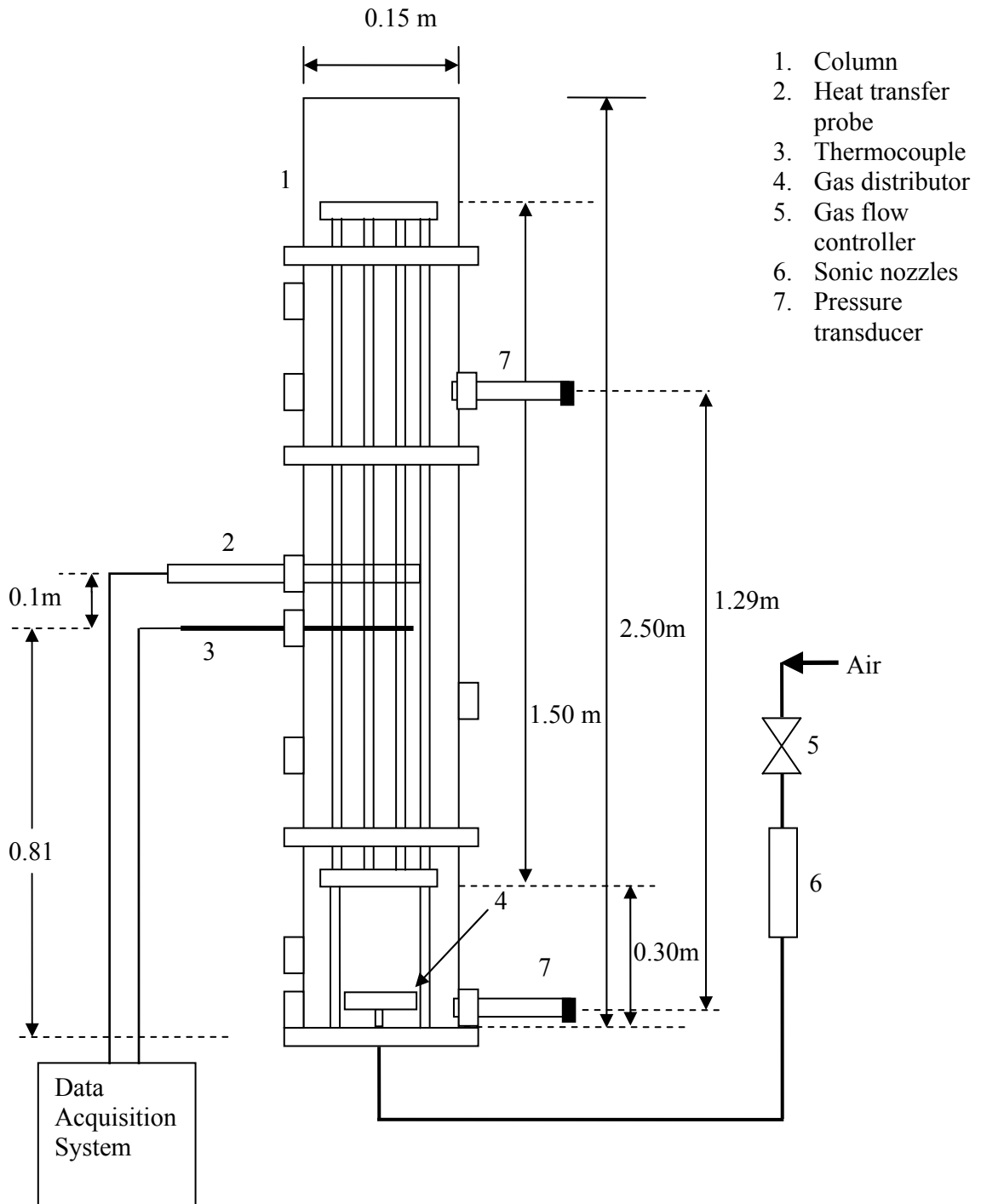


Figure 3.1. Schematic diagram of experimental setup

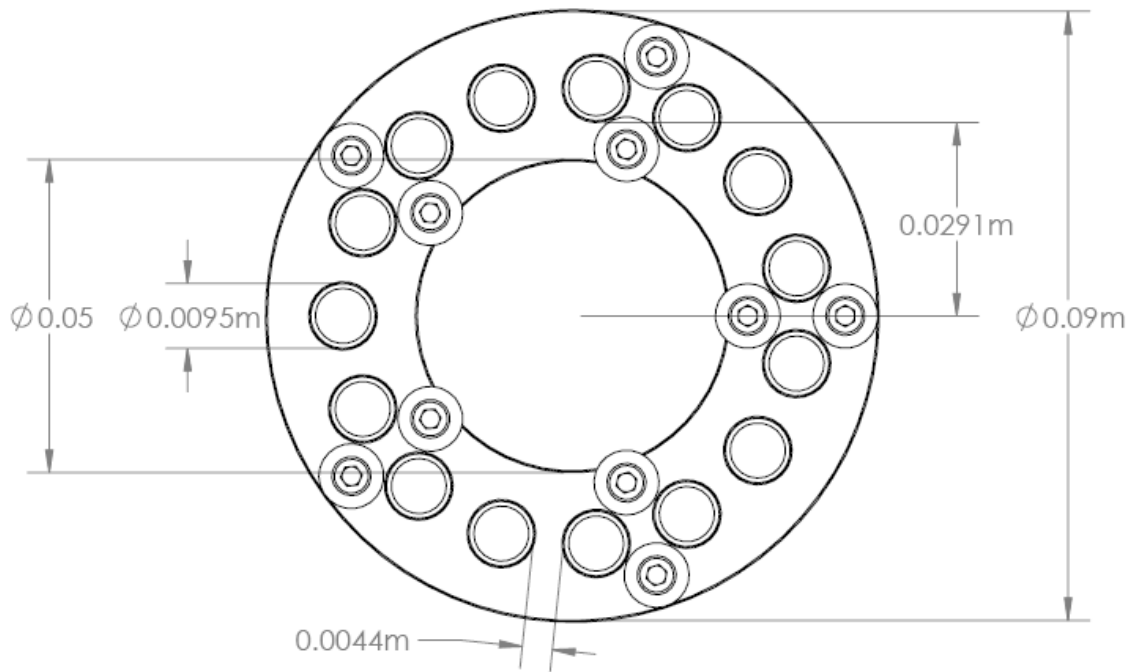


Figure 3.2a. Top view of the tube bundle used (Type A)

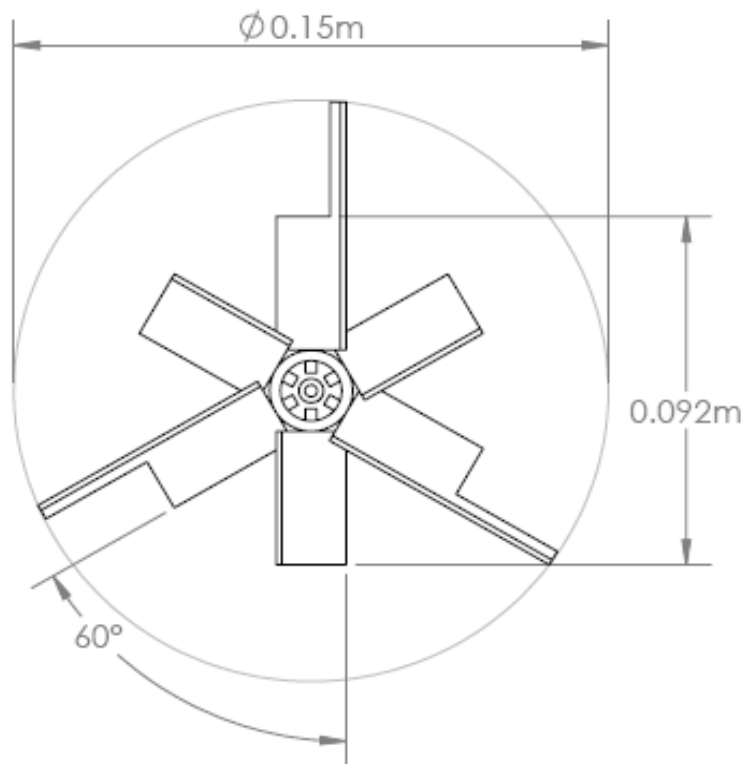


Figure 3.2b. Top view of bubble diffuser used (Type B)

Table 3.1. Details of internals used in air-water system

Internal type	Label	Geometrical details	Comments
Circular tube bundle (z = 0.3 m)	A	No. of tubes: 15 Tube diameter: 0.95 cm Tube length: 150 cm Wall to wall spacing between tubes: 4.4 mm	Adjustable height from column bottom
Concentric baffle (z = 0.21 m)	B1	No. of blades: 6 Length of blade: 3.5 cm Width of blade: 1.9 cm Blade angle: 60° from axis	Adjustable height from column bottom
Concentric baffle (z = 0.36 m)	B2	Same as B1	Adjustable height from column bottom
Circular tube bundle (z = 0.5 m) + baffle (z = 0.36 m)	AB2	Combination of A and B2	

3.3 Results and discussion

3.3.1 Local Heat Transfer Coefficients

Figures 3.3 presents a comparison of average heat transfer coefficient obtained in the bulk section of the column at column center with and without internals. From the figure it is observed that the heat transfer coefficient increases with increase in superficial gas velocity in bubble columns in all cases but at different rates. This increase in heat transfer coefficient with superficial gas velocity can be attributed to the turbulence generated due to the introduction of the gas in the column. It is observed that the heat transfer coefficients obtained with internals types A and AB2 are significantly higher than those obtained in without internals. It should also be noted that the difference between internals A and AB2 is not significant, indicating that internal A is clearly playing a more dominant role here. With internal B2, the difference is not significant for lower velocities (< 0.15 m/s) compared to hollow column but higher values are obtained with increasing velocities. However with internal B1, no significant difference is observed. These differences can be related to

changes in mixing patterns, turbulence and column hydrodynamics caused by the internal type. The intensity and degree of change is expected to vary with specific design of internal. Type A internal due to its circular arrangement of heat exchanger tubes would help direct flow of gas bubbles to column center thus creating additional driving force for liquid circulation rate. The B type internals in this study would have a smaller such effect due to a very different design configuration. However, differences observed with change in axial position of this internal (B1 and B2) indicate the need to consider local variations in the column hydrodynamic behavior.

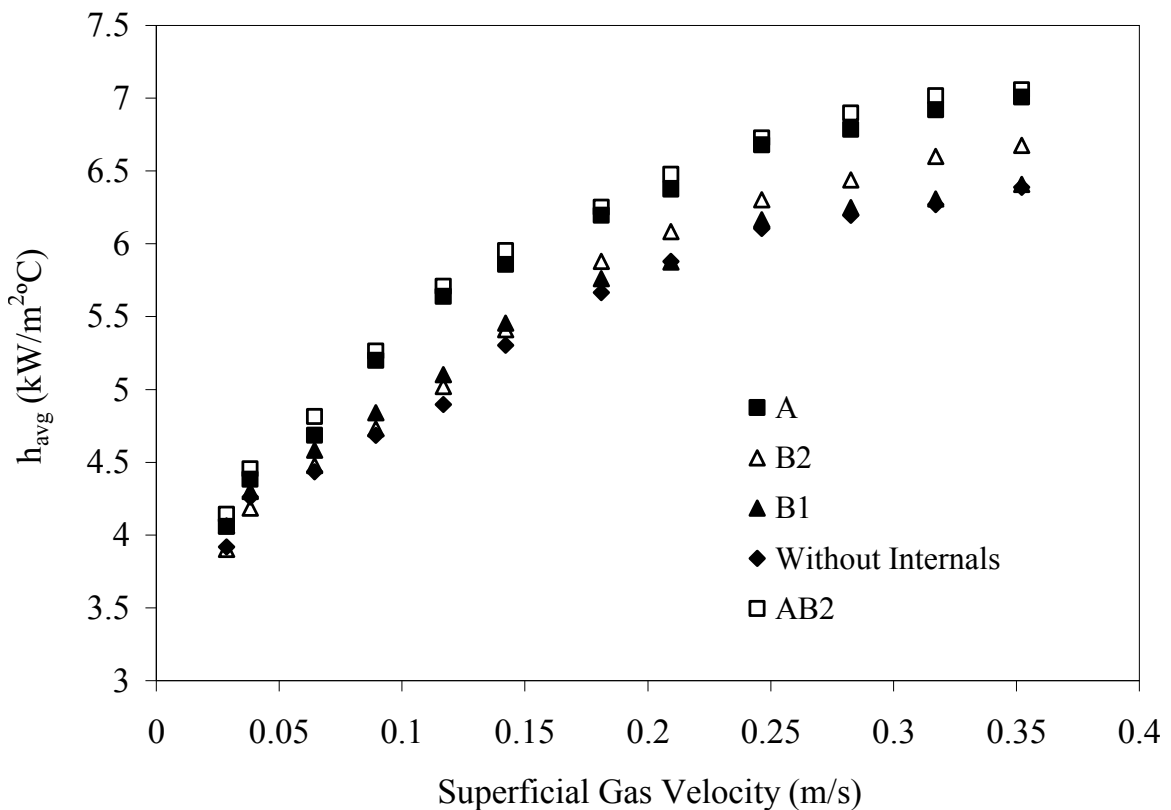


Figure 3.3. Comparison of heat transfer coefficient measurements in bubble column with and without internals, $r/R=0$ (air-water system)

A limited number of literature studies have investigated effects of internals on bubble column hydrodynamics (Youssef and Al-Dahhan, 2009; Larachi et al., 2006; Chen et al., 1999). These studies clearly point to alterations in flow pattern, mixing intensities and general hydrodynamics due to insertion of internals in a hollow bubble column.

Change in design configuration has been reported to clearly affect hydrodynamic behavior which is expected to affect rate of transport processes (Youssef and Al-Dahhan, 2009; Larachi et al., 2006). The fast response heat transfer probe used in this study allowed measurement of temporal variation of local heat transfer coefficient in the column. Therefore to further understand the underlying reasons for the observed increase in heat transfer coefficient with type A internal, the dynamic behavior of heat transfer coefficient was compared for a given gas velocity. It is observed from Figure 3.4a that the peaks obtained in presence of internals are wider and taller as compared to those without the internal. This could be attributed to the passage of clusters of bubble generated with type A internal as a result of directing bubble flow towards central region of the column.

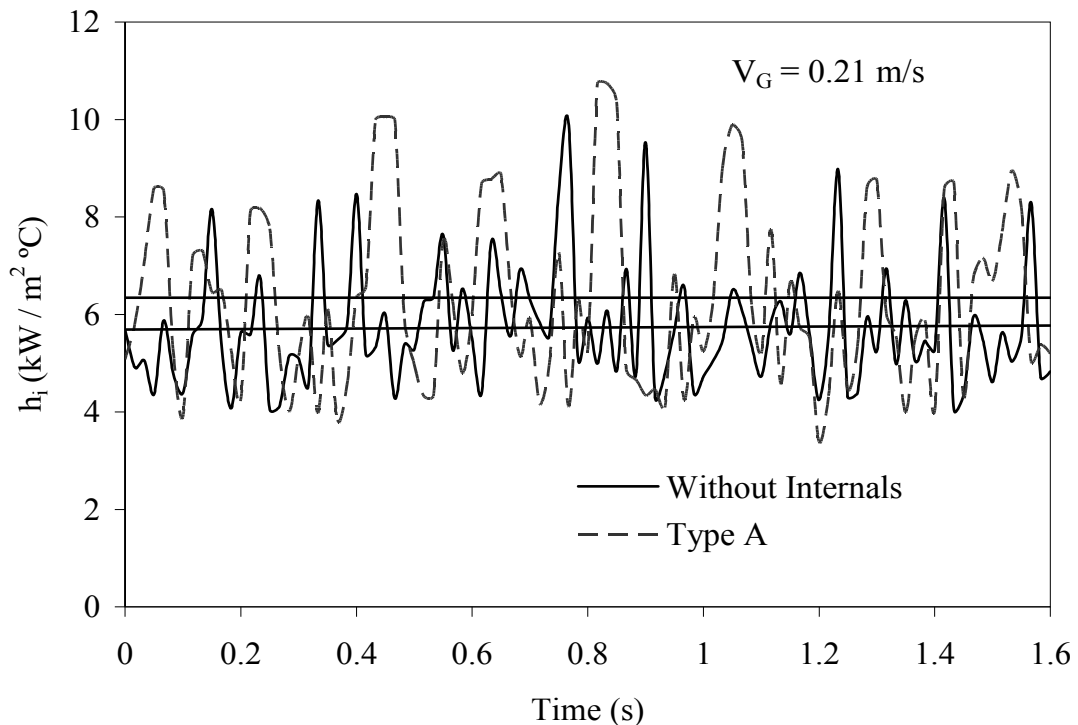


Figure 3.4a. Instantaneous heat transfer coefficients of air-water system (with and without internals) at $r/R=0$

A similar comparison of the behavior of instantaneous heat transfer coefficients obtained in the wall region of the bulk section of the column is shown in Figure 3.4b for the superficial gas velocity of 0.21 m/s. It can be seen in wall region the instantaneous heat transfer coefficient peaks are smaller than central region in

both the cases. This can be attributed to presence of smaller bubbles in the wall region of the column. It is also interesting to see that in bubble column equipped with type A internal the heat transfer coefficient peaks in wall region are smaller compared to hollow bubble column. This could be due to smaller and fewer bubbles in the annular region created due to insertion of this internal type in the column. Visual observations also supports this, smaller bubbles seemed trapped in the annular region given the geometry of the internal and small gap between the tubes (see Table 3.1).

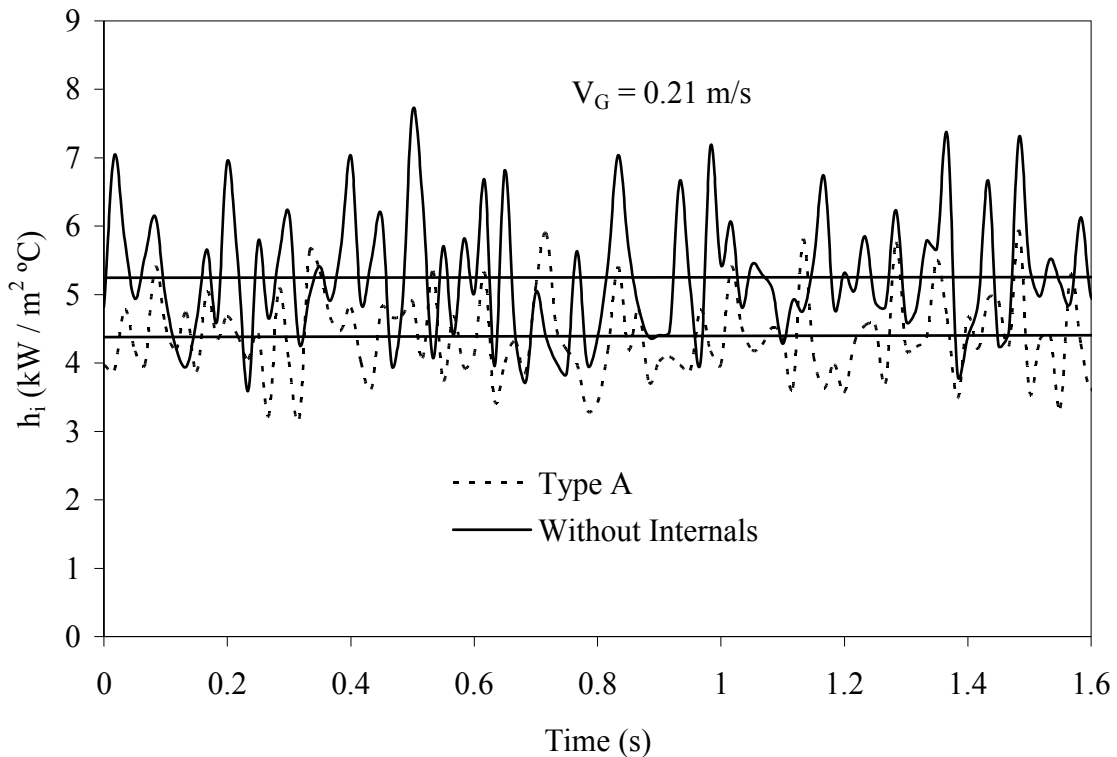


Figure 3.4b. Instantaneous heat transfer coefficients of air-water system (with and without internals) at $r/R=0.624$

Figure 3.5 shows a comparison of average heat transfer coefficient obtained close to the wall ($r/R=0.624$) in the bulk section of the column in presence of different internals. Following observations can be made for data in the wall region, when compared with the heat transfer coefficients obtained at column centre (Figure 3.3).

- Heat transfer coefficients are significantly lower in the wall region.

- The rate of change with gas velocity is slow and decreases further above gas velocity of 0.15 m/s.
- A reverse trend is observed with internals i.e. values are higher with type B and lower with type A internals indicating very different flow patterns with different internals used.
- Combination of internals A and B2 improves heat transfer coefficient in the wall region compared to internal A alone.

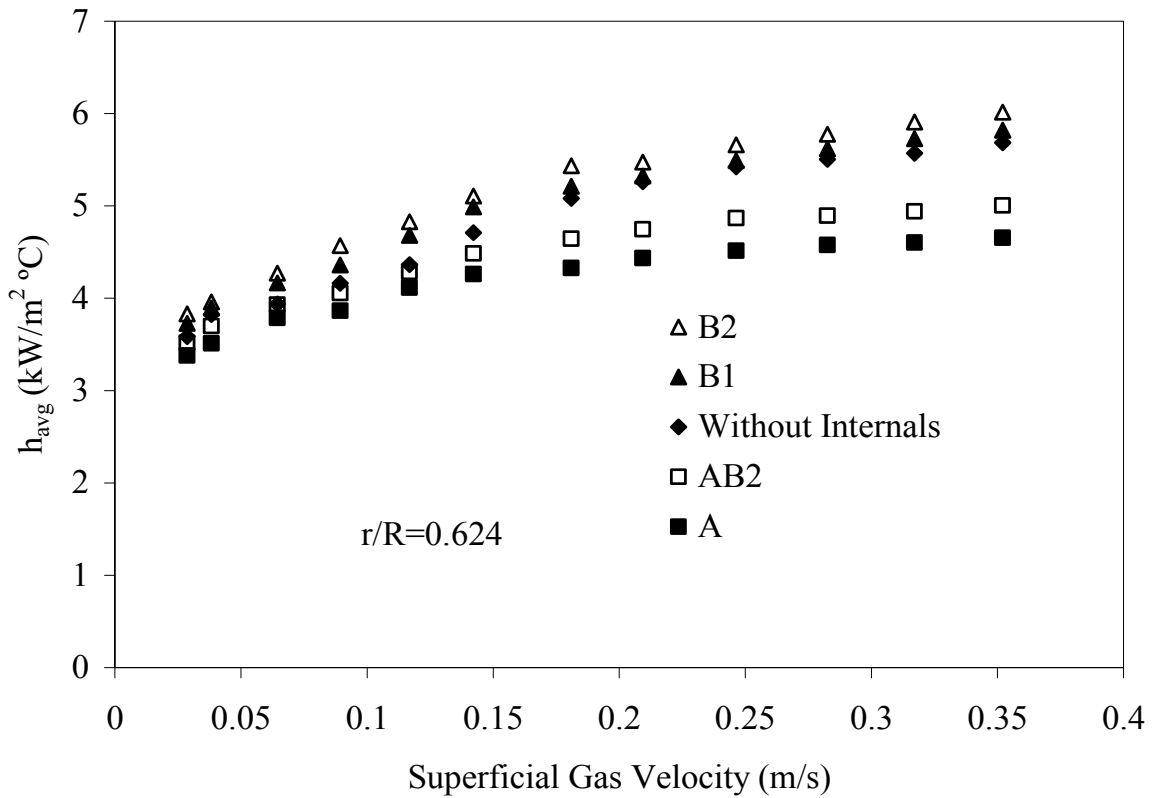


Figure 3.5. Comparison of heat transfer coefficient measurements in bubble column with and without internals, $r/R=0.624$ (air-water system)

A direct comparison of data obtained in the two regions obtained with two different internals is presented in Figure 3.6 to further highlight the differences. It can be noted that the differences between the two regions is higher with type A internal compared to type B2. Very different geometry of these internals of course is the main cause of

the difference. Selection of proper internals for a given application would need to take such differences into consideration.

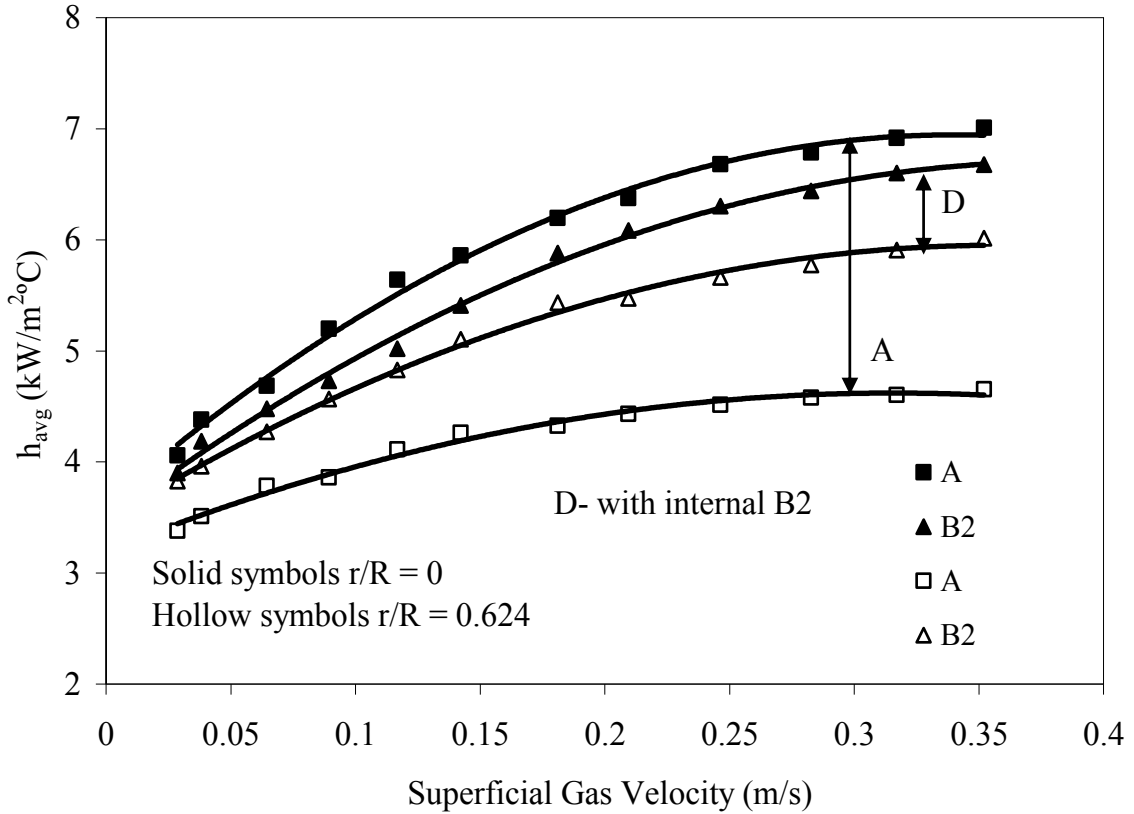


Figure 3.6. Variations of heat transfer coefficient at two radial locations with internal A and B2

The radial direction variations were further investigated with radial profiles of heat transfer coefficients obtained with and without internals as presented in Figure 3.7a. As the radial distance from the center increases the heat transfer coefficient decreases at all superficial gas velocities in all cases. It is also observed that the profiles are much steeper with Type A internal compared to hollow bubble column or other internal type. The radial profiles obtained with type A internal cross the other profile around dimensionless radius of about 0.3 and move below other profiles as it moves into annular region. This difference can be related to the design of type A internal. The tube bundle design would funnel the two phase flow and smaller inter-tube gap would limit flow into annular region thus significantly altering column

hydrodynamics. The steeper profiles obtained in presence of Type A internals show that the lower turbulence is caused by the smaller and fewer bubbles in the wall region. It was visually observed that the bubble size and population decreased in the wall region with type A internals, compared to those without or other type internals.

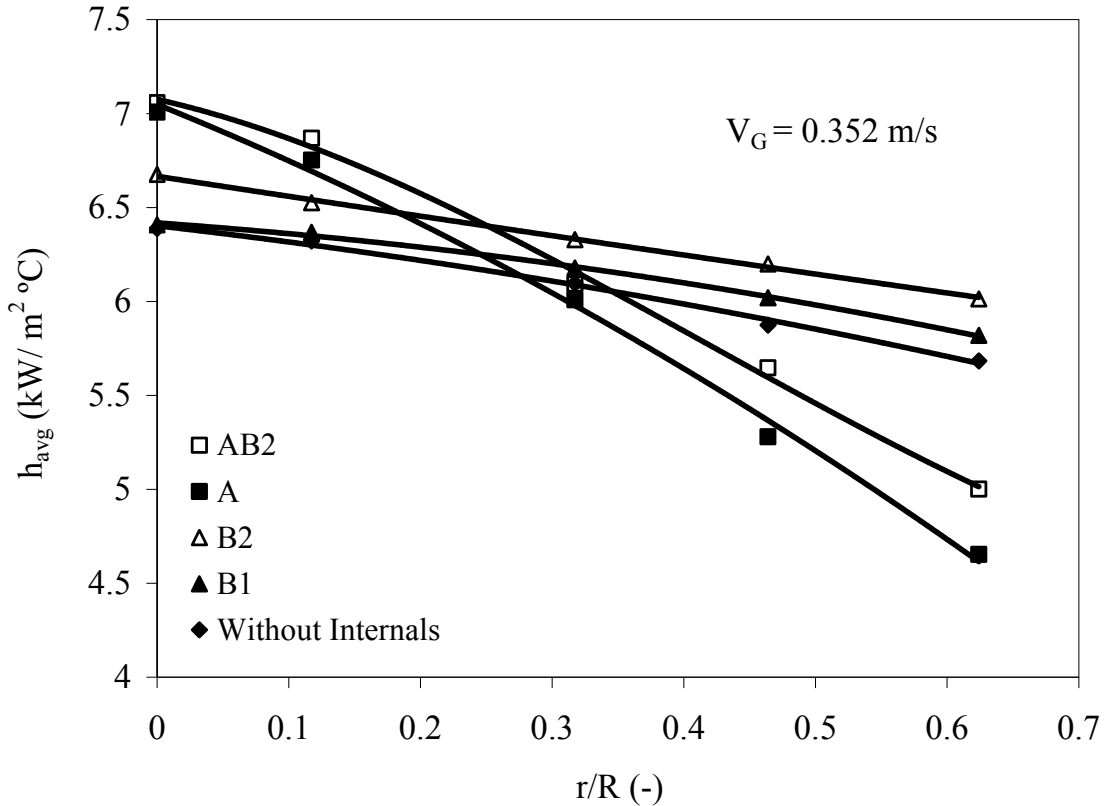


Figure 3.7a. Comparison of the radial profile of heat transfer coefficient obtained with and without internals in air-water system

It is also observed from Figure 3.7a that the radial profile was less steeper with combined AB2 internal compared to internal A alone. Given its design, internal B2 would assist with some flow deflection over the column cross section thus limiting the funneling action of type A internal. It is also observed from Figure 3.7a that insertion of type B internal caused the radial profile to become more gradual compared to hollow column. This effect should lead to reduction in phase back-mixing in the column and requires further investigations. A direct comparison of radial profiles between hollow column and with internal A is presented in Figure 3.7b

at a low and a high gas velocity. It is interesting to note at low gas velocity of 0.038 m/s, the radial profiles obtained in hollow bubble column and with internal A are quite similar. This indicates minimal effect of the internal on column hydrodynamics under the dispersed bubble flow conditions at the low velocity. However, at the high gas velocity of 0.35 m/s when the column is in fully developed heterogeneous regime, the two profiles come apart.

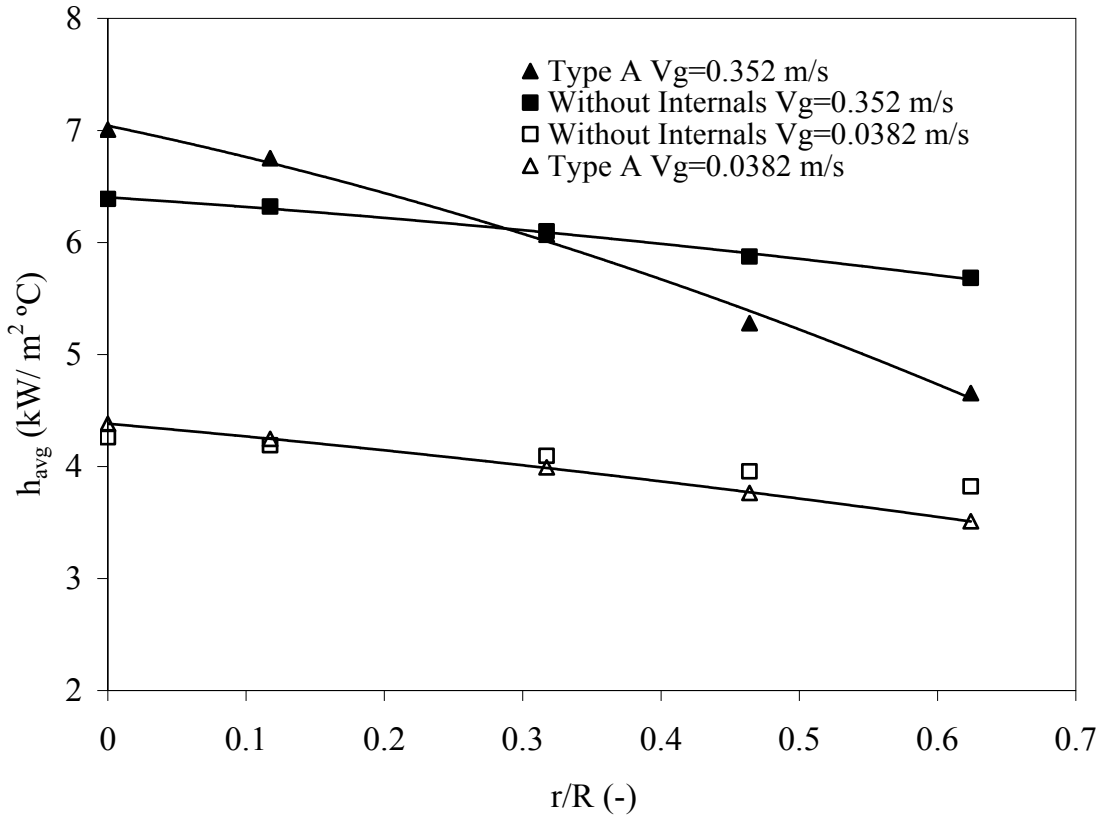


Figure 3.7b. Comparison of the radial profile of heat transfer coefficient obtained with Type A and without internals in air-water system

3.3.2 Gas Holdup and Bubbles Fractions

A comparison of gas holdups measured in bubble column with and without internals in air-water systems is shown in Figure 3.8. Highest gas holdups are obtained with type A internals (A and AB2) followed by B2 while lowest values are obtained with B1. Gas holdups obtained in absence of internal lie between internals B1 and B2. The results in presence of type A internal are consistent with the literature studies, who

used similar internals (Youssef and Al-Dahhan, 2009; Chen et al., 1999; Saxena et al., 1990). The increase in gas holdup in presence of internals can be attributed due to decrease in average bubble size and *vice versa*. With type A internals, it was visually observed in this study that smaller bubbles accumulated in the wall region. But in case of B1, bubble coalescence was visually observed close to the internal especially at low superficial gas velocities. At higher velocities visual observations could not be made as system was very turbulent. As discussed below, the analysis of bubble holdup structure based on gas disengagement studies clearly support the observations that “the average bubble size was increasing” in the presence of internal B1.

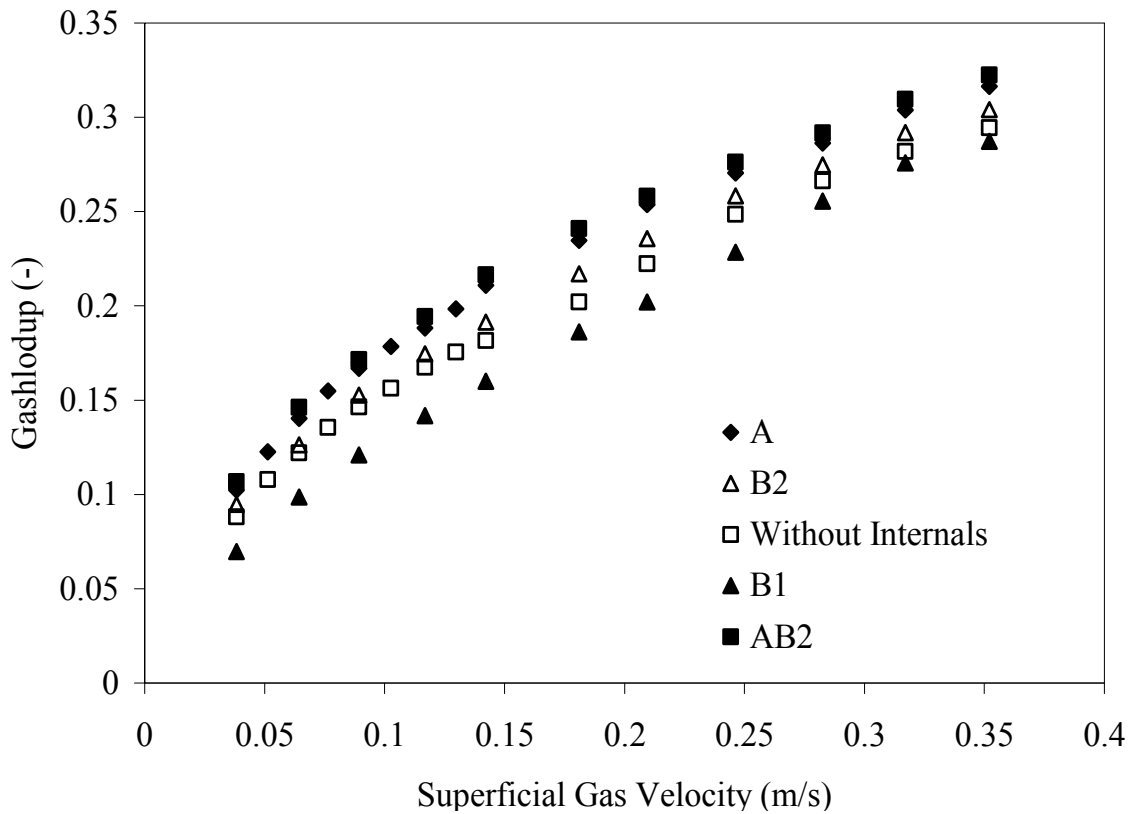


Figure 3.8. Comparison of gas holdup measurements obtained with and without internals (air-water system)

In bubble columns the small bubbles are typically less than 5 mm in diameter and large bubbles are typically 5 cm in diameter or larger (Krishna et al., 1991). Figure 3.9a and b present comparison of gas holdup of small and large bubbles obtained in bubble columns with and without internals in air-water system respectively. The detailed procedure for estimation of bubble holdup is explained elsewhere (Li and

Prakash, 2000). It is observed in Figure 3.9a, that the gas holdup of small bubble is higher in bubble columns equipped with internals A and B2 compared to hollow bubble column. This clearly shows that the average bubble size decreased in presence of these internals. But in case of bubble column equipped with internal B1, the gas holdup of small bubble is lower compared to bubble column without internals. The fact that the presence of this internal in the distributor region actually promotes the coalescence of bubbles was visually observed especially at low superficial gas velocities. From Figure 3.9b it is also interesting to note that there is no much variation in gas holdup of large bubbles fraction in bubble columns equipped with internal A, B2 and without internals. But in case of bubble column equipped with internal B1, the gas holdup of large bubble is significantly higher. This means the average bubble size is increasing.

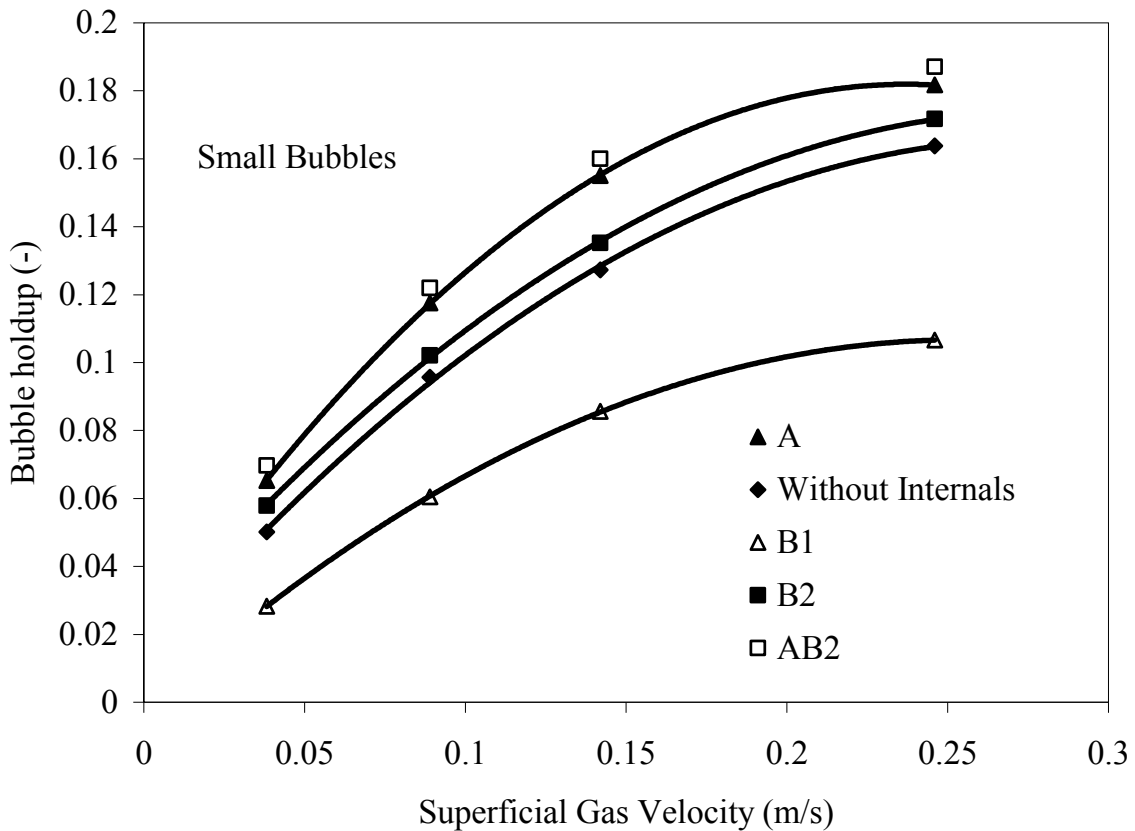


Figure 3.9a. Comparison of small bubbles holdup in bubble columns equipped with and without internals in air-water system

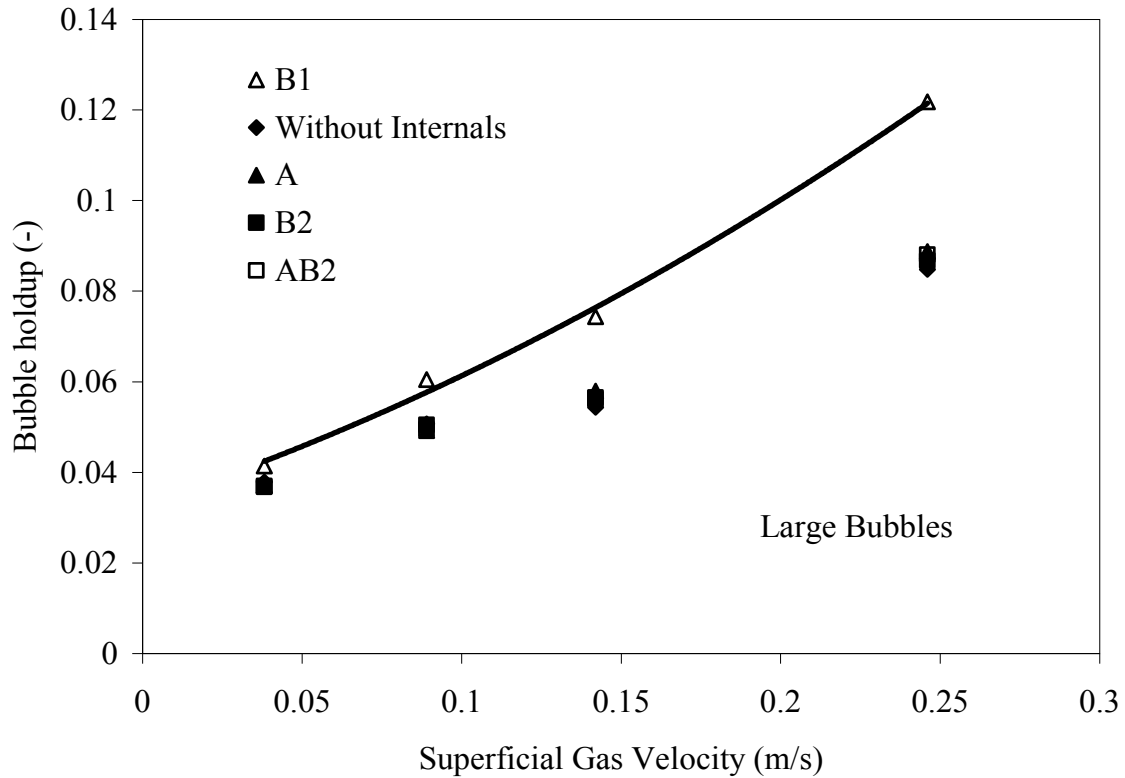


Figure 3.9b. Comparison of large bubbles holdup in bubble columns equipped with and without internals in air-water system

The fast response heat transfer probe used in this study could detect variations due to changes in bubble size distribution which could be reflected in standard deviations of time series data of the heat transfer coefficient. Figures 3.10a and b compare standard deviation of heat transfer data obtained at $r/R=0$ and $r/R=0.624$ in the bulk section of the column for different cases. The standard deviation of heat transfer coefficient in both central and wall region increases with the increase in superficial gas velocity in all cases. However, the rate of increase varies with internal type and radial location and following observations can be made.

- In the central region of column, the standard deviations are highest with internal B1, followed by type A internals while internal B2 and hollow bubble column have similar values. High values obtained with B1 can be related wider variations in bubble size distribution caused by bubble coalesce observed with this internal.

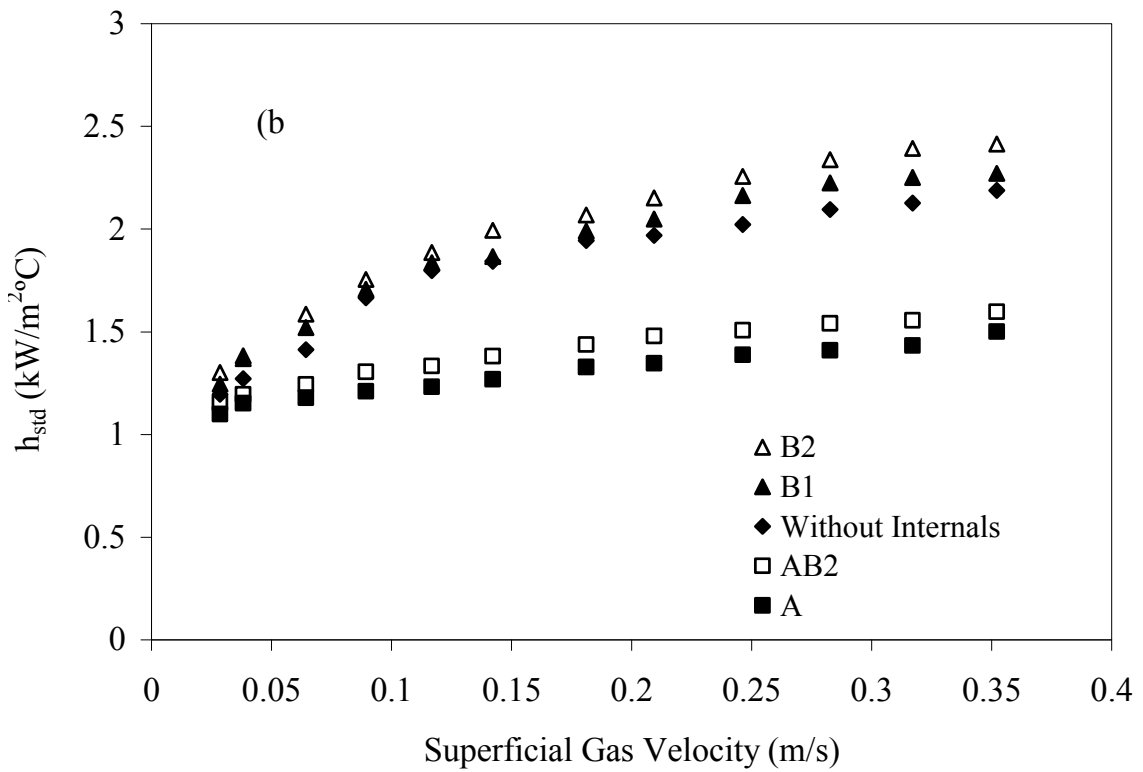
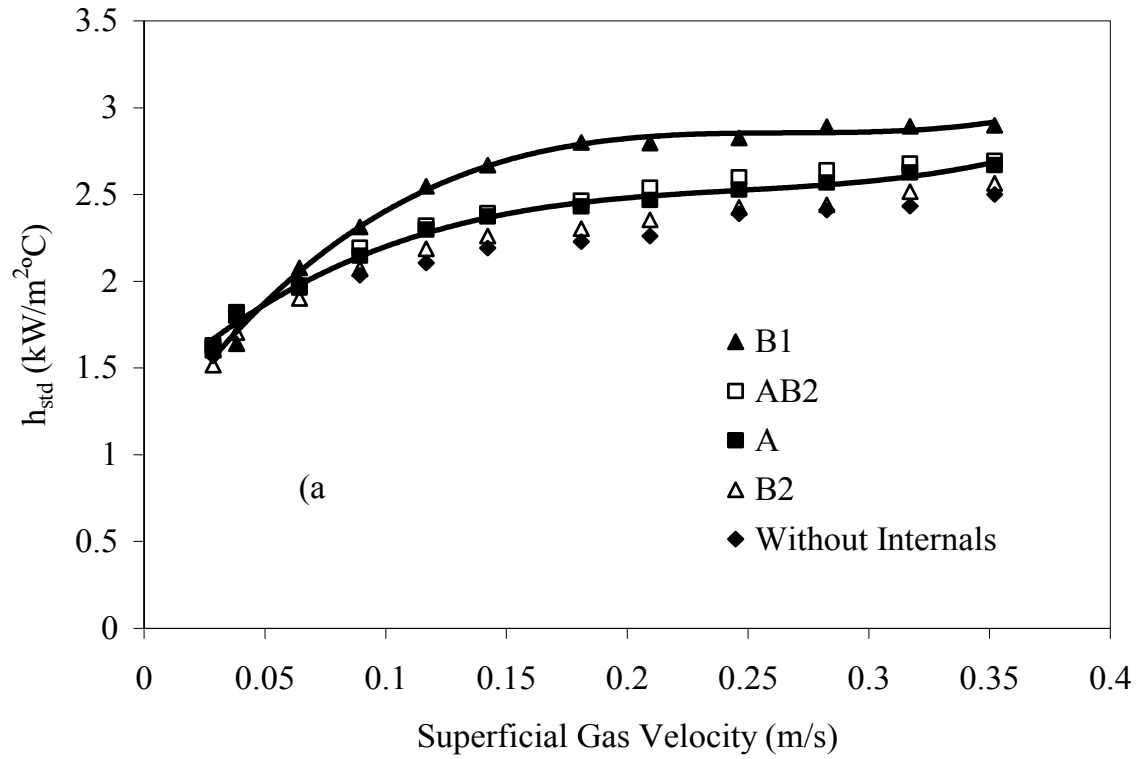


Figure 3.10. Comparison of standard deviation of heat transfer coefficient in bubble columns with and without internals in: (a) central ($r/R=0$) (b) wall region ($r/R=0.624$)

- It can also be noted that differences between different internals are generally small and become insignificant at low gas velocities (< 0.1 m/s) when bubble size distribution may not evolve significantly.
- In the wall region, it can be noted that lowest standard deviations are obtained with type A internals and there is no significant change with gas velocity. This indicates that the bubble size is small and there is little change with gas velocity.
- Higher standard deviation values obtained with type B internals and hollow bubble column point to wider bubble size distribution in the wall region for these cases.

3.3.3 Local Liquid Velocity and Related Hydrodynamics

The heat transfer probe used in this study could also detect flow direction and provide an estimation of local liquid velocity using boundary layer theory (Li and Prakash, 2002). Flow direction could be identified (upward or downward) by measuring the time averaged local heat transfer coefficients using the different orientation of the probe (upward, downward or lateral). Figure 3.11 shows the results obtained at the center ($r/R=0$) in the bulk section of the column with type A internal. The heat transfer coefficients (stagnation point) obtained with the downward orientation of the probe are higher than those obtained with the upward orientation, hence indicating upward liquid flow. Similar studies were conducted without internals and with internals. Li and Prakash (2002) developed a correlation to obtain a local liquid velocity by applying boundary layer theory to the measured stagnation point heat transfer coefficients.

$$\frac{h_{st} D_p}{k_L} = a_s (\text{Pr})^{0.4} \left(\frac{V_L D_p}{\nu_L} \right)^{0.5} \quad (3.3)$$

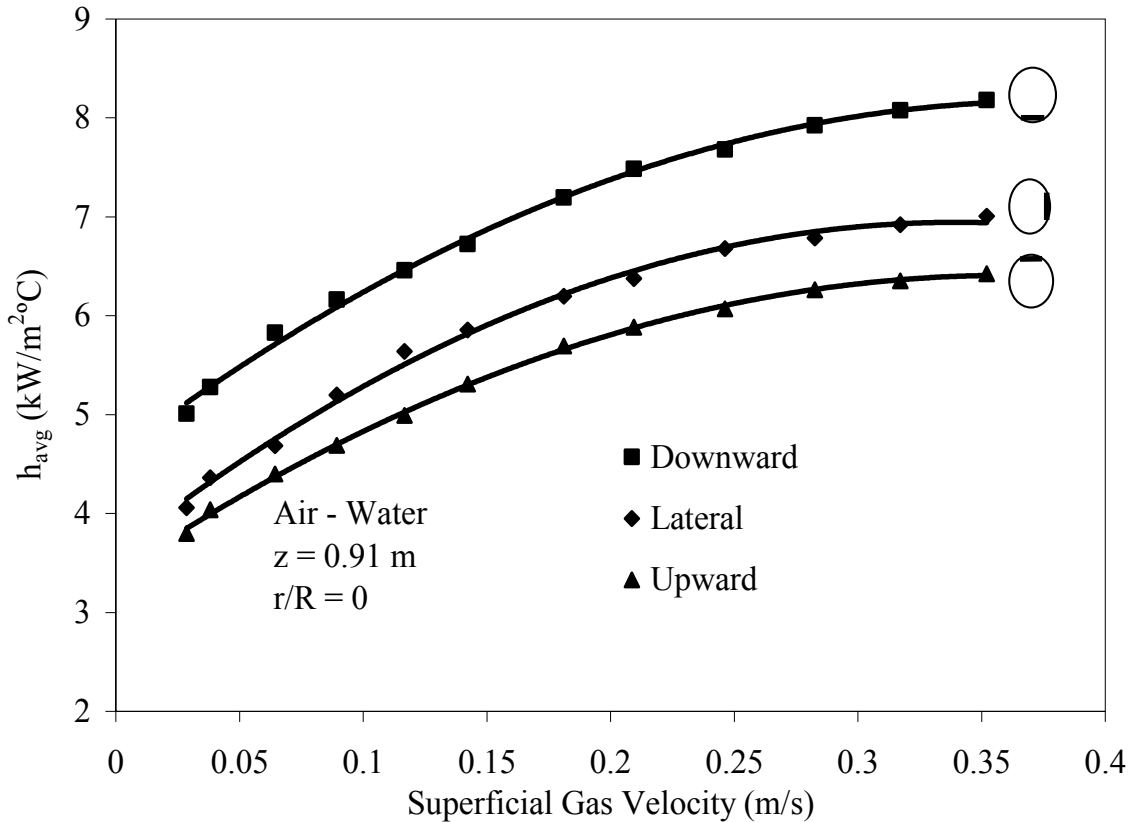


Figure 3.11. Local heat transfer coefficients for different probe orientations in presence of internals Type A in air-water system ($r/R = 0$)

The above equation gives good prediction of liquid velocities in different diameter bubble columns as reported by Li and Prakash (2002) and Jhawar and Prakash (2011). In the above equation, the value of factor a_s depends on several aspects such as probe design, orientation etc. Jhawar and Prakash (2011), recommended value of factor a_s to be 0.7 based on data from their and other literature studies. The results obtained with this procedure at the column centre are shown in Figure 3.12. It is observed that highest local liquid velocities are obtained with internal A and AB2, followed by internal B2. Lowest center line liquid velocities are obtained with internal B1 but the values are quite close to hollow bubble column which tend to be slightly higher. Higher central liquid velocity with type A internal is a result of its vertical tube bundle design creating a funneling effect for gas and entrained liquid flow. B type internals have horizontal blades occupying part of column cross section. Internal B1

is placed close to the distributor in developing zone, where rising bubble clusters and plumes need to pass through the constricted opening, altering bubble dynamics. Internal B2 was placed at higher elevation where bulk region turbulence seems to be helping bubble breakup and dispersion. This indicates existence of different hydrodynamic conditions in bubble columns equipped with different internals. Even though average bubble size was found to increase in bubble columns equipped with internal B1, the turbulence intensity seems to decrease as a result of redispersed flow by the internal.

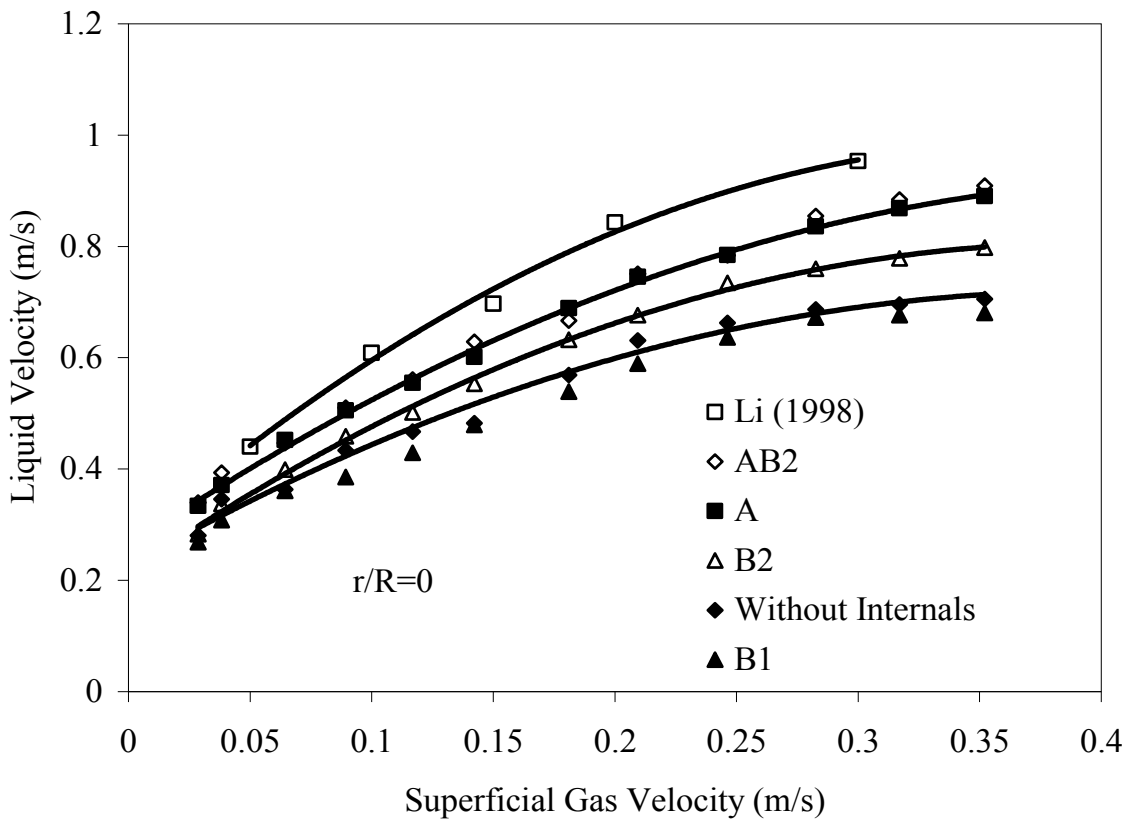


Figure 3.12. Comparison of liquid velocities estimated at the center in bulk section of the column by equation (3.3) in air water system

Liquid velocities in the wall region of bubble columns with and without internals are shown in Figure 3.13. It is observed that trends are quite different compared to central region. The liquid velocities obtained in the wall region are higher with type B internals compared to type A internal. It is also interesting to note that a difference

between internal types is larger and distinct in the wall region. These results indicate important role of internals in altering radial liquid profile in the column and hence column hydrodynamics. The steepness of radial profile is indicative of backmixing effects in the column. Larger the difference or sharper the steep, greater is the backmixing.

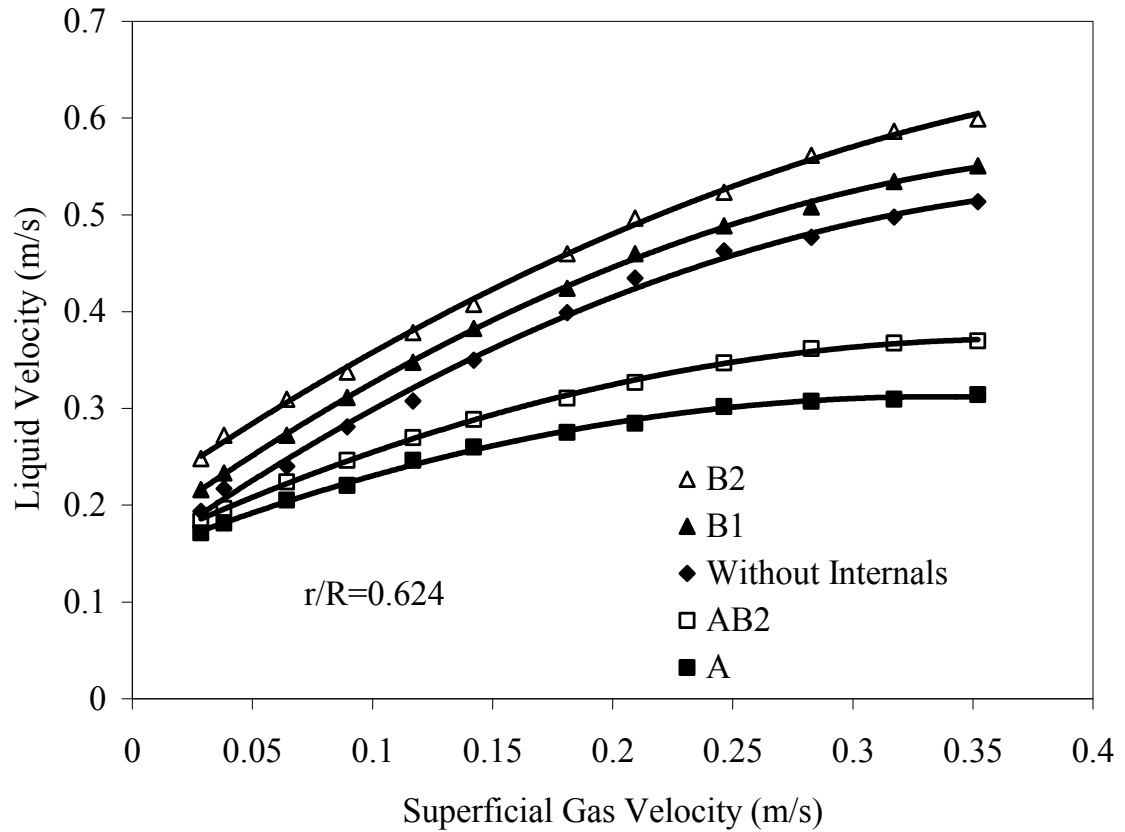


Figure 3.13. Comparison of liquid velocities estimated at the wall ($r/R = 0.624$) in bulk section of the column by equation (3) in air water system

A plot of difference between radial liquid velocities for different internals is presented in Figure 3.14. It can be seen that largest differences are obtained with type A followed by AB2, hollow column B2 and B1 in that order. In addition, following important observations can be made.

- Combining B2 with internal A reduces the differential velocity thereby reducing back mixing especially at higher gas velocities.

- Values with internal B2 are significantly lower than hollow bubble column below gas velocity of 0.15 m/s but approach the hollow column values at higher velocities. This indicates that similar column hydrodynamics are achieved at these high velocities likely due similar bubble breakup and coalescence process.
- Internal B1 remains lower than hollow bubble column for all gas velocities indicating importance of location from the gas distributor.

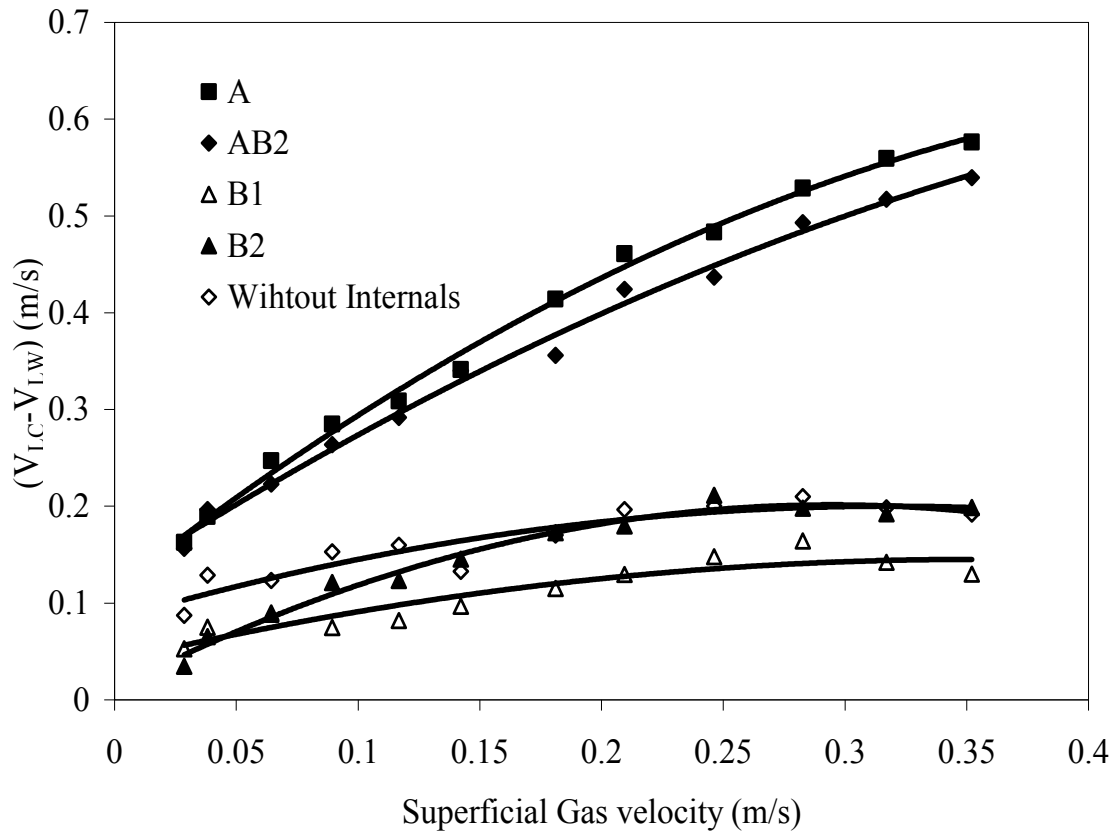


Figure 3.14. Comparison of differential radial liquid velocities with different internals in bulk section of the column

This suggests that with presence of type B internals, there is improvement in column hydrodynamics radially and more uniform mixing is achieved at different radial locations due to uniformity in bubble size and population. This is desired as we can locate the heat transfer surfaces away from the central region there by minimizing the

disturbance to flow and achieving higher heat transfer rates with combination of Type A and Type B internals.

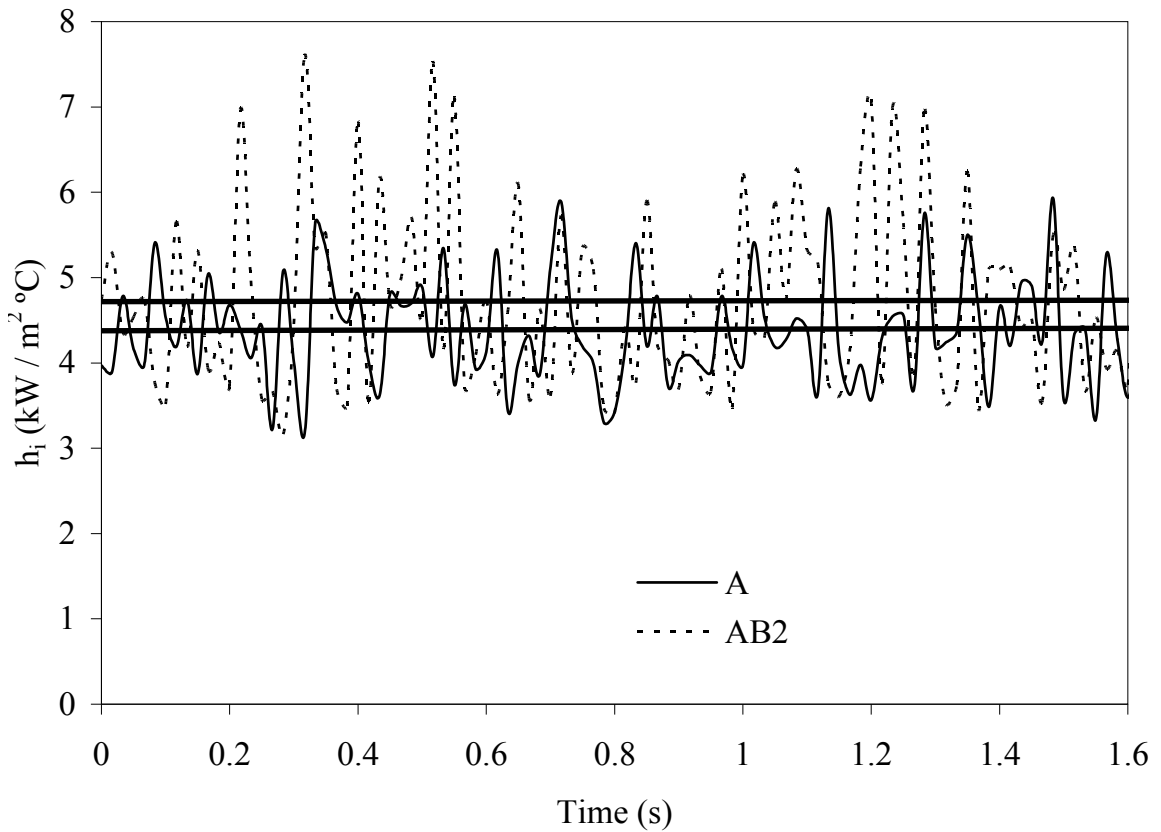


Figure 3.15. Comparison of time series heat transfer coefficients obtained with internals A and AB2 in the annular region

The instantaneous heat transfer coefficient obtained in the annular region in presence of internals A and combination of internal A and B2 (AB2) is presented in Figure 3.15. It is observed that in bubble column equipped with type AB2 internal the heat transfer coefficient peaks in wall region are larger compared to bubble column equipped with internal A. This could be due to passage of few large bubbles in the annular region in bubble columns with AB2. Visual observations also supports this, periodically large bubbles seemed escaping in the annular region because of presence of bubble diffuser B2. Given its design, internal B2 would assist with some flow deflection over the column cross section. This suggests that by using different combination of internals column hydrodynamics can be altered and higher heat transfer can be achieved. The radial improvement in column hydrodynamics with

internal B2 is advantageous, as the combination AB2 improves the heat transfer in annular region.

3.3.4 Estimation of Centerline Liquid Velocity for Type A Internal

The type A internal is close to a concentric wall draft tube type internal air lift reactor which has been well investigated in literature studies (Koide et al., 1983; Koide et al.; 1985; Muroyama et al, 1985; Chisti et al., 1988; Choi and Lee, 1992; Choi et al., 1996; Heijnen et al., 1997). However, there is difference since air lift reactors often have solid wall draft tube while internal A has perforations due to inter-tube gaps. Performing energy balance of an airlift reactor, the energy balance can be written as:

Rate of energy input due to isothermal expansion of gas in the reactor is equal to summation of rate of energy dissipation due to bubble wake, stagnant gas in the downcomer, energy loss due to friction in the riser and downcomer and energy loss due to fluid recirculation at top and bottom of the reactor

The above expression can be written as

$$E_i = E_R + E_D + E_T + E_B + E_F \dots \dots \dots (3.4)$$

Where E_i = Rate of energy input due to isothermal gas expansion

$$E_i = QP_h \ln \left(1 + \frac{\rho_D g h_D}{P_h} \right) \dots \dots \dots (3.5)$$

E_R = Energy dissipation in riser because of bubble wake

E_D = Energy loss due to drag of gas on liquid in downcomer

E_T and E_B = Energy loss due to fluid recirculation at the top and bottom of the reactor

E_F = Energy loss due to wall friction in riser and downcomer.

For low viscosity fluids in airlift reactors the wall (skin) friction energy losses is negligible compared to other energy losses in equation (3.4) (Chisti et al., 1988). This

has been contradicted by Heijnen et al., (1997), who found that the wall friction is significant and depends on aspect ratio of airlift reactor based on draft tube height and effective column height for liquid circulation. But results predicted by Heijnen et al., (1997) using frictional loss at top and wall for data by Livingston and Zhang (1993) are almost similar to those predicted by Chisti et al., (1988) neglecting the loss at top and wall. Thus we will assume that friction energy losses at the wall are negligible. Therefore the equation (3.4) can be rewritten as:

$$E_i = E_R + E_D + E_T + E_B \dots\dots\dots (3.6)$$

Energy loss due to bubble wake in riser is obtained by an energy balance in riser using the liquid in riser as control volume. We know that in the riser the flow is in upward direction means the rising bubbles will gain potential energy, but there will be loss of pressure energy. Assuming the gas is introduced in riser.

Therefore:

$E_i = E_R - \text{Pressure energy loss} + \text{Potential energy gain}$

$$E_i = E_R - U_{Lr} A_r (\rho_L g h_D (1 - \epsilon_r) - \rho_L g h_D) \dots\dots\dots (3.7)$$

The equation (3.7) can be further simplified as

$$E_i = E_R + (\rho_L g h_D U_{Lr} A_r \epsilon_r) \dots\dots\dots (3.8)$$

Rearranging above equation

$$E_R = E_i - (\rho_L g h_D U_{Lr} A_r \epsilon_r) \dots\dots\dots (3.9)$$

Energy loss due to drag of gas on liquid in downcomer (E_D) is obtained by an energy balance in downcomer using the liquid in downcomer as control volume. In downcomer it will be reverse of riser (flow is downward) means there is a pressure energy gain and potential energy loss. Assuming no gas is introduced in downer. In practicality for system like ours, due to its design there will be some gas being

introduced through downcomer, but it will be very small compared to that being introduced in riser, thus assumption seems to be valid.

$0 = E_D + \text{Pressure energy loss} - \text{Potential energy gain}$

$$0 = E_D + U_{Ld} A_d (\rho_L g h_D (1 - \varepsilon_d) - \rho_L g h_D) \dots\dots\dots (3.10)$$

The equation (3.9) can be further simplified as

$$E_D = U_{Ld} A_d (\rho_L g h_D \varepsilon_d) \dots\dots\dots (3.11)$$

The energy loss due to fluid recirculation at the top and bottom of the reactor is calculated in a similar way as for pipe flow (Chisti et al., 1988). But in reality this will be very different for the complex system as ours, where the draft tube is not solid and has perforations (approx. 4.4 mm). This will allow some liquid and most small bubbles to escape to the downcomer. It is known that the average bubble size decreases in presence of internals type A (Youssef and Al-Dahhan, 2009). The reverse flow is not possible because of the pressure difference between riser and downcomer. The bottom and top base plate supporting tube bundle also affects the flow pattern. More over the fluid recirculation is greater at the bottom of the column and decreases as its distance increases from the bottom and is visually observed in this study. It is also observed that some of the entrained bubble from the downcomer in the bottom of the reactor re-enters the riser along with the introduced gas. This makes the hydrodynamics very complex in our system and makes it difficult to model. For the sake of simplicity we will model it based on pipe flow and modify later based on the experimental data and assumptions.

Therefore:

$$E_B + E_T = \frac{1}{2} \rho_L \left[V_{Lr}^3 K_T A_r (1 - \varepsilon_r) + V_{Ld}^3 K_B A_d (1 - \varepsilon_d) \right] \dots(3.12)$$

Where, K_T and K_B are the dimensionless friction loss coefficients at the top and bottom connecting sections of the riser and downcomer in the reactor. The V_{Lr} and V_{Ld} in equation (3.12) are the interstitial liquid velocity in riser and downcomer. From superficial liquid velocity in riser and downcomer the interstitial liquid velocity can be calculated using following equations:

$$V_{Lr} = \frac{U_{Lr}}{1 - \varepsilon_r} \dots\dots\dots (3.13)$$

$$V_{Ld} = \frac{U_{Ld}}{1 - \varepsilon_d} \dots\dots\dots (3.14)$$

The equation of continuity for liquid flow between riser and downcomer can be written as:

$$A_r(1 - \varepsilon_r)V_{Lr} = A_d(1 - \varepsilon_d)V_{Ld} \dots\dots\dots(3.15)$$

$$A_r U_{Lr} = A_d U_{Ld} \dots\dots\dots (3.16)$$

By substituting V_{Lr} and V_{Ld} values from equation (3.13) and (3.14) in equation (3.12) we get

$$E_B + E_T = \frac{1}{2} \rho_L \left[\frac{U_{Lr}^3 K_T A_r}{(1 - \varepsilon_r)^2} + \frac{U_{Ld}^3 K_B A_d}{(1 - \varepsilon_d)^2} \right] \dots\dots\dots(3.17)$$

By substituting equation (3.16) in equation (3.17) and rearranging we get

$$E_B + E_T = \frac{1}{2} \rho_L U_{Lr}^3 A_r \left[\frac{K_T}{(1 - \varepsilon_r)^2} + K_B \left(\frac{A_r}{A_d} \right)^2 \frac{1}{(1 - \varepsilon_d)^2} \right] \dots\dots\dots (3.18)$$

By substituting equation (3.9), (3.11) and (3.18) in equation (3.6) we get

$$E_i = E_i - (\rho_L g h_D U_{Lr} A_r \varepsilon_r) + U_{Ld} A_d (\rho_L g h_D \varepsilon_d) + \frac{1}{2} \rho_L U_{Lr}^3 A_r \left[\frac{K_T}{(1 - \varepsilon_r)^2} + K_B \left(\frac{A_r}{A_d} \right)^2 \frac{1}{(1 - \varepsilon_d)^2} \right] \dots\dots\dots (3.19)$$

By substituting equation (3.16) in equation (3.19) and rearranging we can write an equation for superficial riser velocity in airlift reactors as

$$U_{Lr} = \left[\frac{2gh_D (\varepsilon_r - \varepsilon_d)}{\frac{K_T}{(1 - \varepsilon_r)^2} + K_B \left(\frac{A_r}{A_d} \right)^2 \frac{1}{(1 - \varepsilon_d)^2}} \right]^{0.5} \dots\dots\dots (3.20)$$

Equation (3.20) is the general equation for prediction of liquid velocities in airlift reactors of different configurations. The diameter effect of riser is incorporated in terms of superficial riser liquid velocity. The diameters of riser and downer have significant impact on column hydrodynamics. The ratio (A_r/A_d) does not define the geometry as we can get the same ratio for different configuration.

Chisti et al., (1988) assumed that for concentric tube type internal loop airlift reactor, the energy loss at the top connecting section between riser and downcomer will be small relative to that in the bottom section. This is because the top of the draft tube likely will be an open channel as opposed to constricted flow path at the bottom due to fluid recirculation. The equation (3.20) will be reduced as

$$U_{LR} = \left[\frac{2gh_D (\varepsilon_r - \varepsilon_d)}{K_B \left(\frac{A_r}{A_d} \right)^2 \frac{1}{(1 - \varepsilon_d)^2}} \right]^{0.5} \dots\dots\dots (3.21)$$

The above assumption may not be valid in this case, especially at low gas velocities when the tube bundle is above the gas-liquid dispersion height. It will restrict the fluid flow and there will be energy loss. Also the design of tube bundle A, because of its support plate at top and bottom will also have some impact. But at high velocities the resistance to fluid flow at the top will become negligible compared to the energy loss at the bottom due to increased gas-liquid height and perforation in tube bundle. So the above assumption will affect the liquid velocities at low superficial gas velocities. But our main focus is for high superficial gas velocity (fully developed heterogeneous flow regime), so the above assumption may be valid for our case. K_B is the dimensionless frictional loss coefficient at the riser bottom. Literature studies have reported estimation procedures for conventional airlift reactor (Heijnen et al., 1997; Chisti, et al., 1988).

The tube bundle used in this study, however has different geometry due to inter-tube spacing of 4.4 mm, so there could be flow of liquid and small bubbles from center to the downer region, reverse flow is less likely due to higher pressure inside the bundle. Most of the small bubble will be in the downer region. Thus following assumptions were made for gas holdup based on experimental observations.

- All of large bubble holdup and about 30% of small bubbles holdup is in the riser section.
- Downer has the remaining small bubbles holdup and no large bubbles.

Values of frictional loss coefficient (K_B) in equation (3.21) were first estimated using literature correlations recommended for conventional airlift reactor (Heijnen et al., 1997; Chisti, et al., 1988). However, predicted values of liquid velocities were significantly higher. Since, the tube bundle used in this study has several differences, it was decided to use a value obtained from experimental data. Key differences are discussed below.

- Tube bundle has perforations which allow some liquid and most small bubbles to escape to the downcomer along the length of the tube bundle. This will have impact on riser velocities and make the hydrodynamics more complex.
- It was visually observed that the fluid recirculation was very high at the bottom of the column and decreased as the distance increased from the bottom. This indicates bypassing effects thus reducing velocity.

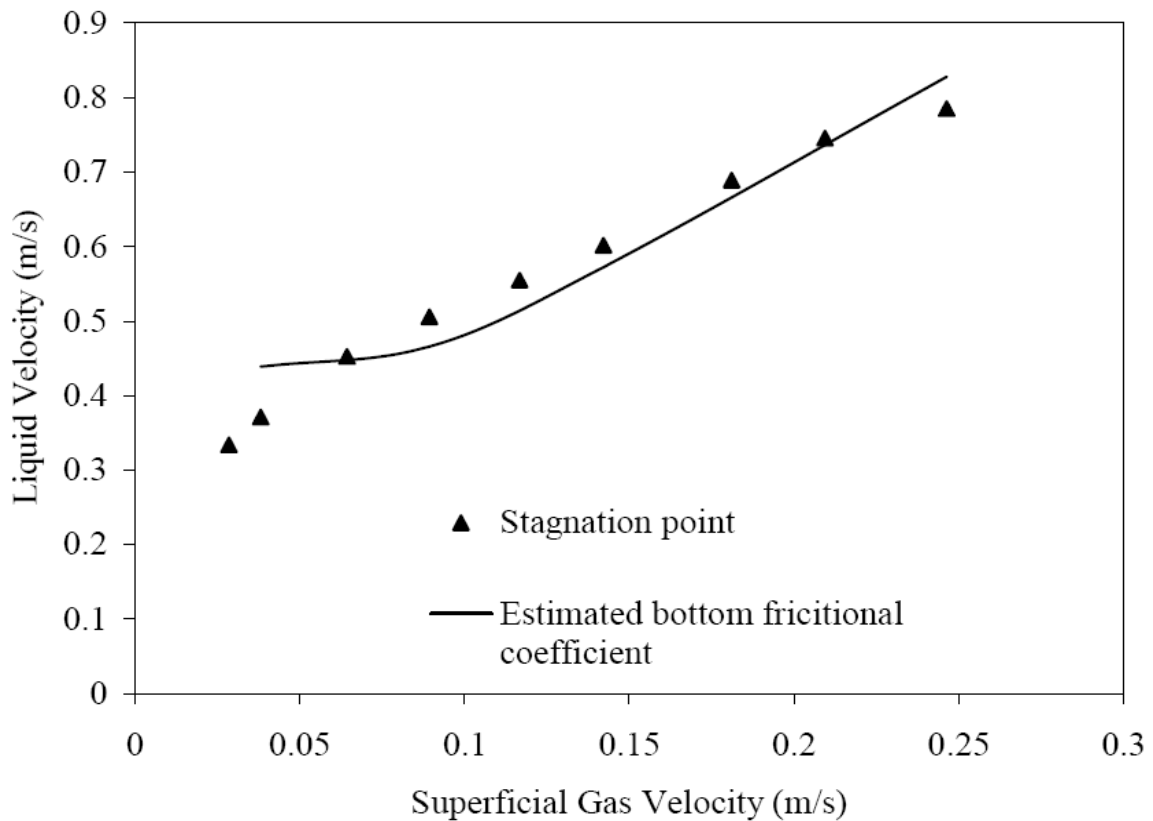


Figure 3.16. Comparison of estimated liquid circulation velocity in core region in bubble columns equipped with Type A internals

A constant value of K_B could be used for gas velocities above 0.05 m/s. This procedure predicted liquid velocity with average error less than 10% as shown in figure 3.16. For low gas velocities, K_T cannot be assumed negligible since the tube bundle was above gas-liquid dispersion height. This resulted in high error in estimated superficial rise velocities at low gas velocities.

3.4 Conclusions

The presences of tube bundle type internal (type A) used in this study results in increase in heat transfer coefficient in the central region, but in wall region the heat transfer coefficients are lower than those obtained in hollow bubble columns or with six-blade baffle (type B). The combination of internals AB2 improved heat transfer coefficient in the wall region compared to internal A alone. The radial profile of heat transfer coefficient was less steeper with combined AB2 internal compared to internal A alone. In case of AB2, given the design, internal B2 would assist with some flow deflection over the column cross section thus limiting the funneling action of type A internal. This study clearly points to alterations in flow pattern, mixing intensities and general hydrodynamics due to insertion of internals in a hollow bubble column. The location of internals can alter the hydrodynamic conditions as observed with change in axial position of B type internal (B1 and B2) indicating the need to consider local variations in the column hydrodynamic behavior for design and location of internals. The average bubble size decreased in presence of internals A and B2, but a reverse trend is found in bubble columns with B1.

3.5 Notations

Δx	Thickness of the thermal barrier, (m)
A	Heat transfer area, (m ²)
A_d	Cross-sectional downer area (m ²)
A_r	Cross-sectional riser area (m ²)
a_s	Constant in equation (3.3)
D_p	Probe diameter (m)
E_B	Energy loss due to fluid recirculation at the bottom of the reactor (W)
E_D	Energy loss due to drag of gas on liquid in downcomer (W)
E_F	Energy loss due to wall friction in riser and downcomer (W)
E_i	Rate of energy input due to isothermal gas expansion (W)
E_R	Energy dissipation in riser because of bubble wake (W)

E_T	Energy loss due to fluid recirculation at the top of the reactor (W)
g	Acceleration due to gravity (m/s^2)
h	Heat transfer coefficient, ($kW/m^2\ ^\circ C$)
h_D	Gas-liquid dispersion height (m)
k	Thermal conductivity, (W/m K)
K_B	Dimensionless friction loss coefficients at the bottom
K_T	Dimensionless friction loss coefficients at the top
N	Number of data points
P_h	Reactor head space pressure (N/m^2)
Pr	Prandtl number, $\left(\frac{C_{p,l} \mu_l}{k_l} \right)$
Q	Gas flow rate (m^3/s)
q	Heat flow rate, (kW)
r	Radial location, (m)
R	Radius of the column, (m)
T	Temperature, ($^\circ C$)
U_{Ld}	Superficial downcomer liquid velocity (m/s)
U_{Lr}	Superficial riser liquid velocity (m/s)
V	Superficial velocity (m/s)
V_{Ld}	Interstitial liquid velocity in downcomer (m/s)
V_{Lr}	Interstitial liquid velocity in riser (m/s)
z	Axial location from the bottom of the column, (m)

Greek Symbols

ε	phase holdup (-)
ν	Kinematic viscosity (m^2/s)
ρ	Density (kg/m^3)
ρ_D	Dispersion density (kg/m^3)
ε_d	Downer holdup (-)
ε_r	Riser holdup (-)

Subscripts

avg	Average
b	Bulk
G	Gas
C	Center
W	Wall
i	Instantaneous
L	Liquid
Su	Surface
st	Stagnation point

3.6 References

- Chen, J., Li, F., Degaleesan, S., Gupta, P., Al-Dahhan, M.H., Dudukovic, M.P., Toseland, B.A., 1999. Fluid dynamic parameters in bubble columns with internals. *Chem. Eng. Sci.* 54, 2187-2197.
- Chen, R.C., Reese, J., Fan, L.S., 1994. Flow structure in a three-dimensional bubble column and three-phase fluidized bed. *AIChE Journal*. 40, 1093-1104.
- Chisti, Y., Halard, B., Moo-Young, M., 1988. Liquid Circulation in Airlift Reactors. *Chemical Engineering Science*. 43, 451-457.
- Choi, K.H., Chisti, Y., Moo-Young, M., 1996. Comparative evaluation of hydrodynamic and gas-liquid mass transfer characteristics in bubble column and airlift slurry reactors. *Chemical Engineering Journal*. 62, 223-229.
- Choi, K.H., Lee, W.K., 1992. Behavior of gas bubbles in a concentric cylindrical airlift column. *Korean Journal of Chemical Engineering*, 9, 66-73.
- Deckwer, W.D., 1980. On the mechanism of heat transfer in bubble column reactors. *Chemical Engineering Science*. 35, 1341-1346.
- Deckwer, W.D., 1992. Bubble column reactors, V. Cottrell (Trans.), R.W. Field (Ed.), John Wiley and Sons, England.
- Deckwer, W.D., Schumpe, A., 1993. Improved tools for bubble column reactor design and scale-up. *Chemical Engineering Science*. 48, 889-911.

Duduković, M.P., Devanathan, N., 1992. Bubble column reactors: some recent developments. *Nato ASI Series E Applied Sciences*. 225, 353-377.

Duduković, M.P., Larachi, F., Mills, P.L., 2002. Multiphase catalytic reactors: a perspective on current knowledge and future trends. *Catalysis Reviews*. 44, 123-246.

Fan, L. S., 1989. *Gas-liquid-solid fluidization engineering*. Butterworths, Stoneham, MA.

Forret, A., Schweitzer, J.M., Gauthier, T., Krishna, R., Schweich, D., 2003. Influence of scale on the hydrodynamics of bubble column reactors: an experimental study in columns of 0.1, 0.4 and 1 m diameters. *Chemical Engineering Science*. 58, 719-724.

Heijnen, J.J., Hols, J., van der Lans, R.G.J.M, van Leeuwen, H.L.J.M, Mulder, A., Weltevrede, R., 1997. A simple hydrodynamic model for the liquid circulation velocity in a full-scale two- and three-phase internal airlift reactor operating in the gas recirculation regime. *Chemical Engineering Science*, 52, 2527-2540.

Jhavar, A.K., Prakash, A., 2007. Analysis of local heat transfer coefficient in bubble column using fast response probes. *Chemical Engineering Science*. 62, 7274-7281.

Jhavar, A.K., Prakash, A., 2011. Influence of bubble column diameter on local heat transfer and related hydrodynamics. *Chemical Engineering Research and Design*. 89, 1996-2002.

Joshi, J.B., Sharma, M.M., Shah, Y.T., Singh, C.P.P., Ally, M., Klinzing, G.E., 1980. Heat transfer in multiphase contactors. *Chemical Engineering Communications*. 6, 257-271.

Kast, W., 1962. Analyse des wärmeübergangs in blasensäulen. *International Journal of Heat and Mass Transfer*. 5, 329-336.

Kluytmans, J.H.J., van Wachem, B.G.M., Kuster, B.F.M., Schouten, J.C., 2001. Gas holdup in a slurry bubble column: influence of electrolyte and carbon particles. *Industrial and Engineering Chemistry Research*. 40, 5326-5333.

Koide, K., Horibe, K., Kawabata, H., Ito, S., 1985. Gas-holdup and volumetric liquid-phase mass transfer coefficient in solid-suspended bubble column with draft tube. *Journal of Chemical Engineering Japan*. 18, 248-254.

Koide, K., Kurematsu, K., Iwamoto, S., Horibe, K., 1983. Gas-holdup and volumetric liquid-phase mass transfer coefficient in bubble column with draft tube with gas dispersion into tube. *Journal of Chemical Engineering Japan*. 16, 407-413.

Krishna, R., Wilkinson, P. M., Van Dierendonck, L.L. A model for gas holdup in bubble columns incorporating the influence of gas density on flow regime and transitions. *Chemical Engineering Science*, 46, 3491-2496.

Krishna, R., Urseanu, M.I., van Baten, J.M., Ellenberger, J., 1999. Influence of scale on the hydrodynamics of bubble columns operating in the churn-turbulent regime: experiment vs. Eulerian simulations. *Chemical Engineering Science*. 54, 4903-4911.

Kulkarni, A.A., Joshi, J.B., Kumar, V.R., Kulkarni, B.D., 2001. Application of multiresolution analysis for simultaneous measurement of gas and liquid velocities and fractional gas hold-up in bubble column using LDA. *Chemical Engineering Science*. 56, 5037-5048.

Larachi, F., Desvigne D., Donnat, L., Schweich, D., 2006. Simulating the effects of liquid circulation in bubble columns with internals. *Chemical Engineering Science*. 61, 4195-4206.

Li, H., 1998. Heat transfer and hydrodynamics in a three-phase slurry bubble column. Thesis, PhD University of Western Ontario, London, Ontario.

Li, H., Prakash, A., 1997. Heat transfer and hydrodynamics in a three-phase slurry bubble column. *Industrial and Engineering Chemistry Research*. 36, 4688-4694.

Li, H., Prakash, A., 2000. Influence of slurry concentrations on bubble population and their rise velocities in a three-phase slurry bubble column. *Powder Technology*. 113, 158-167.

Li, H., Prakash, A., 2001. Survey of heat transfer mechanisms in a slurry bubble column. *Canadian Journal of Chemical Engineering*. 79, 717-725.

Li, H., Prakash, A., 2002. Analysis of flow patterns in bubble and slurry bubble columns based on local heat transfer measurements. *Chemical Engineering Journal*. 86, 269-276.

Li, H., Prakash, A., Margaritis, A., Bergougnou, M.A., 2003. Effects of micron-sized particles on hydrodynamics and local heat transfer in a slurry bubble column. *Powder Technology*. 133, 171-184.

Livingston, A.G., Zhang, S.F., 1993. Hydrodynamic behaviour of three-phase (gas-liquid-solid) airlift reactors. *Chemical Engineering Science*. 48, 1641-1654.

Mudde, R.F., Groen, J.S., Van Den Akker, H.E.A., 1997. Liquid Velocity field in a bubble column: LDA experiments. *Chemical Engineering Science*. 52, 4217-4224.

- Muroyama, K., Mitani, Y., Yasunishi, A., 1985. Hydrodynamic characteristics and gas-liquid mass transfer in a draft tube slurry reactor. *Chemical Engineering communications*, 34, 87-98.
- Prakash, A., Margaritis, A., Li, H., Bergougnou, M.A., 2001. Hydrodynamics and local heat transfer measurements in a bubble column with suspension of yeast. *Biochemical Engineering Journal*. 9, 155-163.
- Prakash, A., Margaritis, A., Saunders, R.C., Vijayan, S., 1999. Ammonia removal at high concentrations by the cyanobacterium *plectonema boryanum* in a photobioreactor system. *Canadian Journal of Chemical Engineering*. 77, 99-106
- Reese, J., Fan, L.S., 1994. Transient flow structure in the entrance region of a bubble column using particle image velocimetry. *Chemical Engineering Science*. 49, 5623-5636.
- Riquarts, H.P., 1981. Strömungsprofile, impulsaustausch und durchmischung der flüssigen phase in bläsensäulen. *Chem Ing Techn*. 53, 60-61.
- Saxena, S.C., Patel, B.B., 1990. Heat transfer and hydrodynamic investigations in a baffled bubble column: air-water-glass bead system. *Chemical Engineering Communications*. 98, 65-88.
- Saxena, S.C., Rao, N.S., 1993. Estimation of gas holdup studies in a slurry bubble column with internals: nitrogen-therminol-magnetite system. *Powder Technology* 75, 153-158.
- Saxena, S.C., Rao, N.S., Saxena, A.C., 1992. Heat transfer and gas holdup studies in a bubble column: air-water-sand system. *The Canadian Journal of Chemical Engineering*. 70, 33-41.
- Saxena, S.C., Rao, N.S., Saxena, A.C., 1990a. Heat transfer from a cylindrical probe immersed in a three-phase slurry bubble column. *Chemical Engineering Journal*. 44, 141-156.
- Saxena, S.C., Rao, N.S., Saxena, A.C., 1990b. Heat-transfer and gas-holdup studies in a bubble column: air-water-glass bead system. *Chemical Engineering Communication*. 96, 31-55.
- Saxena, S.C., Vadivel, R., Saxena, A.C., 1989. Gas holdup and heat transfer from immersed surfaces in two- and three- phase systems in bubble columns. *Chemical Engineering Communications*. 85, 63-83.
- Schlüter, S., Steiff, A., Weinspach, P.M., 1995. Heat transfer in two- and three-phase bubble column reactors with internals. *Chemical Engineering and Processing*. 34, 157-172.

Schumpe, A., Grund, G., 1986. The gas disengagement technique for studying gas holdup structure in bubble columns. *The Canadian Journal of Chemical Engineering*. 64, 891-896.

Shah, Y.T., Kelkar, B.G., Godbole, S.P., Deckwer, W.D., 1982. Design parameters estimations for bubble column reactors. *AIChE Journal*. 28, 353-379.

Su, X., Hol, P.D., Talcott, S.M., Staudt, A.K., Heindel, T.J., 2006. The effect of bubble column diameter on gas holdup in fiber suspensions. *Chemical Engineering Science*. 61, 3098-3104.

Ueyama, K., Morooka, S., Koide, K., Kaji, H., Miyauchi, T., 1980. Behavior of gas bubbles in bubble columns. *Industrial and Engineering Chemistry Process Design and Development*. 19, 592-599.

Wilkinson, P.M., Spek, A.P., van Dierendonck, L.L., 1992. Design parameters estimation for scale-up of high-pressure bubble columns. *AIChE Journal*. 38, 544-554.

Wu, C., Al-Dahhan, M.H., Prakash, A., 2007. Heat transfer coefficients in a high-pressure bubble column. *Chemical Engineering Science*. 62, 140-147.

Youssef, A.A., Al-Dahhan, M.H., 2009. Impact of Internals on the Gas Holdup and Bubble Properties of a Bubble Column. *Industrial and Engineering Chemistry Research*. 48, 8007-8013.

Zahradník, J., Fialová, M., Růžička, M., Drahoš, J., Kaštánek, F., 1997. Duality of the gas-liquid flow regimes in bubble column reactors. *Chemical Engineering Science*. 52, 3811-3826.

CHAPTER 4. INVESTIGATIONS OF HEAT TRANSFER PROFILE AND HYDRODYNAMICS IN A SLURRY BUBBLE COLUMN INSERTED WITH INTERNALS

Abstract

Local heat transfer and column hydrodynamics are investigated in a 0.15m ID bubble column with and without solids in presence of internals of different configurations. Local heat transfers variations are measured with a fast response probe capable of capturing bubble dynamics as well detect local flow direction. Tap water is the liquid phase and the solid particles used are 49 μ m glass beads and their concentration is varied up to 20 vol. %. The static height of the slurry was maintained around 1.45m. Gas phase used is oil free compressed air and its flow rate is varied from 0.03 to 0.35 m/s. Measurements obtained in presence of internals are compared with those without internals to elucidate the effects of internals design. Comparisons are based on average values and fluctuating component of local instantaneous heat transfer coefficient obtained with the fast response probe. The average gas holdup, center line liquid velocity and bubble holdups obtained with and without internals are also compared. The observed differences are discussed based on the insights provided by these comparisons. The heat transfer coefficient and gas holdup can increase or decrease in presence of some internals. The reasons for these deviations are pointed out in this study. Relationships between local heat transfer measurements and hydrodynamic conditions in presence of internals are shown and discussed.

Key words: Bubble columns, Local heat transfer, Internals design, Hydrodynamics, Slurry

4.1 Introduction

Slurry Bubble columns (SBC) are becoming the reactor of choice owing to a number of attractive features the most notable of which is their excellent heat transfer properties. The rule of thumb is that the heat transfer in gas-liquid and gas-liquid-solid dispersion is between 10 and 100 times greater than it is in single-phase liquid flow for the same flow rates with respect to the column cross-section (Kast, 1962; Deckwer, 1980; Deckwer, 1992). The other advantages offered by slurry bubble columns are good mass transfer rates, high selectivity and conversion per pass, isothermal conditions, online catalyst addition and withdrawal, washing effect of the liquid on catalyst, and low maintenance cost due to simple construction and absence of any moving parts (Deckwer and Schumpe, 1993; Kluytmans et al., 2001; Li and Prakash, 2002; Li et al., 2003). The above benefits make these as the reactor of choice in variety of industrial applications such as Fischer-Tropsch synthesis, methanol synthesis, heavy oil upgrading, fermentation, biological waste water treatment, flue gas desulphurization, coal liquefaction, dimethyl ether production, chlorination and hydrogenation (Shah et al., 1982; Fan, 1989; Duduković and Devanathan, 1992; Deckwer and Schumpe, 1993; Li, 1998; Prakash et al., 1999; Prakash et al., 2001; Duduković et al., 2002).

In order to maintain desired temperature and isothermal conditions of operation, slurry bubble columns require internal heat transfer surface to add or remove heat of reaction. Some of these applications include Fischer-Tropsch synthesis, methanol synthesis and production of dimethyl ether (DME). The presence of internals in bubble columns affects the hydrodynamics and mixing pattern, there by affecting the reactor performance and heat transfer. Though these affects have been investigated the reasons for these changes have not been addressed in previous literatures. In this study attempts are made to get further insights into the local hydrodynamics based on heat transfer coefficient measurements and study of bubble populations in presence of internals in slurry bubble columns. The heat transfer coefficient data obtained in this study have been compared with the data obtained without internals to determine the effects. The hydrodynamic parameters such as gas holdup profile, liquid circulation

velocity profile, and bubble holdups are compared with and without internals to get the insights of affect of these parameters on the heat transfer coefficient in air-water-glass beads system.

4.2 Experimental

Experiments were conducted in a Plexiglas column of 0.15 m internal diameter and height of 2.5 m with (Figure 4.1). The column was supported by rigid metallic structure to keep it vertical and minimize mechanical vibrations which might affect pressure and heat transfer signals. The gas was introduced in the column using a coarse sparger. The detailed design of the coarse sparger is explained elsewhere (Gandhi, 1997). The sparger had two levels, upper level had seven (1.9 mm diameter) and lower level had five (1.9 mm diameter) downward facing holes on each of four arms. Two types of internals were used in this study. Top view of tube bundle type internal studied (Type A) is shown in Figure 4.2a. Bubble diffuser type six blade baffle (Type B) studied is shown in Figure 4.2b. Type B internal was located at an axial position of 36 cm from the bottom of the column. The details about internals are provided in Table 4.1. Oil free compressed air was used as gas phase, tap water was used as the liquid phase and 49 μ m glass beads (Potters Industries, spheriglass ® A glass) of density 2500 kg/m³ constituted the solid phase. The gas flow rate was measured using three calibrated sonic nozzles of different diameter (0.7mm, 1.5 mm and 2.5 mm). The superficial gas velocity was varied from 0.03 to 0.35 m/s.

The unaerated slurry height in the column was maintained around 1.45 m. A measuring tape was provided on the column to note the liquid level and dispersion height. The solid concentration was varied from 5 vol% to 20 vol%. Two pressure transducers (OMEGA Type PX541-7.5GI and Type PX541-15GI) were used to measure the pressure fluctuations in distributor ($z = 0.027$ m) and disengagement section ($z = 1.318$ m), as shown in Figure 4.1. The pressure transducers were connected to a DC power supply and generated a voltage proportional to measured

pressure. The response time of the pressure transducers was 2 ms and data were recorded for 180 seconds at a rate of 60 Hz.

Instantaneous heat flux was measured using a micro-foil heat flux sensor (Rdf, Model number 20453-1 G161). The sensor was flush mounted on the surface of a brass cylinder of 11 mm outer diameter. A small cartridge heater (Chromalox, model number CIR-1012) was installed inside the brass cylinder. The AC power was supplied to the cartridge heater through a variac to regulate supplied power in the range of 20 to 40V. The detailed design of the heat flux probe is explained elsewhere (Li and Prakash., 1997; Li, 1998). Probe location could be changed both axially and radially and it could also be rotated to study effects of sensor orientation on measured values. The temperature of the liquid phase was measured using two copper-constantan thermocouples (ANSI type T). These thermocouples were located at two radial locations: one at center and other close to the wall. Axial position of the thermocouple could be changed. The response time of micro-foil heat flux sensor was 20 ms and data were recorded for 180 s at a rate of 60 Hz. The probe generated microvolt signals, which were amplified to millivolts by a suitable amplification circuit using 15V DC supply. A minimum of three test runs were performed at each condition and average values are reported. For the heat flux sensor, the following equation can be derived for liquid film heat transfer coefficient (Li and Prakash, 2001):

$$\frac{1}{h_i} = \frac{T_{Su} - T_b}{q/A} - \frac{\Delta x}{k} \dots\dots\dots(4.1)$$

The second term on the right hand side of Equation (4.1) is negligible compared to the first term (< 1%) due to high conductivity (k) and small thickness (Δx) of the thermal barrier film. Therefore instantaneous heat transfer coefficient could be determined by measurement of heat flux and the difference between surface and bulk temperatures at a given time. The time-averaged heat transfer coefficient at a given location was obtained by averaging the instantaneous heat transfer data collected.

$$h_{avg} = \frac{1}{N} \sum_{i=1}^N \frac{q/A}{T_{Su} - T_b} \dots\dots\dots(4.2)$$

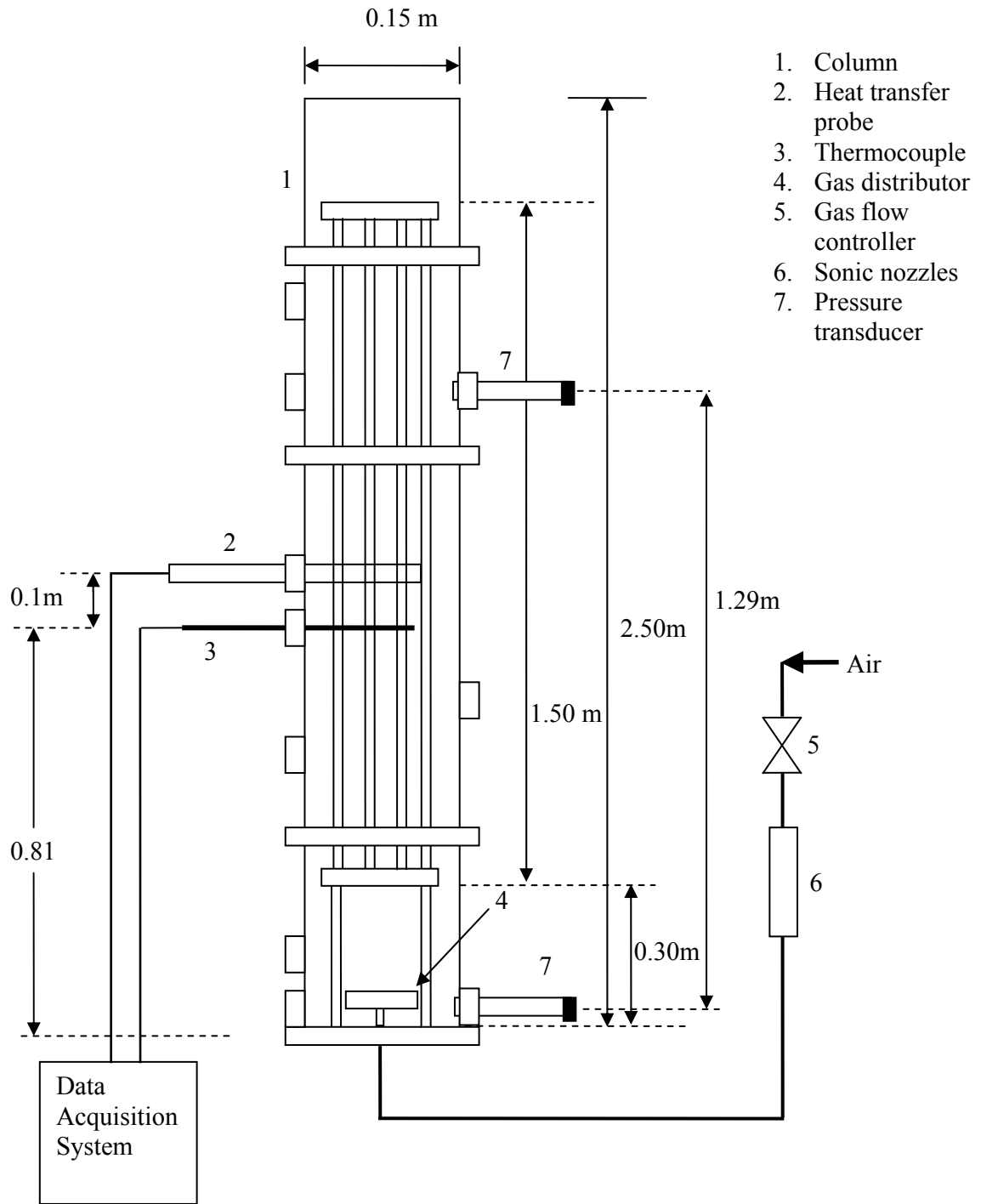


Figure 4.1. Schematic diagram of experimental setup

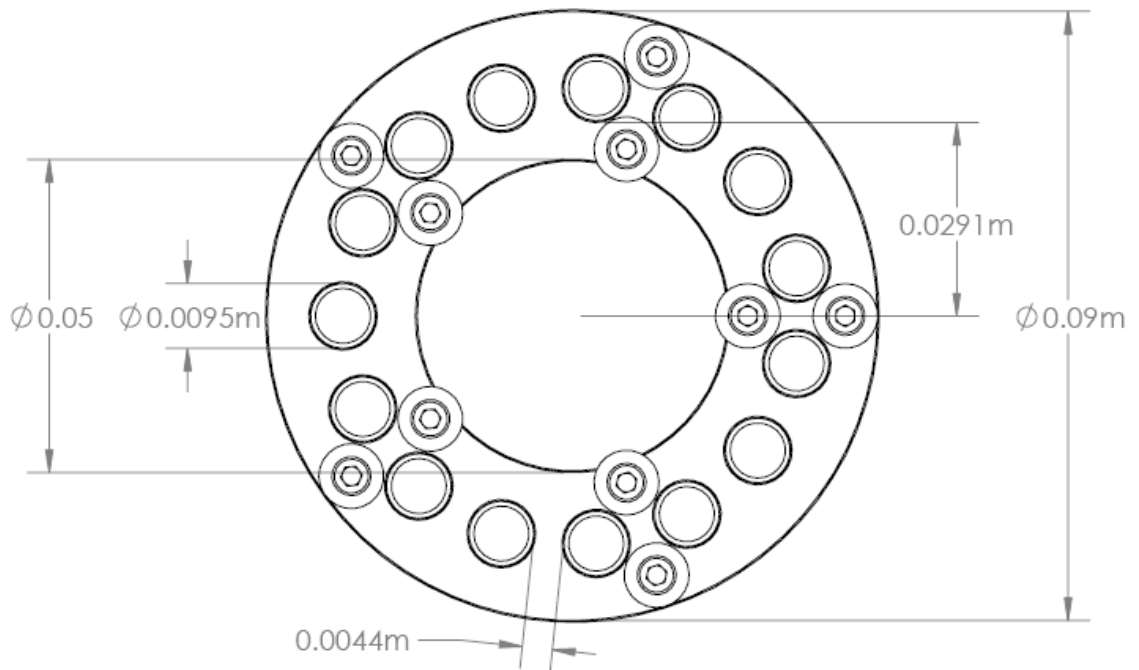


Figure 4.2a. Top view of the tube bundle used (Type A)

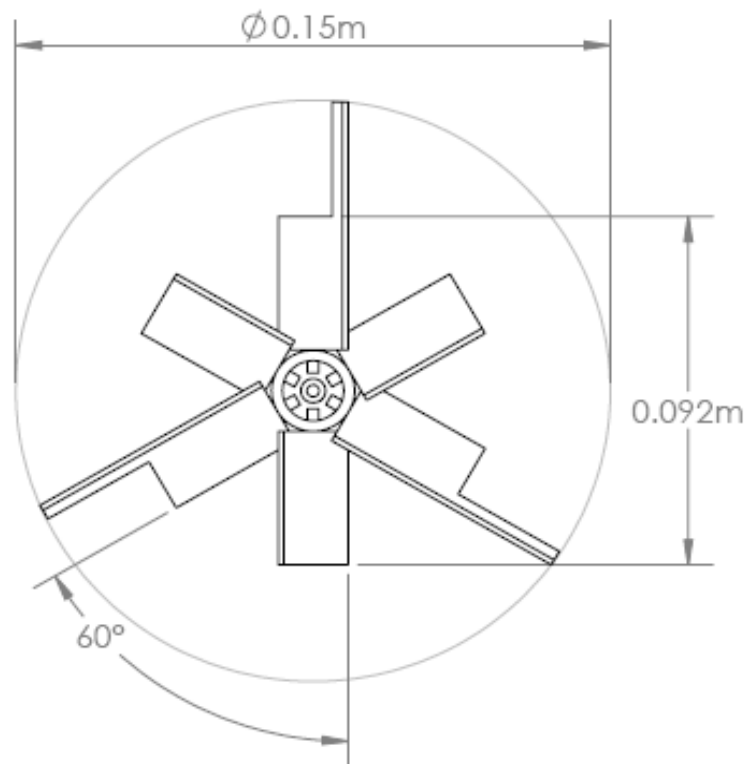


Figure 4.2b. Top view of bubble diffuser used (Type B)

Table 4.1. Details of internals used in air-water-glass beads system

Internal type	Label	Geometrical details	Comments
Circular tube bundle (z = 0.3 m)	A	No. of tubes: 15 Tube diameter: 0.95 cm Tube length: 150 cm Wall to wall spacing between tubes: 4.4 mm	Adjustable height from column bottom
Concentric baffle (z = 0.36 m)	B	No. of blades: 6 Length of blade: 3.5 cm Width of blade: 1.9 cm Blade angle: 60° from axis	Adjustable height from column bottom

4.3 Results and discussion

4.3.1 Local Heat Transfer Coefficients

Figures 4.3 presents a comparison of average heat transfer coefficient obtained in the bulk section of the column at column center, with and without internals for slurry concentrations 10 vol. %. From the figure it is observed that the heat transfer coefficient increases with increase in superficial gas velocity in all cases but at different rates. The rate of increase in heat transfer coefficient is high for gas velocities less than 0.20 m/s and beyond this the increase becomes gradual. It is observed that the heat transfer coefficients obtained are highest with type A internal at the column center followed by type B internal and column without internals at all slurry concentrations. With internal B, the difference is not significant for lower velocities (< 0.15 m/s) compared to hollow column but higher values are obtained and difference increases with increasing velocities. These differences in heat transfer profile in slurry bubble columns with and without internals can be related to changes in mixing patterns, turbulence and column hydrodynamics caused by the internal type. The intensity and degree of change is expected to vary with specific design of internal. Type A internal due to its circular arrangement of heat exchanger tubes would help direct flow of gas bubbles to column center thus creating additional driving force for liquid circulation rate. The B type internals in this study would have a smaller such effect due to a very different design configuration.

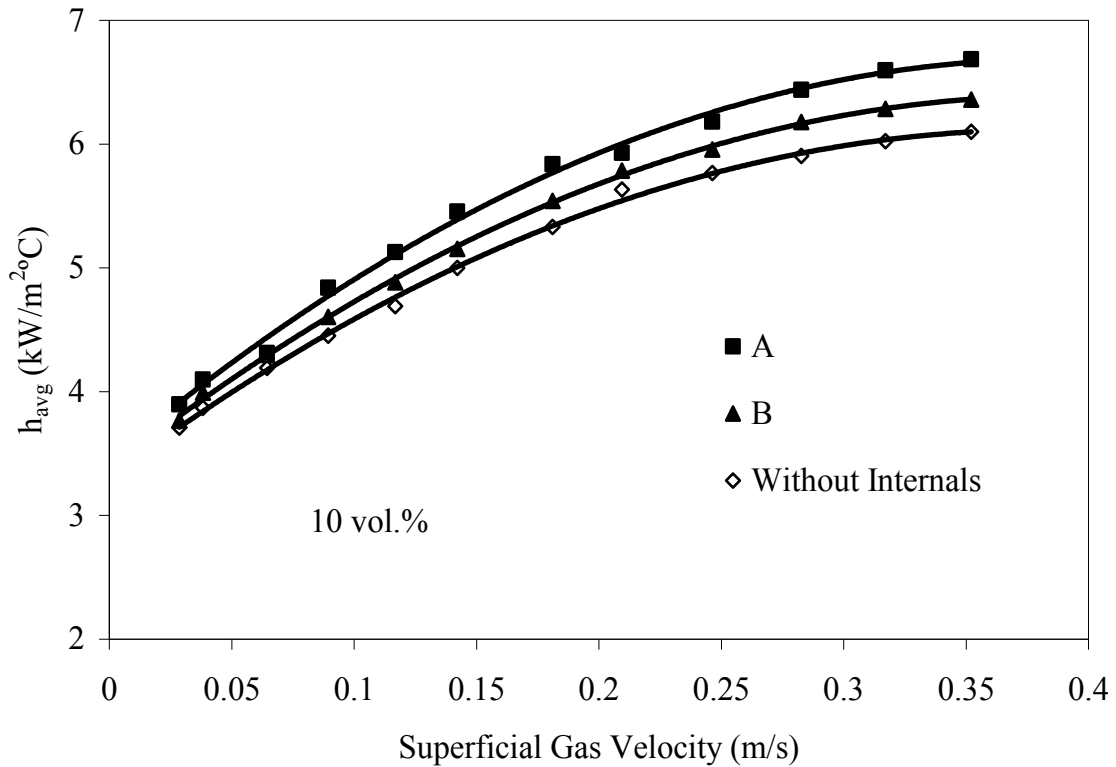


Figure 4.3. Comparison of heat transfer coefficient measurements in bubble column with and without internals, $r/R=0$ (air-water-glass beads system)

Effect of slurry concentration on average heat transfer coefficient obtained in the bulk section of the hollow column and with internal A, at column center are shown in Figure 4.4 a and b respectively. The heat transfer coefficient decreases with increase in slurry concentration in bubble columns with internals A and without, but at different rates. The decrease in heat transfer coefficient with increase in slurry concentration can be attributed to increase in apparent suspension viscosity and decrease in thermophysical properties (glass-beads). The increase in apparent suspension viscosity due to addition of particles results in reduced turbulence, because of the solid particle dampening on the bubble wake turbulence (Li and Prakash, 1997) and also the hydrodynamic boundary layer thickness increases and would have a negative effect on heat transfer coefficient (Jhawar, 2012). In this case there is a decrease in thermophysical properties of the system and these results in a net decrease in heat transfer coefficient with increase in slurry concentration in all cases.

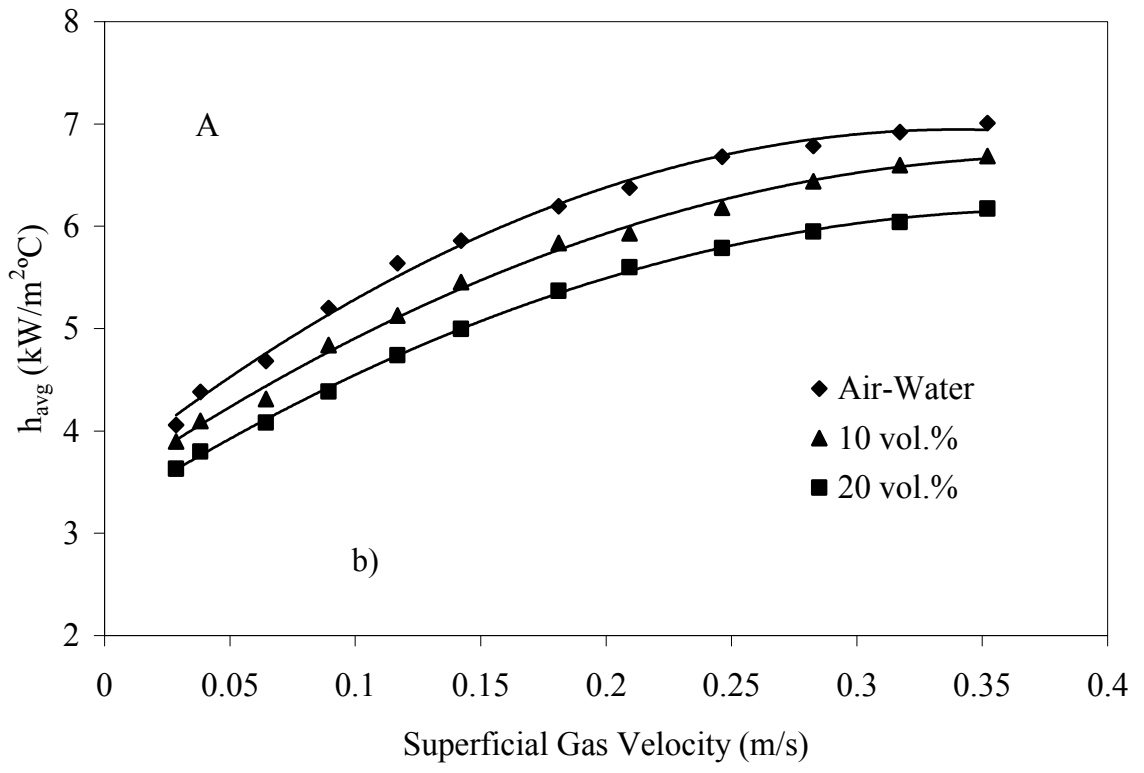
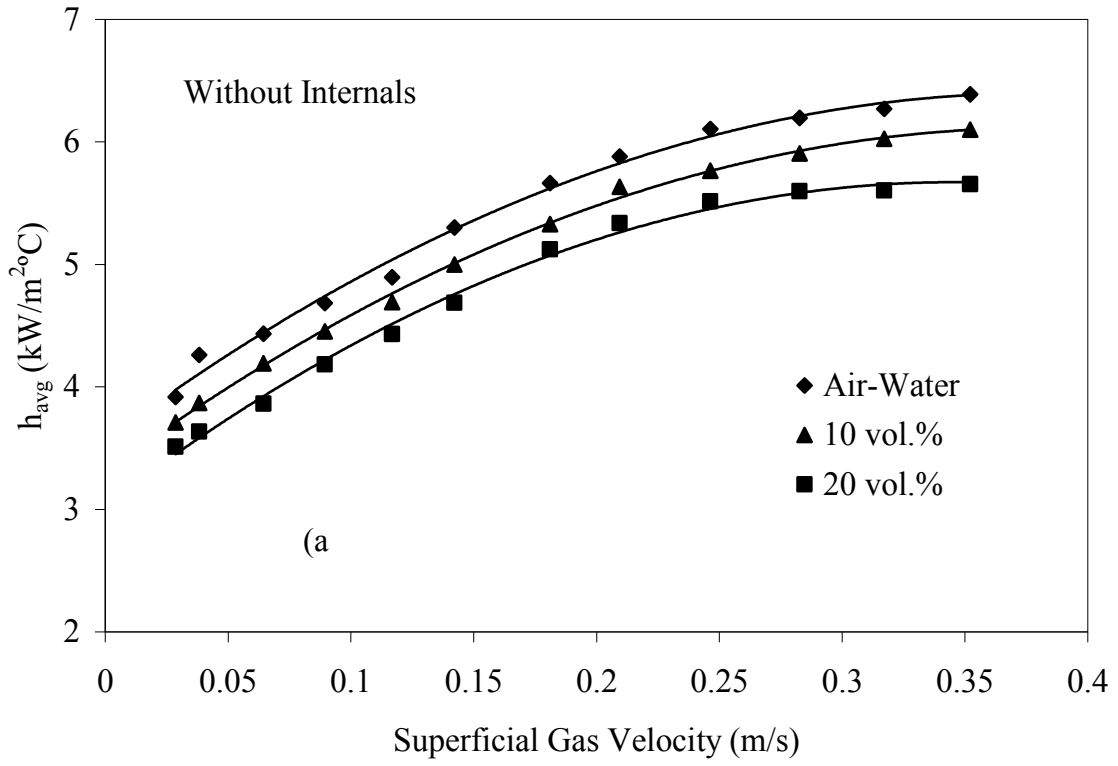


Figure 4.4. Effect of slurry concentration on heat transfer coefficients in bubble columns (a) Without Internals (b) Internals A

For a direct comparison of the effect of internals, the variation of heat transfer coefficients with slurry concentration is re-plotted on Figure 4.5. It is observed that the profiles are much steeper with Type A internal compared to hollow system or other internal type. But in case of hollow bubble column or with internal B, the rate of decrease in heat transfer coefficient is almost similar. Also the differences between the systems decrease with increasing slurry concentration. These observations were analyzed further based on column hydrodynamics and comparison with literature studies.

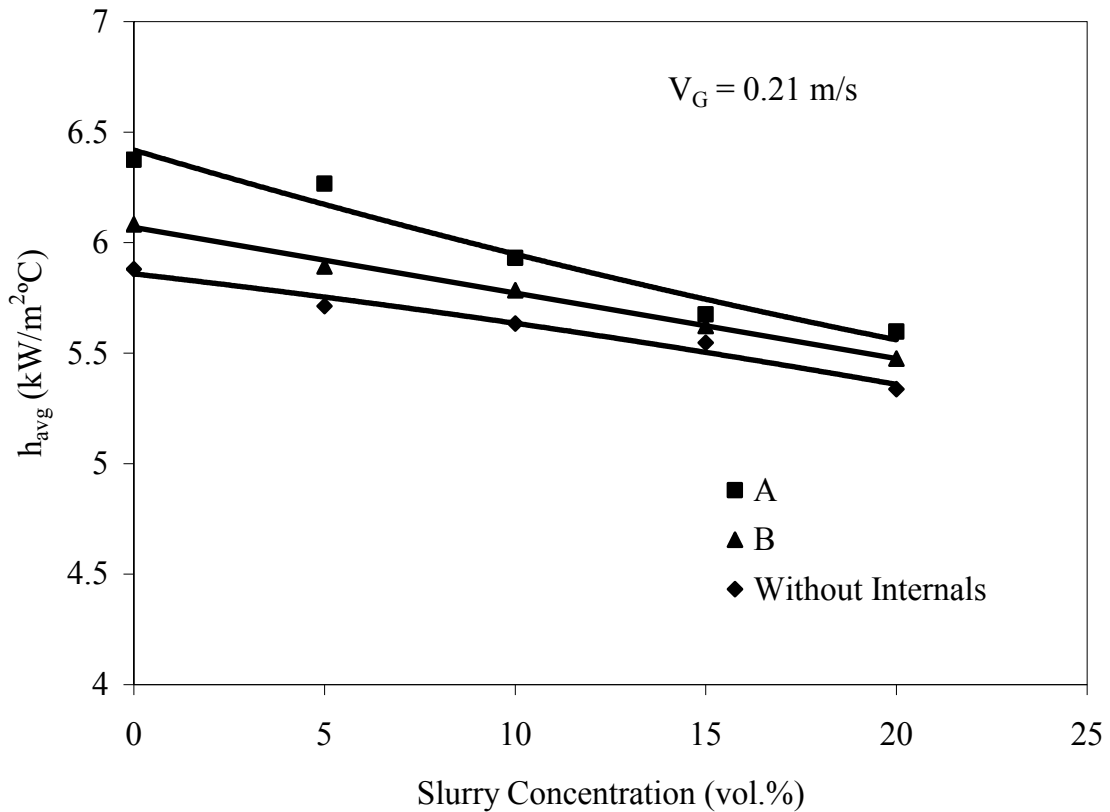


Figure 4.5. Variation of heat transfer coefficient with slurry concentration in bubble columns in central region with and without internals

A limited number of literature studies have investigated effects of internals on bubble column hydrodynamics (Youssef and Al-Dahhan, 2009; Larachi et al., 2006; Chen et al., 1999). But no published open source paper is found to investigate effect of internals in slurry suspensions. These studies clearly point to alterations in flow pattern, mixing intensities and general hydrodynamics due to insertion of internals in

a hollow bubble column. Change in design configuration has been reported to clearly affect hydrodynamic behavior which is expected to affect rate of transport processes (Youssef and Al-Dahhan, 2009; Larachi et al., 2006). The fast response heat transfer probe used in this study allowed measurement of temporal variation of local heat transfer coefficient in the column. Therefore to further understand underlying reason for the observed increase in heat transfer coefficient with type A internal, the instantaneous heat transfer coefficients was compared for a given gas velocity. It is observed from Figure 4.6a that the peaks obtained in presence of internals are wider and taller as compared to those without the internal similar trend is observed in air-water system. This could be attributed to the passage of clusters of bubble generated with type A internal as a result of directing the bubble flow towards central region of the column.

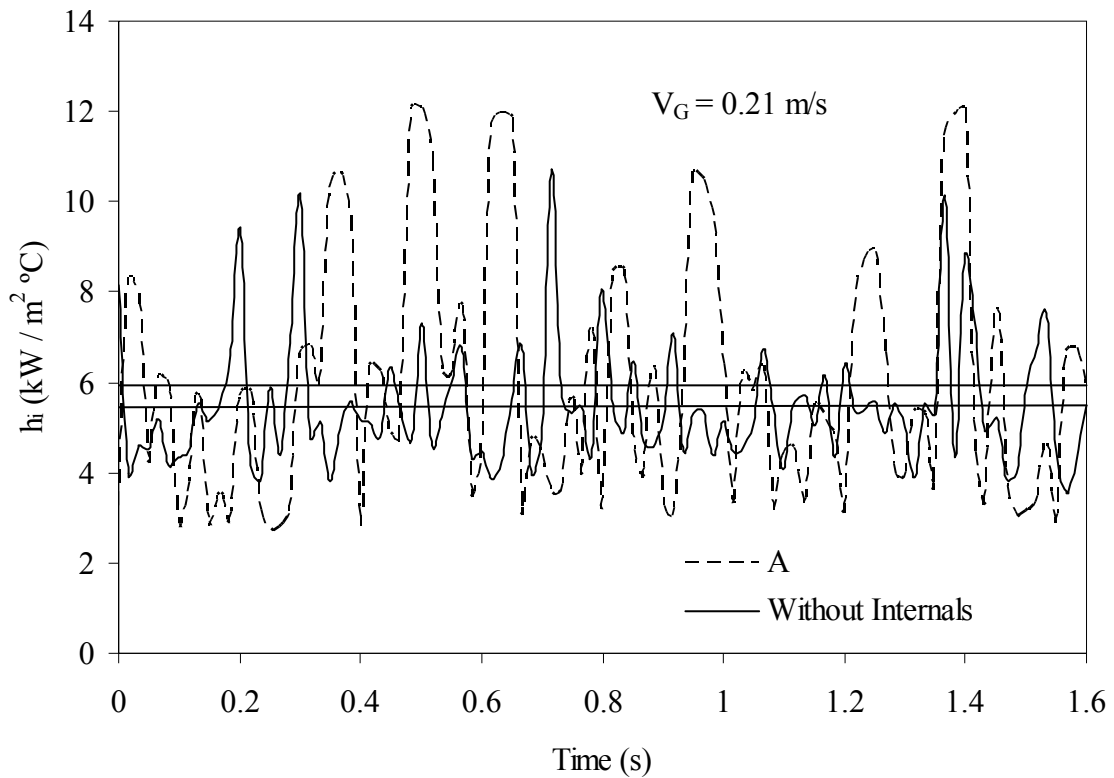


Figure 4.6a. Instantaneous heat transfer coefficients of air-water-glass beads system (with and without internals) at $r/R=0$

A similar comparison of the behavior of instantaneous heat transfer coefficients obtained in the wall region of the bulk section of the column is shown in Figure 4.6b for the superficial gas velocity of 0.21 m/s. It is seen in wall region that the instantaneous heat transfer coefficient peaks are smaller than central region in both the cases. This can be attributed to presence of smaller bubbles in the wall region of the column. It is also interesting to see that in bubble column equipped with type A internal the heat transfer coefficient peaks in wall region are smaller compared to hollow bubble column. This could be due to smaller and fewer bubbles in the annular region created due to insertion of this internal type in the column. Visual observations also supports this, smaller bubbles seemed trapped in the annular region given the geometry of the internal and small gap between the tubes (see Table 4.1).

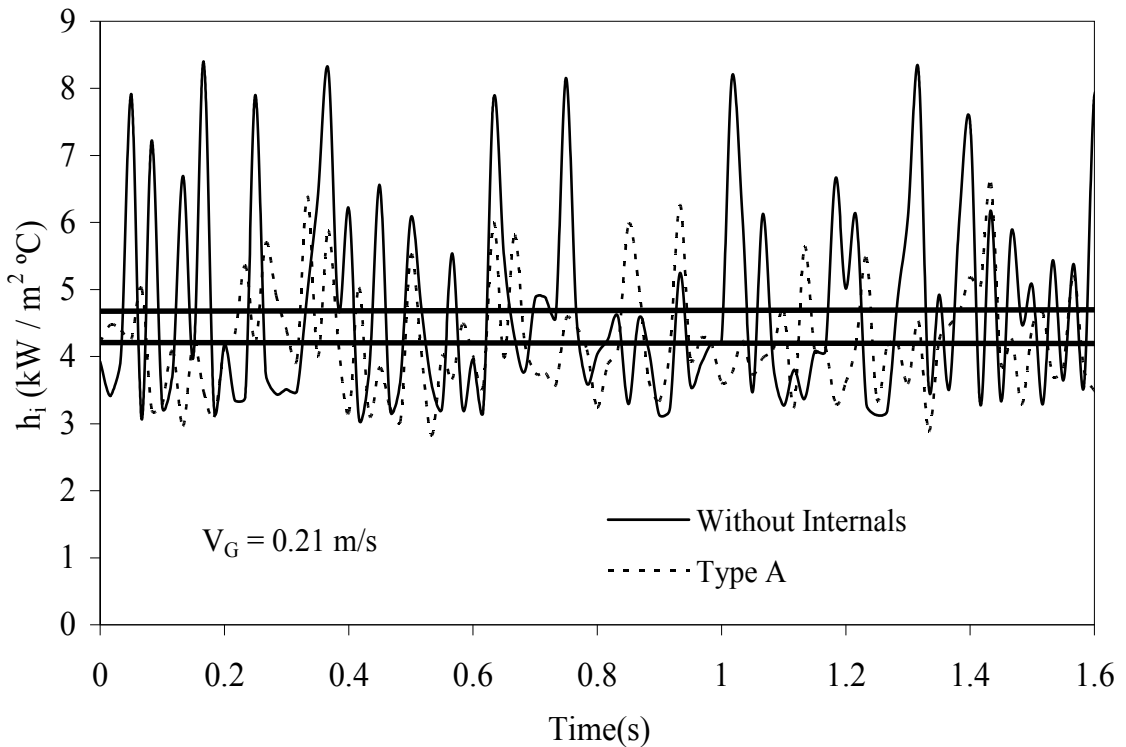


Figure 4.6b. Instantaneous heat transfer coefficients of air-water-glass beads system (with and without internals) at $r/R=0.624$

Figure 4.7 a and b presents the comparison of instantaneous heat transfer coefficient in bubble columns with internals A in bulk section at center and wall region in air-water and air-water-glass beads system at 10 vol.% slurry concentration for a given gas velocity.

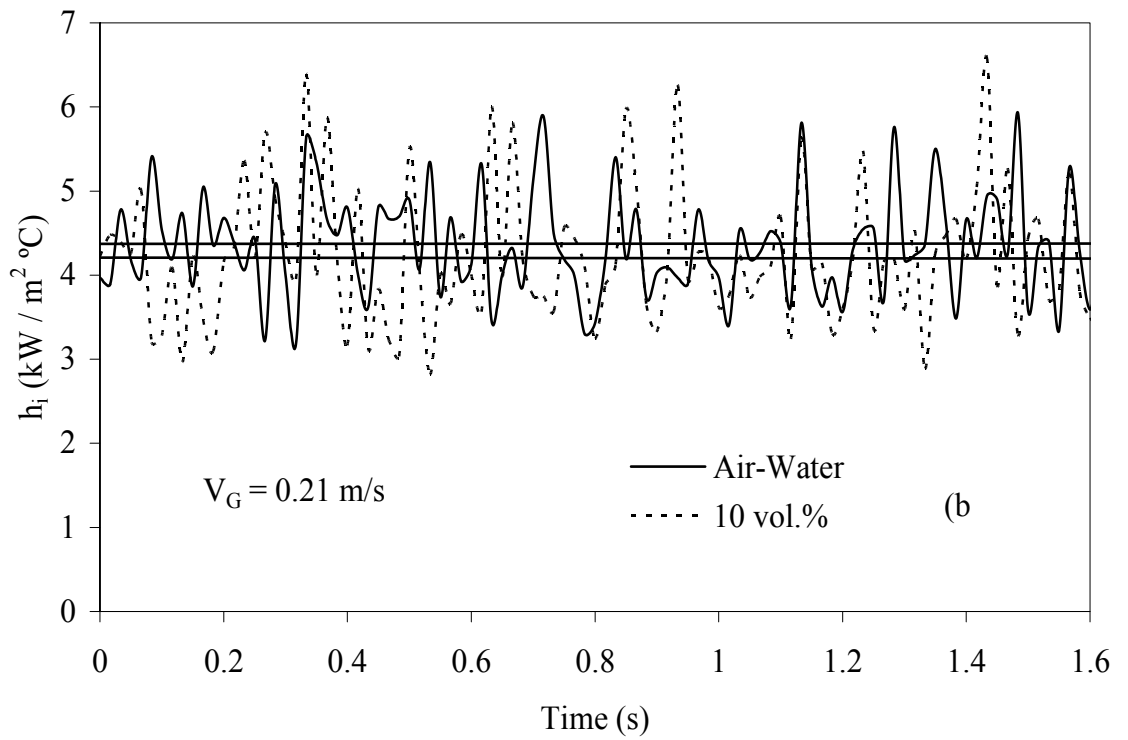
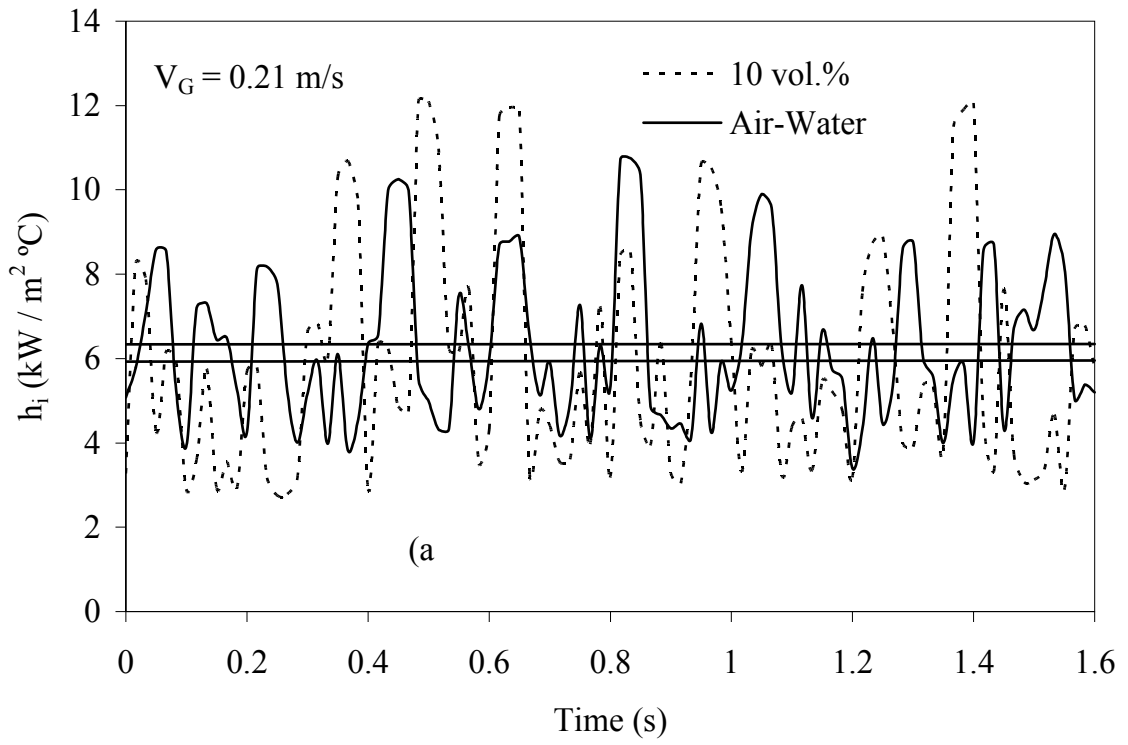


Figure 4.7. Comparison of instantaneous heat transfer coefficients for air-water and air-water-glass beads system with internal type A (a) $r/R = 0$ (b) $r/R=0.624$

From figures it is observed that the heat transfer coefficient peaks obtained in presence of internals in central region are wider and taller as compared to those in the wall region in both the cases. This could be attributed to the passage of clusters of bubble generated with type A internal as a result of directing bubble flow towards central region of the column. It is also observed that with addition of glass-beads the peaks are generally higher but with lower base line value both in the central and wall region compared to those in air-water system with internals A. With addition of solid the apparent slurry viscosity increases, which results in increase in average bubble size. The fast rising large bubbles with addition of glass beads could be responsible for these higher peaks. The lower base line values in both central and wall region can be attributed to combined effect of lower turbulence due to presence of solid particles and increase in hydrodynamic boundary layer thickness (Li and Prakash, 1997, Jhavar, 2012). Both will have negative effect on heat transfer coefficient giving lower base line values.

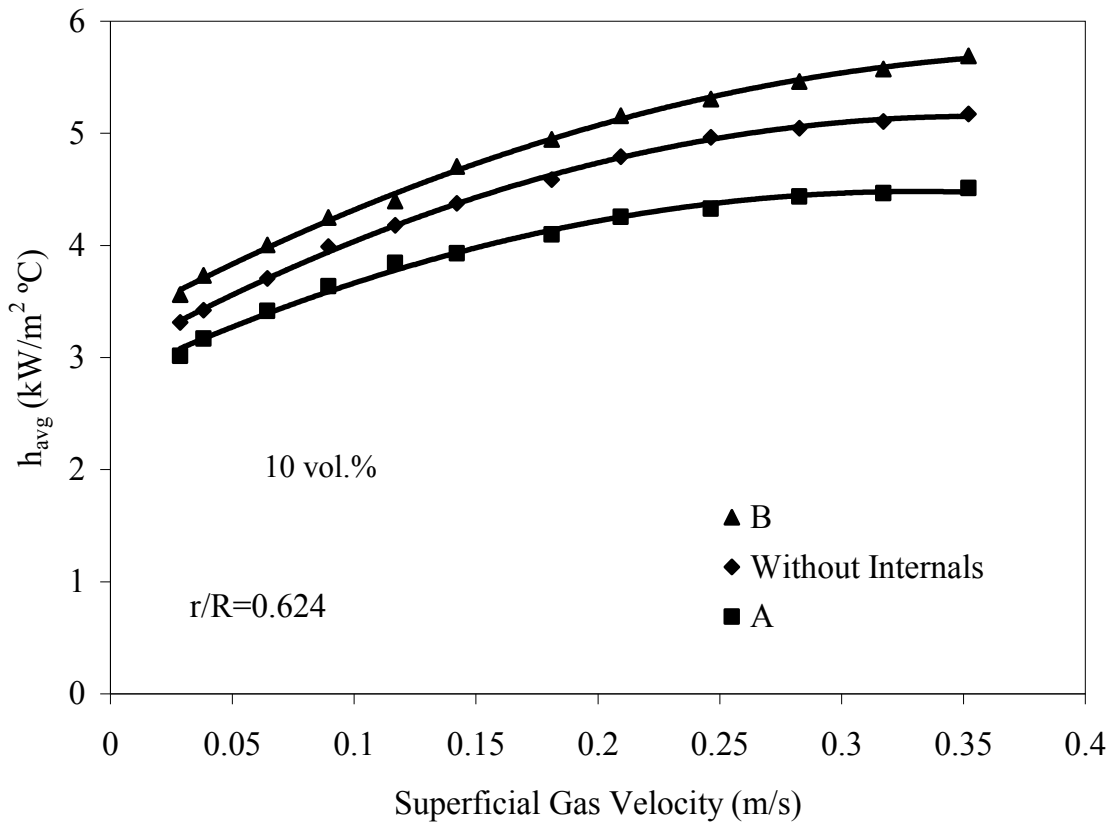


Figure 4.8. Comparison of heat transfer coefficient measurements in slurry bubble column with and without internals, $r/R=0.624$ (air-water-glass beads system)

Figure 4.8 shows a comparison of average heat transfer coefficient obtained close to the wall ($r/R=0.624$) in the bulk section of the column with or without presence of different internals at 10 vol. % slurry concentration. Following observations can be made for data in the wall region, when compared with the heat transfer coefficients obtained at column centre (Figure 4.3).

- Heat transfer coefficients are significantly lower in the wall region
- The rate of increase in heat transfer coefficient with gas velocity is low and it further decreases for gas velocities above 0.2 m/s
- A reverse trend is observed with internals i.e. the heat transfer coefficients with internals A are lower than those with internals B or without indicating existence of very different hydrodynamic conditions with different internals used

Variations of average heat transfer coefficients with slurry concentration in the center and wall regions are presented in Figure 4.9 for different systems. Following observations can be made.

- Heat transfer coefficient are significantly lower in the wall region at all slurry concentrations compared to central region at a given superficial gas velocity
- In hollow bubble column the rate of decrease in heat transfer coefficient with increase in slurry concentration is high in wall region compared to that in central region.
- With internals A, the rate of decrease in heat transfer coefficient with increase in slurry concentration is significantly low in wall region compared to that in central region
- In wall region, it can be noted that lowest heat transfer coefficients are obtained with type A internals and there is little decrease with increase in slurry concentration. This indicates that average bubble size is small and there is very little change with slurry concentrations

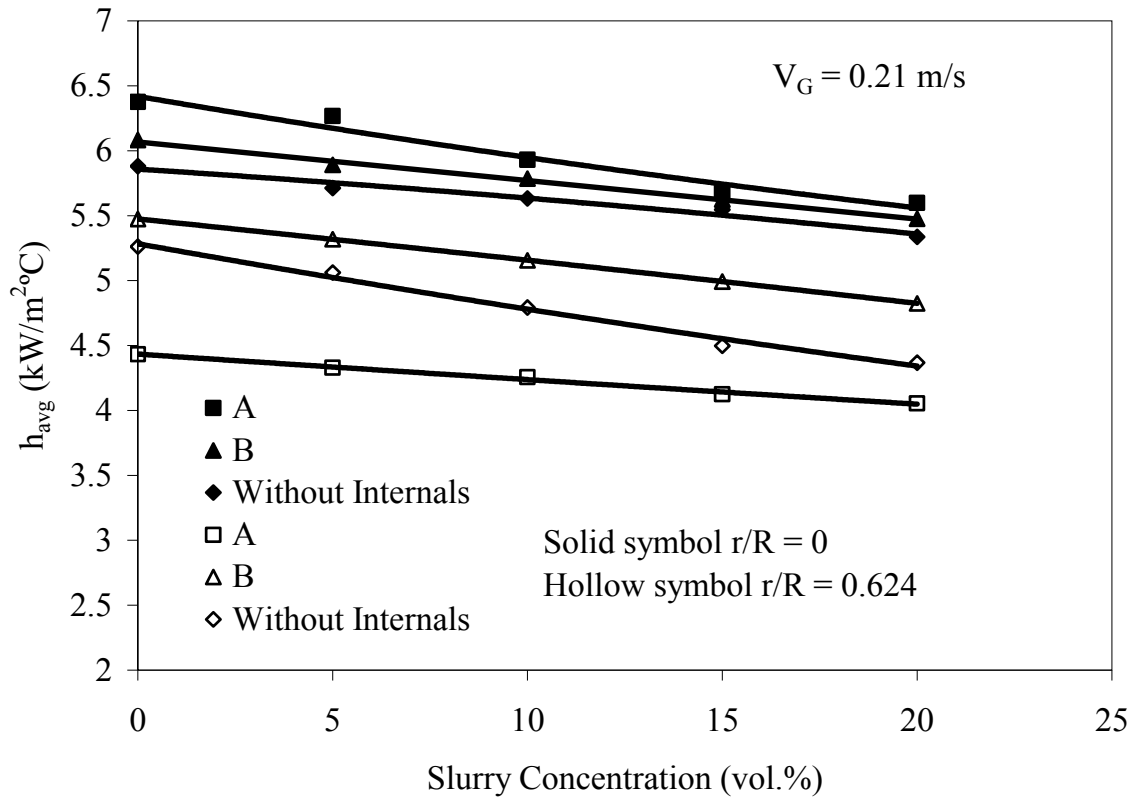


Figure 4.9. Variation of heat transfer coefficient with slurry concentration in bubble columns in central region with and without internals

As discussed in the following sections, these differences in profile of heat transfer coefficient can be related to changes in local column hydrodynamics and bubble size distribution due to the presence of internals and their type. Figure 4.10 shows the comparison of data obtained in the two regions and with two different internals in air-water glass beads system to further highlight the differences in column hydrodynamics due to presence of different internals. It can be noted that the differences between the two regions is higher with type A internal compared to type B. Similar results were obtained in air-water system. Very different geometry of these internals of course is the main cause of the difference. Selection of proper internals for a given application would need to take such differences into consideration. Also combination of different internals and their location need to be tested to improve the column performance.

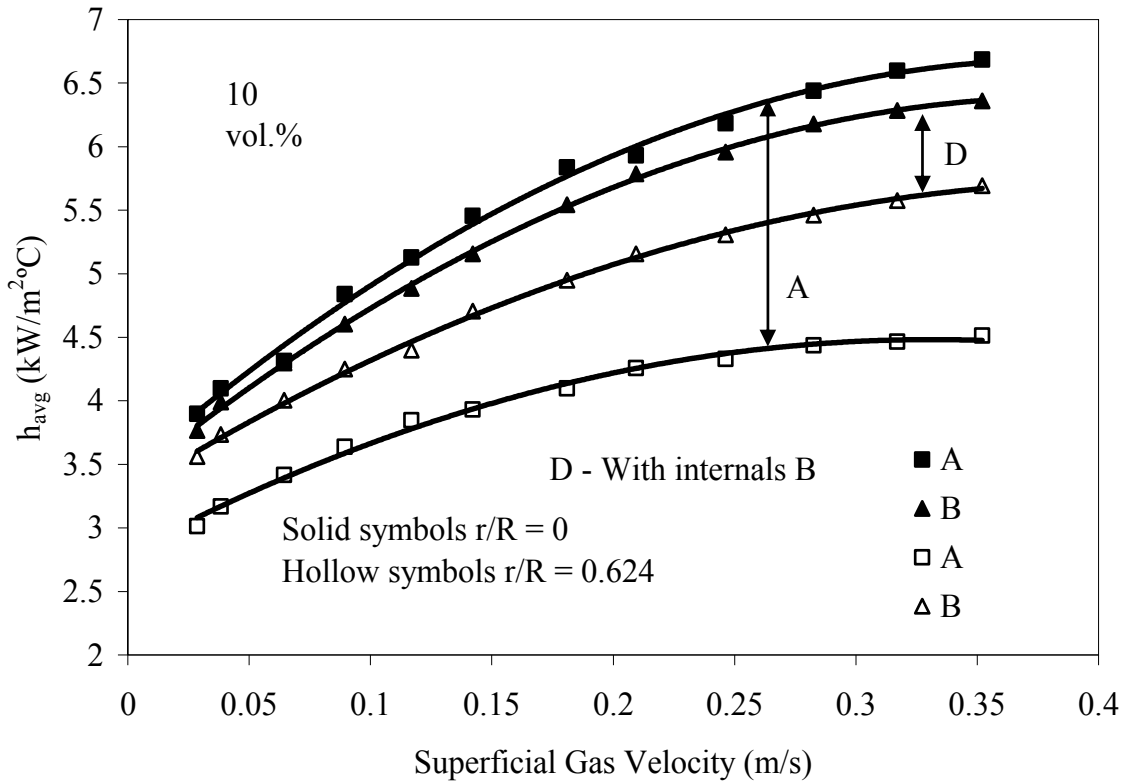


Figure 4.10. Variations of heat transfer coefficient at two radial locations with internal A and B (air-water-glass beads system)

The radial profiles obtained in slurry bubble columns with and without internals are presented in Figure 4.11 to further highlight these radial variations with different internals. As the radial distance from the center increases the heat transfer coefficient decreases at all superficial gas velocities in all cases. But the rate of decreases is different at different superficial gas velocity and in hollow bubble columns or with different internals. Similar trend is observed in air-water system. It is observed that rate of decrease in heat transfer coefficient with increase in radial distance from the center is much higher with internals type A compared to hollow bubble column or with internal B.

The radial profiles obtained with type A internal cross the other profile around dimensionless radius of about 0.3 and move below other profiles as it moves into annular region. This difference can be related to the design of type A internal. The tube bundle design would funnel the two phase flow and smaller inter-tube gap would

limit flow into annular region thus significantly altering column hydrodynamics. The steeper profiles obtained in presence of Type A internals show that lower turbulence is caused by the smaller and fewer bubbles in the wall region. It was visually observed that the bubble size and population decreased in the wall region with type A internals, compared to those without or other type internals.

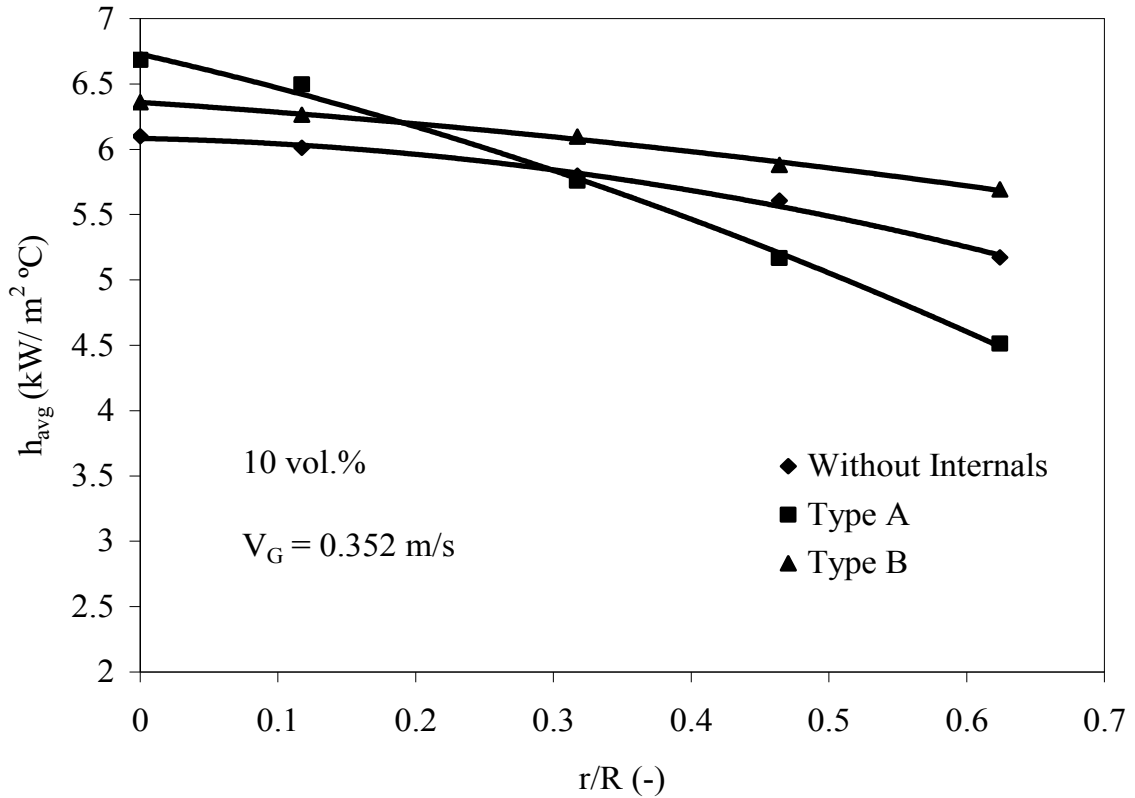


Figure 4.11. Comparison of the radial profile of heat transfer coefficient obtained with and without internals in air-water-glass beads system

Comparison of radial profile of heat transfer coefficient between hollow column and with internal A at a low and high superficial gas velocity is presented in Figure 4.12. It is interesting to note at low gas velocity of 0.038 m/s, the radial profiles obtained in hollow bubble column and with internal A are quite similar. Same trends were also observed in air-water system. This indicates minimal effect of the internal on column hydrodynamics under the dispersed bubble flow conditions at the low velocity. However, at the high gas velocity of 0.35 m/s when the column is in fully developed heterogeneous regime, the two profiles come apart. This suggests that the effect of

internals on column hydrodynamic increases with the increase in superficial gas velocity.

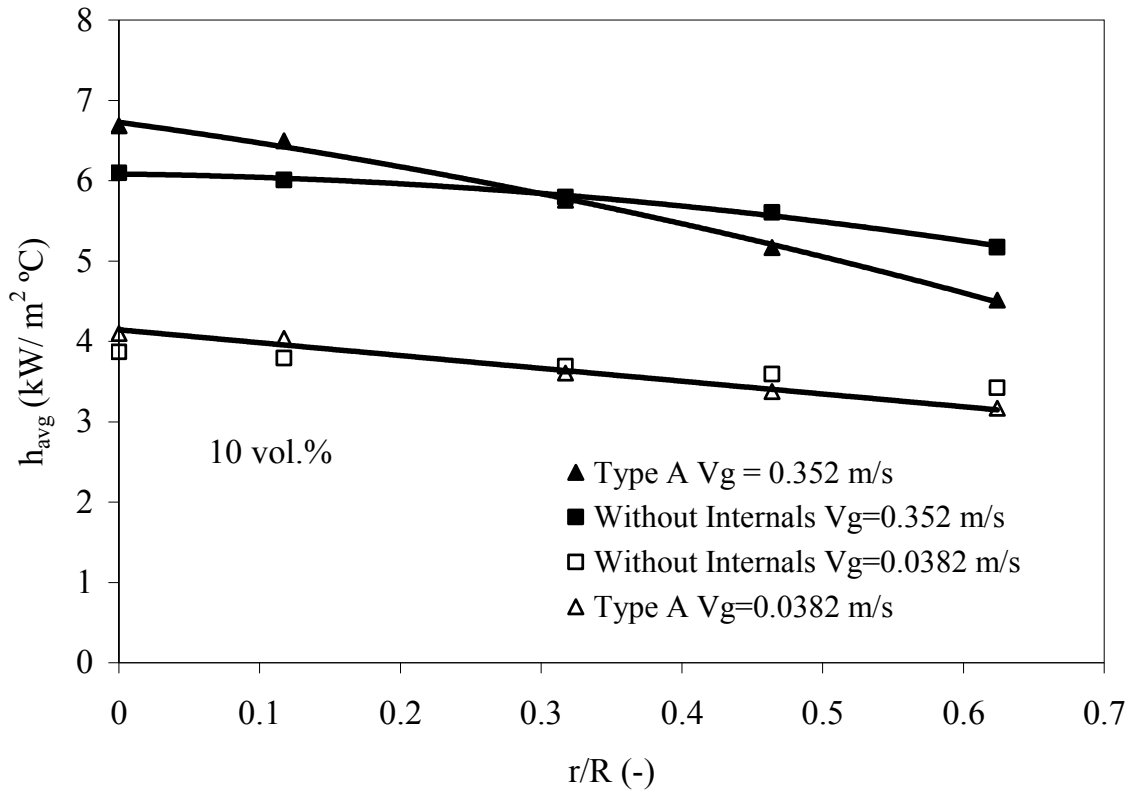


Figure 4.12. Comparison of the radial profile of heat transfer coefficient obtained with type A and without internals (air-water-glass beads system)

4.3.2 Gas Holdup and Bubbles Fractions

A comparison of gas holdups measured in slurry bubble column with and without internals at 10 and 20 vol. % slurry concentrations is presented in Figure 4.13. Gas holdups in presence of internals are higher than those obtained in absence of internals irrespective of slurry concentrations. Highest gas holdups are obtained with internals type A followed by B. The results in presence of type A internal are consistent with the literature studies, who used similar internals (Youssef and Al-Dahhan, 2009; Chen et al., 1999; Saxena et al., 1990). The increase in gas holdup in presence of internals can be attributed due to decrease in average bubble size. With type A internals, it was visually observed that smaller bubbles accumulated in the wall region is also reported by Youssef and Al-Dahhan (2009).

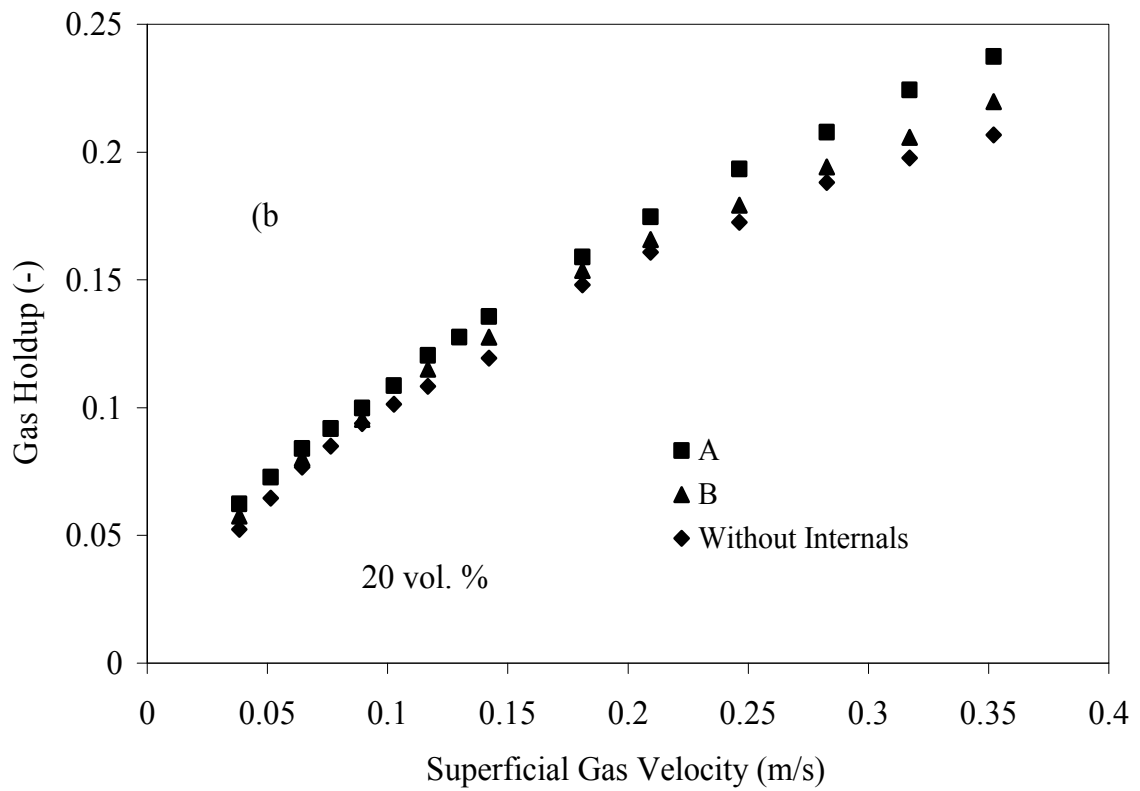
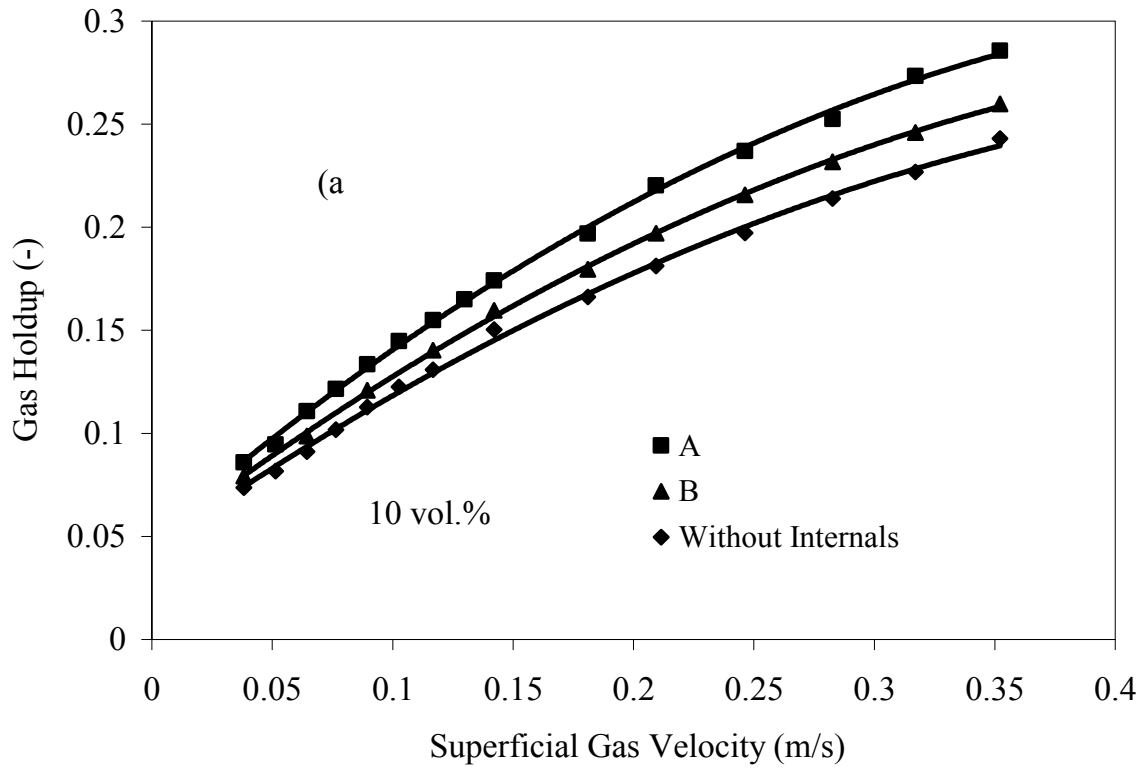


Figure 4.13. Comparison of gas holdup measurements obtained with and without internals (air-water-glass beads systems) (a) 10 vol. % (b) 20 vol. %

From Figure 4.13 it is also observed that the gas holdups decrease with increase in slurry concentration, but the rates of decrease in hollow bubble columns and with internals are different. At high slurry concentration (20 vol. %) the difference in gas holdup obtained in hollow bubble column and with internals B is small at all gas velocities. This indicates minimal effect of the internal B on column hydrodynamics at high slurry concentration owing to its design.

Figure 4.14 a and b presents the comparison of gas holdup of small and large bubbles obtained in slurry bubble columns with and without internals at slurry concentrations, 10 and 20 vol. %. The detailed procedure for estimation of bubble holdup is explained elsewhere (Li and Prakash, 2000). It is observed in Figure 4.14a that the gas holdup of small bubble is highest with internals A, followed by B at all slurry concentrations. This clearly shows that the average bubble size is decreased in presence of these internals. From Figure 4.14b it is also interesting to note that there is no much variation in gas holdup of large bubbles fraction in bubble columns with and without internals irrespective of the slurry concentration. From Figure 4.14 a and b it is also observed that with increase in slurry concentration both gas holdup of small and large bubble decreases in slurry bubble columns with and without internals. This could be due to increase in average bubble size with increase in slurry concentration in presence of fine particles. Because with increase in slurry concentration in presence of fine particles the apparent slurry viscosity increases, this in turn affects the bubble size (Kara et al., 1982; Nigam and Schumpe, 1996).

The comparison of small and large bubble holdup in slurry bubble columns with and without internals with slurry concentration at low and high velocities are presented in figure 4.15 a and b.

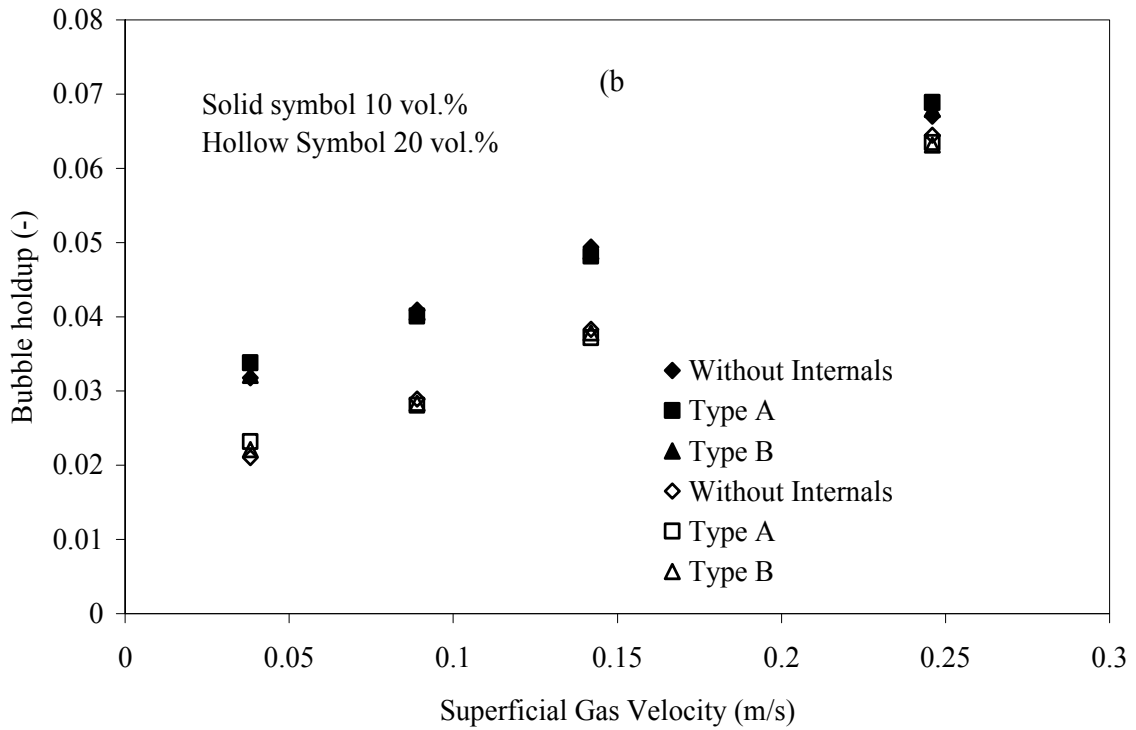
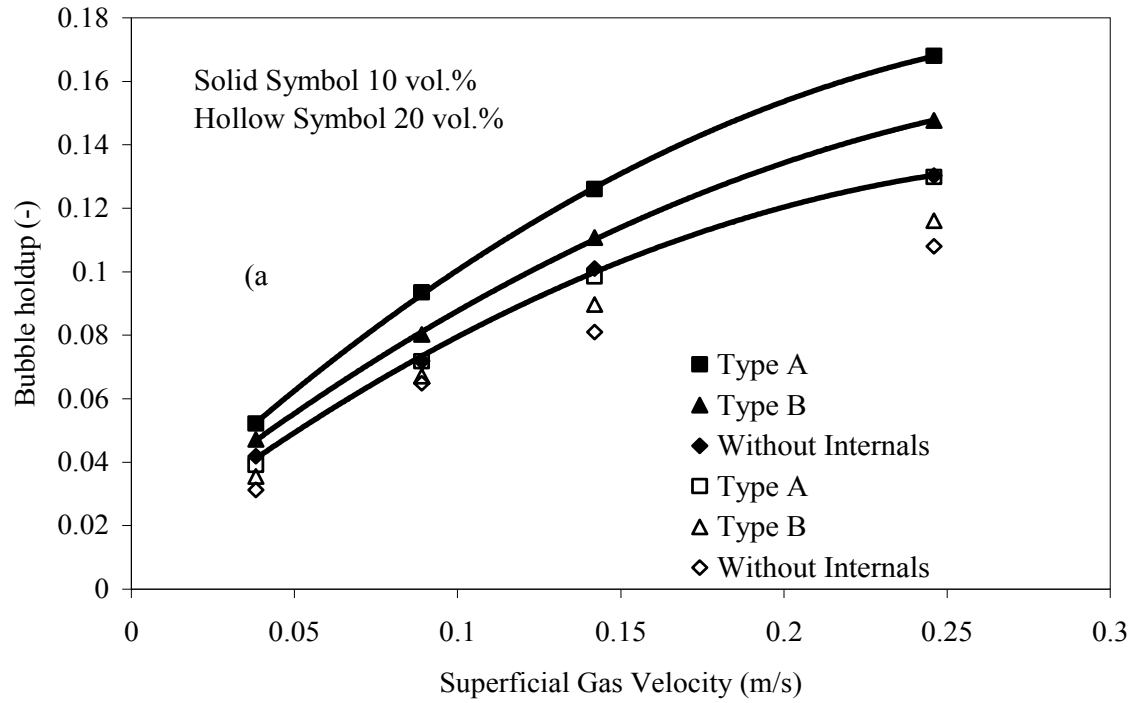


Figure 4.14. Comparison of bubble holdup in slurry bubble columns with and without internals in air-water-glass beads system (a) small (b) large

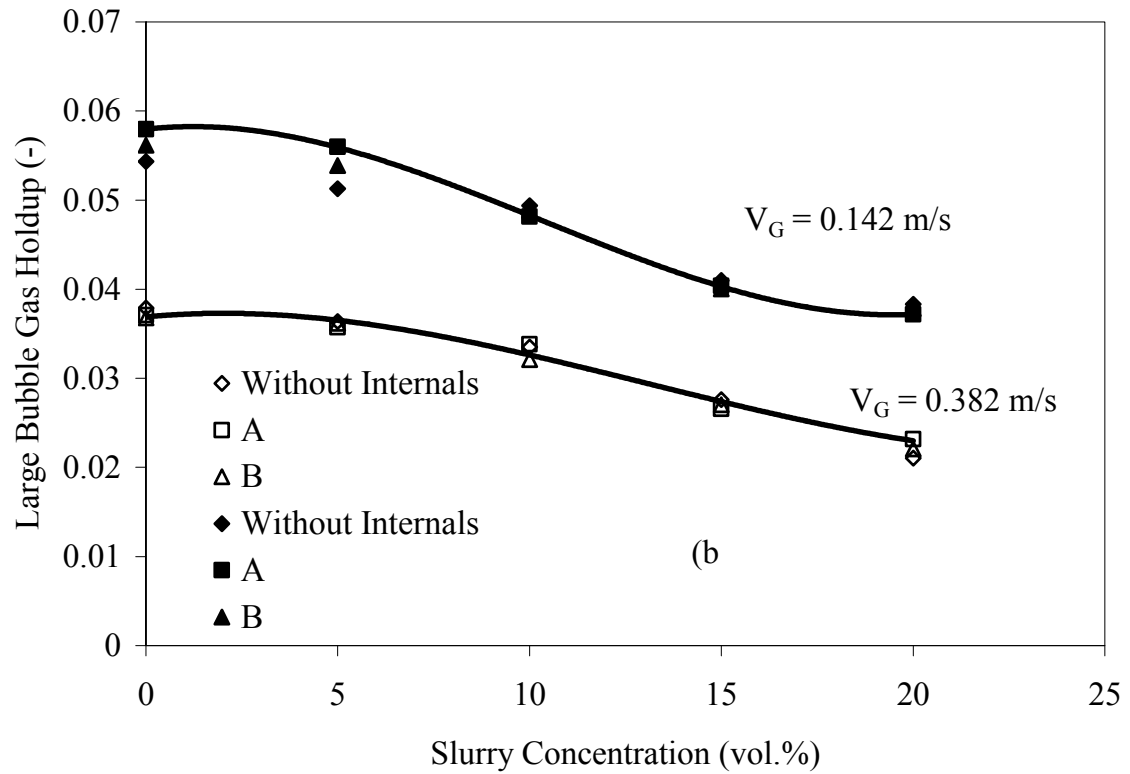
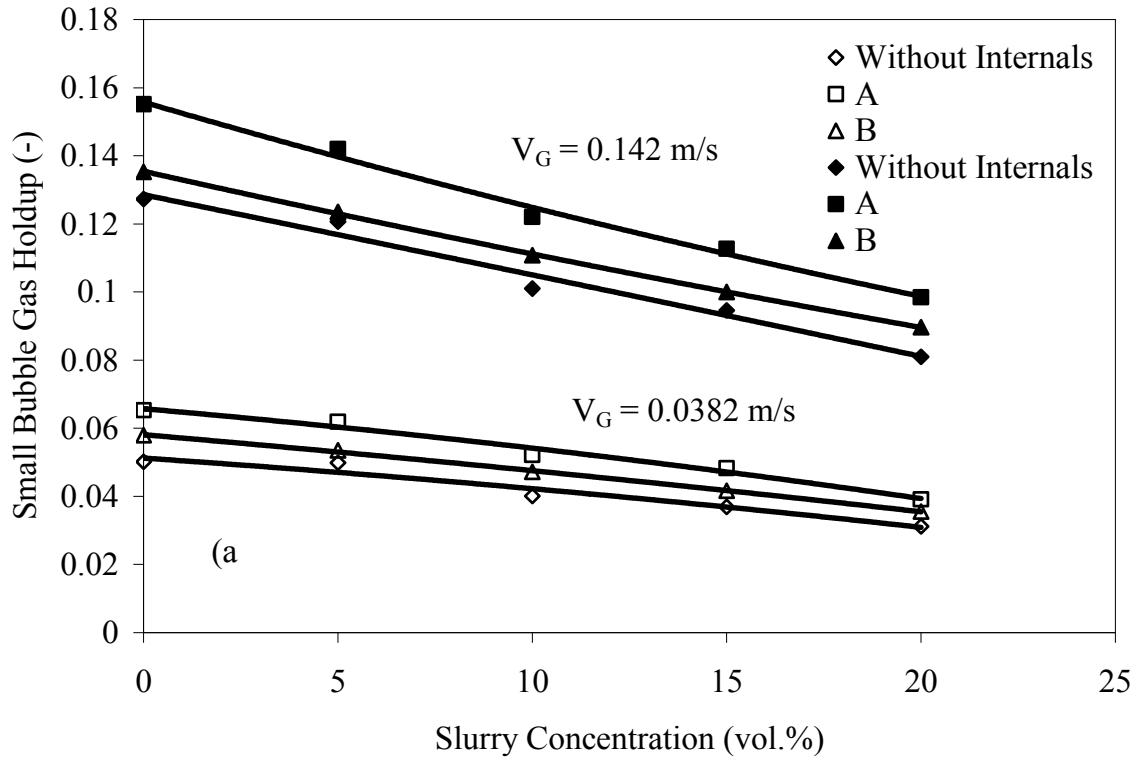


Figure 4.15. Effect of slurry concentration on bubble holdup in slurry bubble columns with and without internals in air-water-glass beads system (a) small (b) large

Following observations can be made for the variation of bubble holdup with slurry concentrations in bubble columns with and without internals.

- The gas holdup of both small and large bubble decreases with increase in slurry concentration in all cases, but at different rates.
- The rate of decrease is high for small bubble holdup compared to that of large bubbles (With slurry concentration)
- The gas holdup of small bubbles is higher in bubble columns with internals compared to those without at all slurry concentration.
- The effect of internals on large bubble holdup is negligible
- The rate of decrease of both small and large bubble holdup with slurry concentration is high at high superficial gas velocities (in fully developed heterogeneous flow regime).

The fast response heat transfer probe used in this study could detect variations due to changes in bubble size distribution which could be reflected in standard deviations of time series data of the heat transfer coefficient. Figures 4.16a and b compare standard deviation of heat transfer data obtained at $r/R=0$ and $r/R=0.624$ in the bulk section of the column for different cases in air-water-glass beads system. The standard deviation of heat transfer coefficient in both central and wall region increases with the increase in superficial gas velocity in all cases. However, the rate of increase varies with internal type and radial location and following observations can be made.

- In the central region of column, the standard deviations are highest with internal type A, followed by internal B. It can also be noted that differences between different internals are generally small and become insignificant at low gas velocities (< 0.1 m/s) when bubble size distribution may not evolved significantly. Similar observations were made in air-water system
- In the wall region, it can be noted that lowest standard deviations are obtained with type A internals and there is no significant change with gas velocity. This

indicates that the bubble size is small and there is little change with gas velocity.

- Higher standard deviation values obtained with type B internals and hollow bubble column point to wider bubble size distribution in the wall region for these cases.

4.3.3 Local Liquid Velocity and Related Hydrodynamics

The heat transfer probe used in this study could also detect flow direction and provide an estimation of local liquid (slurry) velocity using boundary layer theory (Li and Prakash, 2002). Flow direction could be identified (upward or downward) by measuring the time averaged local heat transfer coefficients using the different orientation of the probe (upward, downward or lateral). Figure 4.17 shows the results obtained at the center ($r/R=0$) in the bulk section of the column with internals Type A in air-water-glass beads system at 10 vol. % slurry concentration. The heat transfer coefficients (stagnation point) obtained with the downward orientation of the probe are higher than those obtained with the upward orientation, hence indicating upward liquid flow. Similar studies were conducted without internals and with internals. Li and Prakash (2002) developed a correlation to obtain a local liquid velocity by applying boundary layer theory to the measured stagnation point heat transfer coefficients.

$$\frac{h_{st} D_p}{k_L} = a_s (\text{Pr})^{0.4} \left(\frac{V_L D_p}{\nu_L} \right)^{0.5} \quad (4.3)$$

The above equation gives good prediction of liquid velocities in different diameter bubble columns as reported by Li and Prakash (2002) and Jhavar and Prakash (2011). In the above equation, the value of factor a_s depends on several aspects such as probe design, orientation etc. Jhavar and Prakash (2011), recommended value of factor a_s to be 0.7 based on data from their and other literature studies.

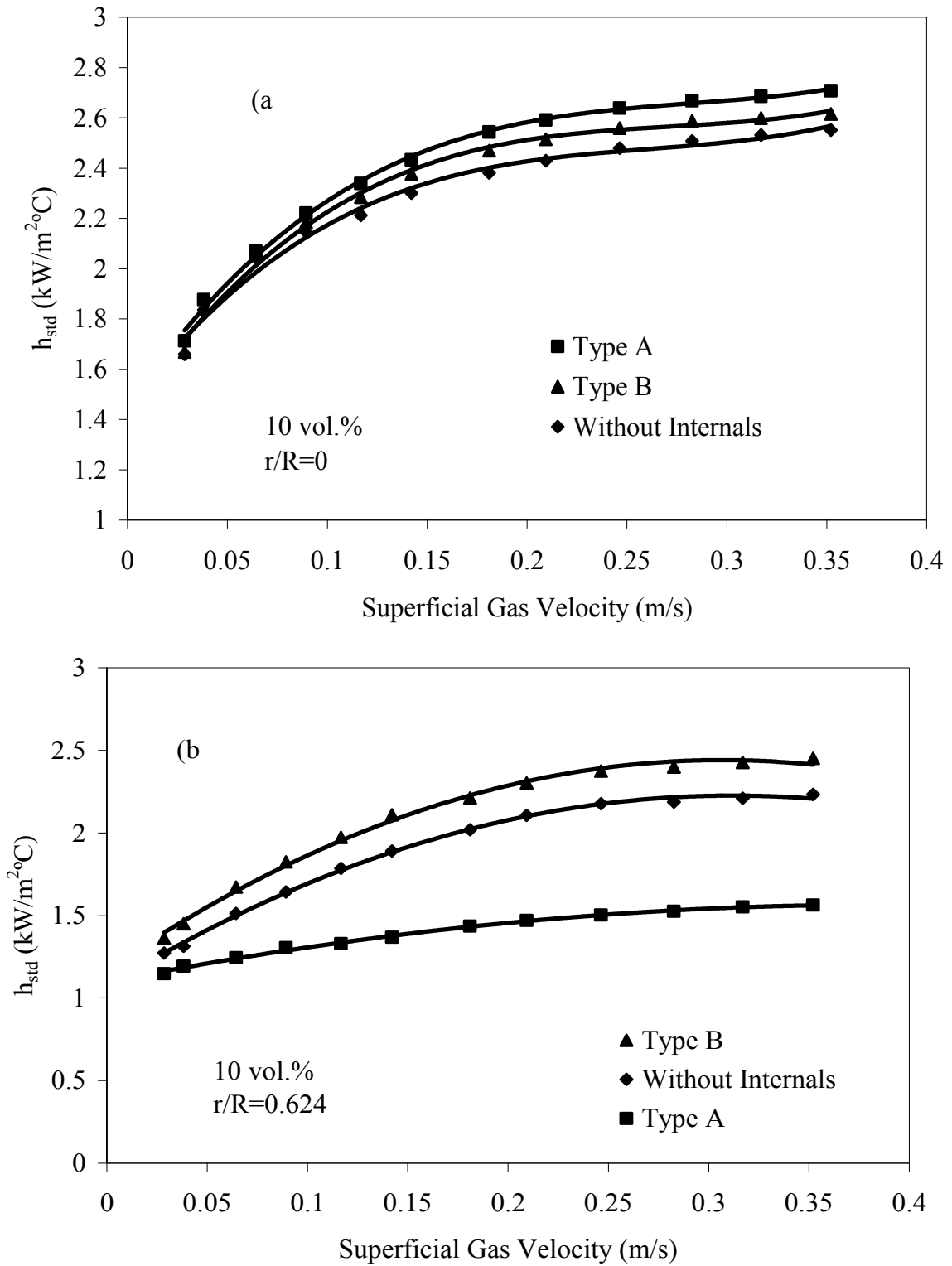


Figure 4.16. Comparison of standard deviation of heat transfer coefficient in slurry bubble columns with and without internals in (a) central (b) wall region

For estimation of slurry velocities the slurry properties needed such as effective densities, heat capacities, thermal conductivities and viscosities of suspensions were estimated based on the equations given elsewhere (Jhavar, 2012). The results obtained with this procedure at the column centre and in region close to wall ($r/R = 0.624$) are shown in Figure 4.18 and 4.19 respectively.

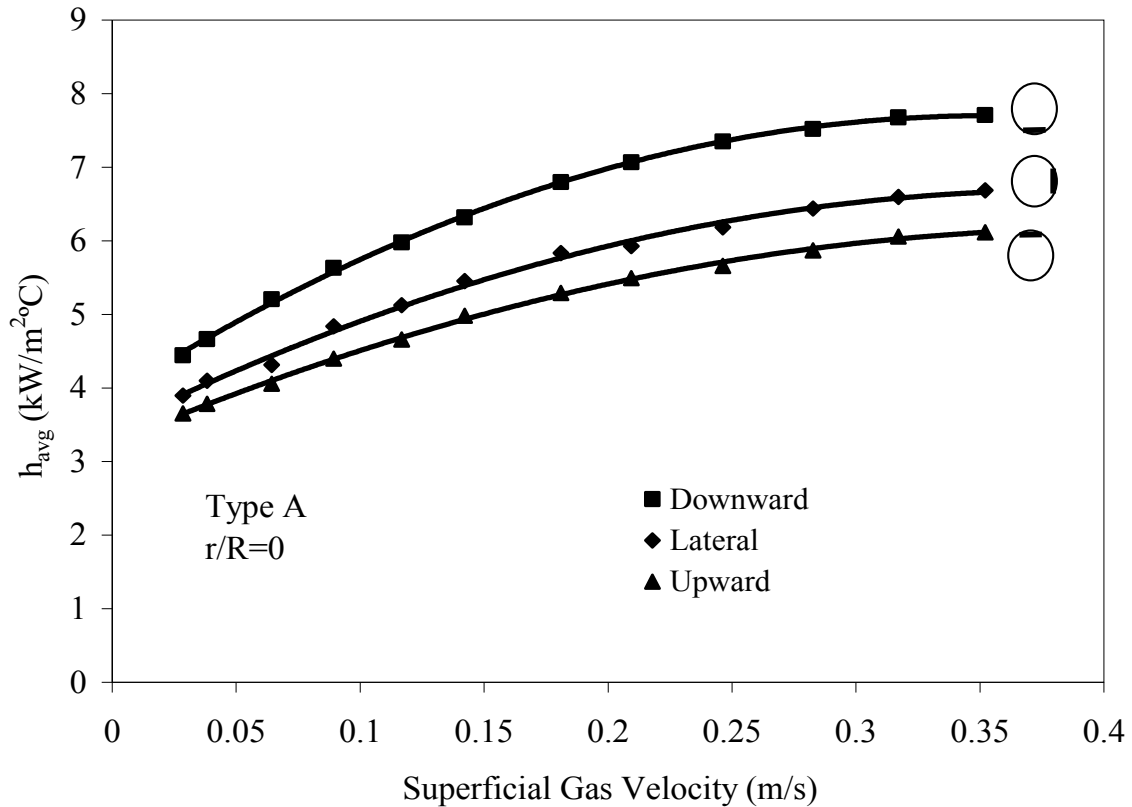


Figure 4.17. Local heat transfer coefficients for different probe orientations in presence of internals Type A in air-water-glass beads system (slurry conc. 10 vol. %) ($r/R = 0$)

It is observed from figure 4.18 that highest local slurry velocities are obtained with internal A, followed by internal B. Higher central slurry velocity with type A internal is a result of its vertical tube bundle design creating a funneling effect for gas and entrained liquid flow. B type internals have horizontal blades occupying part of column cross section. Internal B was placed at higher elevation (36 cm from the bottom) where bulk region turbulence seems to be helping bubble breakup and

dispersion. This indicates existence of different hydrodynamic conditions in bubble columns equipped with different internals. In hollow bubble columns and with internals, there is no significant difference in slurry velocities at low gas velocities (< 0.1 m/s) when bubble size distribution may not evolved significantly.

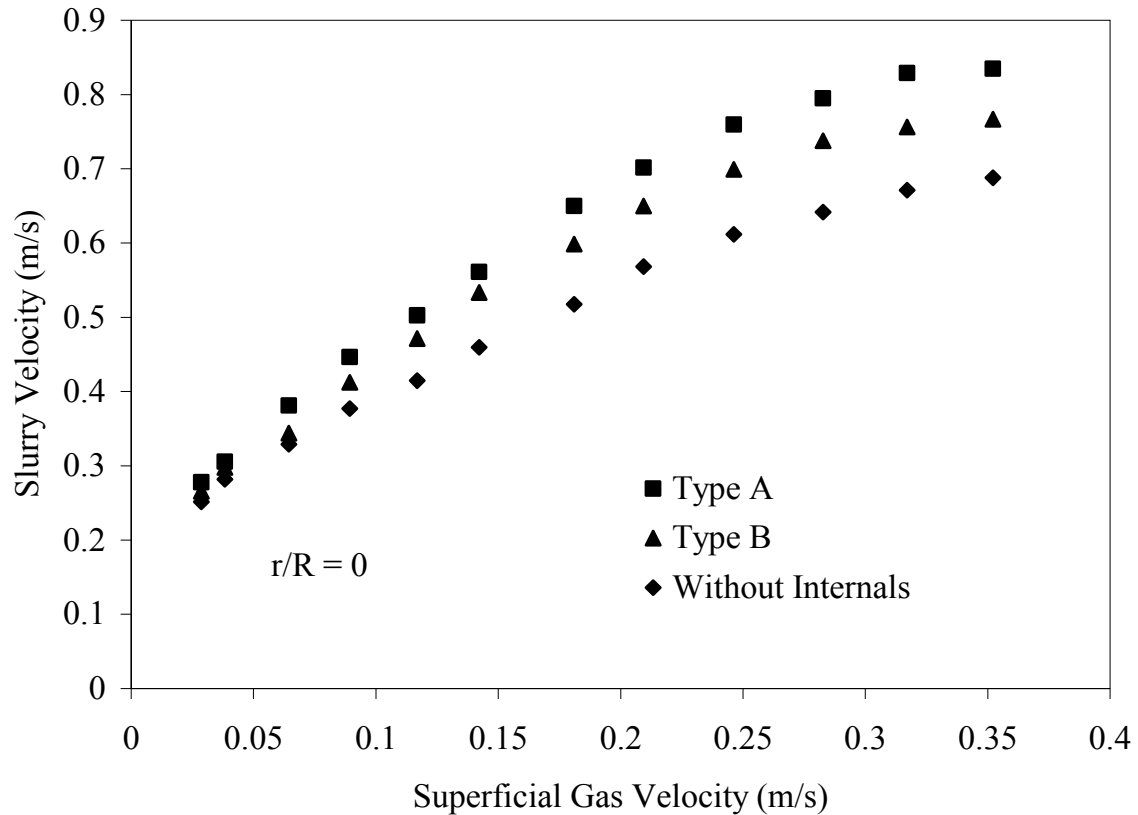


Figure 4.18. Comparison of slurry velocities estimated at the center in bulk section of the column by equation (4.3) in air- water –glass beads system

Figure 4.19 presents the slurry velocities in the wall region of bubble columns with and without internals in bulk section of the column. It is observed that trends are quite different compared to central region. The slurry velocities obtained in the wall region are higher with type B internals compared to type A internal. The slurry velocities with internal type A are lowest in wall region. It is also interesting to note that a difference between internal types is larger and distinct in the wall region. These results indicate important role of internals in altering radial liquid profile in the column and hence column hydrodynamics. The steepness of radial profile is

indicative of backmixing effects in the column. Larger the difference or sharper the steep, greater is the backmixing.

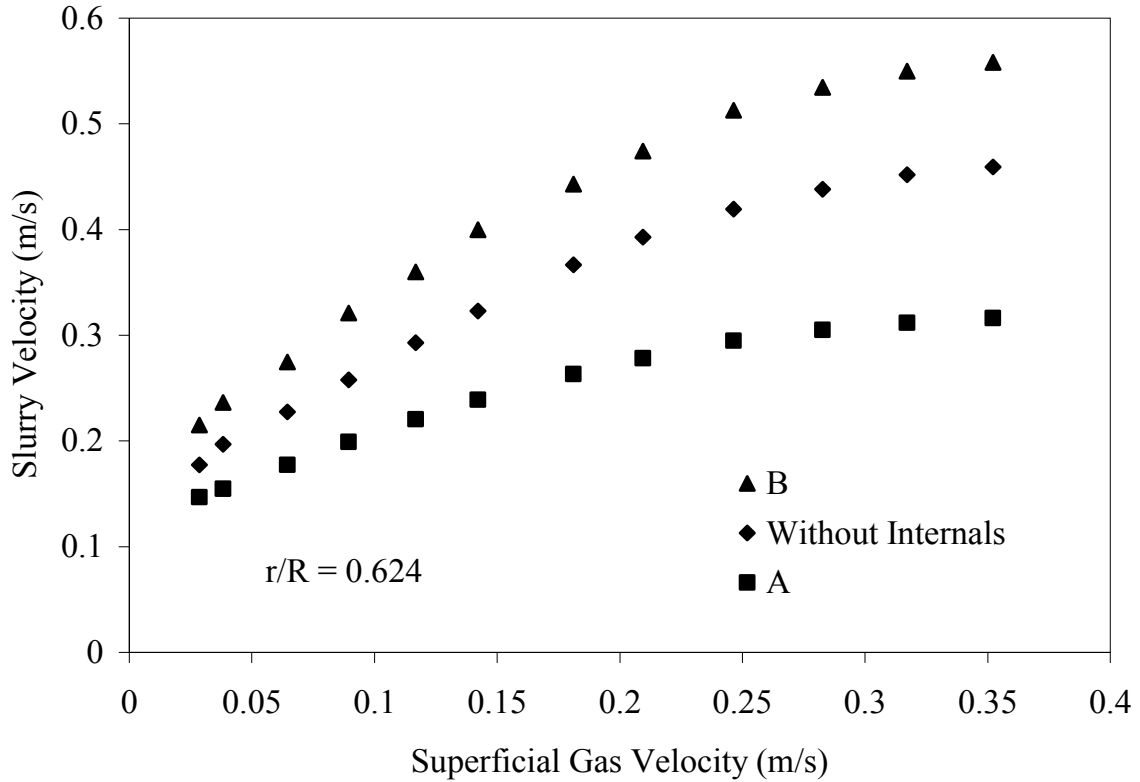


Figure 4.19. Comparison of slurry velocities estimated at the wall ($r/R=0.624$) in bulk section of the column by equation (4.3) in air- water –glass beads system

A plot of difference between radial slurry velocities for different internals is presented in Figure 4.20. It can be seen that largest differences are obtained with type A followed by hollow column and internal B in that order. Backmixing effects are thus expected to highest with type A internal and lowest with type B internal. Combining type B internal with type A should help reduce the large backmixing effects of type A internal alone. Proper positioning of type B internal between column bottom and tube bundle bottom can be investigated for optimization purposes.

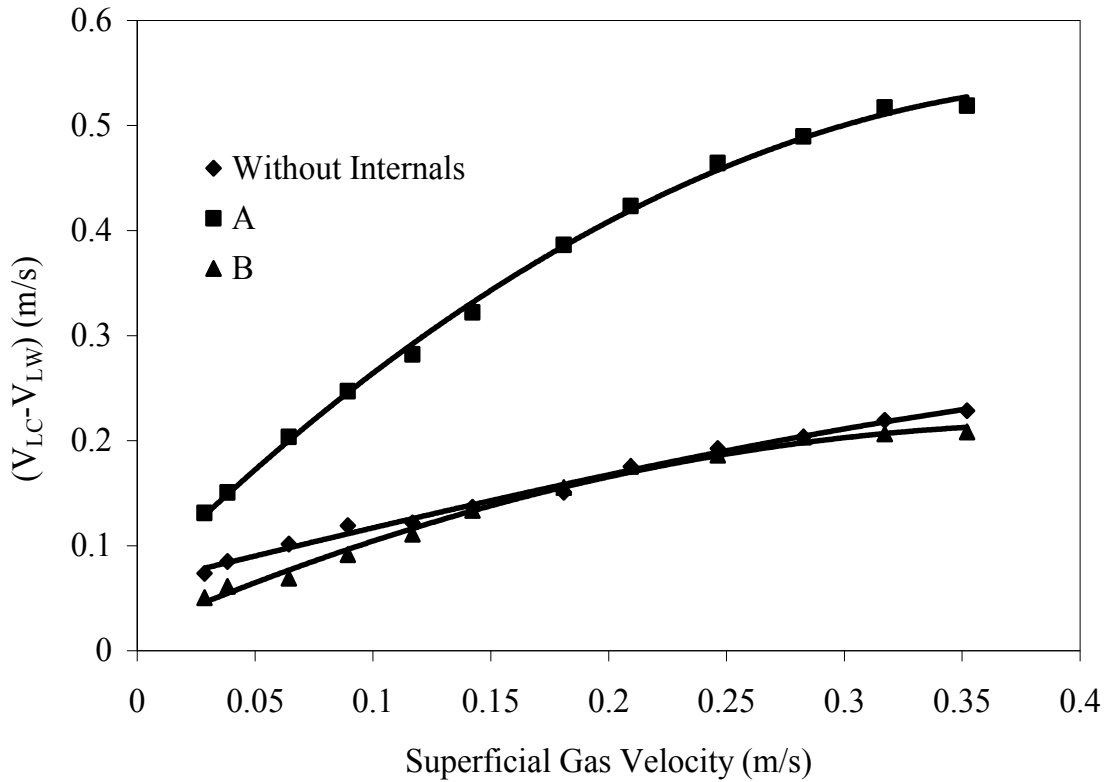


Figure 4.20. Comparison of differential radial liquid velocities with different internals in bulk section of the column

4.4 Conclusions

The fast response heat transfer probe used in the study easily captured local variations in a slurry bubble column caused by internals of different design. It is demonstrated that heat transfer coefficient decreased with increase in slurry concentration. However, rate of decrease is affected by the internal type used. This information can further help improve internals design and their configurations. For example radial variations observed with tube bundle type internal used in this study results in a steeper radial profile which can be altered by suitable design changes, as needed. The ability of the probe to provide local liquid velocity in the column allowed determination of back-mixing effects with different internals. Higher back mixing effects generated with tube bundle type internal may require appropriate mitigation steps for some applications. Further optimization studies in this direction will be helpful.

4.5 Notations

A	Heat transfer area, (m ²)
D _C	Column diameter (m)
D _p	Probe diameter (m)
h	Heat transfer coefficient, (kW/m ² °C)
k	Thermal conductivity, (W/m K)
N	Number of data points
q	Heat flow rate, (kW)
r	Radial location, (m)
R	Radius of the column, (m)
T	Temperature, (°C)
V	Superficial velocity (m/s)
w _S	weight fraction of the solid in the column (kg)
z	Axial location from the bottom of the column, (m)
Δx	Thickness of thermal barrier, (m)
a _s	Constant in equation (4.3)
Pr	Prandtl number, $\left(\frac{C_{p,l} \mu_l}{k_l} \right)$

Greek Symbols

μ	Viscosity (Pa.s)
ρ	Density (kg/m ³)
ν	Kinematic viscosity (m ² /s)

Subscripts

avg	Average
b	Bulk
c	Center
G	Gas
i	Instantaneous

L	Liquid
S	Solid
w	Wall
Su	Surface
st	Stagnation point

4.6 References

Li, H., Prakash, A., (2001). Survey of heat transfer mechanisms in a slurry bubble column. *Canadian Journal of Chemical Engineering*, 79, 717-725.

Li, H., Prakash, A., (1997). Heat transfer and hydrodynamics in a three-phase slurry bubble column. *Industrial and Engineering Chemistry Research*, 36, 4688-4694.

Li, H., (1998). Heat transfer and hydrodynamics in a three-phase slurry bubble column. Thesis, PhD University of Western Ontario, London, Ontario.

Chen, J., Li, F., Degaleesan, S., Gupta, P., Al-Dahhan, M.H., Dudukovic, M.P., Toseland, B.A., 1999. Fluid dynamic parameters in bubble columns with internals. *Chem. Eng. Sci.* 54, 2187-2197.

Chen, R.C., Reese, J., Fan, L.S., 1994. Flow structure in a three-dimensional bubble column and three-phase fluidized bed. *AIChE Journal*. 40, 1093-1104.

Deckwer, W.D., 1980. On the mechanism of heat transfer in bubble column reactors. *Chemical Engineering Science*. 35, 1341-1346.

Deckwer, W.D., 1992. *Bubble column reactors*, V. Cottrell (Trans.), R.W. Field (Ed.), John Wiley and Sons, England.

Deckwer, W.D., Schumpe, A., 1993. Improved tools for bubble column reactor design and scale-up. *Chemical Engineering Science*. 48, 889-911.

Duduković, M.P, Devanathan, N., 1992. Bubble column reactors: some recent developments. *Nato ASI Series E Applied Sciences*. 225, 353-377.

Duduković, M.P., Larachi, F., Mills, P.L., 2002. Multiphase catalytic reactors: a perspective on current knowledge and future trends. *Catalysis Reviews*. 44, 123-246.

Fan, L. S., 1989. *Gas-liquid-solid fluidization engineering*. Butterworths, Stoneham, MA.

Jhawar, A.K., Prakash, A., 2007. Analysis of local heat transfer coefficient in bubble column using fast response probes. *Chemical Engineering Science*. 62, 7274-7281.

Jhawar, A.K., Prakash, A., 2011. Influence of bubble column diameter on local heat transfer and related hydrodynamics. *Chemical Engineering Research and Design*. 89, 1996-2002.

Jhawar, A.K., 2012. Effects of internal on local heat transfer and column hydrodynamics in bubble columns. Thesis, PhD, University of Western Ontario, London, Ontario.

Joshi, J.B., Sharma, M.M., Shah, Y.T., Singh, C.P.P., Ally, M., Klinzing, G.E., 1980. Heat transfer in multiphase contactors. *Chemical Engineering Communications*. 6, 257-271.

Kara, S., Kelkar, B.G., Shah, Y.T., Norman, L.C., 1982. Hydrodynamics and axial mixing in a three-phase bubble column. *Industrial and Engineering Chemistry Process Design and Development*. 21, 584-594.

Kast, W., (1962), Analyse des wärmeübergangs in blasensäulen. *International Journal of Heat and Mass Transfer*, 5, 329-336.

Kluytmans, J.H.J., van Wachem, B.G.M., Kuster, B.F.M., Schouten, J.C., 2001. Gas holdup in a slurry bubble column: influence of electrolyte and carbon particles. *Industrial and Engineering Chemistry Research*. 40, 5326-5333.

Krishna, R., Urseanu, M.I., van Baten, J.M., Ellenberger, J., 1999. Influence of scale on the hydrodynamics of bubble columns operating in the churn-turbulent regime: experiment vs. Eulerian simulations. *Chemical Engineering Science*. 54, 4903-4911.

Kulkarni, A.A., Joshi, J.B., Kumar, V.R., Kulkarni, B.D., 2001. Application of multiresolution analysis for simultaneous measurement of gas and liquid velocities and fractional gas hold-up in bubble column using LDA. *Chemical Engineering Science*. 56, 5037-5048.

Larachi, F., Desvigne D., Donnat, L., Schweich, D., 2006. Simulating the effects of liquid circulation in bubble columns with internals. *Chemical Engineering Science*. 61, 4195-4206.

Li, H., 1998. Heat transfer and hydrodynamics in a three-phase slurry bubble column. Thesis, PhD, University of Western Ontario, London, Ontario.

Li, H., Prakash, A., 1997. Heat transfer and hydrodynamics in a three-phase slurry bubble column. *Industrial and Engineering Chemistry Research*. 36, 4688-4694.

- Li, H., Prakash, A., 2000. Influence of slurry concentrations on bubble population and their rise velocities in a three-phase slurry bubble column. *Powder Technology*. 113, 158-167.
- Li, H., Prakash, A., 2001. Survey of heat transfer mechanisms in a slurry bubble column. *The Canadian Journal of Chemical Engineering*. 79, 717-725.
- Li, H., Prakash, A., 2002. Analysis of flow patterns in bubble and slurry bubble columns based on local heat transfer measurements. *Chemical Engineering Journal*. 86, 269-276.
- Li, H., Prakash, A., Margaritis, A., Bergougnou, M.A., 2003. Effects of micron-sized particles on hydrodynamics and local heat transfer in a slurry bubble column. *Powder Technology*. 133, 171-184.
- Mudde, R.F., Groen, J.S., Van Den Akker, H.E.A., 1997. Liquid Velocity field in a bubble column: LDA experiments. *Chemical Engineering Science*. 52, 4217-4224.
- Nigam, K.D.P; Schumpe, A. 1996. *Three-phase sparged reactors*. Gordon and Breach, London.
- Prakash, A., Margaritis, A., Li, H., Bergougnou, M.A., 2001. Hydrodynamics and local heat transfer measurements in a bubble column with suspension of yeast. *Biochemical Engineering Journal*. 9, 155-163.
- Prakash, A., Margaritis, A., Saunders, R.C., Vijayan, S., 1999. Ammonia removal at high concentrations by the cyanobacterium *Plectonema boryanum* in a photobioreactor system. *Canadian Journal of Chemical Engineering*. 77, 99-106
- Reese, J., Fan, L.S., 1994. Transient flow structure in the entrance region of a bubble column using particle image velocimetry. *Chemical Engineering Science*. 49, 5623-5636.
- Riquarts, H.P., 1981. Strömungsprofile, impulsaustausch und durchmischung der flüssigen phase in bläsensaulen. *Chem Ing Techn*. 53, 60-61.
- Saxena, S.C., Rao, N.S., Saxena, A.C., 1990a. Heat transfer from a cylindrical probe immersed in a three-phase slurry bubble column. *Chemical Engineering Journal*. 44, 141-156.
- Saxena, S.C., Rao, N.S., Saxena, A.C., 1990b. Heat-transfer and gas-holdup studies in a bubble column: air-water-glass bead system. *Chemical Engineering Communication*. 96, 31-55.

Saxena, S.C., Rao, N.S., Saxena, A.C., 1992. Heat transfer and gas holdup studies in a bubble column: air-water-sand system. *The Canadian Journal of Chemical Engineering*. 70, 33-41.

Saxena, S.C., Vandivel, R., Saxena, A.C., 1989. Gas holdup and heat transfer from immersed surfaces in two- and three- phase systems in bubble columns. *Chemical Engineering communications*. 85, 63-83.

Schumpe, A., Grund, G., 1986. The gas disengagement technique for studying gas holdup structure in bubble columns. *The Canadian Journal of Chemical Engineering*. 64, 891-896.

Shah, Y.T., Kelkar, B.G., Godbole, S.P., Deckwer, W.D., 1982. Design parameters estimations for bubble column reactors. *AIChE Journal*. 28, 353-379.

Su, X., Hol, P.D., Talcott, S.M., Staudt, A.K., Heindel, T.J., 2006. The effect of bubble column diameter on gas holdup in fiber suspensions. *Chemical Engineering Science*. 61, 3098-3104.

Ueyama, K., Morooka, S., Koide, K., Kaji, H., Miyauchi, T., 1980. Behavior of gas bubbles in bubble columns. *Industrial and Engineering Chemistry Process Design and Development*. 19, 592-599.

Wilkinson, P.M., Spek, A.P., van Dierendonck, L.L., 1992. Design parameters estimation for scale-up of high-pressure bubble columns. *AIChE Journal*. 38, 544-554.

Wu, C., Al-Dahhan, M.H., Prakash, A., 2007. Heat transfer coefficients in a high-pressure bubble column. *Chemical Engineering Science*. 62, 140-147.

Youssef, A.A., Al-Dahhan, M.H., 2009. Impact of Internals on the Gas Holdup and Bubble Properties of a Bubble Column. *Industrial and Engineering Chemistry Research*. 48, 8007-8013.

Zahradník, J., Fialová, M., Růžička, M., Drahoš, J., Kaštánek, F., 1997. Duality of the gas-liquid flow regimes in bubble column reactors. *Chemical Engineering Science*. 52, 3811-3826.

CHAPTER 5. INFLUENCE OF BUBBLE COLUMN DIAMETER ON LOCAL HEAT TRANSFER AND RELATED HYDRODYNAMICS²

Abstract

Heat transfer coefficients measured in a 0.15m ID bubble column are compared with similar studies in larger diameter columns to identify influence of column diameter. Gas phase used is oil free compressed air and its flow rate is varied from 0.03 to 0.35 m/s. Tap water is the liquid phase and the solid particles used are 49 μ m glass beads and their concentration is varied up to 20 vol.%. The observed increase in heat transfer coefficients can be related to increase in liquid circulation velocity with column diameter which in turn is related to increase in large bubbles rise velocity. A simplified scale-up procedure is presented based on available data and suitably modified literature correlations for heat transfer coefficient.

Keywords: Bubble columns; Column diameter effects; Scale-up; Heat transfer; Radial profile; Hydrodynamics

² A Version of this chapter is accepted for publication in Chemical Engineering Research and Design (2011).

5.1 Introduction

In addition to their good heat transfer characteristics, the bubble columns offer several advantages such as: good mass transfer rates, isothermal conditions, online catalyst addition and withdrawal, washing effect of the liquid on catalyst, and low maintenance cost due to simple construction and absence of any moving parts (Deckwer, 1992; Deckwer and Schumpe, 1993; Kluytmans et al., 2001; Li and Prakash, 2002; Li et al., 2003). These benefits make these as the reactor of choice in a variety of industrial applications such as Fischer-Tropsch synthesis, methanol synthesis, dimethyl ether production, chlorination, hydrogenation and heavy oil upgrading, fermentation, biological waste water treatment, flue gas desulphurization, coal liquefaction etc. (Shah et al., 1982; Fan, 1989; Deckwer, 1992; Duduković and Devanathan, 1992; Deckwer and Schumpe, 1993; Li, 1998; Prakash et al., 1999; Prakash et al., 2001; Duduković et al., 2002; Li et al., 2003).

However scale-up procedures are still evolving primarily due to lack of detailed understanding of flow structure and mixing pattern for optimal design of these reactors (Deckwer and Schumpe, 1993; Li and Prakash, 2002). Saxena et al. (1990) pointed out that the model representation of hydrodynamics and heat transfer behavior of these columns is quite difficult due to the involved and complicated flow and dispersion patterns of the different phases, there by making it difficult and rather impossible to reliably scale these reactors. In last decade, attempts have been made to study the flow structure in bubble and slurry bubble columns using techniques such as particle image velocimetry (Chen et al., 1994; Reese and Fan, 1994), laser Doppler anemometry (Mudde et al., 1997, Kulkarni et al. 2001), single particle tracking techniques (Degaleesan et al., 1996, 1997) and local heat transfer coefficient-based technique (Li and Prakash, 2002; Wu et al., 2007). In this study attempts are made to get further insights into the local hydrodynamics based on heat transfer coefficient measurements and study of bubble populations. The heat transfer coefficient data obtained in this study has been compared with the literature data to determine scale-up effects. The hydrodynamic parameters such as gas holdup profile, liquid circulation velocity profile, and bubble rise velocity are compared with the available

literature data to get the insights of affect of these parameters on the heat transfer coefficient with the increase in column size.

5.2 Experimental Setup

Experiments were conducted in a Plexiglas column of 0.15 m internal diameter and height of 2.5 m (Figure 5.1). The column was supported by rigid metallic structure to keep it vertical and minimize mechanical vibrations which might affect pressure and heat transfer signals. The gas was introduced in the column using a coarse sparger. The detailed design of the coarse sparger is explained elsewhere (Gandhi, 1997). The sparger had five (1.9 mm diameter) downward facing holes on each of four arms. Oil free compressed air was used as gas phase, tap water was used as the liquid phase and 49 μ m glass beads (Potters Industries, spheriglass ® A glass) of density 2500 kg/m³ constituted the solid phase. The gas flow rate was measured using three calibrated sonic nozzles of different diameter (0.7mm, 1.5 mm and 2.5 mm). The superficial gas velocity was varied from 0.03 to 0.35 m/s.

The unaerated water height in the column was maintained around 1.45 m. A measuring tape was provided on the column to note the liquid level and dispersion height. The solid concentration was varied from 5 vol% to 20 vol%. Two pressure transducers (OMEGA Type PX541-7.5GI and Type PX541-15GI) were used to measure the pressure fluctuations in distributor ($z = 0.027$ m) and disengagement section ($z = 1.318$ m), as shown in Figure 5.1. The pressure transducers were connected to a DC power supply and generated a voltage proportional to measured pressure. The response time of the pressure transducers was 2 ms and data were recorded for 105 seconds at a rate of 60 Hz.

Instantaneous heat flux was measured using a micro-foil heat flux sensor (Rdf, Model number 20453-1 G161).The sensor was flush mounted on the surface of a brass cylinder of 11 mm outer diameter. A small cartridge heater (Chromalox, model number CIR-1012) was installed inside the brass cylinder. The AC power was

supplied to the cartridge heater through a variac to regulate supplied power in the range of 20 to 40V. The detailed design of the heat flux probe is explained elsewhere (Li and Prakash., 1997; Li, 1998). Probe location could be changed both axially and radially and it could also be rotated to study effects of sensor orientation on measured values. For most measurements, the sensor was in lateral position with respect to flow, however for some measurements it was oriented to face the flow direction to obtain stagnation point heat transfer coefficient used to estimate local liquid velocity (Li and Prakash, 2002). The temperature of the liquid phase was measured using two copper-constantan thermocouples (ANSI type T). These thermocouples were located at two radial locations: one at center and other close to the wall. Axial position of the thermocouple could be changed. The response time of micro-foil heat flux sensor was 20 ms and data were recorded for 180 s at a rate of 60 Hz. The probe generated microvolt signals, which were amplified to millivolts by a suitable amplification circuit using 15V DC supply. A minimum of three test runs were performed at each condition and average values are reported. For the heat flux sensor, the following equation can be derived for liquid film heat transfer coefficient (Li and Prakash, 2001):

$$\frac{1}{h_i} = \frac{T_{Su} - T_b}{q/A} - \frac{\Delta x}{k} \quad (5.1)$$

The second term on the right hand side of Equation 5.1 is negligible compared to the first term (< 1%) due to high conductivity (k) and small thickness (Δx) of the thermal barrier film. Therefore instantaneous heat transfer coefficient could be determined by measurement of heat flux and the difference between surface and bulk temperatures at a given time. The time-averaged heat transfer coefficient at a given location was obtained by averaging the instantaneous heat transfer data collected.

$$h_{avg} = \frac{1}{N} \sum_{i=1}^N \frac{q/A}{T_{Su} - T_b} \quad (5.2)$$

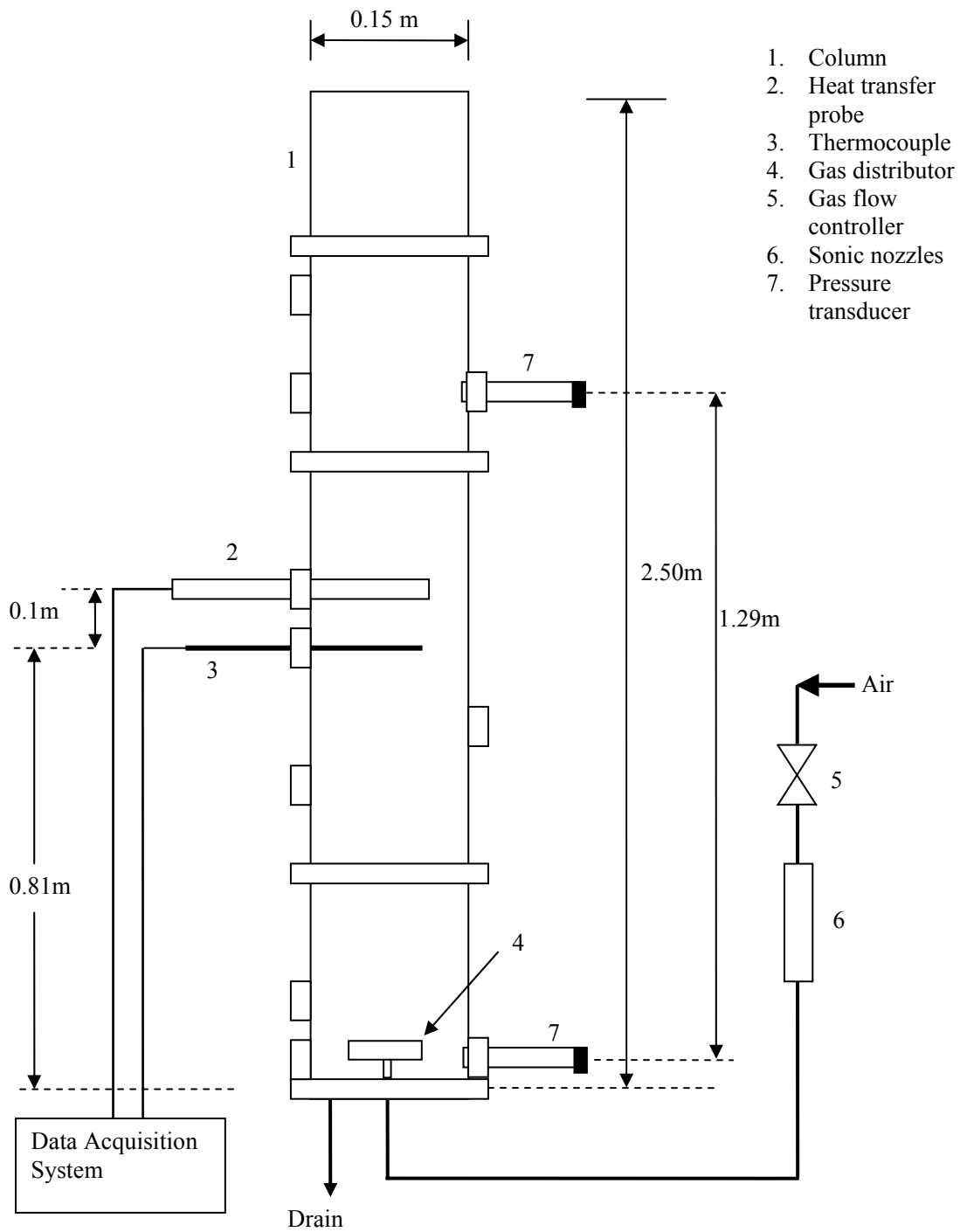


Figure 5.1. Schematic diagram of experimental setup

5.3 Results and Discussion

To analyze the effects of column diameter on heat transfer coefficient, the data of this study were compared with other literature studies (Li, 1998; Li and Prakash, 2001), who used a similar heat flux probe in a larger diameter column. Figure 5.2a shows a comparison of average heat transfer in this study with the heat transfer coefficients obtained in larger diameter column. Comparison of measured heat transfer coefficients were also made in air-water-glass beads system (Figure 5.2b) - the scale effect is observed clearly irrespective of slurry concentration.

Similar trends were observed by Saxena et al. (1989) who compared the results obtained in the central region of bubble columns of 0.108 m and 0.305 m diameter (Figure 5.3). These authors used a 19 mm diameter probe of conventional design placed at column center. The observed increase in heat transfer with column diameter was attributed to better mixing achieved with large diameter by Saxena et al. (1989).

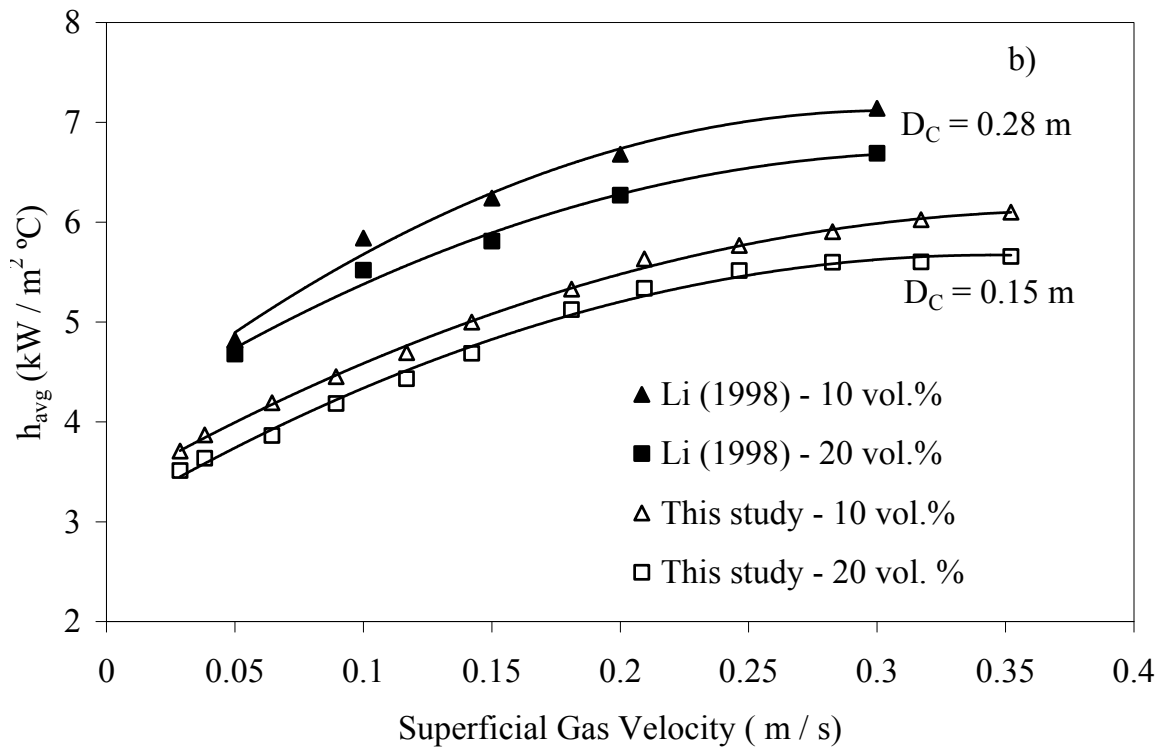
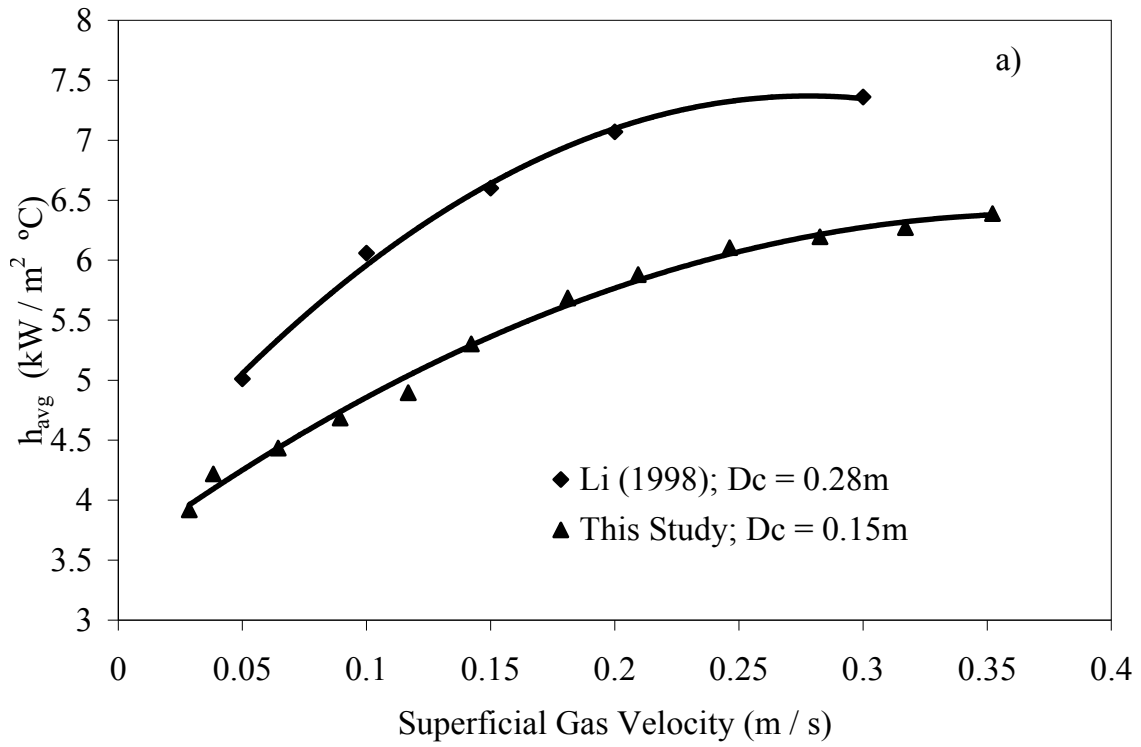


Figure 5.2. Comparison of measured heat transfer coefficients with literature studies effects of column diameter: (a) air-water system. (b) air-water-glass beads system

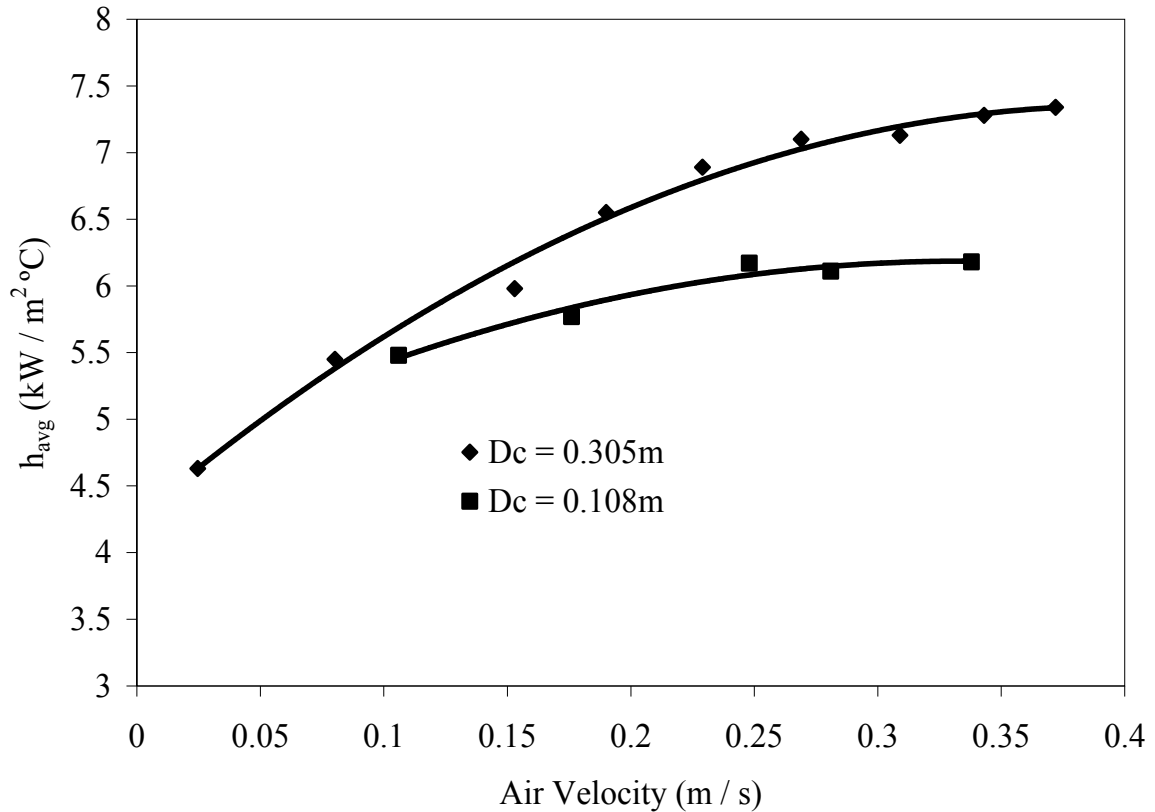


Figure 5.3. Heat transfer coefficient data obtained in different column diameter from Saxena et al. (1989)

A comparison of average gas holdups measured in this study with the data of Li (1998) shows that there is little effect of column diameter on average gas holdups in air-water or air-slurry systems (Figure 5.4). These findings are consistent with other literature studies which report that the average gas holdups become scale independent when $D_c \geq 0.15$ m (Shah et al., 1982; Wilkinson et al., 1992; Zahradník et al., 1997; Su et al., 2006). Since gas holdups alone can't explain the observed increases in heat transfer coefficients with column diameter, gas holdup structure in the columns was analyzed. Populations of different bubble fractions and their rise velocities were obtained by the dynamic gas disengagement (DGD) method. This technique is based on the principle that different bubble classes in dispersion can be distinguished if there are significant differences between their rise velocities (Schumpe and Grund, 1986). The procedure used to obtain bubble fractions and their rise velocities is explained elsewhere (Li and Prakash, 2000).

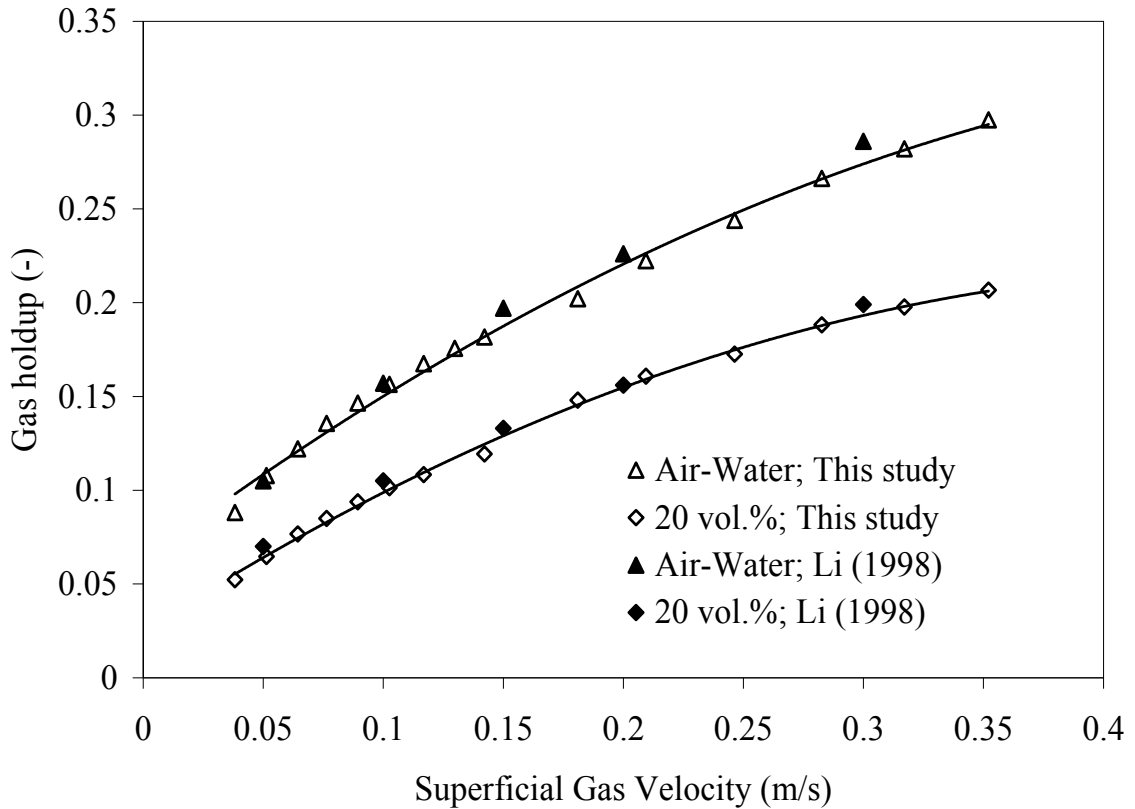
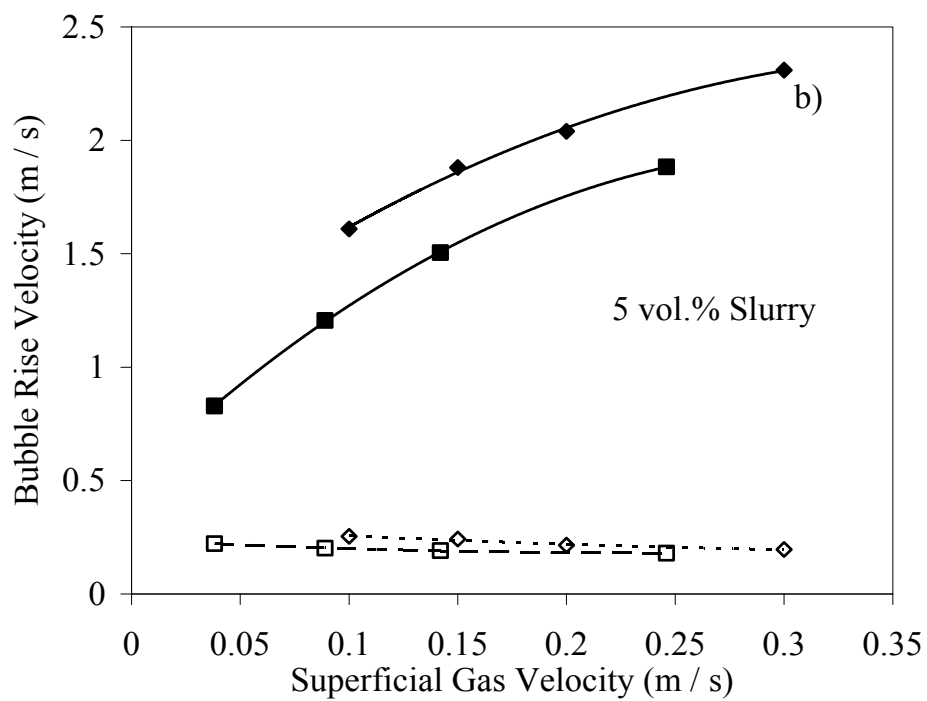
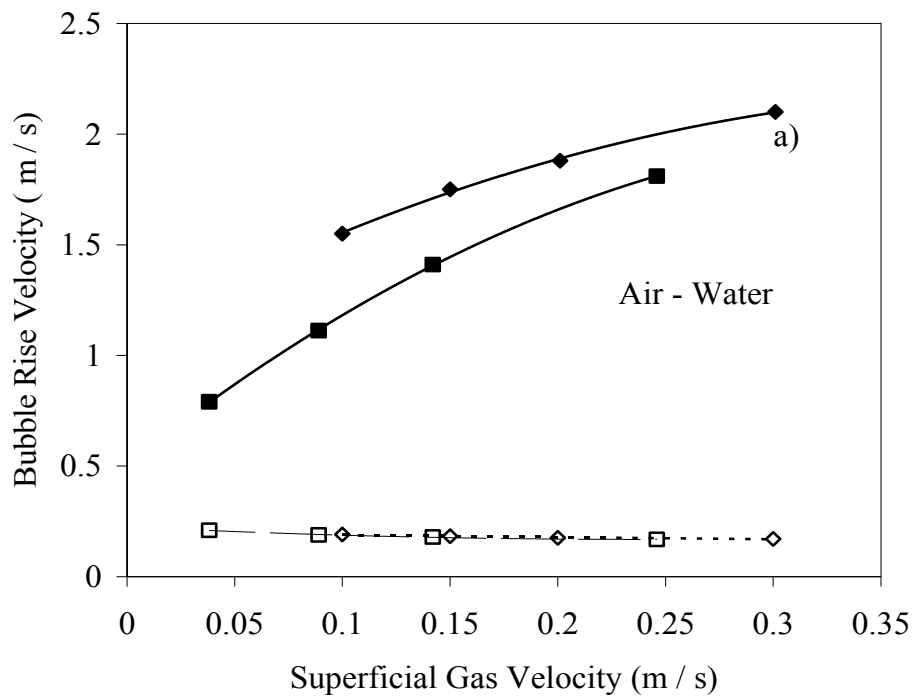


Figure 5.4. Comparison of average gas holdup obtained with literature studies

Figures 5.5 a, b and c compare rise velocities of small and large bubble fractions obtained in air-water and air-water-glass beads (5 vol.% and 10 vol.% slurry concentrations) systems with those obtained by Li and Prakash (2000). The rise velocities of large bubbles obtained in this study ($D_c = 0.15$ m) are lower than those obtained in larger diameter column by Li and Prakash (2000). This variation in bubble rise velocity with column diameter can be attributed to the wall effects on bubble size (Ueyama et al., 1980; Li and Prakash, 2000). The increase in bubble rise velocity with column diameter affects the local liquid (slurry) velocities, which in turn can affect the local heat transfer coefficients and mixing in column. This can be one of the potential reasons for the increase in heat transfer coefficient with column diameter.



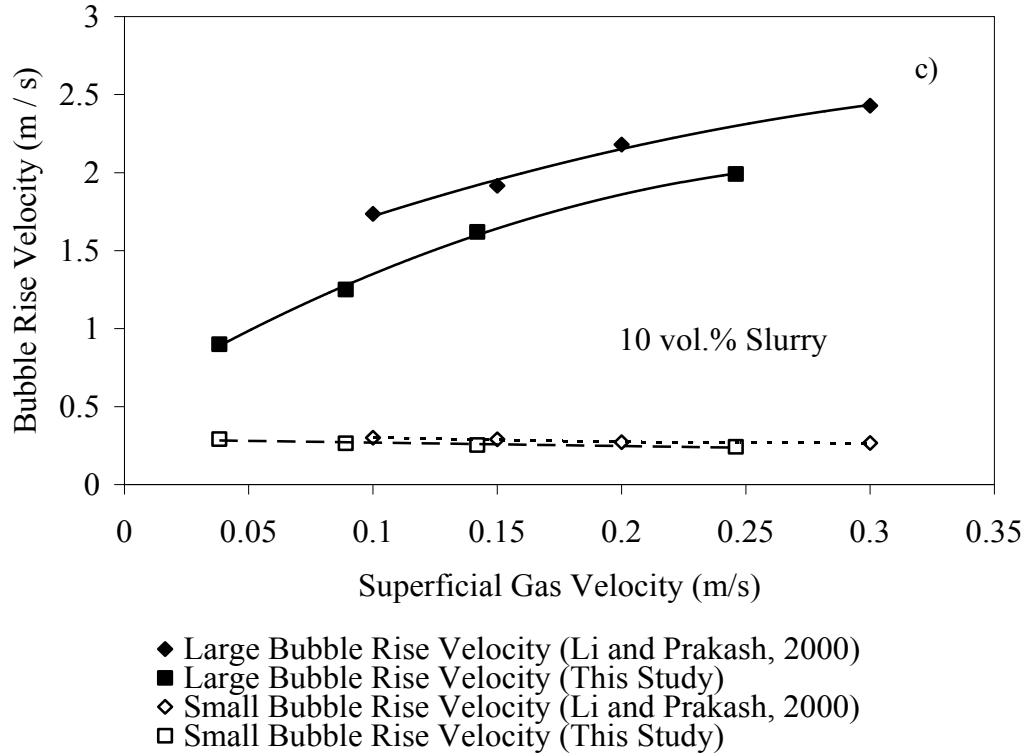


Figure 5.5. Comparison of bubble rise velocity with literature studies: a) air-water system (b) air-water-5 vol.% glass beads systems (c) air-water-10 vol.% glass beads system

The heat transfer probe used in this study could also detect flow direction and provide an estimation of local liquid (slurry) velocity using boundary layer theory (Li and Prakash, 2002). Flow direction could be identified (upward or downward) by measuring the time averaged local heat transfer coefficients using the different orientation of the probe (upward, downward or lateral). Figure 5.6 show the results obtained at the center ($r/R=0$) in the bulk section of the column. The heat transfer coefficients obtained with the downward orientation of the probe are higher than those obtained with the upward orientation, hence indicating upward liquid flow at that location. As pointed out by Li and Prakash (2002), local liquid velocity could be obtained by applying boundary layer theory to the measured stagnation point heat transfer coefficients.

$$\frac{h_{st} D_p}{k_L} = a_s (\text{Pr})^{0.4} \left(\frac{V_L D_p}{\nu_L} \right)^{0.5} \quad (5.3)$$

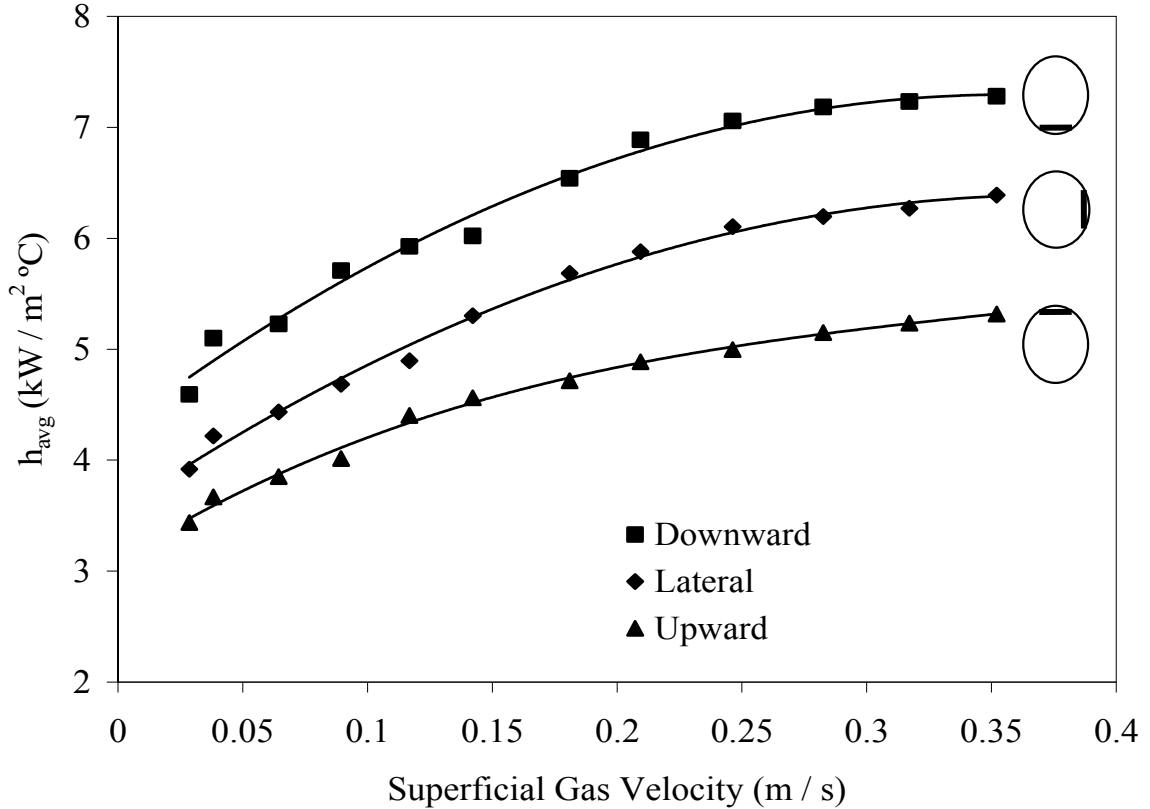


Figure 5.6. Local heat transfer coefficients for different probe orientations in bulk section ($z = 0.91$ m; $r/R = 0.0$) for air-water system

In the above equation, the value of a_s depends on several factors such as probe design, orientation etc. In this study, values of a_s were obtained at a low (0.0382 m/s) and a high superficial gas velocity (0.15 m/s) using the center line liquid velocity reported in 0.15 m diameter column in different literature studies (Kulkarni et al., 2001; Forret et al., 2003) and the local heat transfer coefficient obtained with the downward orientation of the probe. The values of a_s obtained using the above procedure were quite close (within 3%) for the two superficial gas velocities. Hence an average value ($a_s = 0.7$) was used in Equation (5.3) to estimate the liquid velocities at the column center using data of this study and those reported by Li (1998). As shown in Figure 5.7, these values are in good agreement with the predictions by the well tested correlation of Riquarts (1981) - absolute average error less than 5%.

$$V_{L,c} = 0.21\sqrt{gD_C} \left(\frac{V_G^3}{v_L g} \right)^{\frac{1}{8}} \quad (5.4)$$

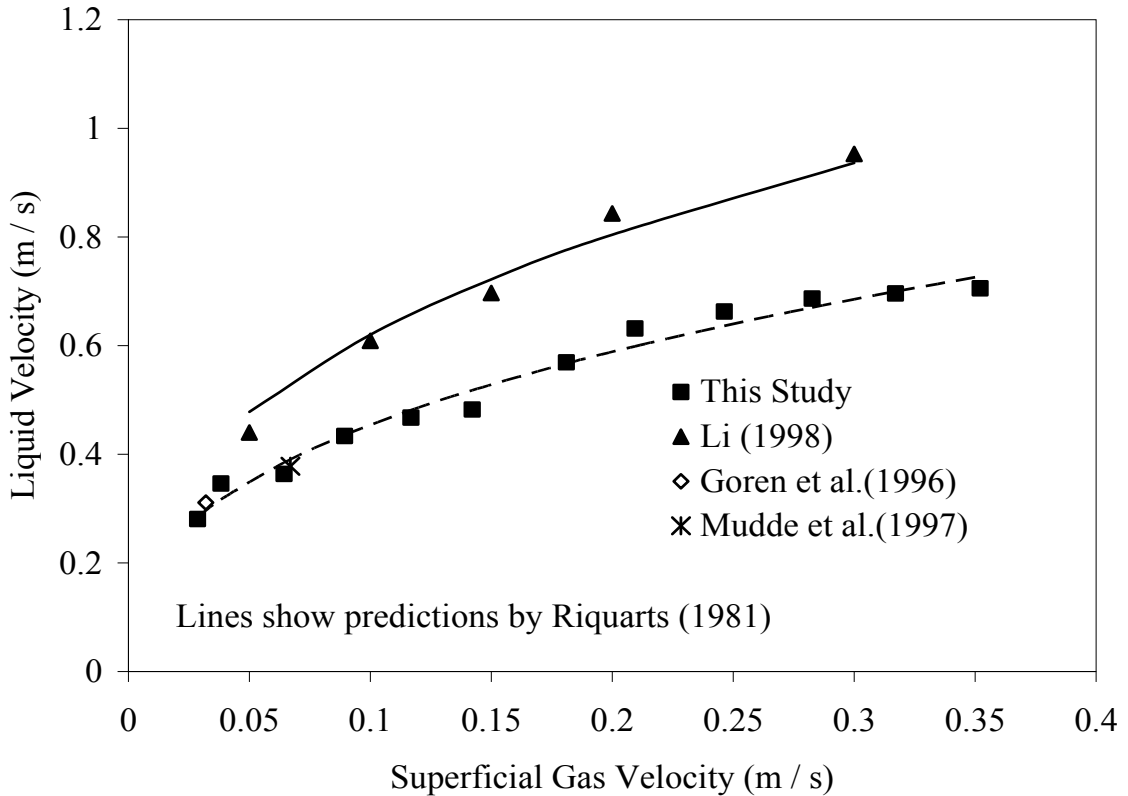


Figure 5.7. Comparison of liquid velocities estimated by equation (5.3) with predictions by literature correlations (air-water system)

The figure also shows that the measured center line liquid velocities by Groen et al. (1996) and Mudde et al. (1997) are also close to the predictions. This indicates that the correlation based on stagnation point heat transfer can provide a good estimate of center line liquid velocity in different diameter columns. In order to further confirm these observations, experimental data of Krishna et al. (1999) for liquid velocity in different diameter bubble columns was also used. As shown in Figure 5.8, these authors measured the effect of column diameter on the radial distribution of the liquid velocity in the heterogeneous regime. The liquid velocity increases with increase in column diameter at all the radial locations except in the region close to the wall. From Figure 5.8, the effect of column diameter on center line liquid velocity is plotted in Figure 5.9 and comparisons are made with the predicted centerline liquid velocity based on heat transfer measurements at the superficial gas velocity of 0.23 m/s. The heat transfer data were interpolated to get the centerline liquid velocities at the

superficial gas velocity of 0.23 m/s. It can be observed from Figure 5.9 that, the values obtained by Krishna et al. (1999) are slightly lower than those based on heat transfer measurements or predicted by Riquart's correlation but approach predictions with increasing column diameter. This could be attributed partially to different measurement techniques and calibration procedures used in these studies.

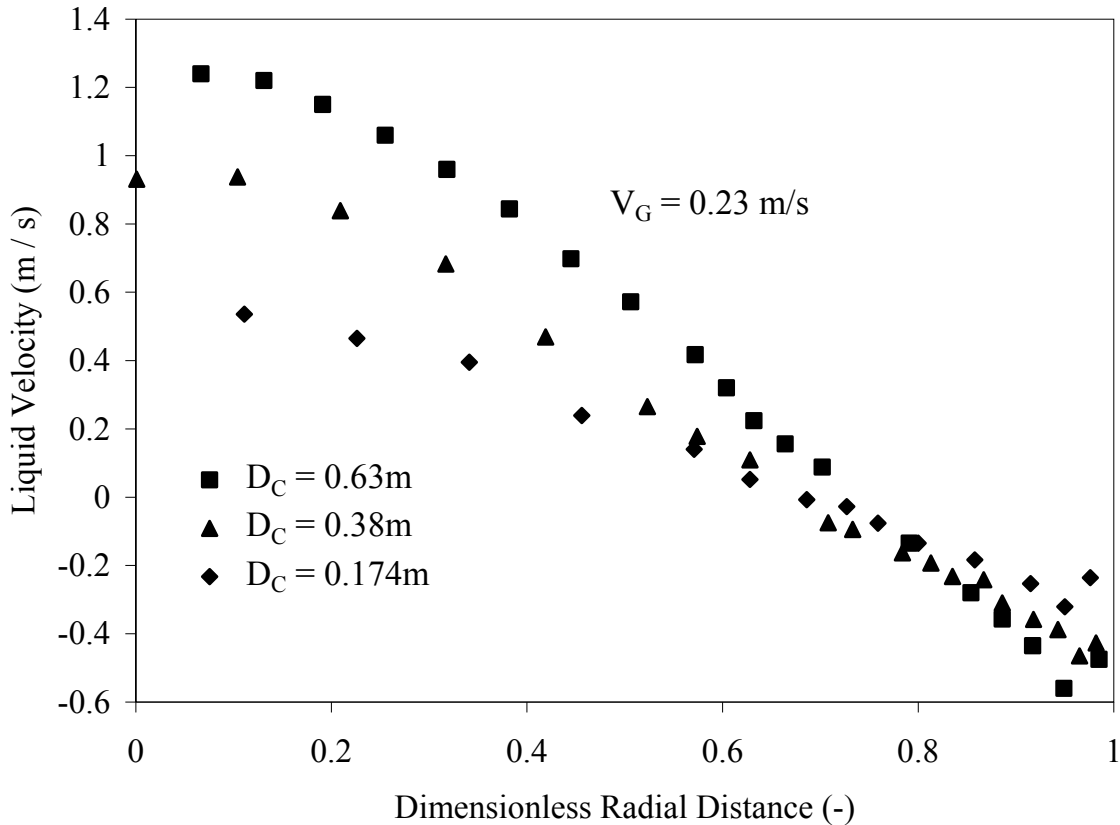


Figure 5.8. Radial distribution of liquid velocity in heterogeneous flow regime from Krishna et al. (1999)

A review of heat transfer studies and proposed correlations in bubble columns showed that literature correlations have either not accounted for column diameter effects (i.e. Deckwer, 1980; Saxena et al., 1992) or shown the effect to be negligibly small (Joshi et al., 1980). It should be pointed out that literature correlations are generally based on bed-to-wall heat transfer where column diameter effects may not be significant due to the damping effect of the wall. This is also supported by the plots of radial profiles of liquid velocity in different diameter columns in Figure 5.8. It can be observed that local liquid velocities are similar in the wall region but the differences

are significant in the central region. A comparison of heat transfer coefficients in different column diameters compared in this study also showed that that wall region heat transfer coefficients are much closer compared to the central region, where differences are significant.

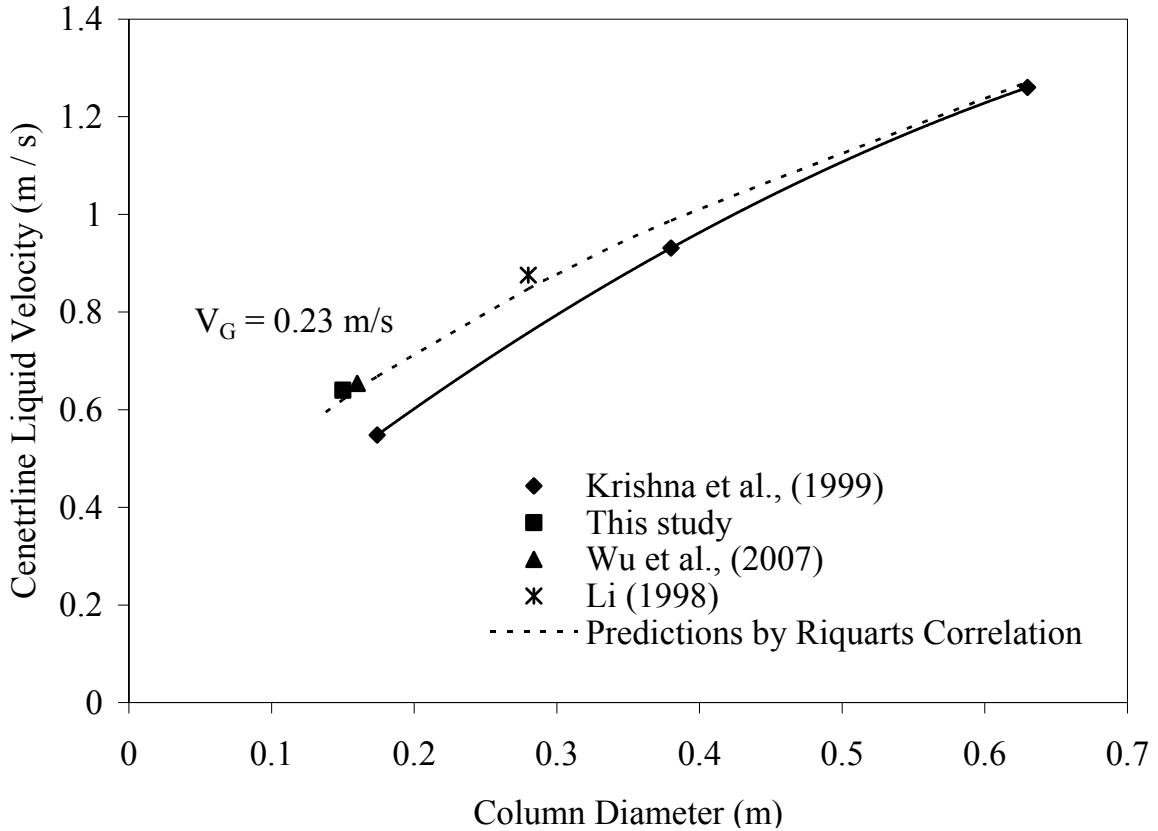


Figure 5.9. Effect of column diameter on centerline liquid velocity

From the above, it can be concluded that a method based on central line liquid velocity needs to be used for the estimation of heat transfer coefficient at the column center. For a given column diameter, first the correlation of Riquarts (1981) can be used to obtain center line liquid velocity. This velocity can be substituted in Equation (5.3) to estimate stagnation point heat transfer coefficient at the column center. However, this value will be high for vertical heat transfer tubes often used in these reactor systems. The data of this study together with that of Li and Prakash (2002) and Wu et al., (2007) was used to get a correction factor based on the lateral (vertical) and downward (stagnation point) orientation of the probe. It was found that average

ratio was essentially constant (about 0.85) for all the column diameters. This procedure was applied to estimate heat transfer coefficients for a vertical tube at column center for two column diameters (0.15m and 0.28m). It can be seen from Figure 5.10 that the predicted values are within 5% of experimental values. This procedure was also used to predict the data reported by Saxena et al., (1989) in 0.108 and 0.305 m diameter columns. It gives good predication of their data (average error < 5%) in 0.305 m diameter column, but the average error increased to 10% for 0.108m column diameter. This increase in error for small column diameter can be attributed to the increased wall effect on column hydrodynamics in small column diameter ($D_c < 15$) as pointed in literature (Shah et al., 1982; Wilkinson et al., 1992; Zahradnik et al., 1997; Su et al., 2006;). This indicates that the wall damping effect would be significant for smaller diameter columns.

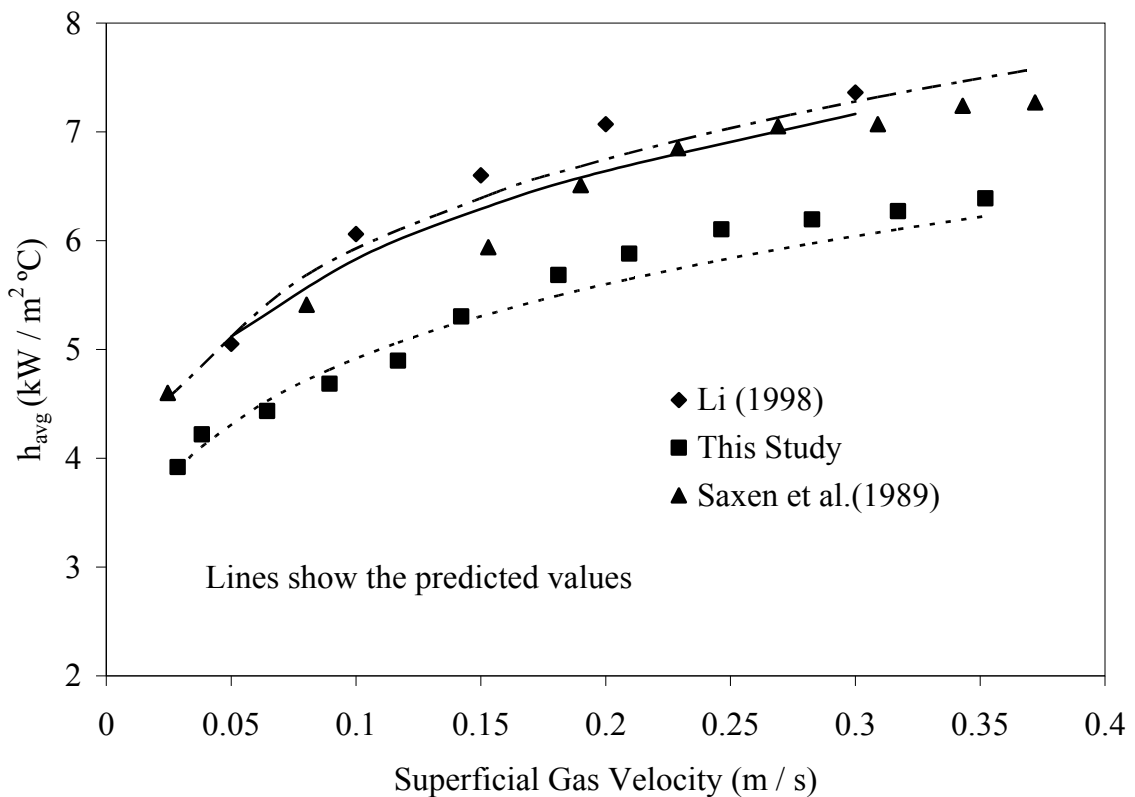


Figure 5.10. Comparison of predicted and experimental value of heat transfer coefficient for vertical orientation of heat flux sensor

A correlation that is based on liquid circulation velocity in bubble columns was proposed by Joshi et al. (1980) for bed to wall heat transfer. This dimensionless correlation shown in its general form below was adapted by these authors from stirred systems.

$$\frac{h_w D_C}{k_L} = C \left(\frac{D_C V_L \rho_L}{\mu_L} \right)^m \left(\frac{C_{p,L} \mu_L}{k_L} \right)^{1/3} \left(\frac{\mu_L}{\mu_{L,w}} \right)^{0.14} \quad (5.5)$$

It was decided to test this correlation for the estimation of central region heat transfer coefficient in bubble columns by using central line liquid velocity. The predicted values by Equation 5.5 for the two column diameters were within 6% for the whole range of gas velocities for selected values of correlation constant and exponent (i.e. $C=0.084$; $m=0.8$). This correlation was also used to predict the data reported by Saxena et al. (1989) in 0.108 and 0.305 m diameter columns. It gives good predication of their data with average error less than 6% in 0.305 m diameter column, but the average error increased to about 8% for 0.108m column diameter. This increase in error can be attributed to the wall effects as discussed above for the smaller diameter column.

While the above procedure gives a good estimate of heat transfer coefficients at the column center, there is often need to determine the values at different radial locations since for different industrial applications, heat transfer surface could be installed at different radial locations in a reactor. Jhawar and Prakash (2007) proposed a correlation to predict the heat transfer coefficient at different radial locations knowing the value at the center.

$$\frac{h_c - h(r)}{h_c} = \left(\frac{n-1}{n} \right) \left(\frac{r}{R} \right)^n \quad (5.6)$$

Figures 5.11a,b, show the radial profiles of the heat transfer coefficients measured in bubble columns with tube bundle type internal (type A) and without, and those reported by other researchers (Li, 1998; Wu et al., 2007). Equation (5.6) well predicted (within 5%) the radial profile in hollow bubble columns in this study and those reported in literature up to $r/R=0.75$ using the recommended value of 1.4 for n . In the region between $r/R=0.75$ to $r/R=1$,

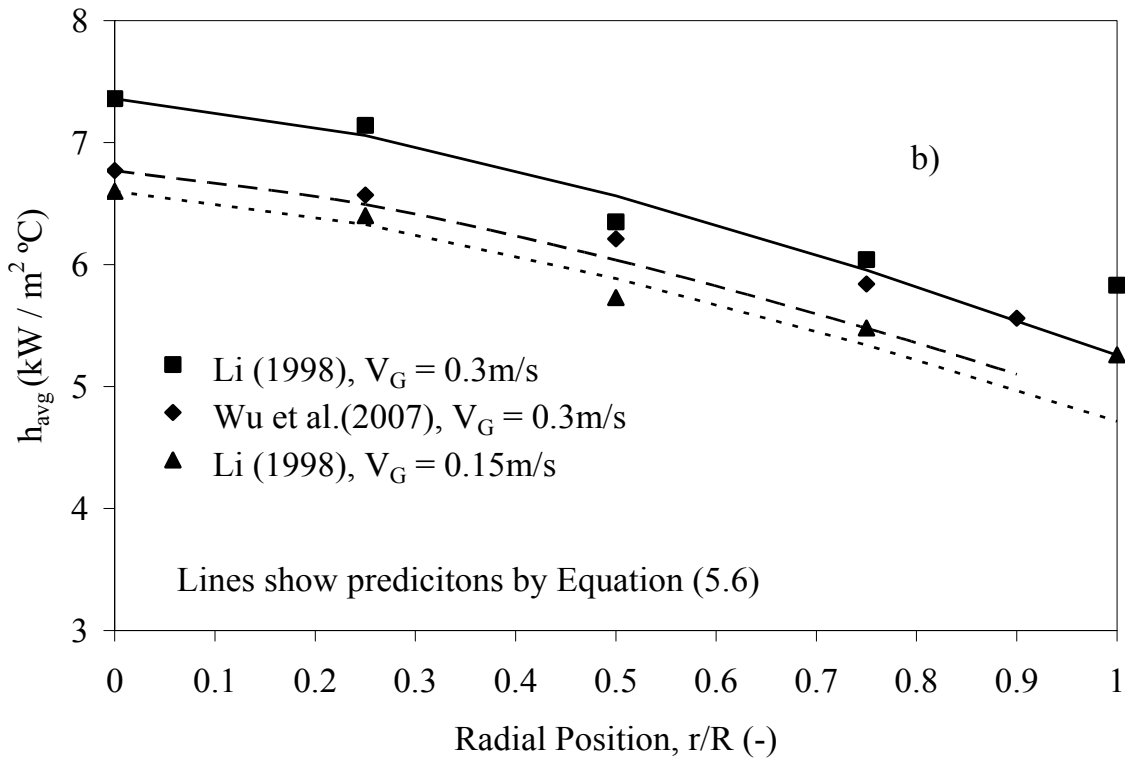
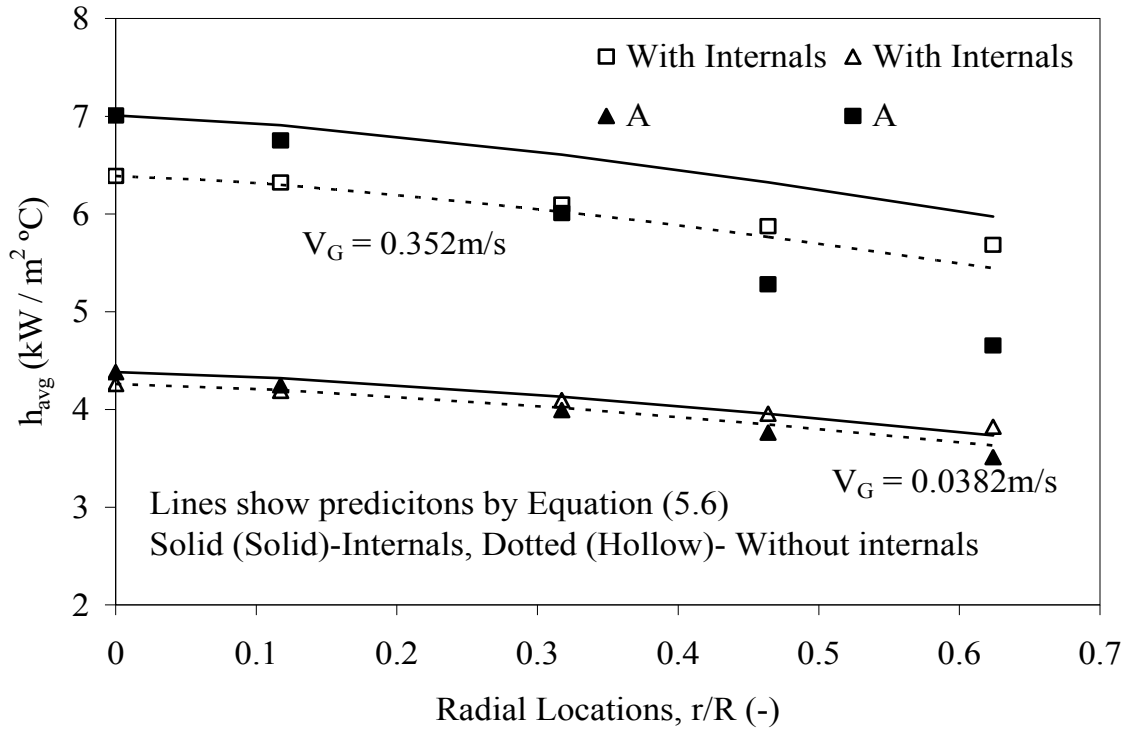


Figure 5.11. Prediction of Radial profile of heat transfer coefficient using equation (5.6): (a) this study (b) literature studies in different column diameter

the correlation predicted lower values than the measured heat transfer coefficients with average error rising to about 12%. It can be observed from Figure 5.11b that the radial profile of heat transfer coefficient becomes relatively flat in this region and equation (5.6) may not be applicable here. In bubble columns with tube bundle (type A) the radial profile is quite different at low velocities the radial profile is almost similar to those obtained in hollow bubble column and are well predicted by equation (5.6) using recommended value of n. But at high superficial gas velocity (in fully developed heterogeneous flow) the radial profile is different in core and annular region. In the core region, equation (5.6) well predicts the data; predictions are higher in annular region. In presence of tube bundle type internal, the variable n in equation (5.6) needs to be modified. The average heat transfer coefficient between two radial positions – where tubes bundle could be arranged- can be obtained by equation 5.7.

$$h_{avg}(r) = \frac{1}{A_{anu}} \int_{r_1}^{r_2} h(r) 2\pi r dr \quad (5.7)$$

Substituting Equation (5.6) into (5.7) and integrating gives.

$$h_{avg}(r) = h_c \left(1 - \frac{0.17}{R^{1.4}} \left(\frac{r_2^{3.4} - r_1^{3.4}}{r_2^2 - r_1^2} \right) \right) \quad (5.8)$$

The value of n in equation (5.6) was taken as 1.4, as suggested by Jhawar and Prakash (2007). Equation (5.8) can be used to calculate the average heat transfer coefficient at any given radial location. The estimated heat transfer coefficient at a superficial gas velocity of 0.35 m/s and at the radial location, $r/R = 0.6$ with the width of 19 mm cross-section is $5.2 \text{ kW/m}^2 \text{ }^\circ\text{C}$, which is within 7% of the experimental value obtained at $r/R=0.624$. It can also be noted from Figure 5.11a that the values obtained for the tube bundle type internal are higher in central and lower in wall regions compared to hollow bubble columns. A quick calculation shows that the differences in central and

wall regions with tube bundle tend to compensate each other. So hollow column n value ($n=1.4$) in equation (5.6) should give reasonable predictions.

5.4 Conclusions

The variation of heat transfer coefficient in bubble columns with diameter was established based on the data of this study and comparison with literature studies. The diameter effect is more prominent in the central region of column. Negligible effect of column diameter in the wall region can be related to turbulence damping effect in that region. The observed increase in heat transfer coefficient in the central region of column is related to increase in liquid circulation velocity with column diameter which can in turn be related to increase in large bubbles rise velocities. A general literature correlation which accounts for diameter effects on heat transfer has been modified to predict center line heat transfer coefficient in bubble columns. A procedure is presented to estimate average heat transfer coefficient for tube bundle placed at a radial location in a bubble column reactor of a given diameter.

5.5 Notations

A	Heat transfer area, (m^2)
C_p	Heat capacity, (J/kg K)
D_C	Column diameter (m)
D_p	Probe diameter (m)
d_p	Diameter of particle (m)
g	Acceleration due to gravity (m/s^2)
h	Heat transfer coefficient, ($kW/m^2\text{ }^\circ C$)
k	Thermal conductivity, (W/m K)
n	Constant in equation (5.6)
N	Number of data points
q	Heat flow rate, (kW)
r	Radial location, (m)
R	Radius of the column, (m)

T	Temperature, (°C)
V	Superficial velocity (m/s)
w _s	weight fraction of the solid in the column (kg)
z	Axial location from the bottom of the column, (m)
Δx	Thickness of thermal barrier, (m)
ΔH	Distance between two transducers (m)
a _s	Constant in equation (5.3)
Pr	Prandtl number, $\left(\frac{C_{p,l} \mu_l}{k_l} \right)$

Greek Symbols

μ	Viscosity (Pa.s)
ρ	Density (kg/m ³)
ν	Kinematic viscosity (m ² /s)

Subscripts

1	any given radial location
2	any given radial location greater than radial location 1
anu	Annular crossection
avg	Average
b	Bulk
c	Center
G	Gas
i	Instantaneous
L	Liquid
S	Solid
w	Wall
Su	Surface
st	Stagnation point
1	Any particular location
2	Any particular location

5.6 References

- Chen, R.C., Reese, J., Fan, L.S., 1994. Flow structure in a three-dimensional bubble column and three-phase fluidized bed. *AIChE Journal*. 40, 1093-1104.
- Deckwer, W.D., 1980. On the mechanism of heat transfer in bubble column reactors. *Chemical Engineering Science*. 35, 1341-1346.
- Deckwer, W.D., 1992. Bubble column reactors, V. Cottrell (Trans.), R.W. Field (Ed.), John Wiley and Sons, England.
- Deckwer, W.D., Schumpe, A., 1993. Improved tools for bubble column reactor design and scale-up. *Chemical Engineering Science*. 48, 889-911.
- Degaleesan, S., Duduković, M.P., Toseland, B.A., Bhatt, B.L., 1997. A two-compartment convective-diffusion model for slurry bubble column reactors. *Industrial and Engineering Chemistry Research*. 36, 4670-4680.
- Degaleesan, S., Roy, S., Kumar, S.B., Duduković, M.P., 1996. Liquid mixing based on convection and turbulent dispersion in bubble columns. *Chemical Engineering Science*. 51, 1967-1976.
- Duduković, M.P., Devanathan, N., 1992. Bubble column reactors: some recent developments. *Nato ASI Series E Applied Sciences*. 225, 353-377.
- Duduković, M.P., Larachi, F., Mills, P.L., 2002. Multiphase catalytic reactors: a perspective on current knowledge and future trends. *Catalysis Reviews*. 44, 123-246.
- Fan, L. S., 1989. Gas-liquid-solid fluidization engineering. Butterworths, Stoneham, MA.
- Forret, A., Schweitzer, J.M., Gauthier, T., Krishna, R., Schweich, D., 2003. Influence of scale on the hydrodynamics of bubble column reactors: an experimental study in columns of 0.1, 0.4 and 1 m diameters. *Chemical Engineering Science*. 58, 719-724.
- Gandhi, B., 1997. Hydrodynamic studies in a slurry bubble column. Thesis, M.E.Sc., University of Western Ontario, London, Ontario
- Groen, J.S., Oldeman, R.G.C., Mudde, R.F., van den Akker, H.E.A., 1996. Coherent structures and axial dispersion in bubble column reactors. *Chemical Engineering Science*. 51, 2511-2520.
- Jhavar, A.K., Prakash, A., 2007. Analysis of local heat transfer coefficient in bubble column using fast response probes. *Chemical Engineering Science*. 62, 7274-7281.

- Joshi, J.B., Sharma, M.M., Shah, Y.T., Singh, C.P.P., Ally, M., Klinzing, G.E., 1980. Heat transfer in multiphase contactors. *Chemical Engineering Communications*. 6, 257-271.
- Kluytmans, J.H.J., van Wachem, B.G.M., Kuster, B.F.M., Schouten, J.C., 2001. Gas holdup in a slurry bubble column: influence of electrolyte and carbon particles. *Industrial and Engineering Chemistry Research*. 40, 5326-5333.
- Krishna, R., Urseanu, M.I., van Baten, J.M., Ellenberger, J., 1999. Influence of scale on the hydrodynamics of bubble columns operating in the churn-turbulent regime: experiment vs. Eulerian simulations. *Chemical Engineering Science*. 54, 4903-4911.
- Kulkarni, A.A., Joshi, J.B., Kumar, V.R., Kulkarni, B.D., 2001. Application of multiresolution analysis for simultaneous measurement of gas and liquid velocities and fractional gas hold-up in bubble column using LDA. *Chemical Engineering Science*. 56, 5037-5048.
- Li, H., 1998. Heat transfer and hydrodynamics in a three-phase slurry bubble column. Thesis, PhD, University of Western Ontario, London, Ontario.
- Li, H., Prakash, A., 1997. Heat transfer and hydrodynamics in a three-phase slurry bubble column. *Industrial and Engineering Chemistry Research*. 36, 4688-4694.
- Li, H., Prakash, A., 2000. Influence of slurry concentrations on bubble population and their rise velocities in a three-phase slurry bubble column. *Powder Technology*. 113, 158-167.
- Li, H., Prakash, A., 2001. Survey of heat transfer mechanisms in a slurry bubble column. *The Canadian Journal of Chemical Engineering*. 79, 717-725.
- Li, H., Prakash, A., 2002. Analysis of flow patterns in bubble and slurry bubble columns based on local heat transfer measurements. *Chemical Engineering Journal*. 86, 269-276.
- Li, H., Prakash, A., Margaritis, A., Bergougnou, M.A., 2003. Effects of micron-sized particles on hydrodynamics and local heat transfer in a slurry bubble column. *Powder Technology*. 133, 171-184.
- Mudde, R.F., Groen, J.S., Van Den Akker, H.E.A., 1997. Liquid Velocity field in a bubble column: LDA experiments. *Chemical Engineering Science*. 52, 4217-4224.
- Prakash, A., Margaritis, A., Li, H., Bergougnou, M.A., 2001. Hydrodynamics and local heat transfer measurements in a bubble column with suspension of yeast. *Biochemical Engineering Journal*. 9, 155-163.

Prakash, A., Margaritis, A., Saunders, R.C., Vijayan, S., 1999. Ammonia removal at high concentrations by the cyanobacterium *Plectonema boryanum* in a photobioreactor system. *Canadian Journal of Chemical Engineering*. 77, 99-106

Reese, J., Fan, L.S., 1994. Transient flow structure in the entrance region of a bubble column using particle image velocimetry. *Chemical Engineering Science*. 49, 5623-5636.

Riquarts, H.P., 1981. Strömungsprofile, impulsaustausch und durchmischung der flüssigen phase in bläsensäulen. *Chem Ing Techn*. 53, 60-61.

Saxena, S.C., Rao, N.S., Saxena, A.C., 1990a. Heat transfer from a cylindrical probe immersed in a three-phase slurry bubble column. *Chemical Engineering Journal*. 44, 141-156.

Saxena, S.C., Rao, N.S., Saxena, A.C., 1990b. Heat-transfer and gas-holdup studies in a bubble column: air-water-glass bead system. *Chemical Engineering Communication*. 96, 31-55.

Saxena, S.C., Rao, N.S., Saxena, A.C., 1992. Heat transfer and gas holdup studies in a bubble column: air-water-sand system. *The Canadian Journal of Chemical Engineering*. 70, 33-41.

Saxena, S.C., Vandivel, R., Saxena, A.C., 1989. Gas holdup and heat transfer from immersed surfaces in two- and three- phase systems in bubble columns. *Chemical Engineering communications*. 85, 63-83.

Schumpe, A., Grund, G., 1986. The gas disengagement technique for studying gas holdup structure in bubble columns. *The Canadian Journal of Chemical Engineering*. 64, 891-896.

Shah, Y.T., Kelkar, B.G., Godbole, S.P., Deckwer, W.D., 1982. Design parameters estimations for bubble column reactors. *AIChE Journal*. 28, 353-379.

Su, X., Hol, P.D., Talcott, S.M., Staudt, A.K., Heindel, T.J., 2006. The effect of bubble column diameter on gas holdup in fiber suspensions. 61, 3098-3104.

Ueyama, K., Morooka, S., Koide, K., Kaji, H., Miyauchi, T., 1980. Behavior of gas bubbles in bubble columns. *Industrial and Engineering Chemistry Process Design and Development*. 19, 592-599.

Wilkinson, P.M., Spek, A.P., van Dierendonck, L.L., 1992. Design parameters estimation for scale-up of high-pressure bubble columns. *AIChE Journal*. 38, 544-554.

Wu, C., Al-Dahhan, M.H., Prakash, A., 2007. Heat transfer coefficients in a high-pressure bubble column. *Chemical Engineering Science*. 62, 140-147.

Zahradník, J., Fialová, M., Růžička, M., Drahoš, J., Kaštánek, F., 1997. Duality of the gas-liquid flow regimes in bubble column reactors. *Chemical Engineering Science*. 52, 3811-3826.

CHAPTER 6. ANALYSIS OF BUBBLE DYNAMICS AND COLUMN HYDRODYNAMICS BASED ON INSTANTANEOUS HEAT TRANSFER COEFFICIENTS IN SLURRY BUBBLE COLUMNS – WITH AND WITHOUT INTERNALS

Abstract

Nearly instant variations of heat transfer coefficient is recorded using a fast response probe in a 0.15m ID bubble column with and without internals at different gas velocities and slurry concentrations. The heat transfer coefficient increases with increase in superficial gas velocity, because of increase in bubble wake turbulence of fast rising large bubbles. This is analyzed in further details in this study using a peak-fitting method to get the peak-height distribution. Then the average peak height, standard deviation and average peak area obtained from the distribution at different slurry concentrations in bubble column with and without internals is further analyzed to understand the bubble dynamics effects in slurries of different concentrations. Gas phase used is oil free compressed air and its flow rate is varied from 0.03 to 0.35 m/s. Tap water is the liquid phase and the solid particles used are 49 μm glass beads and their concentration is varied up to 20 vol. %. Usually it is observed that average peak height and area increases with the increase in superficial gas velocity. The observed increase in average peak height and area in both systems can be related to bubble wake dynamics. The effect of slurry concentration on bubble wake properties is also analyzed based on instantaneous heat transfer coefficients.

Key Words: Slurry bubble column. Heat transfer, Bubble-wake, internals

6.1 Introduction

The advantages provided by bubble columns such as high heat and good mass transfer rates, high selectivity and conversion per pass, isothermal conditions, online catalyst addition and withdrawal, washing effect of the liquid on catalyst, and low maintenance cost due to simple construction and absence of any moving parts (Deckwer and Schumpe, 1993; Kluytmans et al., 2001; Li and Prakash, 2002; Li et al., 2003), made them the reactor of choice in many industrial applications such as Fischer-Tropsch synthesis, methanol synthesis, heavy oil upgrading, fermentation, biological waste water treatment, flue gas desulphurization, coal liquefaction, dimethyl ether production, chlorination and hydrogenation (Shah et al., 1982; Fan, 1989; Duduković and Devanathan, 1992; Deckwer and Schumpe, 1993; Li, 1998; Prakash et al., 1999; Prakash et al., 2001; Duduković et al., 2002). Heat transfer studies in bubble columns and slurry bubble columns have been investigated by many researchers (Saxena et al., 1989; Saxena and Patel, 1990; Saxena et al., 1990a; Saxena et al., 1990b; Saxena et al., 1991a; Saxena et al., 1991b; Saxena et al., 1992; Li and Prakash, 1997; Li and Prakash, 1999; Li and Prakash, 2001; Prakash et al., 2001; Li and Prakash, 2002; Quiroz et al., 2003; Li et al., 2003; Kantarci et al., 2005b; Wu et al., 2007; Jhavar and Prakash, 2007; Jhavar and Prakash, 2011a; Abdulmohsin, 2011) to name a few. While many of these studies focused on time averaged measurement of heat transfer coefficient, few researchers (Kumar et al., 1992; Kumar and Fan 1994; Li, 1998; Li and Prakash, 1997; Li and Prakash, 1999; Li and Prakash, 2001) studied instantaneous heat transfer coefficients in bubble and slurry bubble columns to investigate the effect of bubble dynamics on heat transfer in bubble column reactors. While Kumar et al., (1992) and Kumar and Fan (1994) investigated this effect either with single-bubble injection or chain bubbling at low superficial gas velocities. Li (1998); Li and Prakash, (1997, 1999, 2001) studied the effect of bubble dynamics on heat transfer in bubble and slurry bubble columns based on instantaneous heat transfer coefficient at superficial gas velocities, varying in range 0.05 m/s to 0.3 m/s. They also investigated the effect of slurry concentration in air-water-glass beads system upto 40 vol.% slurry concentrations. In bubble columns, the rising gas bubbles create turbulent conditions and generate flow patterns as they

entrain liquid (slurry) in their wakes. In this study, instantaneous heat transfer measurements are investigated in bubble and slurry bubble columns with and without internals over a range of superficial gas velocities and slurry concentrations of practical importance. The instantaneous heat transfer data are analyzed to investigate local column hydrodynamics under different conditions.

6.2 Experimental

Experiments were conducted in a Plexiglas column of 0.15 m internal diameter and height of 2.5 m, the experimental set up details are provided elsewhere (Jhawar and Prakash, 2011a). The gas was introduced in the column using a coarse sparger. The detailed design of the coarse sparger is explained elsewhere (Gandhi, 1997). The sparger had two levels, upper level had seven (1.9 mm diameter) and lower level had five (1.9 mm diameter) downward facing holes on each of four arms. The internals type A was used in this study. The details of internal type A used are provided in Jhawar and Prakash (2011b). Oil free compressed air was used as gas phase, tap water was used as the liquid phase and 49 μm glass beads (Potters Industries, spheriglass® A glass) of density 2500 kg/m^3 constituted the solid phase. The gas flow rate was measured using three calibrated sonic nozzles of different diameters (0.7mm, 1.5 mm and 2.5 mm). A measuring tape was provided on the column to note the liquid level and dispersion height. An air box of 0.3 m height was used with sintered steel plate distributor. The superficial gas velocity was varied from 0.03 to 0.35 m/s. The unaerated water height in the column was maintained around 1.45 m. The solid concentration was varied from 0 to 20 vol. %. Two pressure transducers (OMEGA Type PX541-7.5GI and Type PX541-15GI) were used to measure the pressure fluctuations in the distributor ($z = 0.027$ m) and the disengagement section ($z = 1.318$ m), as shown in Figure 1. The pressure transducers were connected to a DC power supply and generated a voltage proportional to measured pressure. The response time of the pressure transducers was 2 ms and data were recorded for 180 seconds at a rate of 60 Hz.

Instantaneous heat flux was measured using a micro-foil heat flux sensor (RdF, Model number 20453-1 G161). The sensor was flush mounted on the surface of a brass cylinder of 11 mm outer diameter. A small cartridge heater (Chromalox, model number CIR-1012) was installed inside the brass cylinder. The AC power was supplied to the cartridge heater through a variac to regulate supplied power in the range of 20 to 40V. The detailed design of the heat flux probe is explained elsewhere (Li and Prakash., 1997; Li, 1998). Probe location could be changed both axially and radially. The temperature of the liquid phase was measured using two copper-constantan thermocouples (ANSI type T). These thermocouples were located at two radial locations: one at center and other close to the wall. Axial position of the thermocouple could be changed. The response time of micro-foil heat flux sensor was 20 ms and data were recorded for 180 s at a rate of 60 Hz. The probe generated microvolt signals, which were amplified to millivolts by a suitable amplification circuit using 12V DC supply. A minimum of three test runs were performed at each condition and average values are reported. For the heat flux sensor, the following equation can be derived for liquid film heat transfer coefficient (Li and Prakash, 2001):

$$\frac{1}{h_i} = \frac{T_{Su} - T_b}{q/A} - \frac{\Delta x}{k} \quad (6.1)$$

The second term on the right hand side of Equation 1 is negligible compared to the first term (< 1%) due to high conductivity (k) and small thickness (Δx) of the thermal barrier film. Therefore instantaneous heat transfer coefficient could be determined by measurement of heat flux and the difference between surface and bulk temperatures at a given time. The time-averaged heat transfer coefficient at a given location was obtained by averaging the instantaneous heat transfer data collected.

$$h_{avg} = \frac{1}{N} \sum_{i=1}^N \frac{q/A}{T_{Su} - T_b} \quad (6.2)$$

6.3 Results and Discussion

6.3.1 Response of Probe at Column Center

Figure 6.1 a and b show comparison of time series heat transfer data obtained at center in bulk section of the bubble column with and without internals for low and high superficial gas velocity. It is observed that at high superficial gas velocity the heat transfer coefficient peak are significantly higher than those obtained at low gas velocities. This increase in heat transfer coefficient with superficial gas velocity can be attributed to increase in coalesced bubble size, which in turn generates strong liquid recirculation velocity due to increased bubble-wake-induced turbulence as pointed out by Li and Prakash (1999). In bubble columns without internals the bubble size increases with increase in superficial gas velocity and this has been reported in literature (De Swart et al., 1996; Krishna et al 1997; Li and Prakash, 1999). A comparison of Figure 6.1a and b indicates that at high gas velocity, peaks are taller and wider in presence of internal A, while they are shorter and narrower without internal. Sharper peaks can be associated with fast rising large bubble while a wider and rounded peak indicate closely spaced large bubbles or bubble clusters. However, the differences are less obvious at lower gas velocity, when bubble size and their rate of generation is small. As discussed in following sections, these differences were further analyzed based on peak height and area distributions.

6.3.2 Probe Response in Central and Wall Regions

Figures 6.2 a and b show comparison of instantaneous heat transfer coefficient obtained at center and wall region in bulk section of the bubble column with and without internals at a superficial gas velocity of 0.21 m/s. It is observed that the heat transfer coefficients obtained in the wall region are significantly smaller than in the central region - with or without internals. This indicates the near absence of fast moving bubble chain or large bubbles in this region.

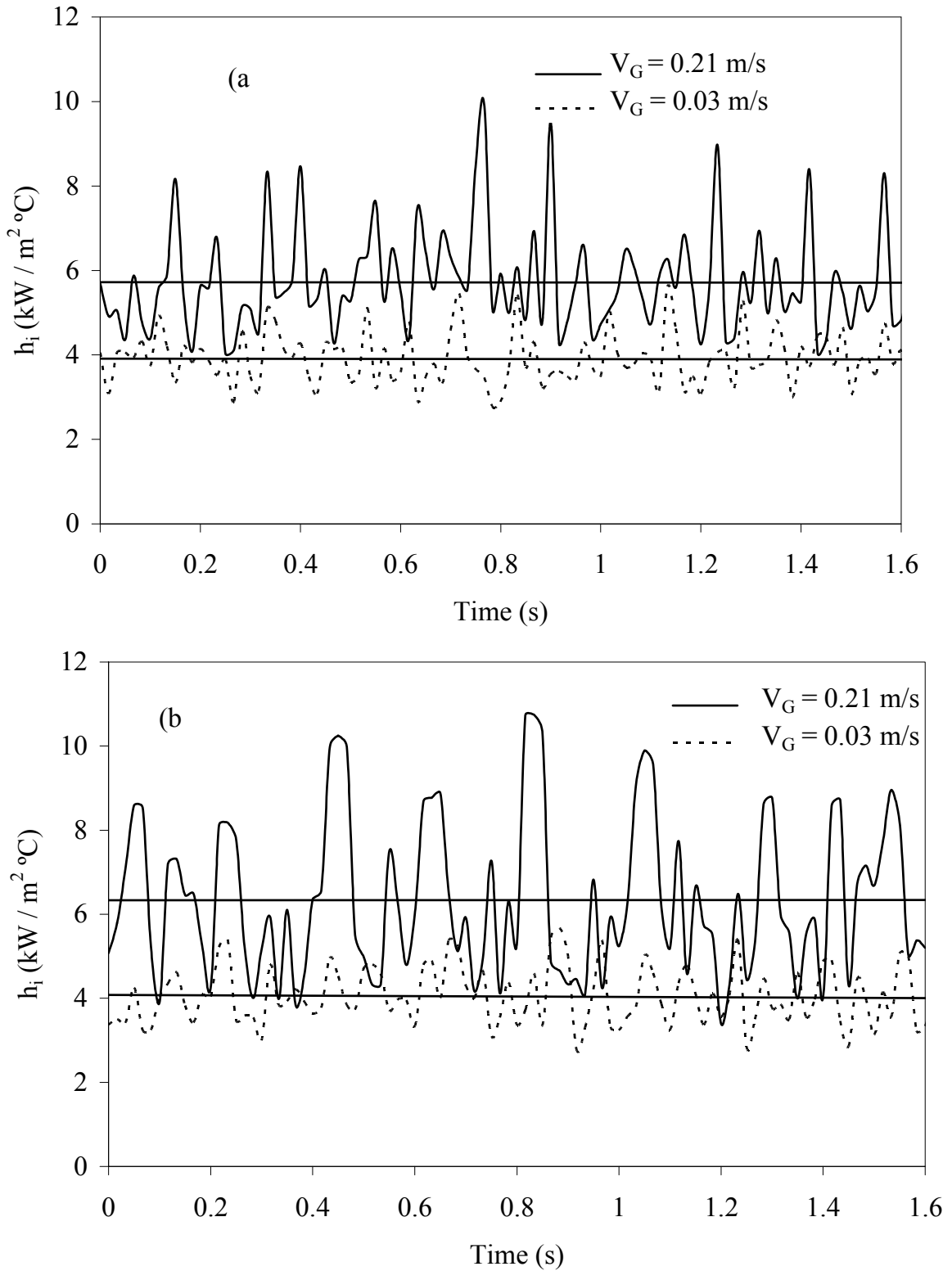


Figure 6.1. Instantaneous heat transfer coefficient obtained at center in bulk section in air – water system (a) Without Internals (b) Type A.

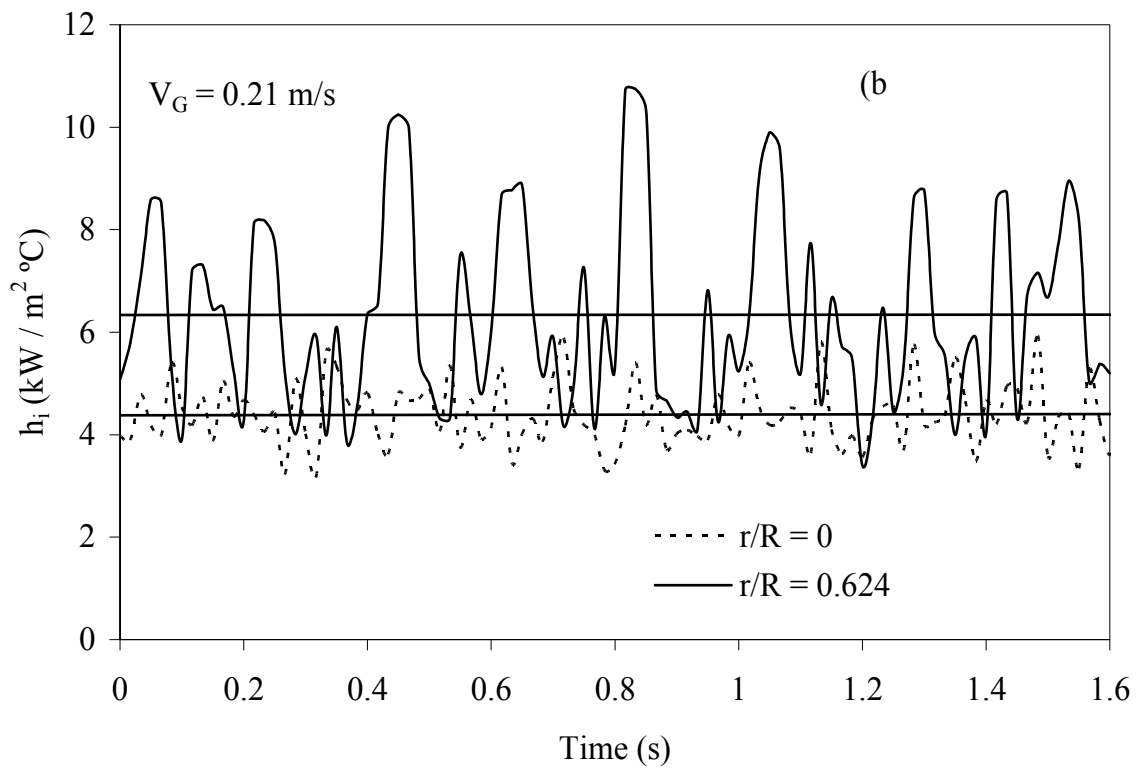
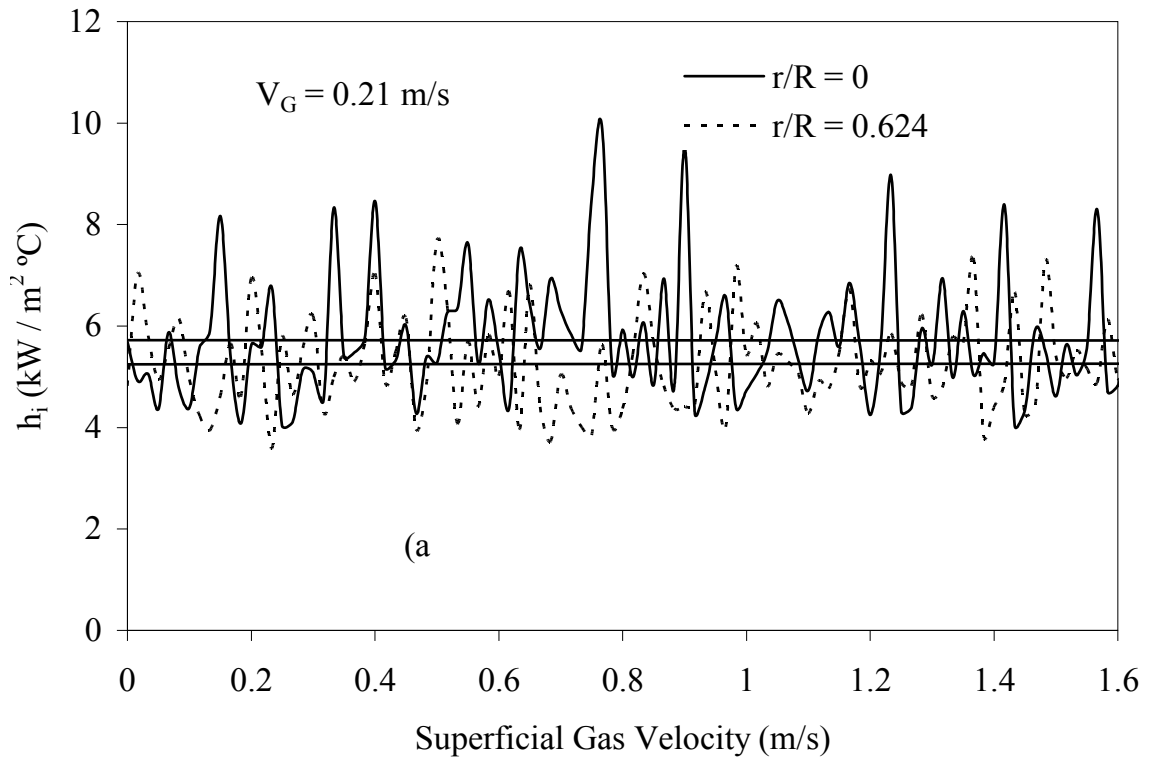


Figure 6.2. Instantaneous heat transfer coefficient obtained at center and in wall region in bulk section in air – water system (a) Without Internals (b) Type A.

Another important thing observed is that the average and instantaneous heat transfer coefficient in central region are higher in bubble columns with internals (core region) compared to those without internals and a reverse trend is observed in the wall region.

A direct comparison of the internal effect at the two radial locations is presented in Figure 6.3a and b. The influence of internal A in the two regions is clearly observable. The widths of tall peaks without internals are nearly half of those obtained with the internal suggesting more large bubbles moving up in close proximity. The reverse trend observable in the wall region (Figure 6.3b) can be attributed to smaller and fewer bubbles in the wall region with internals compared to hollow bubble column. The radial variation of bubble size distribution in bubble columns and three phase fluidized without internals is reported in literature studies (Yu and Kim, 1988; Chen et al., 1994; Kwon et al., 1994). These studies have reported that the average bubble diameter is smaller near the wall region and increases towards the central region in bubble column. Similar observations were reported by Li and Prakash (1999) based on instantaneous heat transfer coefficient measured in bubble column without internals. There is no published literature for the radial variation of bubble size distribution in bubble columns equipped with internals. The data of this study clearly suggests that the radial distribution of average bubble size was significantly affected in presence of the internal type used.

6.3.3 Estimation of peak-height distribution

From the discussion in previous section, instantaneous heat transfer coefficient can be used to describe bubble dynamics and bubble wake behavior. The passing bubble over the heat transfer probe surface enhances the heat transfer coefficient as it creates shear field due to its dynamics and associated turbulent wake region. The fast response probe used in this study is capable of recording this enhanced heat transfer coefficient. From the time series heat transfer coefficient data obtained in this study, it is observed that the instantaneous heat transfer coefficient peaks are not uniformly distributed with time at a given operating condition.

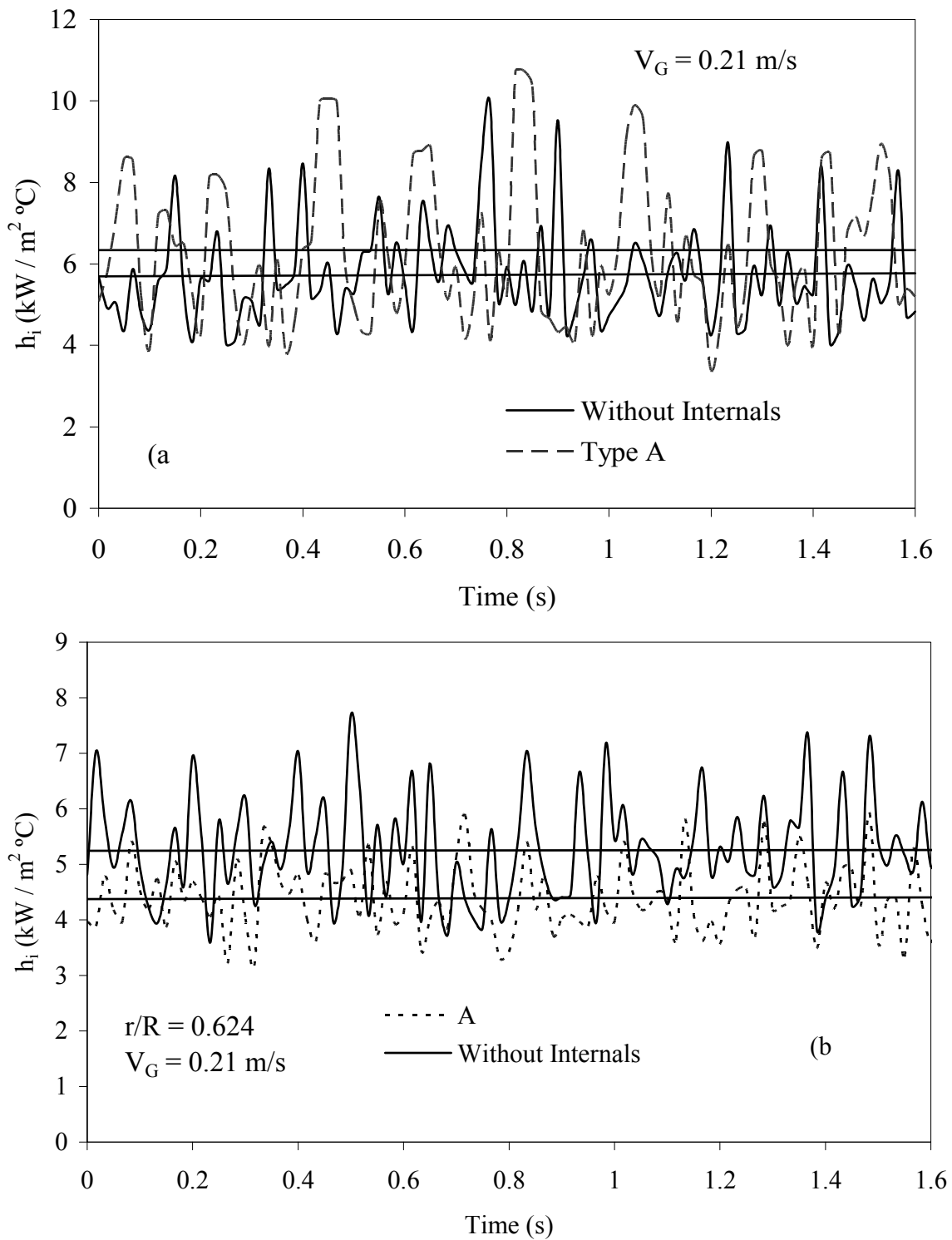


Figure 6.3. Instantaneous heat transfer coefficient obtained in bulk section of the bubble columns with Type A and without internals in air – water system(a) center ($r/R=0$) (b) wall ($r/R=0.624$) region

Therefore, a peak height fitting method developed by Li and Prakash (1999) was adapted to obtain the peak heights distribution in this study. This method is described below in detail. The peak height distribution can be related to bubble dynamics in the column.

The peak heights were divided into 40 equally spaced intervals, for quantitative description. For a given interval, all peak heights were counted as the peak height of mid value of the same interval (the mid value ranged up to 19.75 kW/m²°C). The area of each peak is obtained by multiplying the sampling time with measured heat transfer coefficient above base line. The base line in this study was defined as the average of minimum heat transfer coefficients value obtained, which are lower than the average heat transfer coefficient of the over all data at a given superficial gas velocity. The base line value increases with increase in superficial gas velocity. The heat transfer signal obtained was reconstructed by replacing any instantaneous heat transfer coefficient obtained less than base value line value, with the base line value. To calculate the peak area, both peak height and time length is used. The peak height was defined as the maximum instantaneous heat transfer coefficient obtained for a passing bubble-wake, subtracted base line value from it. The time length of each peak was defined as the time between two minimum heat transfer coefficients in which one is before the peak and other is after the peak. The area of each peak was calculated using Simpson integration method. Once the area of peak was calculated, the areas with same peak height were added to obtain the summed peak area with peak height *i*. The cumulative area with peak height *i* represents total effect of bubble-wake induced turbulence on heat transfer with peak height *i*. Then various cumulative areas with different peak height *i* were classified into an area distribution of various peak-heights. To obtain the distribution independent of sampling time, the distribution was normalized as:

$$\phi_i = \frac{\text{area of peak} - \text{height}_i}{\text{total area}} \quad (6.3)$$

The sampling time independent normalized distribution obtained in bubble columns with and without internals in air-water system at high and low superficial gas

velocities is shown in 6.4. The figure shows that the peak-height distribution is close to Gaussian distribution in bubble columns with and without internals for different superficial gas velocities. Therefore the mean value and standard deviation of Gaussian distribution can be applied to describe the peak height distribution as below:

$$\bar{X} = \frac{\sum_{i=1}^{40} (\text{area of peak} - \text{height}_i) \cdot (\text{peak}_i - \text{height}_i)}{\text{total area}} \quad (6.4)$$

$$SD = \sqrt{\frac{\sum_{i=1}^{40} (\text{area of peak} - \text{height}_i) \cdot [(\text{peak}_i - \text{height}_i) - \bar{X}]^2}{\text{total area}}} \quad (6.5)$$

The mean value of normalized distribution represents an average value of peak height (area average peak height) and standard deviation represents the width of peak height distribution.

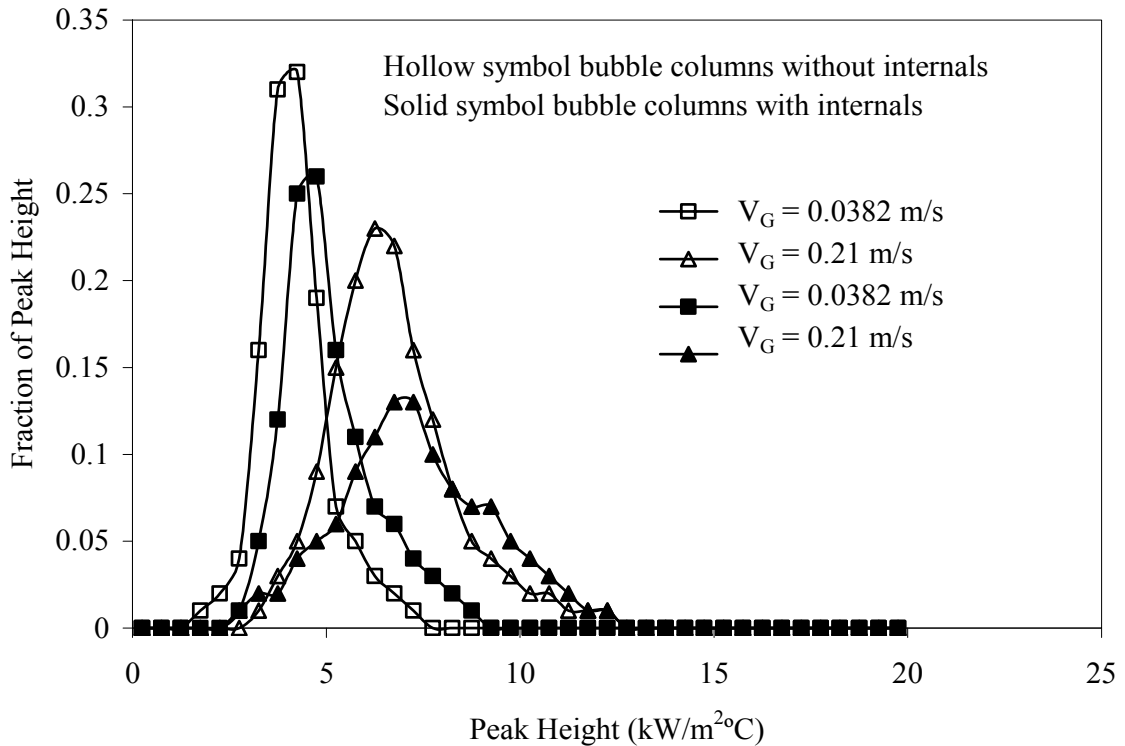


Figure 6.4. Peak-height distribution in bubble columns with Type A and without internals at different gas velocities in air – water system ($r/R=0$).

Average peak area is another important parameter that can be obtained from instantaneous heat transfer coefficients. To estimate average peak area, the number of peaks had to be counted from time series heat transfer data for a given time interval. The individual peak area is obtained by the procedure described previously. From figure 6.1 to 6.3, it is observed that a few of the peaks were close to baseline which could be due to local turbulent fluctuation. In order to avoid counting these low peaks, a minimum peak height was defined as 2.25 (kW/m²C) along the lines, as discussed by Li (1998). The average peak area was obtained by dividing total area by number of peaks. The average area represents a combined effect of both intensity and residence time of bubble wake induced turbulence on heat transfer.

6.3.4 Peak-height distribution

The peak height distributions obtained in bubble columns with and without internals in air-water system at center in bulk section of the column at a low (0.038 m/s) and a high superficial gas velocity (0.21 m/s) is shown in Figure 6.4. The two velocities represent the dispersed flow and heterogeneous flow regimes respectively. It can be observed that the distributions become wider at higher gas velocity. Also for the same gas velocity, the distribution becomes wider in the presence of the internal. It can also be observed that the distribution is nearly Gaussian in bubble columns with and without internals for different superficial gas velocities. These variations in peak height distribution can be compared with change in bubble size distribution and associated column hydrodynamics in presence of the internal.

Variations of average peak heights with superficial gas velocity with and without internal are presented in Figure 6.5 for air-water and air-water-glass beads system. It is observed that average peak height increases with increasing superficial gas velocity in all cases. In addition following observations can be made.

- Higher values obtained with air-water system approach those with slurry system with increase in gas velocity with or without internal.

- Average peak heights are higher with internal and the difference due to internal increases with increasing gas velocity.

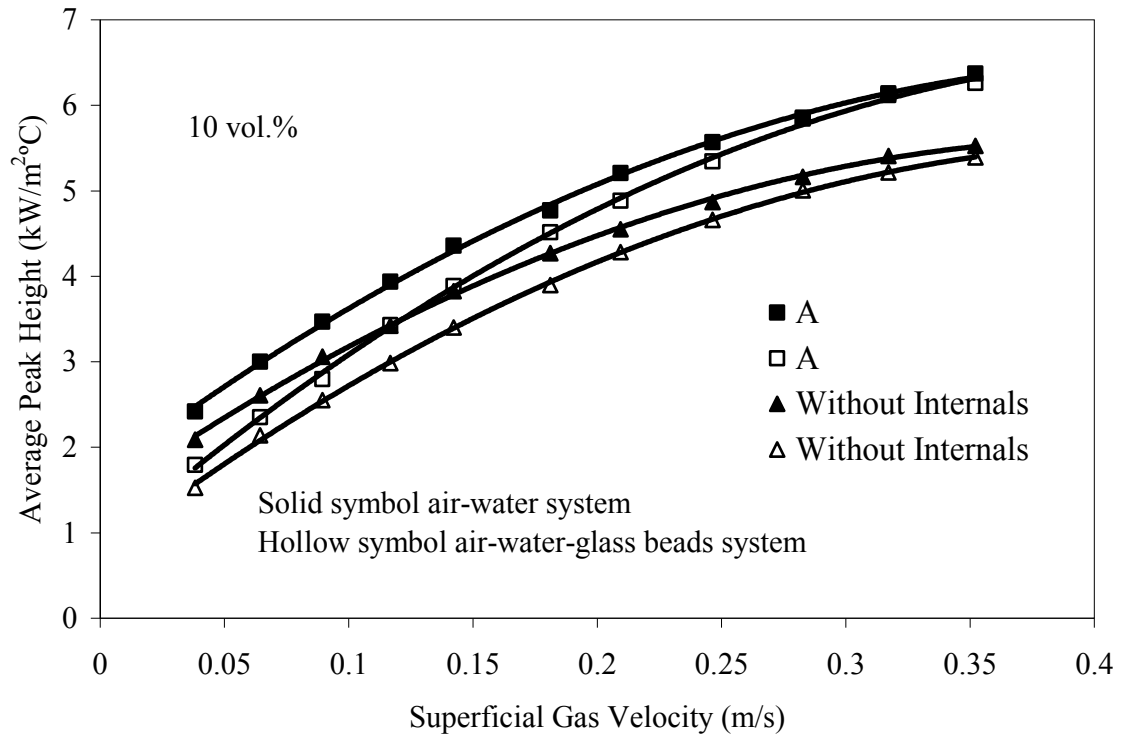


Figure 6.5. Comparison of average peak height in bubble column with and without internals and with literature studies in air-water and air-water-glass beads system

Comparison of standard deviations obtained with average peak heights is presented in Figure 6.6. Following observations can be made from this figure.

- Standard deviations (SD) increase with increasing gas velocity in all cases.
- The rate of increase is faster up to gas velocity of about 0.15 m/s and decreases for higher gas velocities.
- Higher standard deviations are obtained in presence of the internal.
- Also standard deviations are higher with slurry system compared to air-water.

The variation of average peak heights with superficial gas velocities can be compared with variation of bubble size and bubble chord length distribution reported in literature (Rigby et al., 1970; Everson et al., 1993; Kwon et al., 1994; De Swart et al.,

1996; Luo et al., 1999). With increasing superficial gas velocity, the size of large bubble and their distribution width increases (Luo et al., 1999). As the large bubble size increases, their rise velocity also increases (Rigby et al., 1970; Luo et al., 1999). The fast rising bubbles cause strong liquid recirculation, which in turn increases the bubble-wake-induced turbulence, and as a result the heat transfer coefficient peak height increased. The high gas velocity generates higher shear stress, which could result in breakup of the large bubbles, thus the bubble size distribution depends on both bubble coalescence and breakup (De Swart et al., 1996). The bubble size distribution and its standard deviation increases with increasing gas velocity (Everson et al., 1993; Kwon et al., 1994). Thus the increasing average peak height and peak height distribution standard deviation with superficial gas velocity can be related to increase in bubble size distribution and its standard deviation with gas velocity.

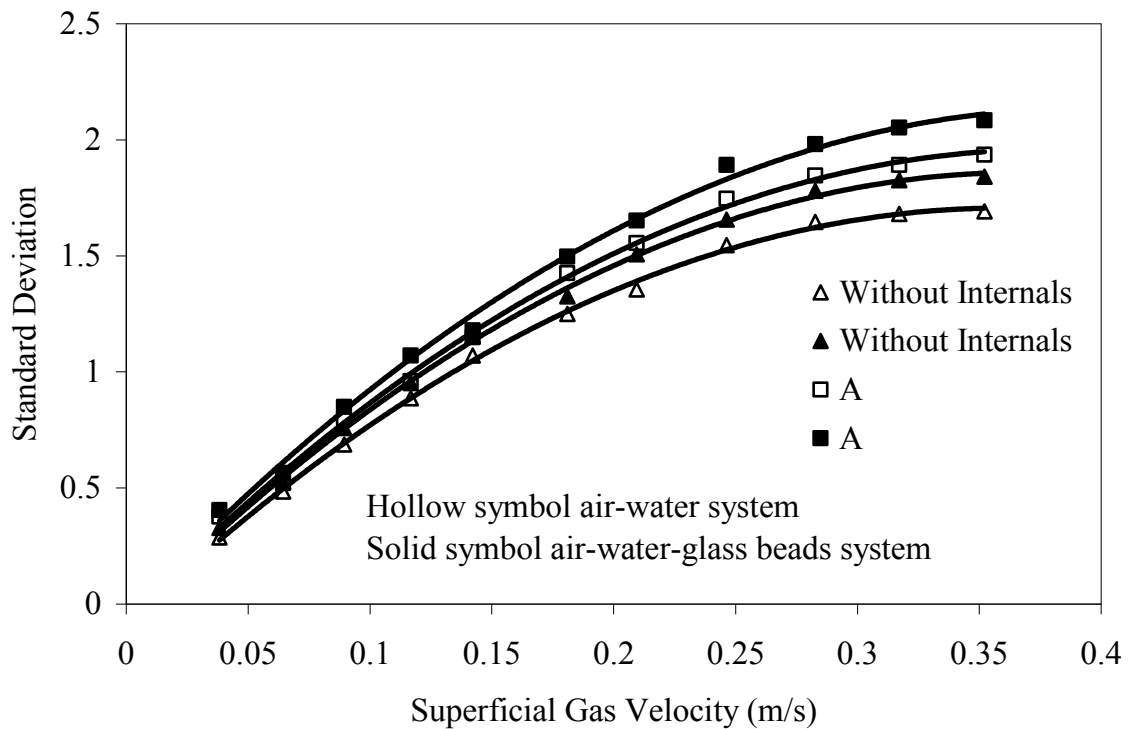


Figure 6.6. Comparison of standard deviation of peak-height distribution in bubble column with and without internals and with literature studies in air-water and air-water-glass beads system

Variations of average peak height with slurry concentration are compared in Figure 6.7 for a low and a high velocity. It is observed that the trends are similar irrespective

of gas velocity or presence of internal. There is a clear tendency for the average peak height to decrease initially with the addition of solid particles up to concentration of about 10 vol.% solids. But at high concentrations (beyond 10 vol. %) the average peak height increases with increase in slurry concentrations and are almost equal or greater than air-water system. The decrease in average peak height with the addition of particles could be attributed to the destruction of ordered motion or circulation in bubble-wake thus reducing vortical strength (hence turbulence) inside the bubble wake as pointed out by Raghunathan et al., (1992). This would result in reduction of bubble wake induced heat transfer rate. The above details explains the reduction in average peak height with addition of particles at low concentrations (< 10 vol. %). The above effect become less significant in bubble column with internals due to increased liquid recirculation and local turbulence, but is not nullified since there is decrease in average peak height, but is less compared to bubble column without internals.

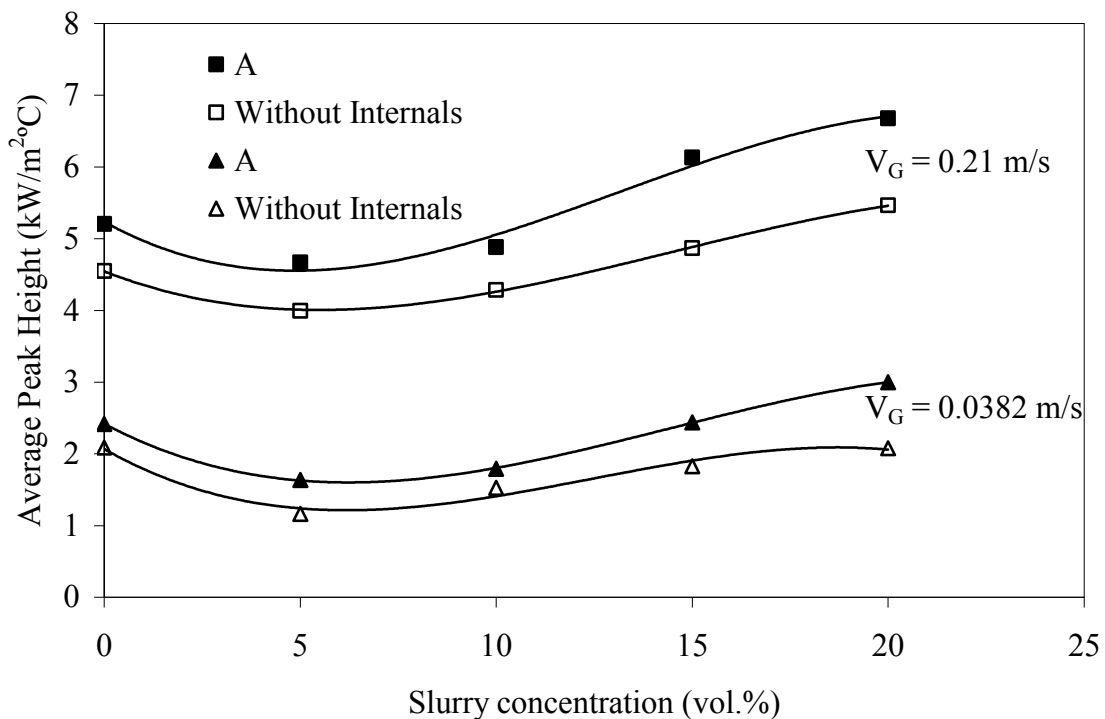


Figure 6.7. Comparison of average peak height with slurry concentration in bubble columns in central region with Type A and without internals

However, when the slurry concentration is increased to 10 vol. % or more, it is observed that the average peak height increases and is almost equal or greater in bubble columns with and without internals. Even though the addition of particles results in reduction in bubble wake induced turbulence, the average peak height is increasing at high concentration, and this could be due to changes in bubble population. With addition of particles, the apparent suspension viscosity is increasing, which results in the increase in bubble size. As the bubble size increases, the rise velocity increases (Luo et al., 1999), which results in strong local shear fields, and also the energy content in the wake region (mainly kinetic energy) of these fast moving large bubbles increases. The combined effect of these two processes will dominate the reduced turbulence due to increasing slurry concentration.

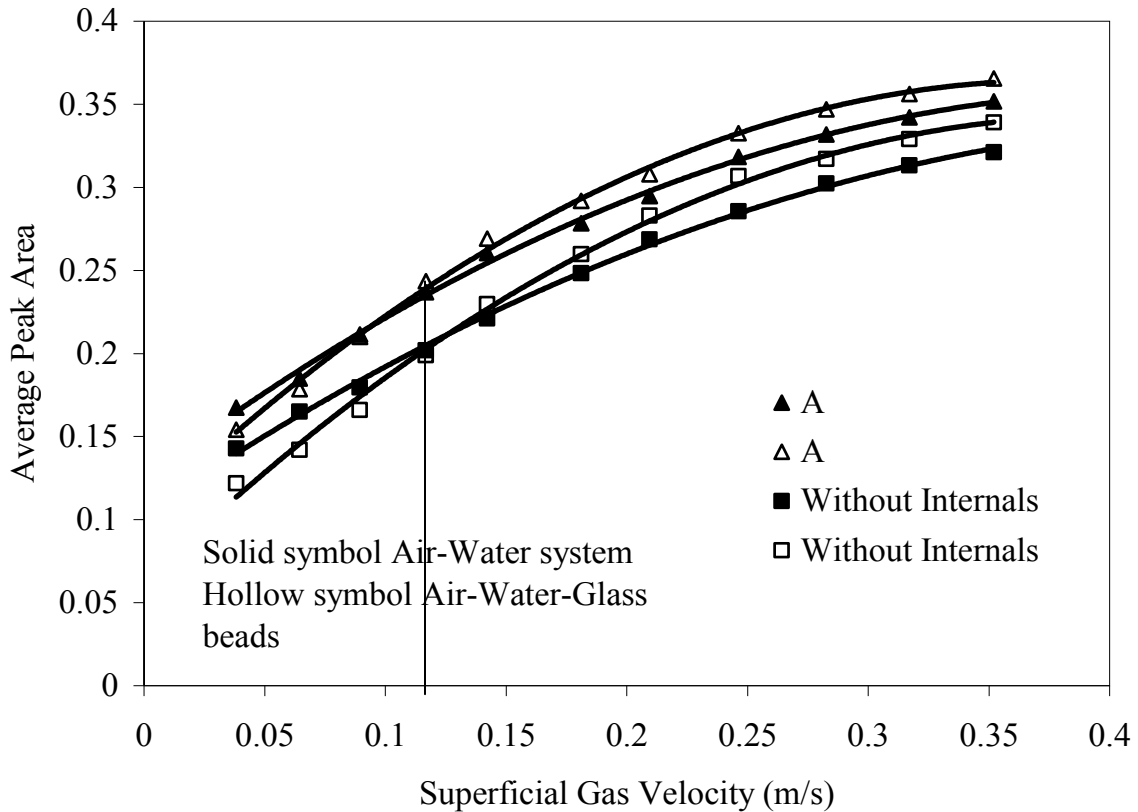


Figure 6.8. Comparison of average peak area in bubble column with and without internals and with literature studies in air-water and air-water-glass beads system

6.3.5 Average Peak Area Analysis

Figure 6.8 compares variations of average peak areas with gas velocity with and without internal in air-water and air-water-glass beads (10 vol. %) system. The peak area represents net effect of both bubble wake size and its energy content (Li and Prakash, 1999). The peak areas increase with the increase in superficial gas velocity in all cases. It can be noted that at low velocities, values obtained in slurry system are lower compared to air-water system but increase at a faster rate with increasing gas velocity and eventually go above air-water values. The gas velocity at which this cross over occurs is lower (≈ 0.09 m/s) with internal compared to hollow bubble column (≈ 0.11 m/s). It seems bubble size is increasing at a faster rate in the slurry system due to the presence of particles and their effects on suspension rheology and this effect is enhanced further in presence of the internal.

Figures 6.9 (a) and (b) show the effect of slurry concentration on average peak area obtained in the central region in bubble columns with and without internals at different superficial gas velocity. Following observation could be made in bubble columns with and without internals

- Variations of peak area have similar trends in both cases.
- Initially there is drop in peak area with addition of fine particles for concentration up to 5 vol.%
- Beyond 5 vol. % slurry concentration there is increasing trend.
- Values with internals are always higher compared to those without internals.
- Higher rate of increase in presence of internals with slurry concentration and superficial gas velocity.

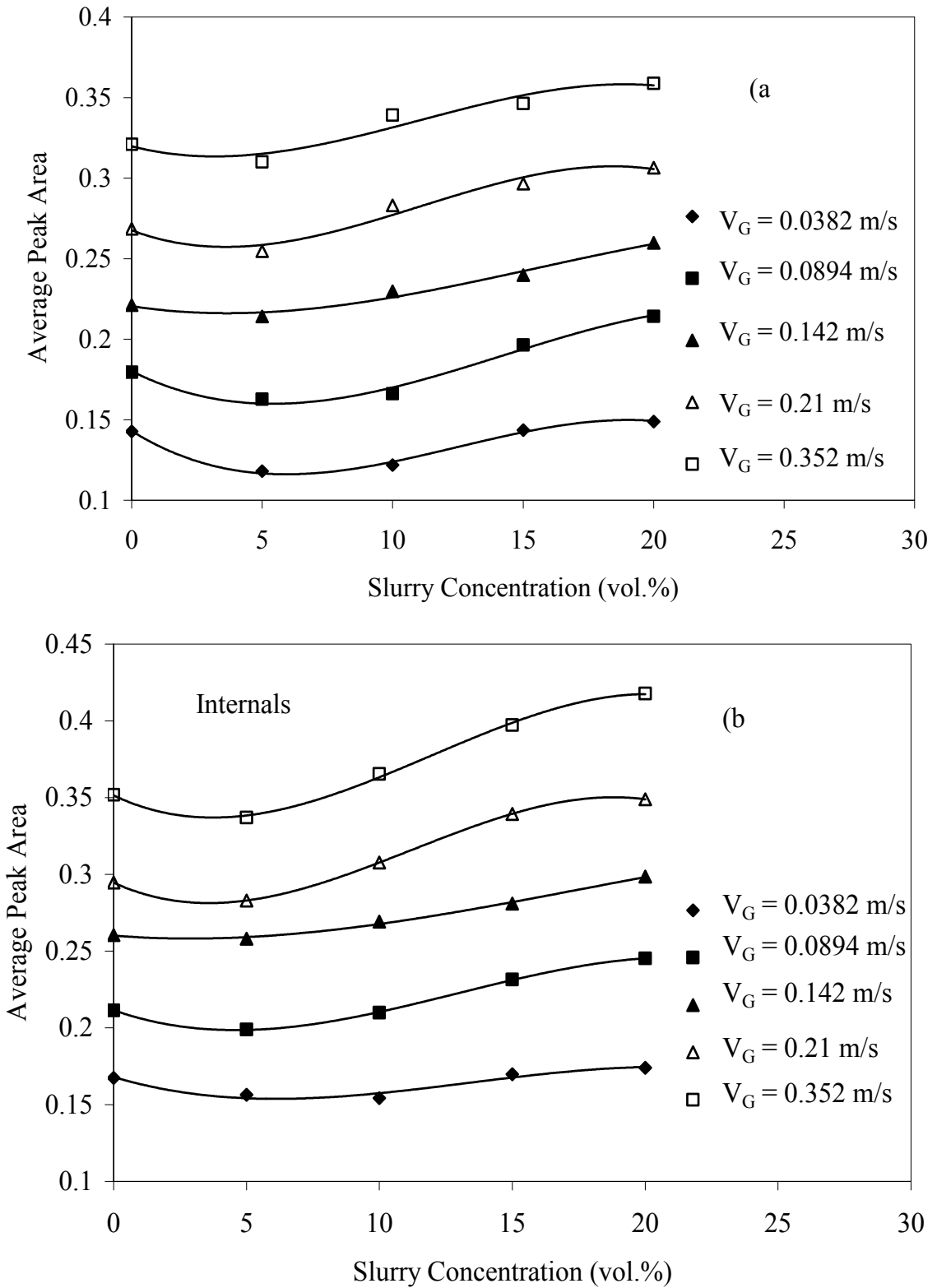


Figure 6.9. Variation of average peak area with slurry concentration in bubble columns in central region (a) Without internals (b) Type A

The average peak area represents the combined effect of both bubble wake size and its turbulence intensity. The initial drop observed in average peak area with addition of fine particles for low slurry concentration (< 5 vol. %) could be explained by boundary layer flow and decrease in bubble wake turbulence with addition of particles. For slurry concentration beyond 5 vol. %, the increase in average peak area can be attributed to the sharp increase in bubble rise velocity Li (1998). With addition of particles, the apparent suspension viscosity is increasing, which results in the increase in bubble size. As the bubble size increases their rise velocity increases (Luo et al., 1999), which results in strong local liquid recirculation, and also the energy content in the wake region (mainly kinetic energy) of these fast moving large bubbles increases. The combined effect of these two will dominate the reduced turbulence due to addition of particles. As a result the average heat transfer peak area increases for slurry concentration in this range (Li and Prakash, 1999). This behavior may change with particle type and size

6.4 Conclusions

The probe is capable of capturing the temporal variation of heat transfer coefficient due to changes in system properties, presence of internals or with addition of particles. This could be further analyzed based on peak height distribution and area to give insights about the bubble size distribution and changes in bubble wake-dynamics. To quantitatively describe the temporal variation of heat transfer coefficient a peak fitting method was developed to obtain average peak height and peak area in bubble columns with and without internals. The average peak height and peak area increases with the increase in superficial gas velocity. The fast response probe can be a useful tool for investigation of bubble size distribution and analysis in different system of practical importance and in large column diameter columns compared to electrical resistance or optical probe as it is not dependent on the system electrical or optical properties.

6.5 Notations

A	Heat transfer area, (m ²)
D _C	Column diameter (m)
h	Heat transfer coefficient, (kW/m ² °C)
k	Thermal conductivity, (W/m K)
N	Number of data points
q	Heat flow rate, (kW)
r	Radial location, (m)
R	Radius of the column, (m)
SD	Standard deviation of peak height distribution
T	Temperature, (°C)
V	Superficial velocity (m/s)
\bar{X}	Average peak height of peak height distribution
z	Axial location from the bottom of the column, (m)
Δx	Thickness of thermal barrier, (m)

Greek Symbols

ν	Kinematic viscosity (m ² /s)
ϕ_i	fraction of area of peak height i in total peak area

Subscripts

avg	Average
b	Bulk
c	Center
G	Gas
i	peak interval number
L	Liquid
S	Solid

w Wall
Su Surface

6.6 References

- Abdulmohsin, R.S., Abid, B.A., Al-Dahhan, M.H., 2011. Heat transfer study in a pilot-plant scale bubble column. *Chemical Engineering Research and Design*. 89, 78-84.
- Chen, R.C., Reese, J., Fan, L.S., 1994. Flow structure in a three-dimensional bubble column and three-phase fluidized bed. *AIChE Journal*. 40, 1093-1104.
- De Swart, J. W. A., van Vliet, R. E., Krishna, R., 1996. Size structure and dynamics of “large” bubbles in a two-dimensional slurry bubble column. *Chemical Engineering Science*, 51, 4619-4629.
- Deckwer, W.D., Schumpe, A., 1993. Improved tools for bubble column reactor design and scale-up. *Chemical Engineering Science*. 48, 889-911.
- Duduković, M.P., Devanathan, N., 1992. Bubble column reactors: some recent developments. *Nato ASI Series E Applied Sciences*. 225, 353-377.
- Duduković, M.P., Larachi, F., Mills, P.L., 2002. Multiphase catalytic reactors: a perspective on current knowledge and future trends. *Catalysis Reviews*. 44, 123-246.
- Everson, R. C., Eyre, D., O'Connor, C. T., Tucker, J. P., 1993. Measurement and analysis of small bubble size distribution. *Chemical Engineering Science*. 48, 3399-3403.
- Fan, L. S., 1989. *Gas-liquid-solid fluidization engineering*. Butterworths, Stoneham, MA.
- Gandhi, B., 1997. *Hydrodynamic studies in a slurry bubble column*. Thesis, M.E.Sc., University of Western Ontario, London, Ontario
- Jhavar, A.K., Prakash, A, 2011a. Influence of bubble column diameter on local heat transfer and related hydrodynamics. *Chemical Engineering Research and Design*. 89, 1996-2002.
- Jhavar, A.K., Prakash, A, 2011b. Effects of internal on local heat transfer and column hydrodynamics in bubble columns. Thesis, PhD, University of Western Ontario, London, Ontario.

- Jhavar, A.K., Prakash, A., 2007. Analysis of local heat transfer coefficient in bubble column using fast response probes. *Chemical Engineering Science*. 62, 7274-7281.
- Kantarci, N., Ulgen, K.O., Borak, F., 2005b. A study on hydrodynamics and heat transfer in a bubble column reactor with yeast and bacterial cell suspensions. *Canadian Journal of Chemical Engineering*. 83, 764-773.
- Kluytmans, J.H.J., van Wachem, B.G.M., Kuster, B.F.M., Schouten, J.C., 2001. Gas holdup in a slurry bubble column: influence of electrolyte and carbon particles. *Industrial and Engineering Chemistry Research*. 40, 5326-5333.
- Krishna, R., De Swart, J. W. A., Ellenberger, J., Martina, G. B., Maretto, C., 1997. Gas holdup in slurry bubble columns: Effect of column diameter and slurry concentrations. *AIChE Journal*, 43, 311-316.
- Kumar, S., Fan, L.S., 1994. Heat-transfer characteristics in viscous gas-liquid and gas-liquid-solid system. *AIChE Journal*. 40, 745-754.
- Kumar, S., Kusakabe, K., Raghuathan, K., Fan, L. S. 1992. Mechanism of heat transfer in bubbly liquid and liquid-solid systems: Single bubble injection. *AIChE Journal*, 38, 733-741.
- Kwon, H. W., Kang, Y., Kim, S. D., Yashima, M., Fan, L., 1994. Bubble-chord length and pressure fluctuations in three-phase fluidized beds. *Industrial and Engineering Chemistry Research*. 33, 1852-1857.
- Li, H., 1998. Heat transfer and hydrodynamics in a three-phase slurry bubble column. Thesis, PhD, University of Western Ontario, London, Ontario.
- Li, H., Prakash, A., 1997. Heat transfer and hydrodynamics in a three-phase slurry bubble column. *Industrial and Engineering Chemistry Research*. 36, 4688-4694.
- Li, H., Prakash, A., 1999. Analysis of bubble dynamics and local hydrodynamics based on instantaneous heat transfer measurements in a slurry bubble column. *Chemical Engineering Science*. 54, 5265-5271.
- Li, H., Prakash, A., 2001. Survey of heat transfer mechanisms in a slurry bubble column. *The Canadian Journal of Chemical Engineering*. 79, 717-725.
- Li, H., Prakash, A., 2002. Analysis of flow patterns in bubble and slurry bubble columns based on local heat transfer measurements. *Chemical Engineering Journal*. 86, 269-276.
- Li, H., Prakash, A., Margaritis, A., Bergougnou, M.A., 2003. Effects of micron-sized particles on hydrodynamics and local heat transfer in a slurry bubble column. *Powder Technology*. 133, 171-184.

Luo, X., Lee, D.J., Lau, R., Yang, G.Q., Fan, L.S., 1999. Maximum stable bubble size and gas holdup in high-pressure slurry bubble columns. *AIChE Journal*. 45, 665-680.

Prakash, A., Margaritis, A., Li, H., Bergougnou, M.A., 2001. Hydrodynamics and local heat transfer measurements in a bubble column with suspension of yeast. *Biochemical Engineering Journal*. 9, 155-163.

Prakash, A., Margaritis, A., Saunders, R.C., Vijayan, S., 1999. Ammonia removal at high concentrations by the cyanobacterium *plectonema boryanum* in a photobioreactor system. *Canadian Journal of Chemical Engineering*. 77, 99-106

Quiroz, I., Herrera, I., Mendizabal, D.G., 2003. Experimental study on convective coefficients in a slurry bubble column. *International Communications in Heat and Mass Transfer*. 30, 775-786.

Raghunathan, K., Kumar, S., Fan, L. S., 1992. Pressure distribution and vortical structure in the wake behind gas bubbles in liquid and liquid-solid systems. *International Journal of Multiphase Flow*. 18, 41-50.

Rigby, G. R., Van Blockland, G. P., Park, W. H., Capes, C. E., 1970. Properties of bubbles in three-phase fluidized beds as measured by electroresistivity probe. *Chemical Engineering Science*. 25, 1729-1741.

Saxena, S.C., Patel, B.B., 1990. Heat transfer and hydrodynamic investigations in a baffled bubble column: air-water-glass bead system. *Chemical Engineering Communications*. 98, 65-88.

Saxena, S.C., Rao, N.S., Saxena, A.C., 1990a. Heat transfer from a cylindrical probe immersed in a three-phase slurry bubble column. *Chemical Engineering Journal*. 44, 141-156.

Saxena, S.C., Rao, N.S., Saxena, A.C., 1990b. Heat-transfer and gas-holdup studies in a bubble column: air-water-glass bead system. *Chemical Engineering Communication*. 96, 31-55.

Saxena, S.C., Rao, N.S., Saxena, A.C., 1992. Heat transfer and gas holdup studies in a bubble column: air-water-sand system. *The Canadian Journal of Chemical Engineering*. 70, 33-41.

Saxena, S.C., Rao, N.S., Yousuf, M., 1991a. Hydrodynamic and heat transfer investigations conducted in a bubble column with fine powders and a viscous liquid. *Powder Technology*. 67, 265-275.

Saxena, S.C., Rao, N.S., Yousuf, M., 1991b. Heat transfer and hydrodynamic investigations conducted in a bubble column with powders of small particles and a viscous liquid. *Chemical Engineering Journal*. 47, 91-103.

Saxena, S.C., Vandivel, R., Saxena, A.C., 1989. Gas holdup and heat transfer from immersed surfaces in two- and three- phase systems in bubble columns. *Chemical Engineering communications*. 85, 63-83.

Shah, Y.T., Kelkar, B.G., Godbole, S.P., Deckwer, W.D., 1982. Design parameters estimations for bubble column reactors. *AIChE Journal*. 28, 353-379.

Wu, C., Al-Dahhan, M.H., Prakash, A., 2007. Heat transfer coefficients in a high-pressure bubble column. *Chemical Engineering Science*. 62, 140-147.

Youssef. A.A., Al-Dahhan, M.H., 2009. Impact of Internals on the Gas Holdup and Bubble Properties of a Bubble Column. *Industrial and Engineering Chemistry Research*. 48, 8007-8013.

Yu, Y. H., Kim, S. D., 1988. Bubble characteristics in the radial direction of three-phase fluidized beds. *AIChE Journal*. 34, 2069-2072.

CHAPTER 7. CONCLUSIONS AND RECOMMENDATIONS

7.1 Conclusions

The following conclusions can be drawn from this study:

1. The presence of internals, their design and location in bubble columns affect heat transfer characteristics, hydrodynamics and mixing pattern. The fast response heat transfer probe used in this study proved to be a valuable tool to investigate these local variations..
2. The presence of tube bundle type internal (type A) increases the heat transfer coefficient in central region compared to hollow bubble column, but a reverse trend is observed in wall region
3. Axial location of six-blade baffle (type B) used in this study was found to be important. When placed at an axial height of 0.36 m from the bottom of the column, the heat transfer coefficients obtained are higher at the center than those obtained in hollow bubble column, but are lower than compared to those obtained with type A.
4. When type B internal was placed at an axial height of 0.21 m, the heat transfer coefficients obtained at the center are similar to those obtained in hollow bubble column.
5. The six-blade baffles (type B) used in this study improved the radial profile of heat transfer coefficients obtained compared to hollow bubble column or with internals type A at both axial locations studied.
6. The combination of type A ($z = 0.50\text{m}$) and B ($z = 0.36\text{m}$) internals studied, shows that the heat transfer characteristics is improved compared to type B alone at the center and the radial profile of heat transfer coefficient is improved compared to those obtained with type A alone.

7. The combination of different design internals can also be used to improve the hydrodynamic characteristics of the bubble column.
8. The presence of type A internal increases the small bubble holdup, but there is negligible affect on large bubble holdup compared to hollow bubble column or with type B ($z = 0.36$ m), resulting in higher average gas holdup.
9. When type B internal is placed at an axial height of 0.36 m, it increases the small bubble holdup, but there is negligible affect on large bubble holdup compared to hollow bubble column, resulting in higher average gas holdup.
10. When type B internal is placed at an axial of 0.21m, the large and small bubble holdup increases and decreases respectively, resulting in lower average gas holdups compared to those obtained at an axial height of 0.36 m and hollow bubble column.
11. The average bubble size decreases in presence of both type A and type B ($z = 0.36$ m) internals. This decrease in bubble size would results in higher interfacial area and residence time there by improving the reactors mass transfer performance.
12. Presence of six-blade baffle internals, improves the column hydrodynamics radially and more uniform mixing is achieved at different radial locations due to uniformity in bubble size and population.
13. The presence of internals and their combination can increase or decrease backmixing depending on their design and arrangement.
14. The addition of fine solid particles (glass-beads) decreases heat transfer coefficient and average gas holdup in hollow bubble columns or with internals.

15. The average heat transfer coefficient obtained in this study is compared with the literature data; it is observed that the heat transfer coefficient increases with the increase in column diameter.
16. The flow direction can be qualitatively identified (upward or downward) by measuring the time averaged local heat transfer coefficients using the different orientation of the probe (upward, downward or lateral) used in this study.
17. The local liquid velocities estimated by using equation (5.3) based on the stagnation point heat transfer coefficients are in good agreement with the other experimental studies.
18. The modified Joshi et al. (1980) correlation (equation 5.5) based on our study gives a good estimate of heat transfer coefficient for column diameters upto 0.3m. This requires further testing for larger column diameters
19. The bubble rise velocity of large bubbles increases with column diameter and slurry concentration. The bubble rise velocity of small bubble increases with slurry concentration, but no significant effect of column diameter was observed based on comparisons with literature studies.

7.2 Recommendations

The following recommendations can be made based on this study:

1. The radial profile of heat transfer coefficient is strongly affected by the presence of internals type and location. There is a need to develop an appropriate flow model to estimate heat transfer coefficient at different radial and axial locations in presence of internals.

2. Internals in bubble column can significantly affect hydrodynamics which need to be taken into consideration for performance modeling. Detailed CFD modeling with appropriate verification could help to understand the variations in hydrodynamics and heat transfer in bubble columns with scale and in presence of internals.
3. Verification experiments are needed in larger diameter column (say 0.6 m) with appropriate theoretical modeling and analysis to confirm that the effect of column diameter becomes small above diameter of 0.3 m.
4. Axial and radial variations of phase holdups in presence of internals need to be investigated as part of verification experiments.
5. Further work can be done to develop scale-up criteria for bubble columns based on the results of this study.
6. Measurement of bubble size and liquid velocities at different axial and radial locations are needed in presence of different type of internals to better understand their effect on the temporal variation of heat transfer coefficient and local column hydrodynamics.
7. Back mixing of liquid and gaseous phase need to be further investigated in presence of internals using suitable tracers.

References:

Joshi, J.B., Sharma, M.M., Shah, Y.T., Singh, C.P.P., Ally, M., Klinzing, G.E., 1980. Heat transfer in multiphase contactors. *Chemical Engineering Communications*. 6, 257-271.

Appendix A.

Local Liquid Velocity

The radial variation of gas holdup provides the driving force for the recirculation flow. An equation for circulating liquid flow was developed by Ueyama and Miyauchi (1979) starting with Navier-Stokes equation and following main assumptions.

- radial pressure remains constant
- molecular viscosity is negligible in turbulent core compared to turbulent viscosity

$$-\frac{1}{r} \frac{d}{dr} (r \tau_s) = \frac{dp}{dz} + (1 - \varepsilon_g(r)) \rho_l g \quad (\text{A.1})$$

In the turbulent core, the shear stress is related to time-averaged vertical velocity of liquid through the turbulent kinematic viscosity as below:

$$\tau_s = \nu_t \rho_l \frac{dU_l}{dr} \quad (\text{A.2})$$

Ueyama and Miyauchi (1979) developed an empirical correlation for turbulent viscosity based on literature data.

$$\nu_t = 0.0322 D_c^{1.7} \quad (\text{A.3})$$

The radial distribution of gas holdup observed in the turbulent flow regime can be approximated as:

$$\varepsilon_{g,loc} = \varepsilon_{g,avg} \left(\frac{m+2}{m} \right) (1 - \theta^m) \quad (\text{A.4})$$

Mean gas holdup is related to local gas holdup as follows:

$$\varepsilon_{g,avg} = \frac{1}{\pi R^2} \int_0^R 2\pi r \varepsilon_{g,loc} dr \quad (A.5)$$

Two boundary conditions are required to solve equation (A.1)

One boundary condition assumes axi-symmetric liquid flow in the column:

$$\frac{dU_l}{dr} = 0 \quad \text{at } r = R \quad (A.6)$$

A second boundary condition is from velocity distribution in turbulent flow. The thickness of the laminar sublayer is much smaller than the column radius R , therefore can be neglected to give the following boundary condition:

$$U = U_w \quad \text{at } r = R \quad (A.7)$$

Equation 2.52 can be integrated with above conditions to obtain local liquid velocity in column. For a value of $m = 2$ (in Eq. A.4), Wachi et al. (1987) obtained the following equation for local liquid velocity.

$$U_l = \frac{\tau_w R}{2\nu_t \rho_l} (1 - \theta^2) + \frac{gR^2 \varepsilon_{g,avg}}{8\nu_t} (1 - \theta^2)^2 + U_{l,w} \quad (A.8)$$

Peripheral or wall liquid velocity ($U_{l,w}$) is related to wall shear stress (τ_w) by the following equation.

$$U_{l,w} = -11.63 \frac{\sqrt{|\tau_w|}}{\rho_l} \quad (\text{A.9})$$

Wachi et al. (1987) have also developed equation for liquid velocity at wall of the column.

References

Ueyama, K., Miyauchi, T., 1979. Properties of recirculating turbulent two phase flow in gas bubble columns. *AIChE Journal*. 25, 258–266.

Wachi, S., Morikawa, H., Ueyama K., 1987. Gas Holdup and Axial Dispersion in Gas-Liquid Cocurrent Bubble Column. *J. of Chem. Eng. of Japan*. Vol. 20, No. 3, p. 309.

Appendix B. Calculation Procedure for Gas Hold-Up from Pressure Difference in Bubble and Slurry Bubble Column

The average gas hold-up can be calculated from the pressure difference between the bottom (sparger region) and the top (disengagement region) pressure transducers. In a three-phase slurry bubble column, the static pressure drop along the bed height is given by

$$-\Delta P = (\rho_g \varepsilon_g + \rho_l \varepsilon_l + \rho_s \varepsilon_s) g \Delta H \quad (\text{B.1})$$

The volume fraction of individual phases is equal to unity.

$$\varepsilon_g + \varepsilon_l + \varepsilon_s = 1 \quad (\text{B.2})$$

The volume fraction of the solid phase in three-phase dispersion is related to the volume fraction in the gas free suspension by

$$\varepsilon_s = (1 - \varepsilon_g) \phi_s \quad (\text{B.3})$$

Substitution of equation B.2 and B.3 into equation B.1 yields an equation for gas hold-up in slurry bubble column after rearrangement,

$$\varepsilon_g = \frac{\left(\frac{\Delta P / \Delta H}{g} \right) + \rho_l \phi_s - \rho_s \phi_s - \rho_l}{\rho_g + \rho_l \phi_s - \rho_s \phi_s - \rho_l} \quad (\text{B.4})$$

For solid-free two-phase bubble column, putting $\phi_s = 0$,

$$\varepsilon_g = \frac{\left(\frac{\Delta P / \Delta H}{g} \right) - \rho_l}{\rho_g - \rho_l} \quad (\text{B.5})$$

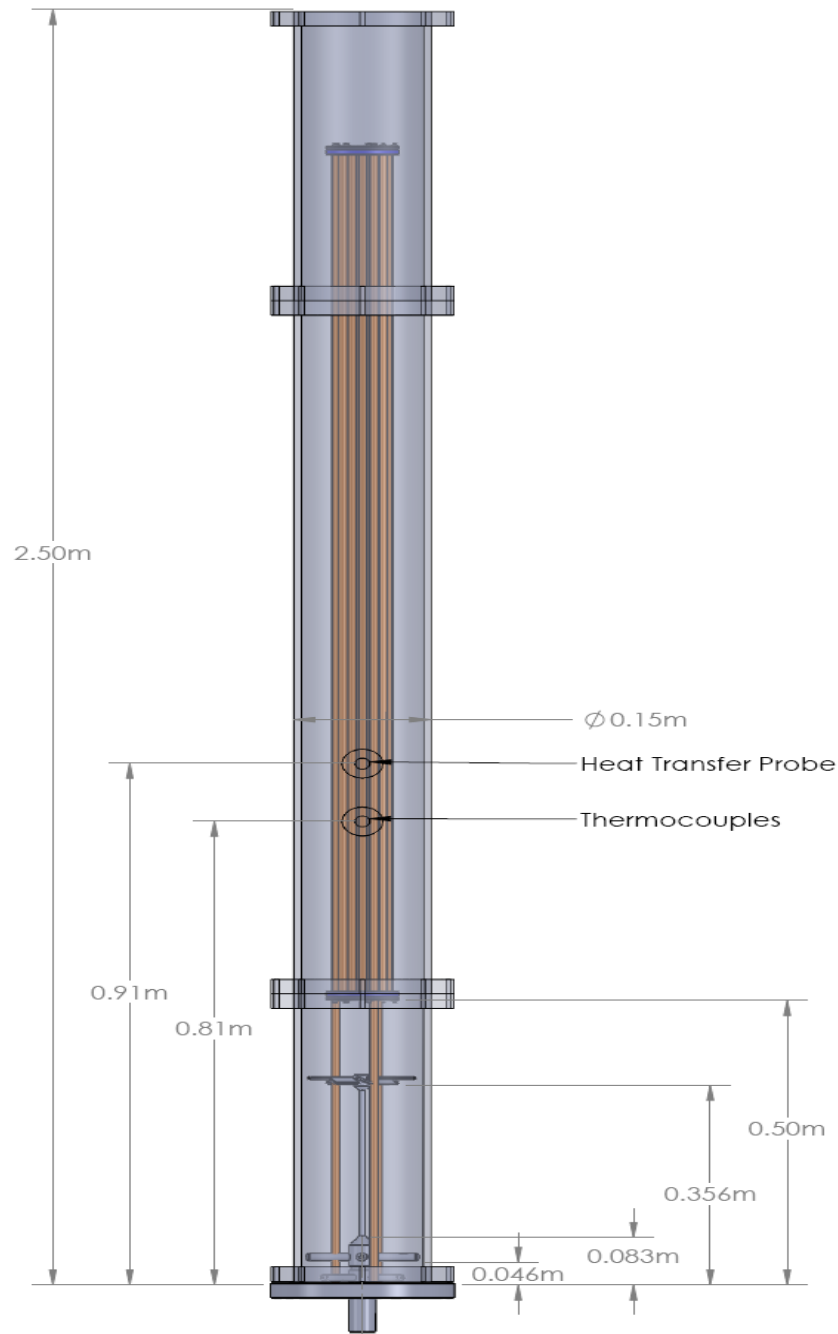
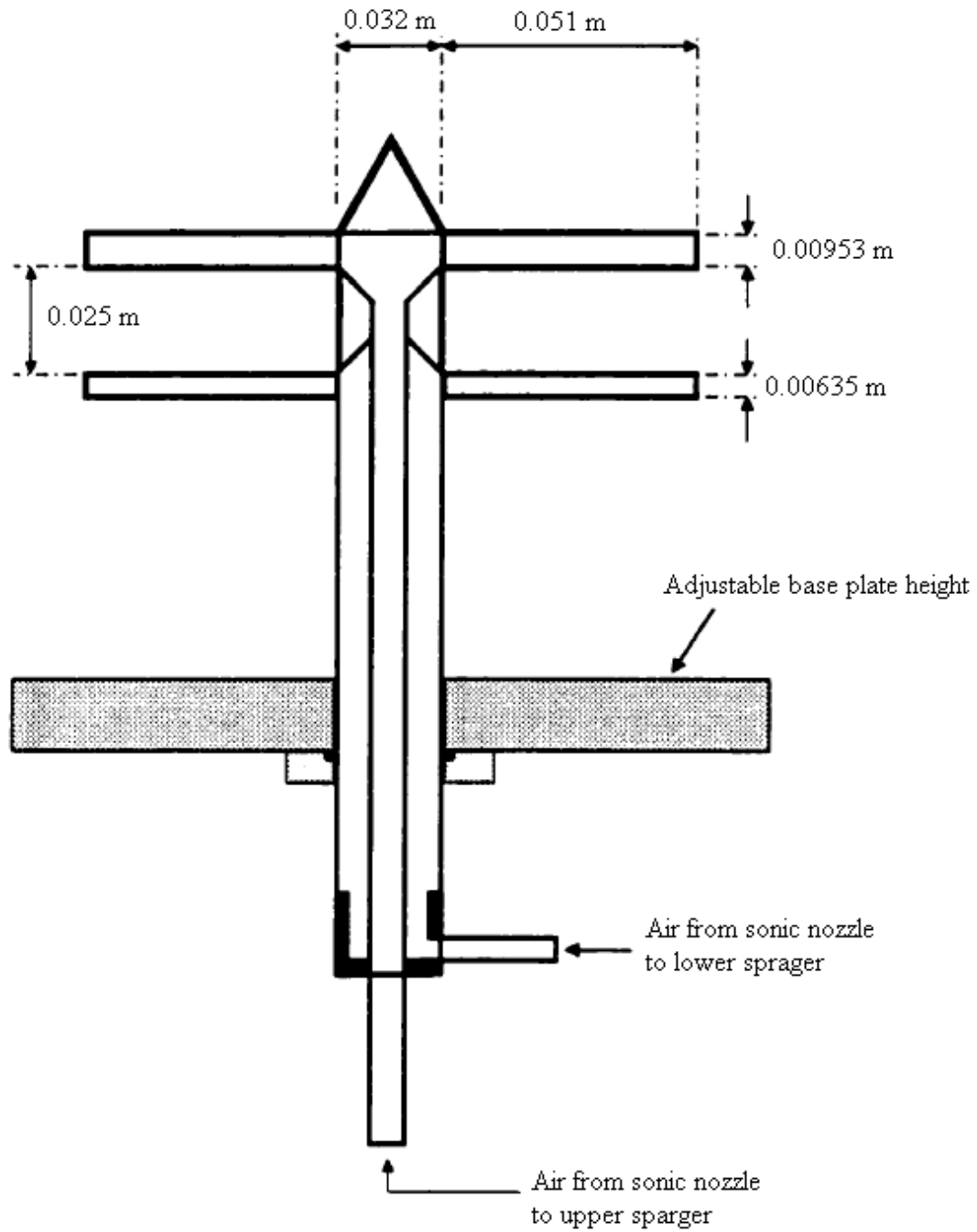


Figure C.1 . Schematic diagram of experimental setup



Upper Sparger – 4 arms with 7 orifices each
 Lower Sparger – 4 arms with 5 orifices each
 Orifices located on the bottom of arms
 Orifice diameter – 1.9 mm

Figure C.2 . Schematic diagram of the dual sparger design (Gandhi, 1997)

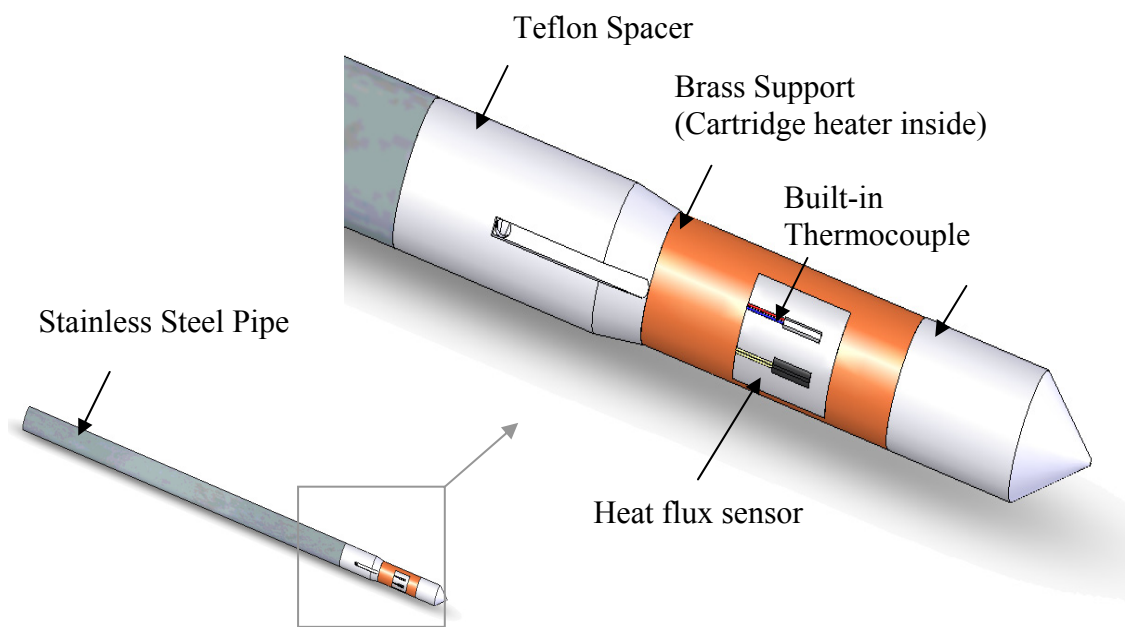


Figure C.3. Schematic diagram of the heat transfer probe

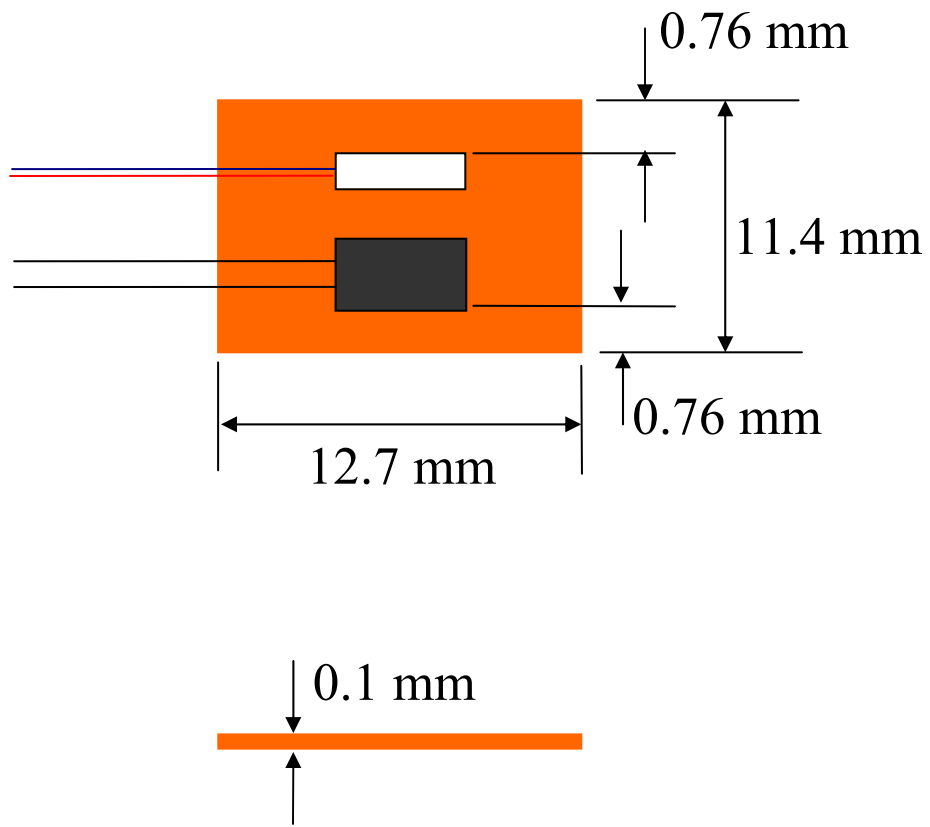


Figure C.4. Microfoil Heat Flux Sensor Dimensions

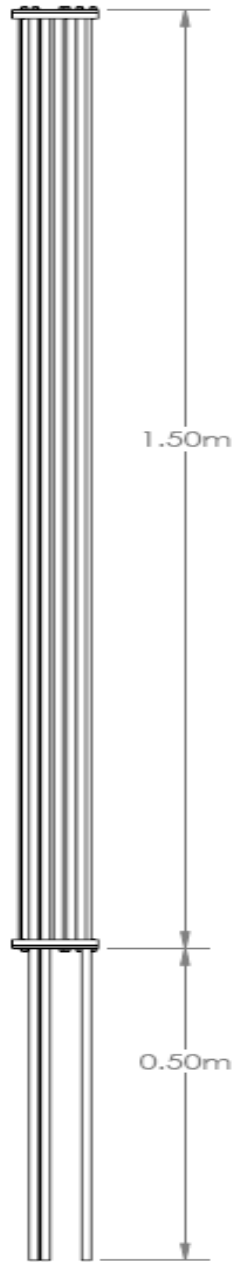


Figure C.5. Schematic diagram of tube bundle internal (type A)

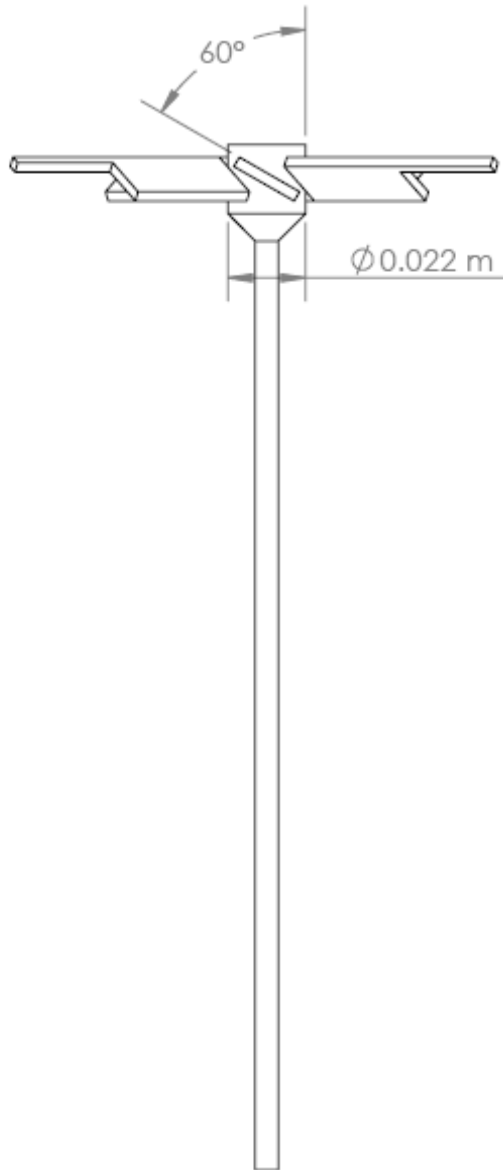


Figure C.6. Schematic diagram of six-blade baffle (type B)

Appendix D. Reproducibility and 95% confidence interval of Heat Transfer and Gas Holdup Data

All heat transfer and gas holdup measurements were done atleast 3 times (maximum 4 times) and the average value is reported in all papers. The reproducibility of heat transfer data in all cases was within 2-3%. In case of gas holdup data the reproducibility of data was within 1%. The 95% confidence interval was calculated for the data reported. Figure D.1 - D.5 shows the 95% confidence interval for heat transfer and gas holdup data in air-water and air-water-glass beads system in hollow bubble columns and with internals.

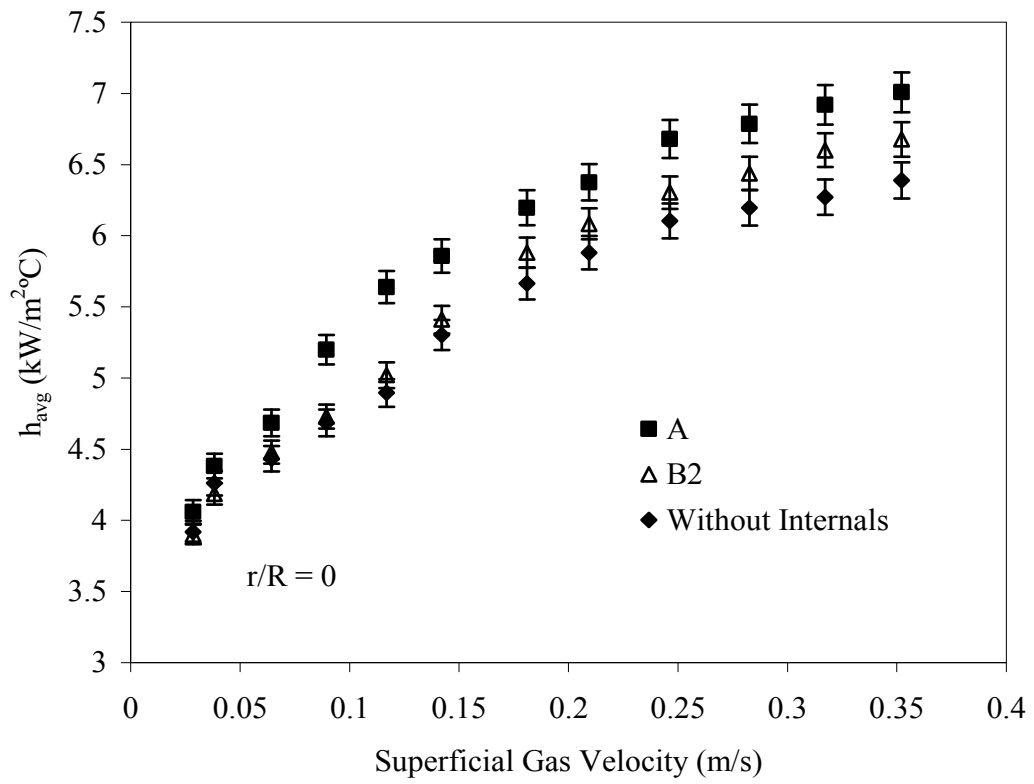


Figure D.1. 95% Confidence interval of heat transfer data in hollow bubble columns and with internals (air-water-system) at center

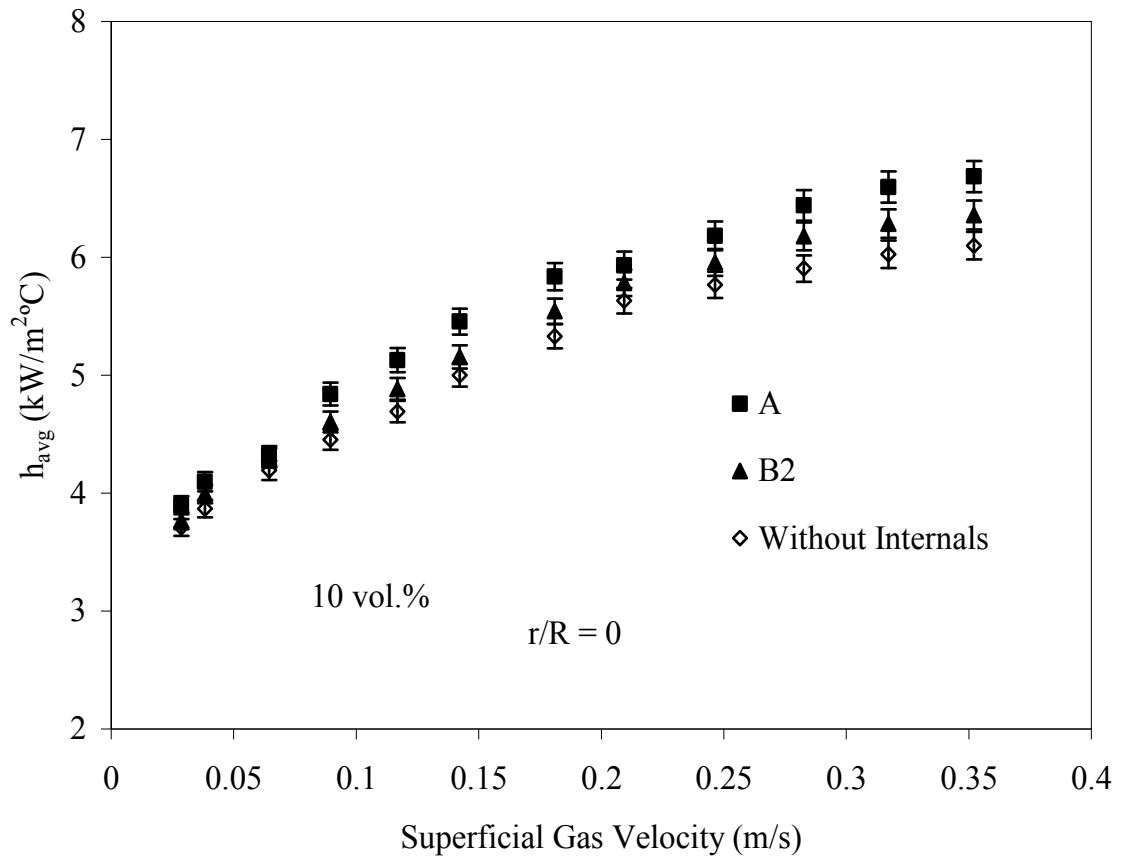


Figure D.2. 95% Confidence interval of heat transfer data in hollow bubble columns and with internals (air-water-glass beads system) at center

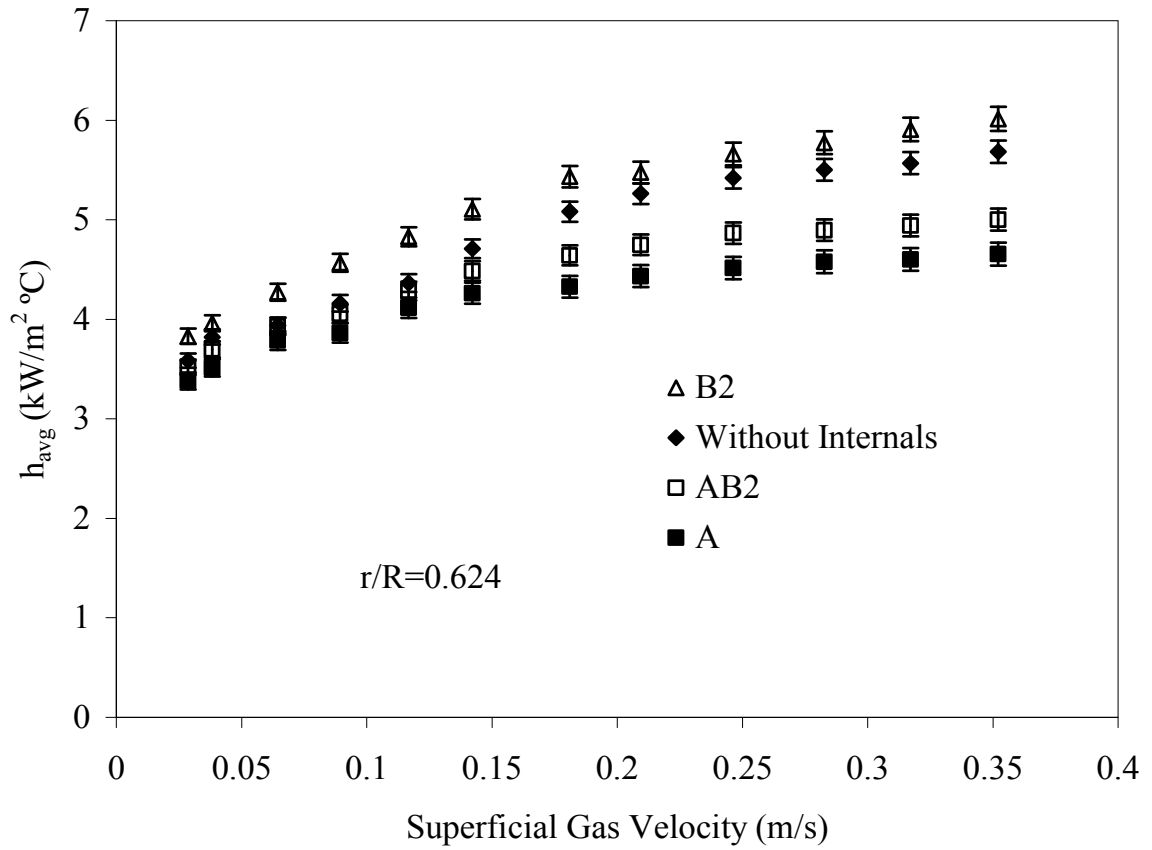


Figure D.3. 95% Confidence interval of heat transfer data in hollow bubble columns and with internals (air-water-system) in wall region

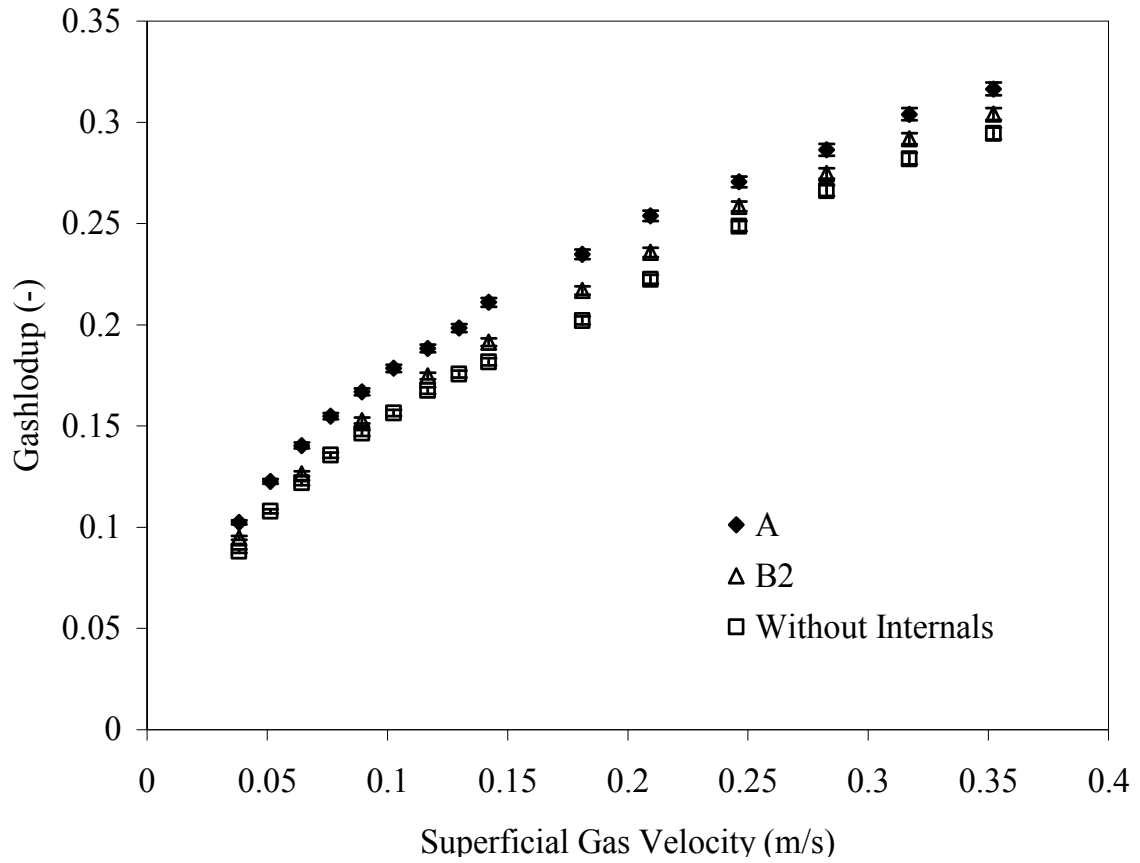


Figure D.4. 95% Confidence interval of gas holdup data in hollow bubble columns and with tube bundle type internal (air-water-system)

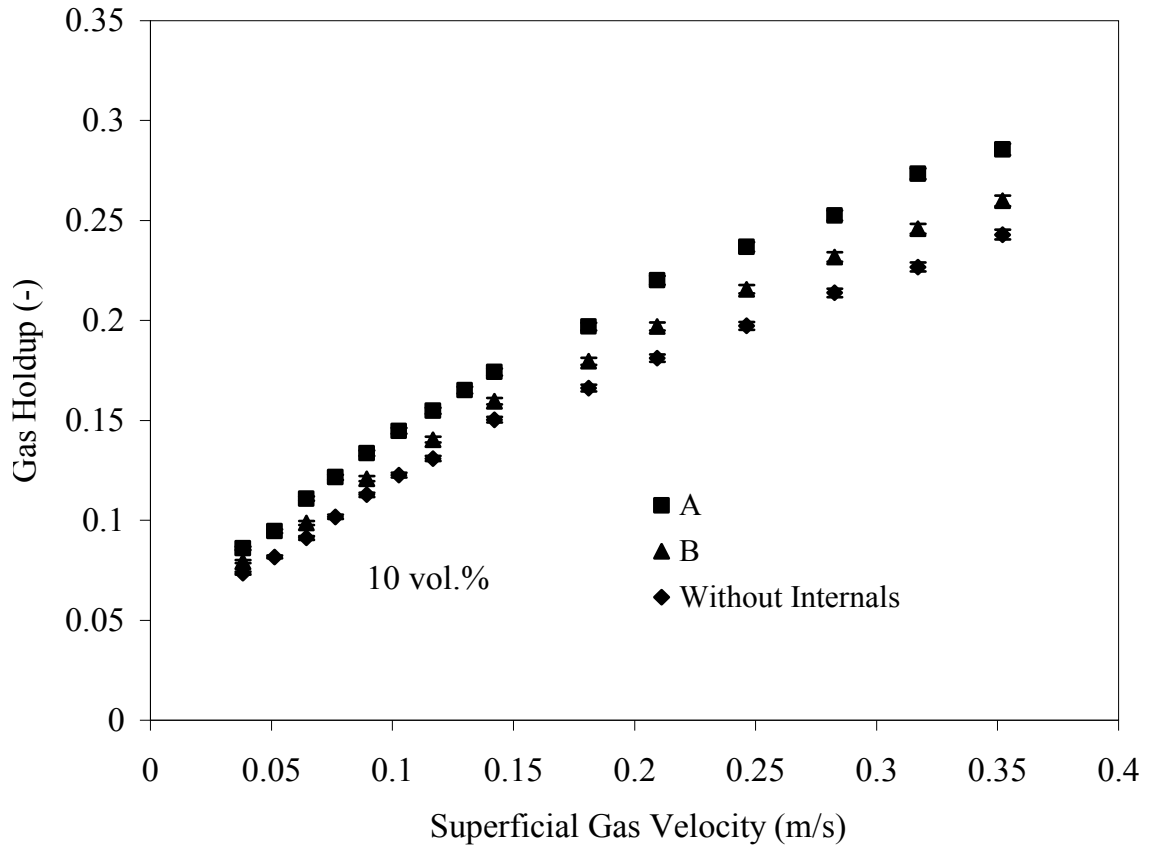


Figure D.5. 95% Confidence interval of gas holdup data in hollow bubble columns and with tube bundle type internal (air-water-glass beads system)

Appendix E. Pressure Transducers Calibration

Three pressure transducers (OMEGA type PX-541) were used to obtain the pressure fluctuation data. One pressure transducer (OMEGA type PX541-15GI) was located in the distributor section at a height of 0.027 m from the bottom of the column. The other pressure transducers (OMEGA type PX541-7.5GI) was located at 1.318 m from the bottom of the column. The pressure transducer were connected a D.C. power supply and generated a voltage proportional to measured pressure.

Calibrations of transducers were repeated before the each set of experiments were done. Figure E.1, E.2, shows the calibration curves obtained with three pressure transducers.

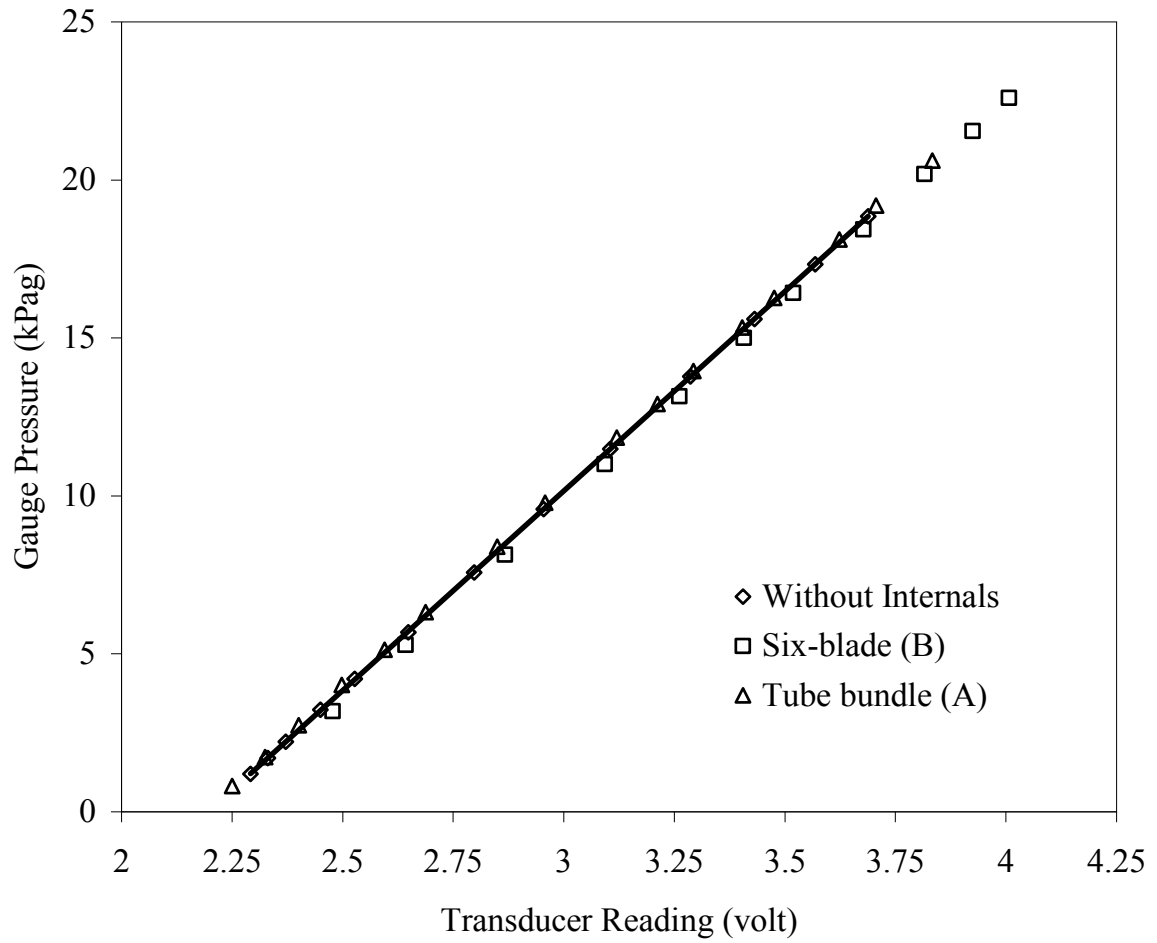


Figure E.1. Calibration curve for distributor section pressure transducer (OMEGA type PX541-15GI)

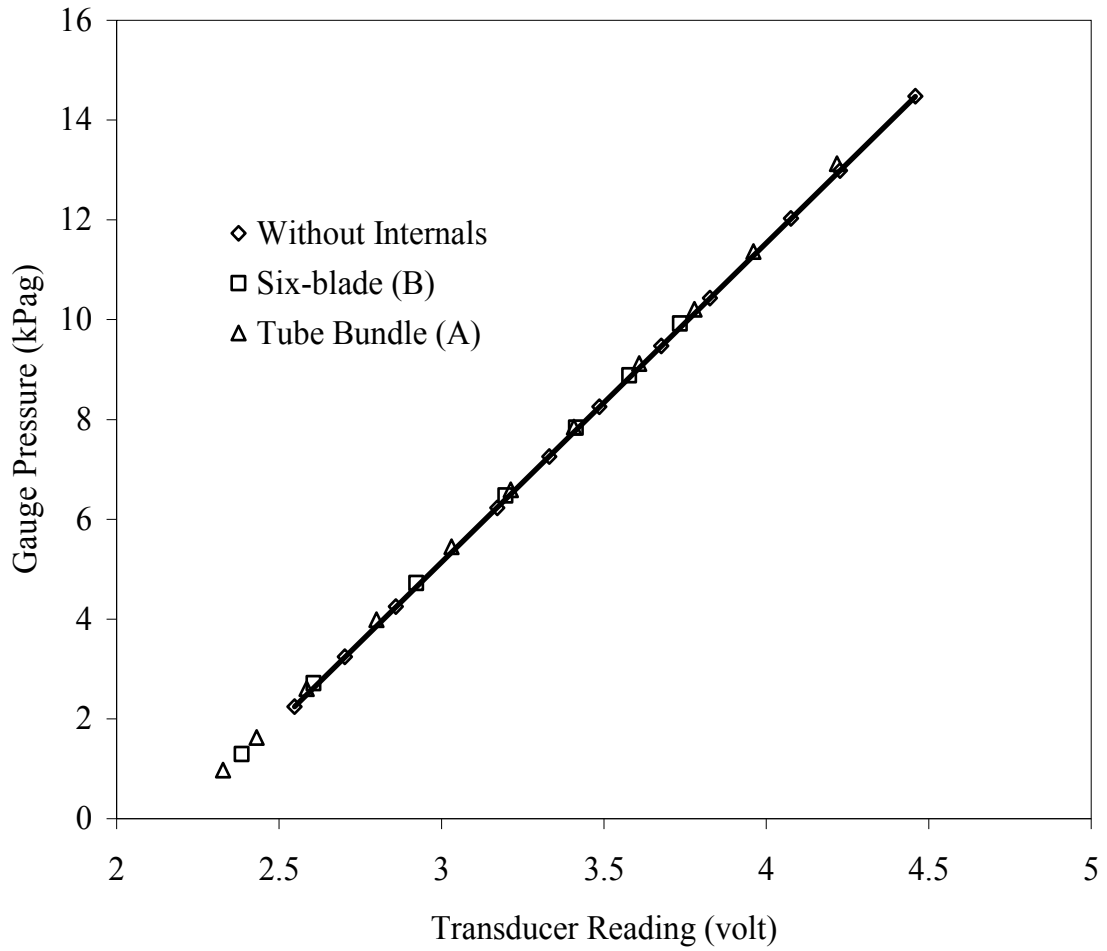


Figure E.2. Calibration curve for disengagement section pressure transducer (OMEGA type PX541-7.5GI)

Appendix F Calibration of Bulk Thermocouples

The bulk temperature was measured using two thermocouples (ANSI type T). One thermocouple was located at the center of the column and the other thermocouple was located close to the wall. The thermocouples were calibrated using the mercury thermometer. The axial locations of the thermocouples could be changed.

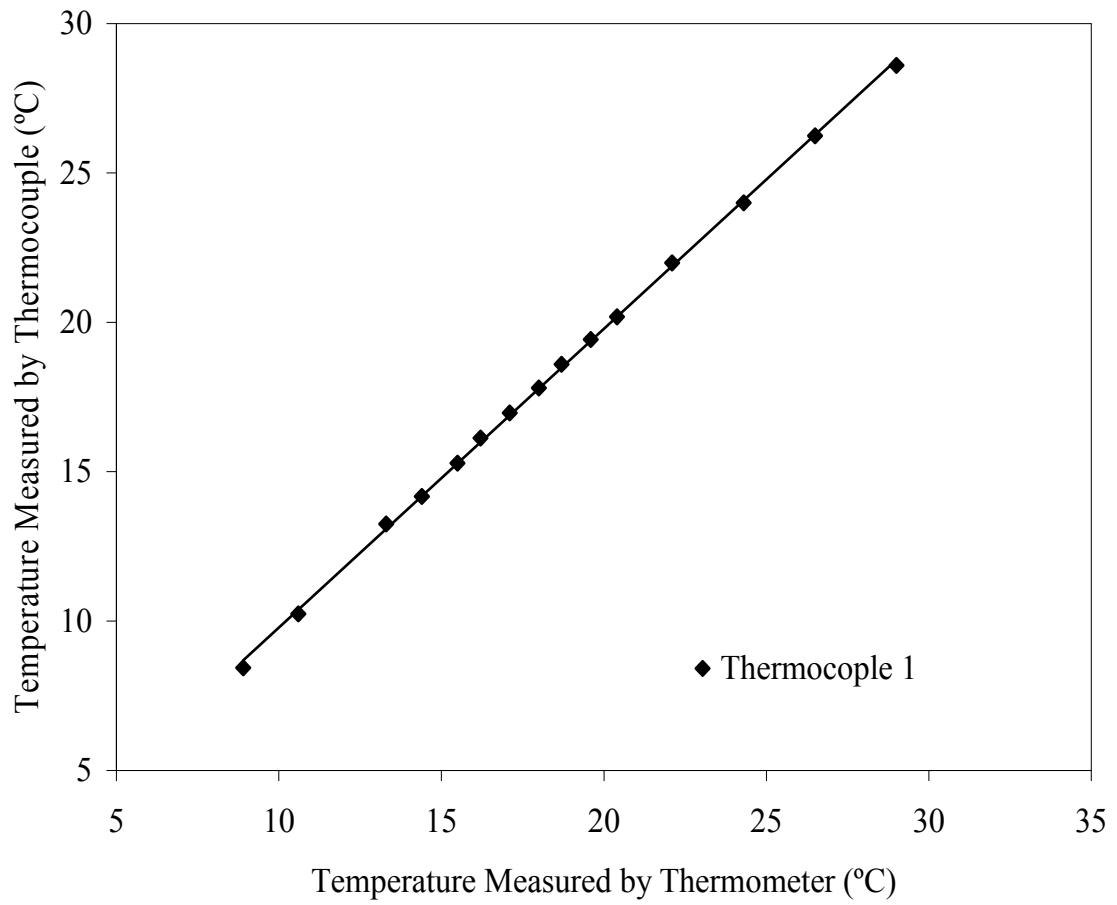


Figure F.1. Calibration curve for bulk thermocouple located at the center

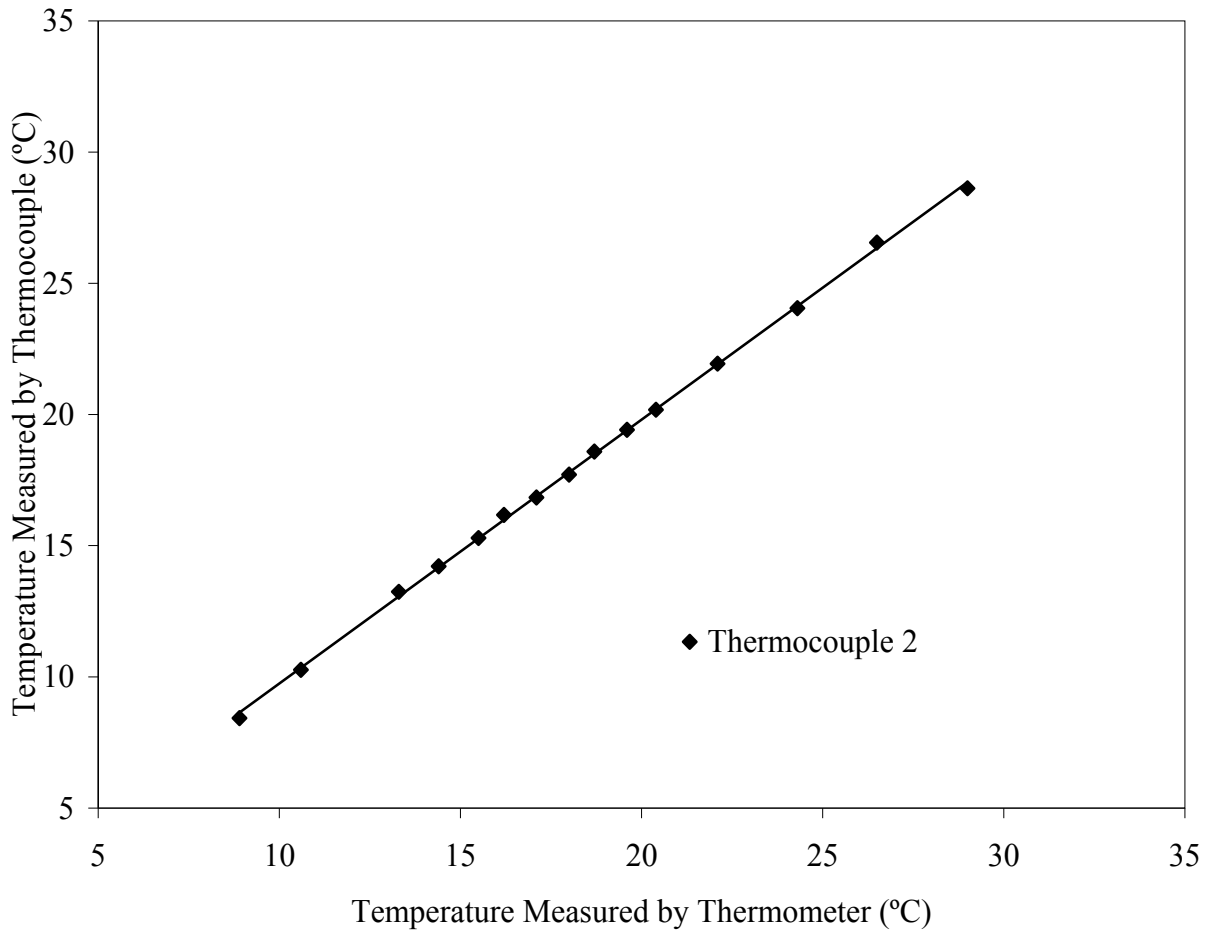


Figure F.2. Calibration curve for bulk thermocouple located close to the wall

Appendix G. Solid Characteristics

The glass beads were purchased from Potters Industries Inc., Valley Forge, PA, USA. The particle size was measured using a Malvern Mastersizer 2000 available in Crystallization and Control Laboratory at the University of Western Ontario. The physicochemical properties of glass beads are presented in Table G.1. The samples were collected from the different heights in the bag. Typical particle size distribution tables and curves obtained for some samples from the Malvern Mastersizer 2000 are presented.

Table G.1. Physicochemical properties of the glass beads

Properties	Values
Particle Size	≈ 49 μm
Density	2500 kg/m ³
Refractive Index	1.51-1.52
Crush Resistance	14000-36000 psi
Heat Capacity	0.84 kJ/kg.K
Thermal Conductivity	0.80 W/m.K
Composition	Soda-Lime Silica Glass
Free Silica	None



MASTERSIZER



Result Analysis Report

Sample Name:
Potters 35micron glass beads
Sample Source & type:
Factory = Potters
Sample bulk lot ref:
25-09-07-b

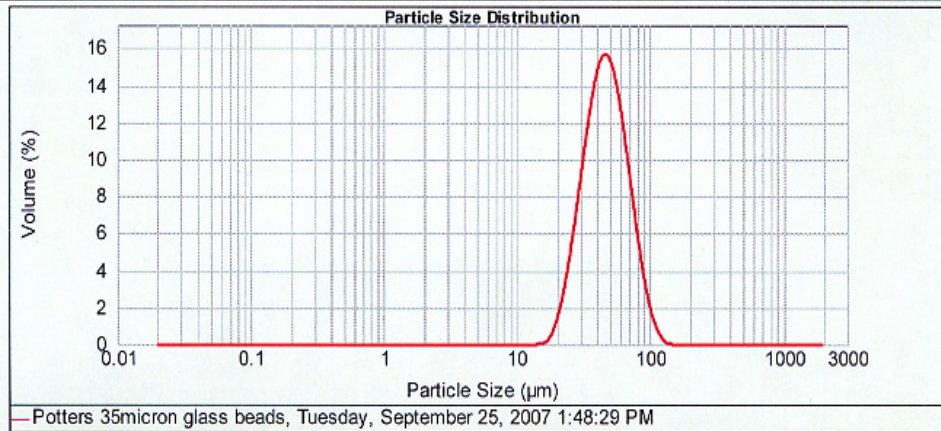
SOP Name:
Glass beads (typical)
Measured by:
CCPL
Result Source:
Measurement

Measured:
Tuesday, September 25, 2007 1:48:29 PM
Analysed:
Tuesday, September 25, 2007 1:48:30 PM

Particle Name: Glass beads (typical)	Accessory Name: Hydro 2000MU (A)	Analysis model: General purpose	Sensitivity: Enhanced
Particle RI: 1.520	Absorption: 0	Size range: 0.020 to 2000.000 um	Obscuration: 10.96 %
Dispersant Name: Water	Dispersant RI: 1.330	Weighted Residual: 0.684 %	Result Emulation: Off

Concentration: 0.0683 %Vol	Span : 1.002	Uniformity: 0.315	Result units: Volume
Specific Surface Area: 0.0577 m ² /g	Surface Weighted Mean D[3,2]: 42.470 um	Vol. Weighted Mean D[4,3]: 48.622 um	

d(0.1): 28.032 um d(0.5): 45.445 um d(0.9): 73.562 um



— Potters 35micron glass beads, Tuesday, September 25, 2007 1:48:29 PM

Size (µm)	Volume In %										
0.010	0.00	0.085	0.00	0.728	0.00	6.213	0.00	53.020	11.25	452.432	0.00
0.011	0.00	0.097	0.00	0.825	0.00	7.048	0.00	60.147	9.04	513.244	0.00
0.013	0.00	0.110	0.00	0.937	0.00	7.996	0.00	68.231	6.51	582.231	0.00
0.015	0.00	0.125	0.00	1.063	0.00	9.071	0.00	77.403	4.14	660.491	0.00
0.017	0.00	0.141	0.00	1.206	0.00	10.290	0.00	87.807	2.25	749.269	0.00
0.019	0.00	0.160	0.00	1.368	0.00	11.673	0.00	99.609	0.99	846.981	0.00
0.021	0.00	0.182	0.00	1.552	0.00	13.242	0.00	112.958	0.30	964.229	0.00
0.024	0.00	0.206	0.00	1.760	0.00	15.022	0.00	128.196	0.01	1093.634	0.00
0.027	0.00	0.234	0.00	1.997	0.00	17.041	0.05	145.416	0.50	1240.860	0.00
0.031	0.00	0.265	0.00	2.265	0.00	19.332	1.50	164.962	0.00	1407.648	0.00
0.035	0.00	0.301	0.00	2.570	0.00	21.930	3.08	187.135	0.00	1596.654	0.00
0.040	0.00	0.342	0.00	2.915	0.00	24.876	5.21	212.298	0.00	1811.492	0.00
0.045	0.00	0.388	0.00	3.307	0.00	28.222	8.76	240.822	0.00	2054.980	0.00
0.052	0.00	0.440	0.00	3.752	0.00	32.015	10.05	273.192	0.00	2331.196	0.00
0.059	0.00	0.499	0.00	4.256	0.00	36.319	11.94	309.913	0.00	2644.539	0.00
0.066	0.00	0.566	0.00	4.828	0.00	41.200	12.88	351.569	0.00	3000.000	0.00
0.075	0.00	0.642	0.00	5.477	0.00	46.736	12.63	398.825	0.00		
0.085	0.00	0.728	0.00	6.213	0.00	53.020		452.432	0.00		

Operator notes:



MASTERSIZER



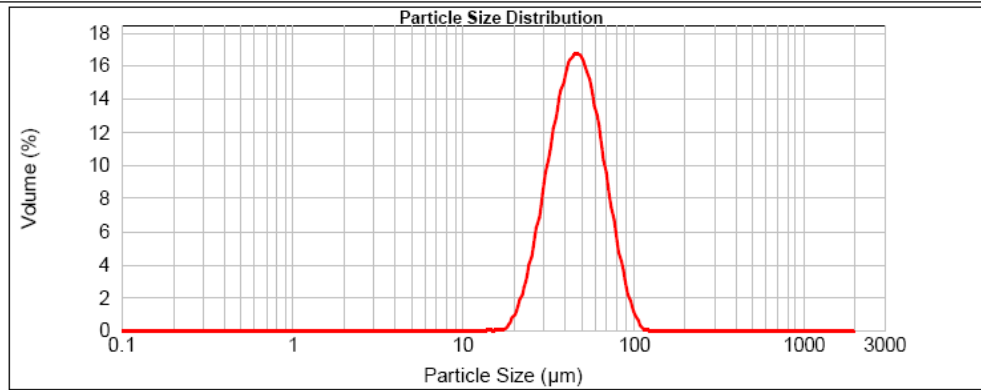
Result Analysis Report

Sample Name: Glass beads 35	SOP Name: New_Glass_beads	Measured: Tuesday, April 27, 2010 3:17:43 PM
Sample Source & type: Factory = Paris	Measured by: CCPL	Analysed: Tuesday, April 27, 2010 3:17:44 PM
Sample bulk lot ref: 123-ABC	Result Source: Measurement	

Particle Name: Default	Accessory Name: Scirocco 2000 (A)	Analysis model: General purpose	Sensitivity: Enhanced
Particle RI: 1.520	Absorption: 0.1	Size range: 0.020 to 2000.000 um	Obscuration: 6.11 %
Dispersant Name:	Dispersant RI: 1.000	Weighted Residual: 0.769 %	Result Emulation: Off

Concentration: 0.0089 %Vol	Span : 0.920	Uniformity: 0.288	Result units: Volume
Specific Surface Area: 0.137 m ² /g	Surface Weighted Mean D[3,2]: 43.644 um	Vol. Weighted Mean D[4,3]: 49.005 um	

d(0.1): 29.478 um d(0.5): 46.439 um d(0.9): 72.207 um



Size (µm)	Volume In %										
0.010	0.00	0.085	0.00	0.728	0.00	6.213	0.00	53.020	12.30	452.432	0.00
0.011	0.00	0.097	0.00	0.826	0.00	7.049	0.00	60.147	9.85	513.244	0.00
0.013	0.00	0.110	0.00	0.937	0.00	7.996	0.00	68.231	6.91	582.231	0.00
0.015	0.00	0.125	0.00	1.063	0.00	9.071	0.00	77.403	4.09	660.491	0.00
0.017	0.00	0.141	0.00	1.206	0.00	10.290	0.00	87.807	1.92	749.269	0.00
0.019	0.00	0.160	0.00	1.368	0.00	11.673	0.00	99.609	0.54	840.981	0.00
0.021	0.00	0.182	0.00	1.552	0.00	13.242	0.00	112.998	0.00	964.229	0.00
0.024	0.00	0.206	0.00	1.760	0.00	15.022	0.00	128.188	0.00	1093.834	0.00
0.027	0.00	0.234	0.00	1.997	0.00	17.041	0.14	145.416	0.00	1240.860	0.00
0.031	0.00	0.265	0.00	2.265	0.00	19.332	0.94	164.962	0.00	1407.648	0.00
0.035	0.00	0.301	0.00	2.570	0.00	21.930	2.33	187.135	0.00	1696.854	0.00
0.040	0.00	0.342	0.00	2.915	0.00	24.878	4.45	212.288	0.00	1811.462	0.00
0.045	0.00	0.388	0.00	3.307	0.00	28.222	7.10	240.822	0.00	2054.960	0.00
0.052	0.00	0.440	0.00	3.752	0.00	32.015	9.88	273.192	0.00	2331.198	0.00
0.058	0.00	0.499	0.00	4.256	0.00	36.319	12.24	309.913	0.00	2644.539	0.00
0.066	0.00	0.566	0.00	4.828	0.00	41.200	13.63	351.569	0.00	3000.000	0.00
0.075	0.00	0.642	0.00	5.477	0.00	46.738	13.67	398.825	0.00		
0.085	0.00	0.728	0.00	6.213	0.00	53.020		452.432	0.00		

Operator notes:
Malvern Instruments Ltd.
Malvern, UK
Tel : +[44] (0) 1684-892468 Fax +[44] (0) 1684-892789

Mastersizer 2000 Ver. 5.22
Serial Number : 34264-51

File name: Glass beads 35.mea
Record Number: 3
27 Apr 2010 03:30:16 PM



MASTERSIZER



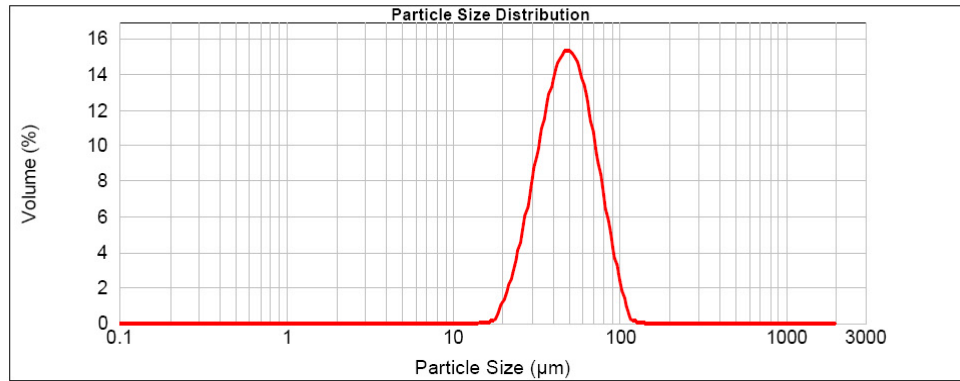
Result Analysis Report

Sample Name: Glass beads 42-1	SOP Name: New_Glass_beads	Measured: Tuesday, April 27, 2010 3:13:55 PM
Sample Source & type: Factory = Paris	Measured by: CCPL	Analysed: Tuesday, April 27, 2010 3:13:56 PM
Sample bulk lot ref: 123-ABC	Result Source: Measurement	

Particle Name: Default	Accessory Name: Scirocco 2000 (A)	Analysis model: General purpose	Sensitivity: Enhanced
Particle RI: 1.520	Absorption: 0.1	Size range: 0.020 to 2000.000 um	Obscuration: 5.16 %
Dispersant Name:	Dispersant RI: 1.000	Weighted Residual: 0.855 %	Result Emulation: Off

Concentration: 0.0077 %Vol	Span : 1.002	Uniformity: 0.309	Result units: Volume
Specific Surface Area: 0.134 m ² /g	Surface Weighted Mean D[3,2]: 44.738 um	Vol. Weighted Mean D[4,3]: 51.235 um	

d(0.1): 29.263 um d(0.5): 48.271 um d(0.9): 77.608 um



— Glass beads 42-1, Tuesday, April 27, 2010 3:13:55 PM

Size (µm)	Volume In %										
0.010	0.00	0.085	0.00	0.728	0.00	6.213	0.00	53.020	12.00	452.432	0.00
0.011	0.00	0.097	0.00	0.826	0.00	7.049	0.00	60.147	10.38	513.244	0.00
0.013	0.00	0.110	0.00	0.937	0.00	7.996	0.00	68.231	8.09	582.231	0.00
0.015	0.00	0.125	0.00	1.063	0.00	9.071	0.00	77.403	5.52	660.491	0.00
0.017	0.00	0.141	0.00	1.206	0.00	10.290	0.00	87.807	3.20	749.269	0.00
0.019	0.00	0.160	0.00	1.368	0.00	11.673	0.00	99.609	1.29	849.981	0.00
0.021	0.00	0.182	0.00	1.552	0.00	13.242	0.00	112.998	0.13	964.229	0.00
0.024	0.00	0.206	0.00	1.760	0.00	15.022	0.03	128.186	0.01	1093.834	0.00
0.027	0.00	0.234	0.00	1.997	0.00	17.041	0.25	145.416	0.00	1240.860	0.00
0.031	0.00	0.265	0.00	2.265	0.00	19.332	1.20	164.962	0.00	1407.648	0.00
0.035	0.00	0.301	0.00	2.570	0.00	21.930	2.51	187.135	0.00	1596.854	0.00
0.040	0.00	0.342	0.00	2.915	0.00	24.878	4.36	212.288	0.00	1811.492	0.00
0.045	0.00	0.388	0.00	3.307	0.00	28.222	6.55	240.822	0.00	2054.980	0.00
0.052	0.00	0.440	0.00	3.752	0.00	32.015	8.83	273.192	0.00	2331.196	0.00
0.058	0.00	0.499	0.00	4.256	0.00	36.319	10.83	309.913	0.00	2644.539	0.00
0.066	0.00	0.566	0.00	4.828	0.00	41.200	12.20	351.569	0.00	3000.000	0.00
0.075	0.00	0.642	0.00	5.477	0.00	46.738	12.63	398.825	0.00		
0.085	0.00	0.728	0.00	6.213	0.00	53.020	12.63	452.432	0.00		

Operator notes:
Malvern Instruments Ltd.
Malvern, UK
Tel : +[44] (0) 1684-892456 Fax +[44] (0) 1684-892789

Mastersizer 2000 Ver. 5.22
Serial Number : 34264-51

File name: Glass beads 42-1.mea
Record Number: 2
27 Apr 2010 03:29:25 PM

CURRICULUM VITAE

Name	Anil Kumar Jhawar
Post-Secondary Education and Degrees	Laxminarayan Institute of Technology, Nagpur University Nagpur - 2000 – 2004 B. Tech (Petroleum Refining and Petrochemical Technology) The University of Western Ontario London, Ontario Canada – 2006-2008 M.E.Sc. (Chemical Engineering) The University of Western Ontario London, Ontario Canada – 2008-2012 Ph.D (Chemical Engineering)
Related Work Experience	Research Assistantship The University Of Western Ontario London, Ontario Canada – 2008 - 2011 Teaching Assistantship The University Of Western Ontario London, Ontario Canada – 2008 - 2011

Publications:

Jhawar, A.K., Prakash, A., 2007. Analysis of local heat transfer coefficient in bubble column using fast response probes. *Chemical Engineering Science*. 62, 7274-7281.

Jhawar, A.K., Prakash, A, 2011. Influence of bubble column diameter on local heat transfer and related hydrodynamics. *Chemical Engineering Research and Design*. 89, 1996-2002.

Jhawar, A.K., Prakash, A, 2012. Heat Transfer in Slurry Bubble Column Reactor – A Critical Overview. *Industrial and Engineering Chemistry Research*. (Accepted for publication)